HORIZONTAL BALL MILLING: A SIMPLE AND EFFECTIVE PER- AND POLYFLUOROALKYL SUBSTANCES (PFAS) DESTRUCTION TECHNIQUE FOR IMPACTED SOILS

BROYAGE À BILLES HORIZONTAL: UNE TECHNIQUE SIMPLE ET EFFICACE DE DESTRUCTION DES SUBSTANCES PER- ET POLYFLUOROALKYLES (SPFA) POUR LES SOLS IMPACTÉS

A Thesis Submitted to the Division of Graduate Studies
of the Royal Military College of Canada
by

Nicholas J. Battye

In Fulfillment of the Requirements for the Degree of
Doctor of Philosophy in Chemistry and Chemical Engineering

May 16, 2025

Arwyn – proof that anything is possible with a little determination and perseverance ☺

Acknowledgements

Was this Ph.D. the product of a mid-life crisis? Maybe not at the start since I did enroll at the age of 38, but it did take a decade to complete in my spare time, so it often felt like it towards the end. There were many moments of fight-or-flight-level panic along the way; thankfully, there was no shortage of individuals who helped me get through those trying times.

First, I would like to acknowledge my supervisor Dr. Kela Weber. He could have had an equally glowing career as a motivational speaker as I seriously tried to quit twice (maybe three times?), but each time, he managed to soothe and inspire, and pull me back from the brink of despair. Thank you for this, and for everything else that you did to help me along the way; it was a lot, and it will forever be appreciated.

I would also like to acknowledge my co-supervisor, Dr. Michael Hulley, whose calm, friendly demeanour, regardless of the work and stress load he was under, as well as his punctuality in getting reviews back to me, is a modus operandi to which we should all aspire.

A special ‘thank you’ to David Patch. Another genius to be sure, but even better, an optimistic, enthusiastic, and inspiring colleague who also helped drag me across the finish line.

Finally, to my family and friends, who learned from my last graduate experience and did not ask, “When will you be done?” nearly so often, I would not have been able to do this without your constant support through it all. All of you kept my spirits high and my heart light, and what more can you ask for in life than that?

Abstract

Per- and polyfluoroalkyl substances (PFAS) are a manufactured class of chemicals used for a variety of common and more specialized consumer and industrial products and processes that are most easily identified by one or more carbon-fluorine bonds. The carbon-fluorine bond is the strongest in organic chemistry, and one that does not exist naturally. This makes them extremely persistent in nature with limited, or a complete lack of, biodegradation pathways. Because of this, they are now found in virtually every environmental matrix around the globe, as well as in human blood. This is a major problem because there are a number of associated health issues attributed to PFAS that can occur at low levels.

Remediating PFAS is difficult. While sorption-based technologies have been used successfully, these do not destroy PFAS, and often create secondary waste streams. Destructive technologies are few and are mostly applicable to water. To address many of the most significant PFAS point sources in the environment, a simple and efficient PFAS-destruction technology for soil is critically needed.

One such method is ball milling. The mechanochemical processes that occur inside ball mills, namely friction, impact, collision, and grinding, enable solid-state reactions to occur that are not otherwise attainable in ambient conditions. While successful destruction of PFAS has been shown using planetary ball mills (PBMs), the double axis of rotation (mimicking planetary motion) currently precludes easy scale-up beyond the benchtop. Alternatively, horizontal ball mills (HBMs) function on a single axis of rotation (like a wheel); while this produces lower energy environments, large-scale HBMs are readily available, being prevalent in the mining, metallurgy and agricultural industries. Such mills could easily be repurposed and transported to impacted sites for on-site remediation purposes.

This work pursued the potential of HBMs to be a simple and efficient PFAS-destruction technique for impacted soils. Spiked nepheline syenite sand (NSS) and PFAS-impacted field soils were used in the trials. Analysis included liquid chromatography tandem mass spectrometry (LC-MS/MS) to track 21 target PFAS and liquid chromatography high-resolution mass spectrometry (LC-HRMS) was used to track 19 non-target PFAS. Combined, the two analytical techniques allowed the tracking of both target and non-target PFAS transformation chemistry. The first trials were conducted using 1 L and 25 L cylinders. In the presence of potassium hydroxide (KOH), used as a co-milling reagent, the spiked perfluorooctanesulfonate (PFOS), 6:2 fluorotelomer sulfonate (6:2 FTS), and non-target PFAS in the aqueous film-forming foam (AFFF) underwent 42.85 ± 4.81, 97.21 ± 0.90, and 90.97 ± 1.76 % degradation, respectively. Despite the inherent added complexity associated with

field soils, higher PFOS degradation was achieved at both scales, up to 81 % at the 1 L scale, and up to 85 % at the 25 L scale. Subsequent experiments using an industrial-scale HBM (267 L cylinder) degraded 6:2 FTS by 97 % and the non-target PFAS in AFFF by 98 %, in their respective NSS spiked trials with KOH. PFOS achieved 70 % degradation with KOH and 69 % without. Perfluorooctanoate (PFOA) behaved similarly: 74 % with KOH and 70 % without. Highly challenging field soils from a former firefighting training area (FFTA) were purposefully used to test the limits of the HBM. To quantify effectiveness, free fluoride analysis had to be used; the difference between unmilled and milled soil was up to 7.8 mg/kg, which is the equivalent of 12 mg/kg PFOS, a sizable amount considering typical field impact levels. Soil health, evaluated by key microbial and plant health parameters, was not significantly affected by of milling though it was characterized as poor to begin with. Leachability reached 100 % in milled soil with KOH, but already ranged from 81 to 96 % in unmilled soil. A limited assessment of the hazards associated with the inhalation of PFAS-impacted dust from milling, as well as the cross-contamination potential to the environment, showed risk to be low in both cases. In the final experiments for this work, performed in preparation for on-site pilot tests, AFFF-impacted field soil was run at three different scales: a benchtop PBM (0.25 L cylinder), a commercial-scale HBM (1 L cylinder), and an industrial-scale HBM (267 L cylinder) to further understand the critical parameters behind PFAS destruction. Results showed that with the right milling parameters the majority of non-target PFAS, up to 93 % on a HBM system, can be degraded (on the PBM it was up to 97 %). The amount of KOH used was clearly the most critical factor related to PFAS degradation. Media:soil ratios and soil moisture content were also influential factors. Experiments seeking to restart higher rates of degradation, often observed in the first few minutes of milling, showed some indications of success.

These experiments represent the first attempted use of a HBM to destroy PFAS. Several logistical and analytical opportunities were identified to guide future work. Heterogeneity of PFAS concentrations, primarily in unmilled (i.e. starting) soil, was problematic. The problems encountered with this will likely be proportional to the volumes used. Sieving, more robust initial characterization, and larger subsample sizes during analysis should be considered; however, even quantifying the total amount of PFAS present in AFFF remains analytically challenging due to the presence of non-target PFAS. Novel analytical methodologies should be incorporated as they become available. Existing, unconventional, but complimentary analytical techniques, including X-ray diffraction analysis (XRD) and proton induced gamma-ray emission (PIGE), could also assist with interpretation and a better understanding of the insoluble fluoride complex developments that can form as a result of milling, which in turn would help close the mass balance.

The conclusion of this work is that HBMs can successfully destroy PFAS in soil, making it a promising and much needed soil remediation technology. Further study of the highlighted critical factors will make on-site field remediation efforts more efficient and cost-effective.

Résumé

Les substances per- et polyfluoroalkylées (SPFA) sont une classe de produits chimiques manufacturés, utilisés dans divers produits et procédés destinés aux consommateurs et aux industries, à la fois commun et spécialisé. Leur identification se fait facilement par une ou plusieurs liaisons carbone-fluor. Cette liaison est la plus forte en chimie organique et n'existe pas à l'état naturel. Cela les rend extrêmement persistantes dans la nature, avec des voies de biodégradation limitées, voire inexistantes. De ce fait, on les retrouve aujourd'hui dans la quasi-totalité des matrices environnementales autour du monde, ainsi que dans le sang humain. Il s'agit d'un enjeu de taille, puisque de nombreux troubles de santé liés aux SPFA peuvent apparaître même à faibles concentrations.

La dépollution des SPFA est complexe. Bien que les technologies de sorption aient été utilisées avec succès, elles ne détruisent pas les SPFA et génèrent souvent des flux de déchets secondaires. Les technologies destructives sont peu nombreuses et s'appliquent principalement à l'eau. Pour traiter les principales sources ponctuelles de SPFA dans l'environnement, une technologie simple et efficace de destruction des SPFA pour les sols est indispensable.

L'une de ces méthodes est le broyage à boulets. Les processus mécanochimiques qui se produisent à l'intérieur des broyeurs à boulets, à savoir la friction, l'impact, la collision et le broyage, permettent des réactions à l'état solide impossibles à obtenir autrement dans des conditions ambiantes. Si la destruction des SPFA a été démontrée avec des broyeurs planétaires à boulets (PBM), le double axe de rotation (imitant le mouvement planétaire) empêche actuellement une transposition aisée au-delà de la paillasse. Par ailleurs, les broyeurs horizontaux à boulets (HBM) fonctionnent sur un seul axe de rotation (comme une roue); bien que cela produise des environnements à plus faible énergie, les HBM à grande échelle sont facilement disponibles et sont répandus dans les industries minière, métallurgique, et agricole. Ces machines pourraient facilement être réaffectées et transportées vers les sites touchés à des fins d’assainissement sur place.

Ces travaux ont exploré le potentiel des HBM comme technique simple et efficace de destruction des SPFA dans les sols contaminés. Du sable de syénite néphélinique (NSS) enrichi et des sols contaminés par des SPFA ont été utilisés dans les essais. L'analyse a inclus la chromatographie liquide couplée à la spectrométrie de masse en tandem (LC-MS/MS) pour suivre 21 SPFA cibles et la chromatographie liquide couplée à la spectrométrie de masse à haute résolution (LC-HRMS) pour suivre 19 SPFA non cibles. Combinées, ces deux techniques analytiques ont permis de suivre la chimie de transformation des SPFA cibles et non cibles. Les premiers essais ont

été réalisés avec des cylindres de 1 L et 25 L. En présence d'hydroxyde de potassium (KOH), utilisé comme réactif de co-broyage, l'acide perfluorooctanesulfonique (PFOS) enrichi, le sulfonate de perfluorooctane 6:2 (6:2 FTS) et les SPFA non ciblés dans la mousse à film aqueux (AFFF) ont subi respectivement une dégradation de 42,85 ± 4,81, 97,21 ± 0,90, et 90,97 ± 1,76 %. Malgré la complexité accrue inhérente aux sols de terrain, une dégradation plus élevée du PFOS a été obtenue aux deux échelles, jusqu'à 81 % à l'échelle de 1 L et jusqu'à 85 % à l'échelle de 25 L. Des expériences ultérieures utilisant un HBM à l'échelle industrielle (cylindre de 267 L) ont dégradé le 6:2 FTS de 97 % et les SPFA non ciblés dans l'AFFF de 98 %, dans leurs essais respectifs enrichis en NSS avec du KOH. Le PFOS a atteint 70 % de dégradation avec du KOH et 69 % sans KOH. L'acide perfluorooctanoïque (PFOA) s'est comporté de manière similaire: 74 % avec du KOH et 70 % sans KOH. Des sols de terrain très difficiles provenant d'une aire de formation pour pompiers (FFTA) ont été délibérément utilisés pour tester les limites du HBM. Pour quantifier l'efficacité, une analyse du fluorure libre a dû être utilisée; la différence entre le sol non broyé et le sol broyé pouvait atteindre 7,8 mg/kg, ce qui équivaut à 12 mg/kg de PFOS, une quantité considérable compte tenu des niveaux d'impact typiques sur le terrain. La santé du sol, évaluée par des paramètres microbiens et phytosanitaires clés, n'a pas été significativement affectée par le broyage, bien qu'elle ait été qualifiée de mauvaise au départ. La lixiviabilité a atteint 100 % dans les sols broyés avec du KOH, mais variait déjà entre 81 et 96 % dans les sols non broyés. Une évaluation limitée des dangers liés à l'inhalation de poussières de broyage contenant des SPFA, ainsi que du potentiel de contamination croisée de l'environnement, a montré que le risque était faible dans les deux cas. Dans les expériences finales de ce travail, réalisées en préparation des essais pilotes sur site, le sol de terrain impacté par l'AFFF a été testé à trois échelles différentes: un PBM de paillasse (cylindre de 0,5 L), un HBM à l'échelle commerciale (cylindre de 1 L) et un HBM à l'échelle industrielle (cylindre de 267 L) afin de mieux comprendre les paramètres critiques derrière la destruction des SPFA. Les résultats ont montré qu'avec les bons paramètres de broyage, la majorité des SPFA non ciblés, jusqu'à 93 % sur un système HBM, peuvent être dégradés (sur le PBM, ce taux atteignait jusqu'à 97 %). La quantité de KOH utilisée était clairement le facteur le plus critique lié à la dégradation des SPFA. Les rapports milieu:sol et la teneur en humidité du sol étaient également des facteurs influents. Les essais visant à relancer la cinétique de premier ordre souvent observée dans les premières minutes de broyage ont montré des indications de succès.

Ces essais représentent la première tentative d'utilisation d'un HBM pour détruire les SPFA. Plusieurs pistes logistiques et analytiques ont été identifiées pour orienter les travaux futurs. L'hétérogénéité des concentrations de SPFA, principalement dans le

sol non broyé (c'est-à-dire de départ), était problématique. Les difficultés rencontrées seront probablement proportionnelles aux volumes utilisés. Un tamisage, une caractérisation initiale plus robuste et des sous-échantillons plus importants lors de l'analyse doivent être envisagés. Cependant, la quantification de la quantité totale de SPFA présente dans l'AFFF reste un défi analytique en raison de la présence de SPFA non ciblés. De nouvelles méthodologies analytiques devraient être intégrées dès qu'elles seront disponibles. Des techniques analytiques existantes, non conventionnelles mais complémentaires, notamment la diffraction des rayons X (XRD) et l'émission gamma induite par des protons (PIGE), pourraient également faciliter l'interprétation et une meilleure compréhension des complexes de fluorure insolubles qui peuvent se former suite au broyage, ce qui contribuerait à clôturer le bilan massique.

La conclusion de ces travaux est que les HBM peuvent détruire efficacement les SPFA dans le sol, ce qui en fait une technologie de dépollution des sols prometteuse et indispensable. Une étude plus approfondie des facteurs critiques mis en évidence rendra les efforts de dépollution sur site plus efficaces et plus rentables.

Co-authorship Statement

This thesis is written in manuscript format, with Nicholas Battye being the primary author of the six chapters. Co-author contributions are highlighted below.

Chapter 3, "Use of a horizontal ball mill to remediate per- and polyfluoroalkyl substances in soil," was co-authored by Nicholas Battye, David Patch, Dylan Roberts, Natalia O'Connor, Lauren Turner, Bernard Kueper, Michael Hulley, and Kela Weber. It was published in Science of the Total Environment. Conceptualization was conducted by Nicholas Battye, Lauren Turner, Bernard Kueper, and Kela Weber. Investigation and experimental work were performed by Nicholas Battye and Dylan Roberts. Formal analysis was performed by Nicholas Battye, David Patch, Natalia O'Connor, and Dylan Roberts. Original draft writing was performed by Nicholas Battye. Editing and review was performed by all co-authors. [Battye, N. J., Patch, D. J., Roberts, D. M. D., O'Connor, N. M., Turner, L. P., Kueper, B. H., Hulley, M. E., & Weber, K. P. (2022). Use of a horizontal ball mill to remediate per- and polyfluoroalkyl substances in soil. Science of The Total Environment, 835, 155506. https://doi.org/https://doi.org/10.1016/j.scitotenv.2022.155506]

Chapter 4, "Mechanochemical degradation of per- and polyfluoroalkyl substances in soil using an industrial-scale horizontal ball mill with comparisons of key operational metrics," was co-authored by Nicholas Battye, David Patch, Iris Koch, Ryan Monteith, Dylan Roberts, Natalia O'Connor, Bernard Kueper, Michael Hulley, and Kela Weber. It was published in Science of the Total Environment. Conceptualization was conducted by Nicholas Battye and Kela Weber. Investigation and experimental work were performed by Nicholas Battye and Dylan Roberts. Formal analysis was performed by Nicholas Battye, David Patch and Natalia O'Connor. Original draft writing was performed by Nicholas Battye. Editing and review was performed by all co-authors. [Battye, N., Patch, D., Koch, I., Monteith, R., Roberts, D., O'Connor, N., Kueper, B., Hulley, M., & Weber, K. (2024). Mechanochemical degradation of per- and polyfluoroalkyl substances in soil using an industrial-scale horizontal ball mill with comparisons of key operational metrics. Science of the Total Environment, 928, 172274. https://doi.org/10.1016/j.scitotenv.2024.172274]

Chapter 5, "Mechanochemical degradation of per- and polyfluoroalkyl substances in soil from at a firefighter training area at three scales," was co-authored by Nicholas Battye, Dean Morrow, Michael Hulley, and Kela Weber. It is being prepared for submission. Conceptualization was conducted by Nicholas Battye and Kela Weber. Investigation and experimental work were performed by Nicholas Battye and Dean

Morrow. Formal analysis was performed by Nicholas Battye, Adrian Pang and Tim Brown. Original draft writing was performed by Nicholas Battye. Editing and review was performed by all co-authors.

Table of Contents

List of Tables

List of Figures

List of Acronyms

AFFF: aqueous film forming foam
ECF: electrochemical fluorination
BAF: bioaccumulation factors
BCF: bioconcentration factors
CIC: combustion ion chromatography
EOF: extractable organic fluorine
FASA: perfluoroalkane sulphonamide
FFTA: firefighting training area
FSA: perfluorosulfonamides
FtB: fluorotelomer betaines
FtOHs: fluorotelomer alcohols
FTS: fluorotelomer sulfonate
FtSaAm: fluorotelomer sulfonamido amine
FtSaB: fluorotelomer sulfonamido betaine
FtSam: fluorotelomer sulfonamide
FtTAoS: fluorotelomer thioamido sulfonate
FtUAl: fluorotelomer unsaturated aldehyde
FtUSam: fluorotelomer unsaturated sulfonamide
GC-MS: gas chromatography mass spectrometry
HBM: horizontal ball mill
HFPO-DA: hexafluoropropylene oxide dimer acid
HPLC: high-pressure liquid chromatography
LC-HRMS: liquid chromatography high-resolution mass spectrometry
LC-MS: liquid chromatography-mass spectrometry
LC-MS/MS: liquid chromatography tandem mass spectrometry
KF: potassium fluoride
KOH: potassium hydroxide
NSS: nepheline syenite sand
PBM: planetary ball mill
PCBs: polychlorinated biphenyls
PFAA: perfluoroalkyl acid
PFAS: per and polyfluoroalkyl substances
PFBA: perfluorobutanoate
PFBS: perfluorobutane sulfonic acid
PFCA: perfluoroalkyl carboxylic acid
PFDA: perfluorodecanoate
PFDoA: perfluorododecanoate
PFHpA: perfluoroheptanoate
PFHxA: perfluorohexanoate
PFHxS: perfluorohexane sulfonate
PFNA: perfluorononanoate

PFOA: perfluorooctanoic acid
PFOS: perfluorooctane sulfonate
PFPA: perfluoroalkyl phosphonic acid
PFPeA: perfluoropentanoate
PFSA: perfluoroalkyl sulphonic acids
PFSAm: perfluoroalkyl sulfonamide
PFUnA: perfluoroundecanoate
PIC: product of incomplete combustion
PIGE: photon-induced gamma ray emission
POP: persistent organic pollutant
RPM: rotations per minute
SERS: surface enhanced ramen spectroscopy
TOP assay: total oxidizable precursor assay
USEPA: United States Environmental Protection Agency
XRD: x-ray diffraction analysis

1 Chapter 1: Introduction

1.1 Background

Per- and polyfluoroalkyl substances (PFAS) are aliphatic substances containing one or more carbon atoms that have had one or more of the hydrogen atoms replaced by fluorine (Buck et al., 2011). They represent synthetic organic chemicals that do not exist naturally. Coveted for their unique physicochemical properties, including high thermal/chemical stability, high tensioactivity, hydrophobicity, and oleophobicity, they have been produced commercially for a variety of applications in the modern industrial world since the 1950s (Lindstrom et al., 2011; Prevedouros et al., 2006). Typical uses include surface treatments to provide water, oil, grease, and stain resistance, but also in specialty products that require dispersant, emulsifying and/or surfactant properties, such as paints, coatings and lubricants, and aqueous film-forming foam (AFFF), which is used to extinguish fuel-based fires.

There are currently 14,735 individual PFAS listed on the USEPA's CompTox Chemicals Dashboard (v2.4.1, accessed October 8, 2024). Many of them have been shown to have the defining characteristics of persistent organic pollutants (POPs): they are toxic, extremely resistant to degradation to the point that they are often referred to as "forever chemicals", bioaccumulate in food chains, and have long-half lives in humans (Lindstrom et al., 2011). PFAS are now found in air, water, soil, sediment, glacier ice, and various biological organisms, including humans, all over the world (Chen et al., 2017; Ericson Jogsten et al., 2012; Garnett et al., 2021; John P Giesy & Kannan, 2001; Hogue, 2020; Huber & Brox, 2015; Jian et al., 2017; Kahkashan et al., 2019; Kwok et al., 2013; Möller et al., 2010; Paul et al., 2009; Quiñones & Snyder, 2009; Wang et al., 2014; Zacs & Bartkevics, 2016); and despite numerous warnings related to their toxicity (Gaber et al., 2023; Grandjean, 2018), PFAS applications continue to expand. Almost all human blood samples worldwide now contain measurable quantities of many PFAS at the µg/L level (Kannan et al., 2004), with a large body of research identifying their toxicological impacts, including links to cancer, kidney/liver disease, neurological and development issues in children, and reduced vaccination immune response (Bell et al., 2021; Caverly Rae et al., 2015; Olsen et al., 2017; Pelch et al., 2019; Shih et al., 2021, 2022; J. Zhang et al., 2024; X. Zhang et al., 2022)

Although many sources of PFAS have contributed to the current global contaminant burden, firefighting training areas (FFTAs) represent some of the most significant PFAS-impacted sites because of copious and chronic use of AFFF for training exercises at a singular location. Historically, FFTAs were nothing more than open fields with a burn pit, with no engineered controls to contain and/or recycle the liquids used (e.g., geomembrane liners, pump and treat systems, etc.). Unburnt fuel and AFFF product were allowed to percolate down into the soil, leading to the

contamination of the underlying groundwater and/or the surrounding surface water bodies from surface water runoff. Impacts to various ecological and human receptors then follow.

Available remedial options for PFAS are matrix-dependent; remediation of PFAS in water is typically limited to sorption-based technologies (e.g., ion exchange resin, granular activated carbon, etc.) (Du et al., 2014; España et al., 2015; Phong Vo et al., 2020; D. Q. Zhang et al., 2019), but these result in secondary waste streams. Destructive PFAS technologies for water are in development, such as ultraviolet activated reduction (Bentel et al., 2019; Z. Liu et al., 2022; O'Connor et al., 2023). While promising and necessary, these "downstream" technologies do not address "upstream" sources. At many contaminated sites, such as FFTAs, the historically impacted soil now acts as an ongoing secondary source of PFAS to the environment with the PFAS sorbed onto the soil readily partitioning into groundwater at levels that can easily exceed drinking water guidelines. Because drinking water guidelines are so low for PFAS, often set at the single- or double-digit ng/L level, in most instances, without intervention, they will essentially exceed in perpetuity. Therefore, impacted soil must be addressed to stop the downstream impacts. Dig and dump practices are questionable, as even in engineered landfills PFAS have been shown to penetrate liners (Di Battista et al., 2020). Theoretically, high-temperature incineration works, and was being used in certain circumstances to destroy PFAS impacted media until questions and concerns were raised regarding the potential for products of incomplete combustion (PICs). This led to a temporary prohibition (Cramer, 2022) so that these issues could be more thoroughly evaluated to determine any associated risk. This has now been shown to be analytically difficult as complex PFAS transformation chemistry complicates both emissions capture and mass balance closure (Crownover et al., 2019; Duchesne et al., 2020; Stoiber et al., 2020; Watanabe et al., 2016, 2018). Other traditional methods of contaminant destruction in soil have not yet been fully demonstrated (Mahinroosta & Senevirathna, 2020). Thus, there remains a critical need for a simple, proven, PFAS soil destruction technology.

1.2 Objectives

The overall goal of this work was to develop a simple and efficient PFAS-destruction technique for impacted soils using a horizontal ball mill (HBM). While successful destruction of PFAS has been shown using planetary ball mills (PBMs), the double axis of rotation (mimicking planetary motion) currently precludes easy scale-up beyond the benchtop. Alternatively, horizontal ball mills (HBMs) function on a single axis of rotation (like a wheel); while this produces lower energy environments, large-scale HBMs are readily available, being prevalent in the mining, metallurgy and agricultural industries. Such mills could easily be repurposed and transported to

impacted sites for on-site remediation purposes. To achieve the overall goal, the following objectives were carried out in succession:

1. Assess, for the first time, whether a HBM is capable of remediating PFAS impacted soil.

2. Scale up the HBM to an industrial size typically used by the industry before field applications.

3. Compare geophysical and geochemical properties in both unmilled and milled soil, as well as health and safety factors to provide insight into critical logistical and operational concerns pertinent to a field remediation project deployment.

4. In preparation for the first in-field ball milling pilot test, perform a final evaluation of PFAS destruction via ball milling using an AFFF impacted field soil at three scales, evaluating influential factors such as KOH and soil:media ratios, soil moisture content, as well as a method to restart higher rates of degradation.

1.3 Thesis Organization

This thesis is presented in manuscript style and consists of six chapters. Chapters 3 and 4 have been published in academic journals; herein, they have been slightly modified from their published versions. The intent is to publish Chapter 5 following the completion of this thesis. This thesis is organized in the following manner:

Chapter 1: background on research topic, objectives, and thesis structure.

Chapter 2: comprehensive literature review pertinent to the thesis; specifically, background information on PFAS and ball milling.

Chapter 3: evaluation of a HBM (1 L and 25 L cylinders) for degrading perfluorooctanesulfonate (PFOS), 6:2 fluorotelomer sulfonate (6:2 FTSA), and aqueous film forming foam (AFFF) spiked on nepheline syenite sand (NSS), as well as on two different soil types collected from an actual firefighting training area (FFTA).

Chapter 4: assessment of PFAS degradation using a scaled up, 267 L cylinder HBM. PFOS, perfluorooctanoate (PFOA), 6:2 FTS, and AFFF spiked NSS, along with soil obtained from another FFTA was milled. Additional analytical methods included free fluoride analysis, a soil health suite, and leachability tests. An exposure assessment for dust intake via oral ingestion was also performed.

Chapter 5: testing of the effectiveness of ball milling PFAS-impacted soil from a FFTA at three different scales: a benchtop planetary ball mill (cylinder size: 0.25 L),

a commercial-scale horizontal ball mill (cylinder size: 1.0 L), and an industrial-scale horizontal ball mill (cylinder size: 267 L).

Chapter 6: summary of the overall conclusions of the thesis and recommendations for future work.

Each chapter includes a short introduction complementing the general introduction provided above.

Appendices A-C contain supplemental information related to Chapters 3-5.

1.4 Chapter 1 References

Bell, E. M., De Guise, S., McCutcheon, J. R., Lei, Y., Levin, M., Li, B., Rusling, J. F., Lawrence, D. A., Cavallari, J. M., O'Connell, C., Javidi, B., Wang, X., & Ryu, H. (2021). Exposure, health effects, sensing, and remediation of the emerging PFAS contaminants – Scientific challenges and potential research directions. *Science of The Total Environment*, *780*, 146399. https://doi.org/https://doi.org/10.1016/j.scitotenv.2021.146399

Bentel, M. J., Yu, Y., Xu, L., Li, Z., Wong, B. M., Men, Y., & Liu, J. (2019). Defluorination of Per- and Polyfluoroalkyl Substances (PFASs) with Hydrated Electrons: Structural Dependence and Implications to PFAS Remediation and Management. *Environmental Science & Technology*, *53*(7), 3718–3728. https://doi.org/10.1021/acs.est.8b06648

Buck, R. C., Franklin, J., Berger, U., Conder, J. M., Cousins, I. T., de Voogt, P., Jensen, A. A., Kannan, K., Mabury, S. A., & van Leeuwen, S. P. J. (2011). Perfluoroalkyl and polyfluoroalkyl substances in the environment: terminology, classification, and origins. *Integrated Environmental Assessment and Management*, *7*(4), 513–541. https://doi.org/10.1002/ieam.258

Caverly Rae, J. M., Craig, L., Slone, T. W., Frame, S. R., Buxton, L. W., & Kennedy, G. L. (2015). Evaluation of chronic toxicity and carcinogenicity of ammonium 2,3,3,3-tetrafluoro-2-(heptafluoropropoxy)-propanoate in Sprague–Dawley rats. *Toxicology Reports*, *2*, 939–949. https://doi.org/https://doi.org/10.1016/j.toxrep.2015.06.001

Chen, H., Reinhard, M., Nguyen, T. V., You, L., He, Y., & Gin, K. Y.-H. (2017). Characterization of occurrence, sources and sinks of perfluoroalkyl and polyfluoroalkyl substances (PFASs) in a tropical urban catchment. *Environmental Pollution*, *227*, 397–405. https://doi.org/https://doi.org/10.1016/j.envpol.2017.04.091

Cramer, P. D. (2022). *Temporary Prohibition on Incineration of Materials Contamining Per- and Polyfluoroalkyl Substances (PFAS)*.

Crownover, E., Oberle, D., Kluger, M., & Heron, G. (2019). Perfluoroalkyl and polyfluoroalkyl substances thermal desorption evaluation. *Remediation Journal*, *29*(4), 77–81. https://doi.org/https://doi.org/10.1002/rem.21623

Di Battista, V., Rowe, R. K., Patch, D., & Weber, K. (2020). PFOA and PFOS diffusion through LLDPE and LLDPE coextruded with EVOH at 22 °C, 35 °C, and 50 °C. *Waste Management (New York, N.Y.)*, *117*, 93–103. https://doi.org/10.1016/j.wasman.2020.07.036

Du, Z., Deng, S., Bei, Y., Huang, Q., Wang, B., Huang, J., & Yu, G. (2014). Adsorption behavior and mechanism of perfluorinated compounds on various adsorbents--a review. *Journal of Hazardous Materials*, *274*, 443–454. https://doi.org/10.1016/j.jhazmat.2014.04.038

Duchesne, A. L., Brown, J. K., Patch, D. J., Major, D., Weber, K. P., & Gerhard, J. I. (2020). Remediation of PFAS-Contaminated Soil and Granular Activated Carbon by Smoldering Combustion. *Environmental Science & Technology*, *54*(19), 12631–12640. https://doi.org/10.1021/acs.est.0c03058

Ericson Jogsten, I., Nadal, M., van Bavel, B., Lindström, G., & Domingo, J. L. (2012). Per- and polyfluorinated compounds (PFCs) in house dust and indoor air in Catalonia, Spain: Implications for human exposure. *Environment International*, *39*(1), 172–180. https://doi.org/https://doi.org/10.1016/j.envint.2011.09.004

España, V. A. A., Mallavarapu, M., Naidu, R., & Naidu, R. (2015). Treatment technologies for aqueous perfluorooctanesulfonate (PFOS) and perfluorooctanoate (PFOA): A critical review with an emphasis on field testing. *Environmental Technology and Innovation*, *4*, 168–181.

Gaber, N., Bero, L., & Woodruff, T. J. (2023). The Devil they Knew: Chemical Documents Analysis of Industry Influence on PFAS Science. *Annals of Global Health*, *89*(1), 37. https://doi.org/10.5334/aogh.4013

Garnett, J., Halsall, C., Thomas, M., Crabeck, O., France, J., Joerss, H., Ebinghaus, R., Kaiser, J., Leeson, A., & Wynn, P. M. (2021). Investigating the Uptake and Fate of Poly- and Perfluoroalkylated Substances (PFAS) in Sea Ice Using an Experimental Sea Ice Chamber. *Environmental Science & Technology*, *55*(14), 9601–9608. https://doi.org/10.1021/acs.est.1c01645

Giesy, J. P., & Kannan, K. (2001). Global Distribution of Perfluorooctane Sulfonate in Wildlife. *Environmental Science & Technology*, *35*(7), 1339–1342. https://doi.org/10.1021/es001834k

Grandjean, P. (2018). Delayed discovery, dissemination, and decisions on intervention in environmental health: a case study on immunotoxicity of

perfluorinated alkylate substances. *Environmental Health*, *17*(1), 62. https://doi.org/10.1186/s12940-018-0405-y

Hogue, C. (2020). US military sued to stop PFAS incineration. *C&EN Global Enterprise*, *98*(9), 27–27. https://doi.org/10.1021/cen-09809-polcon3

Huber, S., & Brox, J. (2015). An automated high-throughput SPE micro-elution method for perfluoroalkyl substances in human serum. *Analytical and Bioanalytical Chemistry*, *407*(13), 3751–3761. https://doi.org/10.1007/s00216-015-8601-x

Jian, J.-M., Guo, Y., Zeng, L., Liang-Ying, L., Lu, X., Wang, F., & Zeng, E. Y. (2017). Global distribution of perfluorochemicals (PFCs) in potential human exposure source–A review. *Environment International*, *108*, 51–62. https://doi.org/https://doi.org/10.1016/j.envint.2017.07.024

Kahkashan, S., Wang, X., Chen, J., Bai, Y., Ya, M., Wu, Y., Cai, Y., Wang, S., Saleem, M., Aftab, J., & Inam, A. (2019). Concentration, distribution and sources of perfluoroalkyl substances and organochlorine pesticides in surface sediments of the northern Bering Sea, Chukchi Sea and adjacent Arctic Ocean. *Chemosphere*, *235*, 959–968. https://doi.org/https://doi.org/10.1016/j.chemosphere.2019.06.219

Kannan, K., Corsolini, S., Falandysz, J., Fillmann, G., Kumar, K. S., Loganathan, B. G., Mohd, M. A., Olivero, J., Wouwe, N. Van, Yang, J. H., & Aldous, K. M. (2004). Perfluorooctanesulfonate and Related Fluorochemicals in Human Blood from Several Countries. *Environmental Science & Technology*, *38*(17), 4489–4495. https://doi.org/10.1021/es0493446

Kwok, K. Y., Yamazaki, E., Yamashita, N., Taniyasu, S., Murphy, M. B., Horii, Y., Petrick, G., Kallerborn, R., Kannan, K., Murano, K., & Lam, P. K. S. (2013). Transport of Perfluoroalkyl substances (PFAS) from an arctic glacier to downstream locations: Implications for sources. *Science of The Total Environment*, *447*, 46–55. https://doi.org/https://doi.org/10.1016/j.scitotenv.2012.10.091

Lindstrom, A. B., Strynar, M. J., & Libelo, E. L. (2011). Polyfluorinated compounds: Past, present, and future. *Environmental Science and Technology*. https://doi.org/10.1021/es2011622

Liu, Z., Chen, Z., Gao, J., Yu, Y., Men, Y., Gu, C., & Liu, J. (2022). Accelerated Degradation of Perfluorosulfonates and Perfluorocarboxylates by UV/Sulfite + Iodide: Reaction Mechanisms and System Efficiencies. *Environmental Science & Technology*, *56*(6), 3699–3709. https://doi.org/10.1021/acs.est.1c07608

Mahinroosta, R., & Senevirathna, L. (2020). A review of the emerging treatment

technologies for PFAS contaminated soils. *Journal of Environmental Management*, *255*, 109896. https://doi.org/10.1016/j.jenvman.2019.109896

Möller, A., Ahrens, L., Surm, R., Westerveld, J., van der Wielen, F., Ebinghaus, R., & de Voogt, P. (2010). Distribution and sources of polyfluoroalkyl substances (PFAS) in the River Rhine watershed. *Environmental Pollution*, *158*(10), 3243–3250. https://doi.org/https://doi.org/10.1016/j.envpol.2010.07.019

O'Connor, N., Patch, D., Noble, D., Scott, J., Koch, I., Mumford, K. G., & Weber, K. (2023). Forever no more: Complete mineralization of per- and polyfluoroalkyl substances (PFAS) using an optimized UV/sulfite/iodide system. *The Science of the Total Environment*, *888*, 164137. https://doi.org/10.1016/j.scitotenv.2023.164137

Olsen, G. W., Mair, D. C., Lange, C. C., Harrington, L. M., Church, T. R., Goldberg, C. L., Herron, R. M., Hanna, H., Nobiletti, J. B., Rios, J. A., Reagen, W. K., & Ley, C. A. (2017). Per- and polyfluoroalkyl substances (PFAS) in American Red Cross adult blood donors, 2000-2015. *Environmental Research*, *157*, 87–95. https://doi.org/10.1016/j.envres.2017.05.013

Paul, A. G., Jones, K. C., & Sweetman, A. J. (2009). A First Global Production, Emission, And Environmental Inventory For Perfluorooctane Sulfonate. *Environmental Science & Technology*, *43*(2), 386–392. https://doi.org/10.1021/es802216n

Pelch, K. E., Reade, A., Wolffe, T. A. M., & Kwiatkowski, C. F. (2019). PFAS health effects database: Protocol for a systematic evidence map. *Environment International*, *130*, 104851. https://doi.org/https://doi.org/10.1016/j.envint.2019.05.045

Phong Vo, H. N., Ngo, H. H., Guo, W., Hong Nguyen, T. M., Li, J., Liang, H., Deng, L., Chen, Z., & Hang Nguyen, T. A. (2020). Poly-and perfluoroalkyl substances in water and wastewater: A comprehensive review from sources to remediation. *Journal of Water Process Engineering*, *36*, 101393. https://doi.org/https://doi.org/10.1016/j.jwpe.2020.101393

Prevedouros, K., Cousins, I. T., Buck, R. C., & Korzeniowski, S. H. (2006). Sources, fate and transport of perfluorocarboxylates. In *Environmental Science and Technology*. https://doi.org/10.1021/es0512475

Quiñones, O., & Snyder, S. A. (2009). Occurrence of perfluoroalkyl carboxylates and sulfonates in drinking water utilities and related waters from the United States. *Environmental Science & Technology*, *43*(24), 9089–9095. https://doi.org/10.1021/es9024707

Shih, Y.-H., Blomberg, A. J., Bind, M.-A., Holm, D., Nielsen, F., Heilmann, C.,

Weihe, P., & Grandjean, P. (2021). Serum vaccine antibody concentrations in adults exposed to per- and polyfluoroalkyl substances: A birth cohort in the Faroe Islands. *Journal of Immunotoxicology*, *18*(1), 85–92. https://doi.org/10.1080/1547691X.2021.1922957

Shih, Y.-H., Blomberg, A. J., Jørgensen, L. H., Weihe, P., & Grandjean, P. (2022). Early-life exposure to perfluoroalkyl substances in relation to serum adipokines in a longitudinal birth cohort. *Environmental Research*, *204*, 111905. https://doi.org/https://doi.org/10.1016/j.envres.2021.111905

Stoiber, T., Evans, S., & Naidenko, O. V. (2020). Disposal of products and materials containing per- and polyfluoroalkyl substances (PFAS): A cyclical problem. *Chemosphere*, *260*, 127659. https://doi.org/10.1016/j.chemosphere.2020.127659

Wang, Z., Cousins, I. T., Scheringer, M., Buck, R. C., & Hungerbühler, K. (2014). Global emission inventories for C4-C14 perfluoroalkyl carboxylic acid (PFCA) homologues from 1951 to 2030, Part I: production and emissions from quantifiable sources. *Environment International*, *70*, 62–75. https://doi.org/10.1016/j.envint.2014.04.013

Watanabe, N., Takata, M., Takemine, S., & Yamamoto, K. (2018). Thermal mineralization behavior of PFOA, PFHxA, and PFOS during reactivation of granular activated carbon (GAC) in nitrogen atmosphere. *Environmental Science and Pollution Research*, *25*(8), 7200–7205. https://doi.org/10.1007/s11356-015-5353-2

Watanabe, N., Takemine, S., Yamamoto, K., Haga, Y., & Takata, M. (2016). Residual organic fluorinated compounds from thermal treatment of PFOA, PFHxA and PFOS adsorbed onto granular activated carbon (GAC). *Journal of Material Cycles and Waste Management*, *18*. https://doi.org/10.1007/s10163-016-0532-x

Zacs, D., & Bartkevics, V. (2016). Trace determination of perfluorooctane sulfonate and perfluorooctanoic acid in environmental samples (surface water, wastewater, biota, sediments, and sewage sludge) using liquid chromatography - Orbitrap mass spectrometry. *Journal of Chromatography. A*, *1473*, 109–121. https://doi.org/10.1016/j.chroma.2016.10.060

Zhang, D. Q., Zhang, W. L., & Liang, Y. N. (2019). Adsorption of perfluoroalkyl and polyfluoroalkyl substances (PFASs) from aqueous solution - A review. *The Science of the Total Environment*, *694*, 133606. https://doi.org/10.1016/j.scitotenv.2019.133606

Zhang, J., Hu, L., & Xu, H. (2024). Dietary exposure to per- and polyfluoroalkyl substances: Potential health impacts on human liver. *Science of The Total*

Environment, *907*, 167945. https://doi.org/https://doi.org/10.1016/j.scitotenv.2023.167945

Zhang, X., Xue, L., Deji, Z., Wang, X., Liu, P., Lu, J., Zhou, R., & Huang, Z. (2022). Effects of exposure to per- and polyfluoroalkyl substances on vaccine antibodies: A systematic review and meta-analysis based on epidemiological studies. *Environmental Pollution*, *306*, 119442. https://doi.org/https://doi.org/10.1016/j.envpol.2022.119442

2 Chapter 2: Literature Review

2.1 Per- and Polyfluoroalkyl Substances (PFAS)

PFAS represent a large group of fluorinated polymers and non-polymers (Figure 2-1). These two classes of PFAS are broken down into subclasses, for which there are groups and sub-subgroups. Each sub-subgroup consists of many individual homologous members and isomers. At the time of writing, there are 14,735 individual PFAS listed on the USEPA's CompTox Chemicals Dashboard (v2.4.1, accessed October 8, 2024). Depending on the specific definition used for PFAS, it is estimated that over 38,000 PFAS molecules have been identified, with the list continuing to grow daily (Buck et al., 2021; Lea et al., 2022; Williams et al., 2022).

On the non-polymer side, the difference between the per- and polyfluoralkyl substances subclasses is that perfluoroalkyl substances have had all the hydrogen atoms replaced with fluorine atoms, while in polyfluoroalkyl substances, only some of the hydrogen atoms (not all) have been replaced with fluorine atoms. In many of the industrial and commercial applications in which they are used, the perfluoroalkyl substances are superior to the polyfluoroalkyl substances because of their enhanced chemical properties in three unique areas:

1. The carbon-fluorine bond is very strong in comparison to the carbon-hydrogen bond (O'Hagan, 2008). In fact, the carbon-fluorine bond is considered to be the strongest single bond in organic chemistry and second only to the silicon-fluorine bond as the strongest single bond for any pair of atoms. The carbon-fluorine bond also strengthens and shortens as more fluorine is added to the same carbon. Complete coverage of the carbon chain renders perfluoroalkyl substances more resistant to oxidation, microbial degradation, digestion and hydrolysis, and to photodegradation as the carbon chain becomes more difficult to access and break apart.
2. The fluorocarbon tail is hydrophobic (similar to most hydrocarbon compounds), meaning that water is not attracted to the molecule; therefore, perfluoroalkyl substance coatings tend to be water-repellent.
3. Many perfluoroalkyl substances are also lipophobic (or oleophobic) (J P Giesy et al., 2006); that is, they are not soluble in lipids or other non-polar solvents.

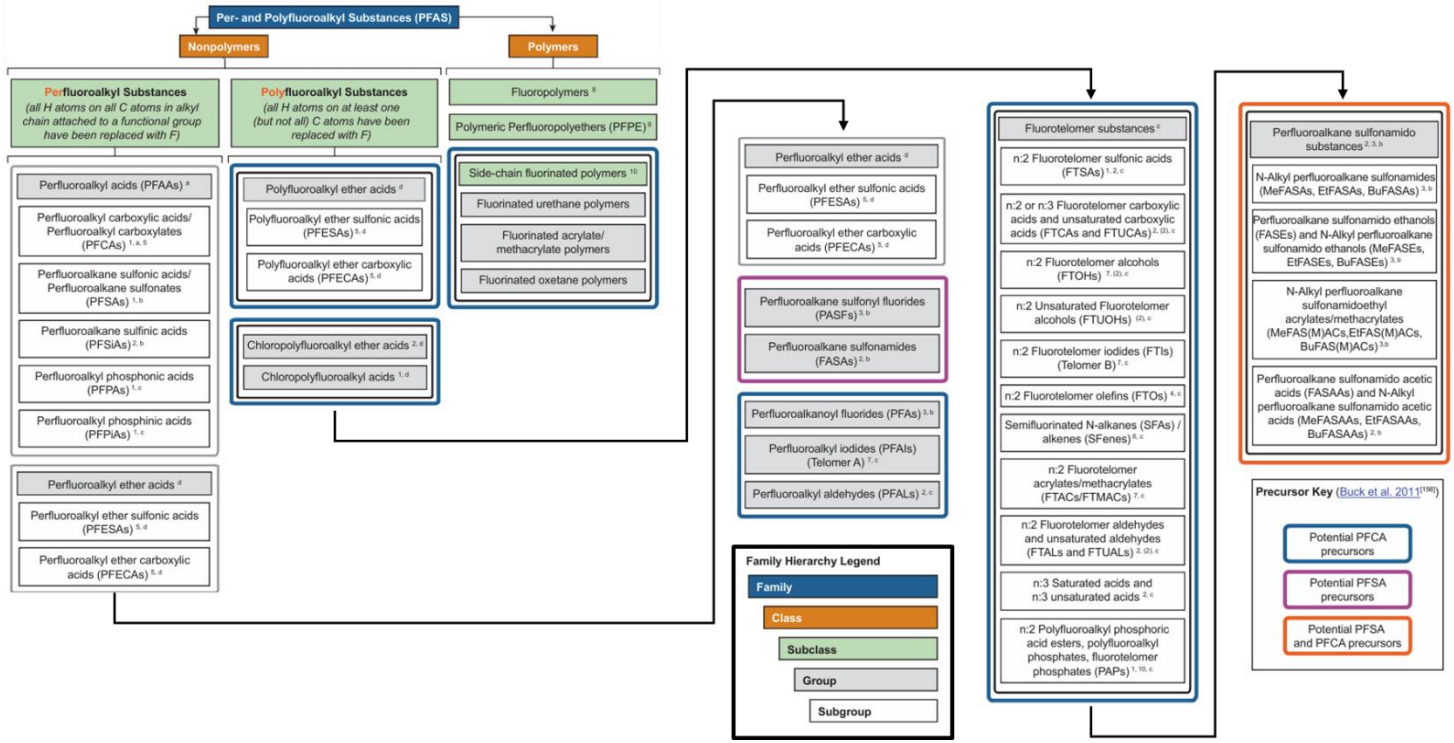

Figure 2-1: The PFAS family tree (modified from the Interstate Technology & Regulatory Council (ITRC) PFAS Technical and Regulatory Guidance Document and Fact Sheets (2021)).

The combination of hydrophobic and lipophobic is unusual, since hydrophobic compounds tend to interact similarly through weak dispersion forces, and usually mix with non-polar solvents without phase separation. These interactions are dominated by weak London dispersion forces, which have their origin in the polarizability of the hydrocarbon framework. In the case of many perfluoroalkyl substances, either the strong carbon-fluorine bond dipole or their substitution with charged or dipolar groups promotes strong interactions amongst the perfluoroalkyl substances themselves that are even able to displace other hydrocarbons. Perfluoroalkyl substances are therefore unique, as they fall into a small class of compounds that dissolve equally poorly in both water and non-polar solvents.

In Figure 2-2, the chemical structure of nine perfluoroalkyl carboxylic acids (PFCAs), three perfluoroalkyl sulfonic acids (PFSAs), and perfluorooctanesulfonamide (PFOSA), a perfluoroalkane sulphonamide (FASA), are shown. For the PFCAs, these are perfluorobutanoate (PFBA), perfluoropentanoate (PFPeA), perfluorohexanoate (PFHxA), perfluoroheptanoate (PFHpA), perfluorooctanoic acid (PFOA), perfluorononanoate (PFNA), perfluorodecanoate (PFDA), perfluoroundecanoate (PFUnA) and perfluorododecanoate (PFDoA). For the PFSAs, these are perfluorobutane sulfonate (PFBS), perfluorohexane sulfonate (PFHxS) and perfluorooctane sulfonate (PFOS). The first two groups are characterized by the carboxylate (CO_2^-) and sulfonate (SO_3^-) functional end groups, respectively. PFOSA, the FASA, has a sulfonamide (SO_2NH_2) functional end group. Although other PFCAs and PFSAs exist (in addition to other PFAS in general), these compounds have formed the backbone of analytical suites since PFAS started being tested commercially through LC-MS/MS.

Notably, PFOA and PFHxS are listed under Annex A, and PFOS is listed under Annex B, of the Stockholm Convention for Persistent Organic Pollutants (POPs). In Canada, risk management controls were enacted by prohibiting the manufacture, use, sale, offer for sale, and import of PFOS, PFOA, long-chain PFCAs, and their salts and precursors under the Prohibition of Certain Toxic Substances Regulations; however, it was observed that shorter-chain PFAS and/or PFAS from other groups started to be used as substitutes following the implementation of regulatory restrictions on the latter (Government of Canada, 2024).

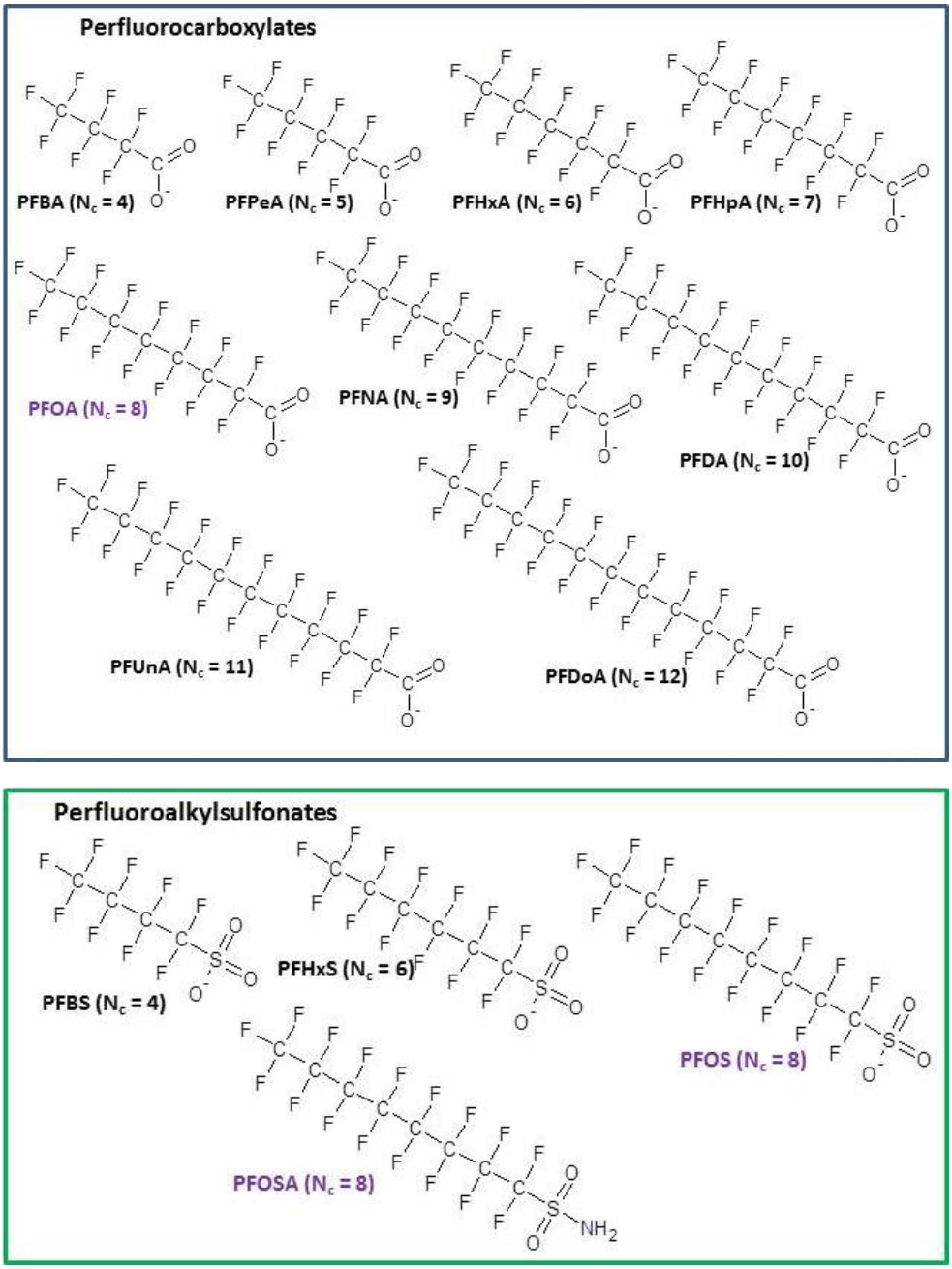

Figure 2-2: Identity and chemical structure of 13 PFAS commonly analyzed at commercial laboratories.

The functional head-groups and carbon chain length of the molecules affect the chemical and physical properties. For example, acidic functional groups like carboxylate (CO_2^-) and sulfonate (SO_3^-) generally exist as anions (i.e., the hydrogen is removed) under normal environmental conditions of approximately neutral pH; thus, the end of the molecule with the anionic group is water-soluble. Water solubility and volatility decrease with increasing carbon numbers (Bhhatarai & Gramatica, 2011; Dreyer et al., 2009; Stock et al., 2004; Thuens et al., 2008). The functional head-group and the carbon chain length also impact the distribution coefficient (K_d), a factor relating the partitioning of a contaminant between the solid and aqueous phases, the organic carbon partitioning coefficient (K_{oc}), the dissolved organic carbon partitioning coefficient (K_{doc}), the octanol-water partitioning coefficient (K_{ow}) and biological absorption measures like bioaccumulation factors (BAFs), reflecting uptake from all sources, and bioconcentration factors (BCFs), which refer to direct uptake from water. These measures all increase with increasing carbon numbers (Awad et al., 2011; Bhhatarai & Gramatica, 2011; Carmosini & Lee, 2008; Higgins & Luthy, 2007; P. Jing et al., 2009; J. Liu & Lee, 2007; Rayne & Forest, 2009; Sepulvado et al., 2011).

PFAS that have acidic (i.e., negatively charged) functional end groups are also surfactants. Surfactants are organic compounds that have both a hydrophobic and a hydrophilic end to the molecule and lower the surface tension of a liquid, or the interfacial tension between two liquids, or between a liquid and a solid. With respect to PFAS, the carbon-fluorine chain represents the hydrophobic end of the molecule and the anionic functional end group represents the hydrophilic end. The extent of fluorination and location of the fluorine atoms affect the surfactant properties, but in general, PFAS excel in lowering aqueous surface tensions at very low concentrations, in addition to being excellent wetting and levelling agents, emulsifiers, foaming agents and dispersants (Kissa, 2001; Taylor, 1999). PFOS was the originally intended compound used in these types of applications.

Rayne & Forest (2009) state that PFCAs and PFSAs generally have $K_{oc}>1$, indicating that they would accumulate in soils and sediments and be removed to some extent from groundwater. With calculated log K_{oc} values generally between 2 and 3 (Higgins & Luthy, 2007), which are substantially lower than those for other POPs, it would be unlikely that PFOS and PFOA would be removed from water to a significant extent by organic carbon sources like those in waste water treatment facility sludge (Y. Jing & Jiangyong, 2011). Log K_{ow} has historically been difficult to measure for PFAS because they can form multiple layers within water and octanol. Log K_{ow} values were estimated potentiometrically for PFCAs with four to nine carbons in the chain, which gave a range of values from -1 to 2 for PFOS. Notably, these are all substantially lower values than those for polychlorinated biphenyls (PCBs), another group of well-studied POPs, which have log K_{ow} of 4.7–6.8 (ATSDR, 2021; Hawthorne et al., 2011).

The toxicity of PFAS has been studied to the largest extent for PFOS and PFOA and has been presented in several Health Canada reviews (Government of Canada, 2012; Health Canada, 2006, 2010, 2013). In general, many PFAS have high uptake by animals (Stock et al., 2010); however, unlike other POPs, they do not accumulate in lipids but rather in the liver, blood serum, and kidneys, through protein binding. Differences are seen in elimination rates between species and also between genders (e.g., elimination rates are faster for rats than for humans and faster for female rats than for male rats) (Stock et al., 2010). The carcinogenicity data for certain PFAS are consistent with United States Environmental Protection Agency (USEPA) guidelines for compounds that are "likely to be carcinogenic to humans" (USEPA, 2024). More generally, PFAS have been linked to several negative health effects, including increases to cholesterol, changes in liver function, reduced vaccination response, neurological/development issues in children, and cancer (Ahrens & Bundschuh, 2014; Caverly Rae et al., 2015; Granum et al., 2013; Shih et al., 2022; X. Zhang et al., 2022).

PFAS were never manufactured in Canada, but they were in the United States (US). Following negotiations between the USEPA and 3M in 2000, a voluntary phase out of PFOS was agreed to over the next two years, which ended PFOS production in the US in 2002. PFOS was later listed as a POP in Annex B (restriction) of the Stockholm Convention in 2009. The USEPA's 2010/2015 PFOA Stewardship Program was initiated in 2006, which was a global stewardship program with the goal of significantly reducing (i.e., by 95 %) PFOA, as well as the PFAS precursors that could break down to PFOA, or related higher homologue chemicals, in both facility emissions and other released media, as well as all manufactured products by 2010, with complete elimination by 2015. PFOA, part of the group of PFAS called perfluorocarboxylic acids (PFCAs), was listed in Annex A (elimination) in 2019. At the 10th meeting of the Conference of the Parties in 2022, PFHxS was listed as a POP. And more recently, the entire PFCA group was made a candidate for listing. Despite this, PFOS, and the other Stockholm Convention PFAS are still produced in several countries, notably Russia, China, and India. Although Western countries may abide by the Convention, many have simply altered their PFAS formulations as each new regulatory restriction was introduced. Thus, PFAS are still present and/or used in AFFF, metal plating, electric and electronic parts, photo imaging, hydraulic fluids, and textiles, for example. These 'modern' PFAS formulations typically include fluorotelomers, such as fluorotelomer sulfonates (FtSs), fluorotelomer alcohols (FtOHs), and fluorotelomer sulfonamido betaines (FtSaBs), perfluoroethers (also known as GenX), and perfluorosulfonamides (FSAs) (Barzen-Hanson & Field, 2015; Gomis et al., 2015; Heydebreck et al., 2015; Rayne & Forest, 2009; Strynar et al., 2015; Wang et al., 2013). The USEPA's 2010/2015 PFOA Stewardship Program created a categorization difference between 'modern' and 'legacy' PFAS formulations. While both types contain PFAS, legacy formulations may contain or degrade into long-chain PFAS (i.e., those with ≥ eight carbon atoms), notably PFOS

or PFOA, while modern formulations will not (they will degrade into short-chain PFAS, which are ≤ six carbon atoms).

With respect to AFFF, formulations are highly variable in terms of the PFAS they contain, as they vary by both manufacturer and by year (Houtz et al., 2013; Place & Field, 2012). A timeline of AFFF manufacture by manufacturer is provided in Figure 2-3 below. The manufacturer of 3M was the sole supplier of AFFF until 1973 and used the electrochemical fluorination (ECF) method, which resulted in formulations that were dominantly PFOS, with lesser concentrations of other PFAS. Beginning in 1973, other companies started manufacturing AFFF using the telomerization method; this created AFFF formulations that were primarily fluorotelomers, which can break down in the environment (a process called transformation) into terminal PFAS (PFCAs and PFSAs). Because of this, they are also known as PFAS precursors. FFTAs that operated for many years would have been exposed to many different formulations resulting in a multitude of PFAS being present (Table 2-1).

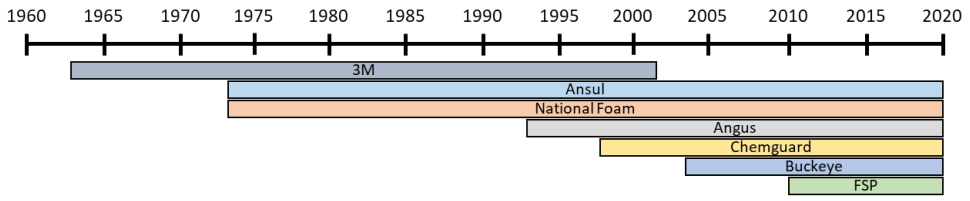

Figure 2-3: Timeline of AFFF manufacture by various manufacturers (modified from Place and Field 2012).

Table 2-1: Concentrations of PFAS (g/L) found in various commercial AFFF formulations over the years (from Houtz et al 2013).

	Precursors (g/L)						Perfluorinated sulfonates (g/L)				Perfluorinated Carboxylates (g/L)				
Formulation and Year	PFBSAm[a]	PFPeS-Am[a]	PFHxS-Am[a]	PFBS-AmA[a]	PFPeS-AmA[a]	PFHxS-AmA[a]	PFBS	PFHxS	PFHpS	PFOS	PFBA	PFPeA	PFHxA	PFHpA	PFOA
3M 1988			0.4				0.1	1.4	0.3	11		0.3	0.1		0.1
3M 1989	0.1		1.1			0.1	0.1	0.9	0.2	11		0.5	0.3		0.1
3M 1992	0.9	0.6	4.8	1.0	0.4	2.2	0.0	0.5	0.1	5.1		0.2	0.1		0.1
3M 1993	1.3	0.8	5.1	1.3	0.6	2.7	0.1	0.6	0.1	5.6		0.3	0.1		0.1
3M 1993	0.7	0.5	3.0	1.1	0.6	2.4	0.0	0.6	0.1	5.3		0.2	0.1		0.1
3M 1998	1.3	0.9	4.7	1.4	0.6	2.6	0.1	0.8	0.1	5.7		0.5	0.1		0.1
3M 1998	1.1	0.8	5.1	1.3	0.5	2.6	0.0	0.7	0.1	4.9		0.1	0.1		0.1
3M 1999	0.8	0.6	3.8	1.2	0.5	2.5	0.1	0.6		4.9		0.2	0.1		0.1
3M 2001	0.6	0.5	4.2	1.5	0.7	3.6	0.2	1.0	0.1	8.0		0.5	0.2		0.1
	6:2 FtTAoS[b]	8:2 FtTAoS[c]													
Chemguard 2008	17														
Chemguard 2010	21														
Ansul 1986	9	3.1													
Ansul 1987	10	2.7													
Ansul 2009	18														
Ansul 2010	10														
	5:1:2 FtB[b]	7:1:2 FtB[b]	9:1:2 FtB[b]	5:3 FtB[b]	7:3 FtB[b]	9:3 FtB[b]									
Buckeye 2009	2.3	4.3	1.4	0.6	1.0	0.3									
	6:2 FtSaB[b]	8:2 FtSaB[c]	10:2 FtSaB[c]	6:2 FtSaAm[b]	6:2 FtS	8:2 FtS									
National Foam 2005	7.0	0.5	0.1	1.8	0.2	0.0									
National Foam 2005	4.8	0.3	0.0	0.4	0.1	0.0									
National Foam 2008	7.5	0.5	0.0	1.4	0.2	0.0									

[a] These compounds were quantified using the precursor oxidation assay as described earlier.
[b] These compounds were quantified using the reference materials provided by the Fire Fighting Foam Coalition
[c] These compounds were quantified using the calibration of an alternate analyte as described earlier.

Despite the large number of PFAS in existence, less than 50 PFAS can easily be quantified. These are referred to as target PFAS (e.g., PFOS). Others, referred to as non-target PFAS (e.g., 6:2 FtOH), can only be semi-quantified because there are no readily available reference standards. Further, some PFAS are charged and can be anionic (e.g., perfluoroalkyl acids (PFAAs) and fluorotelomer sulfonates (FtSs)), cationic (e.g., perfluoroalkyl sulfonamido amines (PFSaAms)), or zwitterionic (e.g., fluorotelomer betaines (FtBs) and fluorotelomer sulfonamido betaines (FtSaBs)), while several classes of PFAS are neutral and / or volatile, which makes them unable to be detected using standard liquid chromatography-mass spectrometry (LC-MS) techniques (Rehman et al., 2023). Mass balance studies on abiotic and biotic samples using fluorine have shown that a large proportion of the extractable organic fluorine (EOF) (15 to 99 %) remains unidentified (Y. Liu et al., 2015). While extensive progress has been made in analyzing PFAS over the years, achieving complete characterization remains elusive unless multiple techniques are used, not all of which are readily available or affordable, and all requiring extensive operator experience and expertise.

The most common pathway of PFAS exposure for humans is through drinking water, and regulatory values are extremely low. Canada has recently established a drinking water quality objective for PFAS of 30 ng/L as the sum total of 25 individual PFAS (Health Canada, 2024). In Europe, total PFAS in drinking water is limited at 500 ng/L, with individual PFAS limited at 100 ng/L (Sadia et al., 2023). And in the

United States, the USEPA set Maximum Contaminant Levels for PFOS / PFOA at 4 ng/L, PFHxS, PFNA, and hexafluoropropylene oxide dimer acid (HFPO-DA) at 10 ng/L, and a hazard index of 1 (unitless) for mixtures of PFHxS, PFNA, HFPO-DA, and PFBS under the Clean Water Act (United States Environmental Protection Agency, 2024). At these extremely low levels, PFAS-free soil becomes critical; otherwise, any associated PFAS will leach to groundwater and surface water, which may be a drinking water source. Comparing the levels of PFOS, PFOA, PFHxS, and PFNA in various global environmental media (i.e., rainwater, soils, and surface waters), Cousins et al. (2024) concluded that the levels of PFOS and PFOA in rainwater are often greater than the USEPA's Lifetime Drinking Water Health Advisory levels; the sum of PFOS, PFOA, PFHxS, and PFNA in rainwater is often above the Danish drinking water limit value (2 ng/L); PFOS in rainwater is often above the Environmental Quality Standard for Inland European Union Surface Water (0.65 ng/L); and atmospheric deposition also leads to global soils being ubiquitously impacted, often above the proposed Dutch soil guideline values (>0.1 μg/kg dry weight (dw) of either PFOS or PFOA). Based on this, it was concluded that the global spread of these four PFAAs in the atmosphere has led to the planetary boundary for chemical pollution being exceeded (Cousins et al., 2022).

2.2 Mechanochemistry

Mechanochemistry is broadly defined as chemical reactivity induced by external mechanical energy. This typically comes in the form of friction, impact, collision, or grinding. Thus, mechanochemistry has been used by humans throughout their entire existence, likely beginning with the discovery of fire by rubbing two sticks together (creating heat through friction), or by striking iron with a flint (impact / collision). Grinding can also be traced back to the Stone Age through the use of the traditional mortar and pestle, which was used to prepare foodstuffs, and treat other types of materials, such as minerals, paints, and medicines (Lynch & Rowland, 2005). Because of this, grinding can be regarded as the first engineering technology by humans (Takacs, 2013).

The first documented mechanical reaction is attributed to Theophrastus of Eresus, student of Aristotle and his successor as head of the Lyceum, the Peripatetic school of philosophy in Athens, Greece. He wrote a short booklet titled "On Stones" in about 315 B.C.E. (Before Current Era) that describes the extraction of mercury by grinding cinnabar in a copper mortar in the presence of vinegar (Takacs, 2000, 2013). (Interestingly, Takacs (2000) also points out that this work happens to be the earliest surviving document related to chemistry.)

While no other reference to mechanochemical processes has been found in historical records before the 19th century, its importance throughout history is well known, as

grinding and milling was the main process behind the working of agricultural grains (e.g. to make flour) and the extraction of minerals and ores, as well as the creation of building materials, pharmaceuticals, and black powder, for example (Takacs, 2013). Grinding for transformation processes was also the basis behind alchemy (Marchini et al., 2024), the medieval chemical science that sought to change less valuable metals into gold, discover a single cure for all diseases, and everlasting life. To this point, in a paper published in 1820 by Michael Faraday, the English physicist and chemist who contributed to the study of electromagnetism and electrochemistry, the grinding procedure used in the reduction of silver chloride with zinc, tin, iron, and copper in a mortar, was referred to casually as the "dry way" of inducing reactions (Faraday, 1820). This suggests that the induction of a chemical reaction through grinding was a familiar procedure by this time (Takacs, 2013).

The first systematic investigations using mechanochemistry were performed by Spring and Lea at the end of the 19th century (Takacs, 2018), and over the next few decades, mechanochemistry developed slowly, with minerals, inorganic compounds, and polymers being the primary areas of interest (Takacs, 2013). The field became more organized in the 1960s when several large groups were established and the first dedicated conferences were held. By the end of 20th century, interest in mechanochemistry had developed into applications of grinding and milling as a means to conduct environmentally friendly and solvent-free preparations of host-guest inclusion complexes (Stojakovic & MacGillivray, 2017).

Modern mechanochemistry is now tightly associated with supramolecular chemistry, with advances in the latter discipline being credited to mechanochemistry. As a result, recent years have witnessed rapid developments in uses of mechanochemistry to generate complex organic molecules, supramolecular assemblies, and metal-organic frameworks (Stojakovic & MacGillivray, 2017). The invention of the atomic force microscope has provided new ways to manipulate atoms and molecules by direct mechanical action (Takacs, 2013).

Understanding the fundamental nature of mechanochemical reactions is still an ongoing pursuit. Mechanochemical processes are complex and involve multiple length and time scales. They are also system specific, and take place under a broad variety of conditions. Thiessen proposed the first theory, the magma–plasma model, in 1967 (Thiessen, P. A.; Meyer, K.; Heinicke, 1967). Atomic force microscopy, invented in 1986, has been, and remains, a promising tool to address fundamental questions on the scale of atoms and molecules, but macroscopic experimental investigations, empirical models, and the characterization of mechanically activated materials are also pursued, as they remain important sources of information (Takacs, 2013). Computer simulation is also becoming an increasingly important component

of theoretical investigations, from modelling the macroscopic operation of milling devices to molecular dynamics and quantum chemical calculations on deformed molecules (Takacs, 2013).

2.2.1 Ball Mills

The most important tool of practical mechanochemistry is the ball mill. A ball mill is a device that breaks solid materials into finer sizes via the impact and frictional forces that are created when the mill is rotated. A mill is typically made up of a cylindrical shell and grinding media is often included to assist in this action, typically steel balls (Figure 2-4). They can be operated in continuous or batch operation, wet or dry. In a typical wet, continuous operation, water is added to the feed to produce a slurry, and the slurry is allowed to overflow out of the mill at the discharge end where particle size can be classified with a screen or a hydrocyclone. Coarse fractions can be returned back to the mill, with fines being the final product. Water is typically used to ease material transport and reduce dust. Dry grinding means that when the material is ground to a required particle size, the material will be fed into and removed from the mill without the use of water. In continuous, dry grinding operations, an air swept system is used to remove fine material from the mill as it is produced.

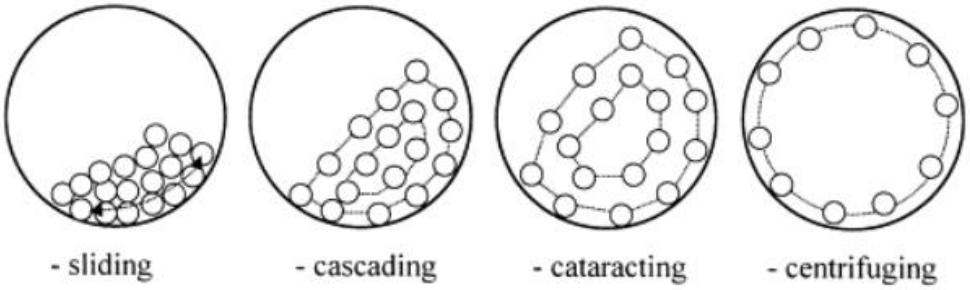

Figure 2-4: Modes of ball motions with rotational speed in a cylindrical shell (from Hong and Kim, 2002).

Parameters that influence the grinding of material include:

- mill speed, which is determined as a percentage of the critical speed (N_c) (the speed at which the centrifugal forces equal gravitational forces, which keeps that ball on the outside wall of the cylinder through full rotation rather than falling),

- ball filling ratio (ball to internal mill volume) (J),
- powder filling ratio (f_c) (ball to solid material weight ratio; only valid in batch milling),
- ball size distribution (%) (controlled in a batch milling setup), and,
- grinding residence time (in minutes).

The mill critical speed is a function of the internal grinding mill diameter (D) and is shown in equation 1 (Bond & Company, 1961).

$$\text{Eq. 1: } Nc = 42.3 \,/\, \sqrt{([D]\,)}$$

The ball filling ratio is determined by the mass and density of the grinding media ratio to the milling volume and is outlined in equation 2 (Cayirli, 2018).

$$\text{Eq. 2: } J = (mass\ of\ balls \,/\, ball\ density) \,/\, mill\ volume \times (1.0 \,/\, 0.64)$$

The powder filling ratio follows a similar formula, shown in equation 3, but is a factor of the materials mass and density ratio to the milling volume (Cayirli, 2018).

$$\text{Eq. 3: } fc = (mass\ of\ powder \,/\, powder\ density) \,/\, mill\ volume \times (1.0 \,/\, 0.64)$$

When ball mill grinding is being completed efficiently, where the factors of speed, powder and grinding media filling ratios are optimized, the breakage rate of any given size fraction typically follows a first order equation where the rate of breakage of a given size fraction i, is equal to the product of the total weight W, times the specific weight fraction w_i, times the rate of breakage constant S_i of the given size fraction (equation 4) (Austin & Bagga, 1981).

$$\text{Eq. 4: } i = S_i w_i W$$

Grinding residence times are utilized to control the final energy transferred from the mill to the media and then to the material to be ground based upon the discussed parameters to achieve a specific final material target size. When size reduction of the material is the governing mechanism, then these standard equations apply; however, energy requirements will also vary with the material to be ground. The characteristics of the material that will have an impact on the milling performance are material hardness, moisture content, feed particle size distribution, and target product size distribution. Because of this, material-specific optimization is required, which, in principle, necessitates experimentation. In practice, sufficient knowledge has now been gained from experience that for common materials, experimentation is no longer required.

Ball mills are available in a wide variety of configurations and sizes. A common benchtop laboratory version is a planetary ball mill (PBM), which is named for the planet-like movement of the cylinder on a sun-wheel or planetary disk (Figure 2-5). In this type of setup the contents inside the cylinder (maximum size is typically 0.5 L or smaller) experience both rotary motion around the sun-wheel axis (Ω) and planetary motion around the cylinder's axis (ω). The PBM uses the principle of centrifugal acceleration over gravitational acceleration to achieve an enhanced force as a result of the two centrifugal fields. This creates a very high energy milling environment, capable of achieving accelerations of 50–100 g (g = gravity, 9.81 m/s^2), as well as an energy density 100–1,000 times that of conventional (i.e., one axis of rotation) milling equipment (Fokina et al., 2004).

Over the last two decades ball milling has been used successfully to remediate other POPs (Aresta et al., 2003, 2004; Birke et al., 2006; Cao et al., 1999; Hall et al., 1996; Intini et al., 2007; Korolev et al., 2003; Monagheddu et al., 1999; J. H. Yan et al., 2007; K. Zhang et al., 2012; W. Zhang et al., 2014), including PFAS (Cagnetta et al., 2017; Turner et al., 2021; X. Yan et al., 2015; K. Zhang et al., 2013, 2016). The mechanism of destruction is mechanical force (e.g., grinding, shearing or impacts), which initiates chemical reactions that lead to the breakup of the targeted pollutants (Friščić, 2018; Loiselle et al., 1997; Nah et al., 2008; Sui et al., 2018). More specifically, the environment created by a rotating ball mill promotes reactivity and surface chemistry states (e.g., surface plasma generation, piezoelectric effects, and high energy emission of electrons, ions, radicals, neutral particles, and photons) that are not attainable in ambient conditions, with excitation periods (a process where molecules absorb energy, and their electrons are promoted temporarily to a higher state of energy) of around 10^{-7} seconds (Kajdas, 2005; Kaupp, 2009; Marinescu et al., 2013).

The limitations with the aforementioned studies is that they all used PBMs, for which scale-up to industrial levels required for the remediation of many tonnes of impacted soil is not feasible. Conversely, large-scale HBMs are readily available, being prevalent in the mining, metallurgy, and agricultural industries. If HBMs were shown to be equally capable of remediating PFAS, a field-capable remedial technology would instantly be available. The variously-sized HBMs used for the work conducted as part of this thesis are presented in Figure 2-6, Figure 2-7, and Figure 2-8.

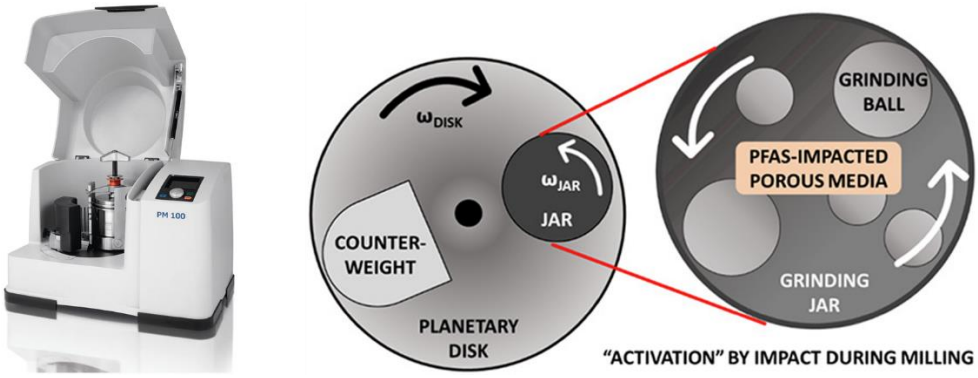

Figure 2-5: A Retsch PM 100 bench top PBM (https://www.retsch.com/products/milling/ball-mills/planetary-ball-mill-pm-100/) and the principle of motion (modified from Turner et al., 2020).

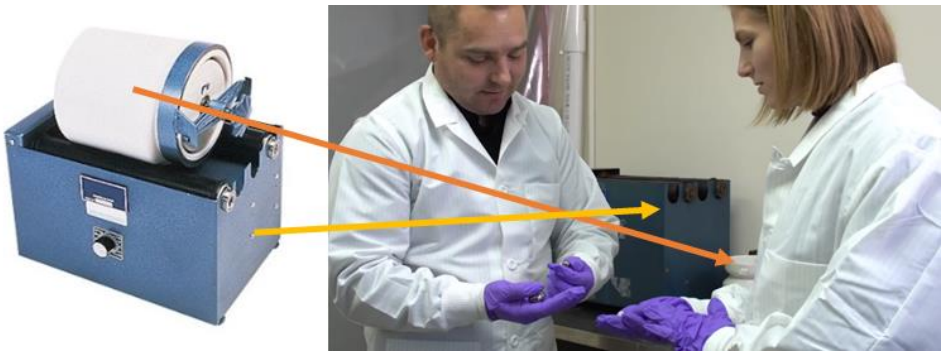

Figure 2-6: A U.S. Stoneware general utility unitized HBM with 1 L ceramic cylinder. Photo at right for sense of scale.

Figure 2-7: A U.S. Stoneware 3-tier long roll HBM (model #803DVM) with 25 L stainless steel cylinder. Photo at right for sense of scale.

Figure 2-8: A Titan Process Equipment Ltd. custom process HBM with 267 L cylinder with and without the protective cage. Photo at right for sense of scale.

Co-milling reagents are often used in ball milling to further enhance the desired reactivity and surface chemistry states. Among the variety of co-milling reagents explored for the destruction of PFAS (e.g., CaO, KOH, Al_2O_3, La_2O_3, ferrate, persulfate, and SiO_2), KOH has emerged as the most successful (Ateia et al., 2021; Lu et al., 2017; Turner et al., 2021; K. Zhang et al., 2013), as it provides a potassium ion for free fluoride to form soluble potassium fluoride (KF) (Ateia et al., 2021; Turner et al., 2021; K. Zhang et al., 2013), which can be measured for mass balance calculations, thereby proving PFAS defluorination/destruction (i.e., severing of the C-F bonds). It is critical that the resulting fluorinated molecule be soluble so that it can be picked up in subsequent free fluoride analyses. In this sense, KOH may not be the best reagent to aid in the destruction of PFAS, but it allows the greatest recovery of the fluorine to prove destruction. Calcium and silicon, for example, create stronger attractions for fluorine, but the resulting molecules are insoluble and not picked up in free fluoride analysis.

Ball milling stands out as a remedial option when considering not just feasibility, but sustainability; it can be performed at environmental temperatures and pressures, and does not require harsh solvents, which allows it to be classified as a green technology (Wieczorek-Ciurowa & Gamrat, 2007). In this thesis, the term "destruction" is only used if corresponding free fluoride analysis is available, as this is the only way to confirm that defluorination was indeed achieved. Otherwise, transformation can take one PFAS and alter it into another with little to no severing of the C-F bonds. Despite the analytical elimination of the original PFAS, this is not PFAS destruction. Therefore, in the absence of free fluoride data, the term degradation is used.

2.3 Chapter 2 References

Ahrens, L., & Bundschuh, M. (2014). Fate and effects of poly- and perfluoroalkyl substances in the aquatic environment: A review. *Environmental Toxicology and Chemistry*, *33*(9), 1921–1929. https://doi.org/https://doi.org/10.1002/etc.2663

Aresta, M, Caramuscio, P., De Stefano, L., & Pastore, T. (2003). Solid state dehalogenation of PCBs in contaminated soil using NaBH4. *Waste Management*, *23*(4), 315–319. https://doi.org/https://doi.org/10.1016/S0956-053X(03)00029-1

Aresta, Michele, Dibenedetto, A., Fragale, C., & Pastore, T. (2004). High-energy milling to decontaminate soils polluted by polychlorobiphenyls and atrazine. *Environmental Chemistry Letters* , *2*(1), 1–4. https://doi.org/10.1007/s10311-003-0057-0

ATSDR. (2021). *Toxicological Profile for Perfluoroalkyls - Release May 2021*. https://www.atsdr.cdc.gov/toxprofiles/tp200.pdf

Austin, L. G., & Bagga, P. (1981). An analysis of fine dry grinding in ball mills. *Powder Technology*, *28*(1), 83–90. https://doi.org/https://doi.org/10.1016/0032-5910(81)87014-3

Awad, E., Zhang, X., Bhavsar, S. P., Petro, S., Crozier, P. W., Reiner, E. J., Fletcher, R., Tittlemier, S. A., & Braekevelt, E. (2011). Long-Term Environmental Fate of Perfluorinated Compounds after Accidental Release at Toronto Airport. *Environmental Science & Technology*, *45*(19), 8081–8089. https://doi.org/10.1021/es2001985

Barzen-Hanson, K. A., & Field, J. A. (2015). Discovery and Implications of C2 and C3 Perfluoroalkyl Sulfonates in Aqueous Film-Forming Foams and Groundwater. *Environmental Science & Technology Letters*, *2*(4), 95–99. https://doi.org/10.1021/acs.estlett.5b00049

Bhhatarai, B., & Gramatica, P. (2011). Prediction of Aqueous Solubility, Vapor Pressure and Critical Micelle Concentration for Aquatic Partitioning of Perfluorinated Chemicals. *Environmental Science & Technology*, *45*(19), 8120–8128. https://doi.org/10.1021/es101181g

Birke, V., Mattik, J., Runne, D., Benning, H., & Zlatovic, D. (2006). Dechlorination of Recalcitrant Polychlorinated Contaminants Using Ball Milling. In V. M. Kolodkin & W. Ruck (Eds.), *Ecological Risks Associated with the Destruction of Chemical Weapons* (pp. 111–127). Springer Netherlands.

Bond, F. C., & Company, A.-C. M. (1961). *Crushing and Grinding Calculations*. Allis-Chalmers Manufacturing Company. https://books.google.ca/books?id=aQUuGwAACAAJ

Buck, R. C., Korzeniowski, S. H., Laganis, E., & Adamsky, F. (2021). Identification and classification of commercially relevant per- and poly-fluoroalkyl substances (PFAS). *Integrated Environmental Assessment and Management*, *17*(5), 1045–1055. https://doi.org/https://doi.org/10.1002/ieam.4450

Cagnetta, G., Zhang, Q., Huang, J., Lu, M., Wang, B., Wang, Y., Deng, S., & Yu, G. (2017). Mechanochemical destruction of perfluorinated pollutants and mechanosynthesis of lanthanum oxyfluoride: A Waste-to-Materials process. *Chemical Engineering Journal*, *316*, 1078–1090. https://doi.org/https://doi.org/10.1016/j.cej.2017.02.050

Cao, G., Doppiu, S., Monagheddu, M., Orrù, R., Sannia, M., & Cocco, G. (1999). Thermal and Mechanochemical Self-Propagating Degradation of Chloro-organic Compounds: The Case of Hexachlorobenzene over Calcium Hydride. *Industrial & Engineering Chemistry Research*, *38*(9), 3218–3224. https://doi.org/10.1021/ie980790+

Carmosini, N., & Lee, L. S. (2008). Partitioning of Fluorotelomer Alcohols to Octanol and Different Sources of Dissolved Organic Carbon. *Environmental Science & Technology*, *42*(17), 6559–6565. https://doi.org/10.1021/es800263t

Caverly Rae, J. M., Craig, L., Slone, T. W., Frame, S. R., Buxton, L. W., & Kennedy, G. L. (2015). Evaluation of chronic toxicity and carcinogenicity of ammonium 2,3,3,3-tetrafluoro-2-(heptafluoropropoxy)-propanoate in Sprague–Dawley rats. *Toxicology Reports*, *2*, 939–949. https://doi.org/https://doi.org/10.1016/j.toxrep.2015.06.001

Cayirli, S. (2018). Influences of operating parameters on dry ball mill performance. *Physicochemical Problems of Mineral Processing*, *54*(3), 751–762. https://doi.org/10.5277/ppmp1876

Cousins, I. T., Johansson, J. H., Salter, M. E., Sha, B., & Scheringer, M. (2022). Outside the Safe Operating Space of a New Planetary Boundary for Per- and Polyfluoroalkyl Substances (PFAS). *Environmental Science & Technology*, *56*(16), 11172–11179. https://doi.org/10.1021/acs.est.2c02765

Dreyer, A., Langer, V., & Ebinghaus, R. (2009). Determination of Octanol−Air Partition Coefficients (KOA) of Fluorotelomer Acrylates, Perfluoroalkyl Sulfonamids, and Perfluoroalkylsulfonamido Ethanols. *Journal of Chemical & Engineering Data*, *54*(11), 3022–3025. https://doi.org/10.1021/je900082g

Faraday, M. (1820). No Title. *Quarterly Journal of Science, Literature and the Arts*, *8*(374).

Fokina, E., Budim, N., Kochnev, V., & Chernik, G. (2004). Planetary mills of periodic and continuous action. *Journal of Materials Science*, *39*, 5217–5221. https://doi.org/10.1023/B:JMSC.0000039213.44891.7d

Friščić, T. (2018). Mechanochemistry in Co-crystal Synthesis. In C. B. Aakeröy & A. S. Sinha (Eds.), *Co-crystals: Preparation, Characterization and Applications* (p. 0). The Royal Society of Chemistry. https://doi.org/10.1039/9781788012874-00147

Giesy, J. P., Mabury, S. A., Martin, J. W., Kannan, K., Jones, P. D., Newsted, J. L., & Coady, K. (2006). Perfluorinated Compounds in the Great Lakes. In R. A. Hites (Ed.), *Persistent Organic Pollutants in the Great Lakes* (pp. 391–438). Springer Berlin Heidelberg. https://doi.org/10.1007/698_5_046

Gomis, M. I., Wang, Z., Scheringer, M., & Cousins, I. T. (2015). A modeling assessment of the physicochemical properties and environmental fate of emerging and novel per- and polyfluoroalkyl substances. *The Science of the Total Environment*, *505*, 981–991. https://doi.org/10.1016/j.scitotenv.2014.10.062

Government of Canada. (2012). *Final Screening Assessment on Perfluorooctanoic Acid (PFOA), its Salts and its Precursors*.

Government of Canada. (2024). *Updated Draft State of Per- and Polyfluoroalkyl Substances (PFAS) Report*.

Granum, B., Haug, L. S., Namork, E., Stølevik, S. B., Thomsen, C., Aaberge, I. S., van Loveren, H., Løvik, M., & Nygaard, U. C. (2013). Pre-natal exposure to perfluoroalkyl substances may be associated with altered vaccine antibody levels and immune-related health outcomes in early childhood. *Journal of Immunotoxicology*, *10*(4), 373–379. https://doi.org/10.3109/1547691X.2012.755580

Hall, A. K., Harrowfield, J. M., Hart, R. J., & McCormick, P. G. (1996). Mechanochemical Reaction of DDT with Calcium Oxide. *Environmental Science & Technology*, *30*(12), 3401–3407. https://doi.org/10.1021/es950680j

Hawthorne, S. B., Grabanski, C. B., Miller, D. J., & Arp, H. P. H. (2011). Improving Predictability of Sediment-Porewater Partitioning Models using Trends Observed with PCB-Contaminated Field Sediments. *Environmental Science & Technology*, *45*(17), 7365–7371. https://doi.org/10.1021/es200802j

Health Canada. (2006). *State of the Science Report for a Screening Health Assessment, Perfluorooctane Sulfonate, Its Salts and Its Precursors that Contain the C8F17SO2 or C8F17SO3 Moiety*.

Health Canada. (2010). *Report on Human Biomonitoring of Environmental Chemicals in Canada: Results of the Canadian Health Measures Survey Cycle 1 (2007–2009)*.

Health Canada. (2013). *Second Report on Human Biomonitoring of Environmental Chemicals in Canada: Results of the Canadian Health Measures Survey Cycle 2 (2009–2011)*.

Health Canada. (2024). *Objective for Canadian Drinking Water Quality Per- and Polyfluoroalkyl Substances*.

Heydebreck, F., Tang, J., Xie, Z., & Ebinghaus, R. (2015). Alternative and Legacy Perfluoroalkyl Substances: Differences between European and Chinese River/Estuary Systems. *Environmental Science & Technology*, *49*(14), 8386–8395. https://doi.org/10.1021/acs.est.5b01648

Higgins, C. P., & Luthy, R. G. (2007). Modeling Sorption of Anionic Surfactants onto Sediment Materials: An a priori Approach for Perfluoroalkyl Surfactants and Linear Alkylbenzene Sulfonates. *Environmental Science & Technology*, *41*(9), 3254–3261. https://doi.org/10.1021/es062449j

Houtz, E. F., Higgins, C. P., Field, J. A., & Sedlak, D. L. (2013). Persistence of Perfluoroalkyl Acid Precursors in AFFF-Impacted Groundwater and Soil. *Environmental Science & Technology*, *47*(15), 8187–8195. https://doi.org/10.1021/es4018877

Intini, G., Cangialosi, F., L.Liberti, D.Lupo, Notarnicola, M., & Pastore, T. (2007). Mechanochemical treatment of contaminated marine sediments for PCB degradation. *Chemistry for Sustainable Development*, *15*, 147–156.

Jing, P., Rodgers, P. J., & Amemiya, S. (2009). High Lipophilicity of Perfluoroalkyl Carboxylate and Sulfonate: Implications for Their Membrane Permeability. *Journal of the American Chemical Society*, *131*(6), 2290–2296. https://doi.org/10.1021/ja807961s

Kajdas, C. K. (2005). Importance of the triboemission process for tribochemical reaction. *Tribology International*, *38*(3), 337–353. https://doi.org/https://doi.org/10.1016/j.triboint.2004.08.017

Kaupp, G. (2009). Mechanochemistry: the varied applications of mechanical bond-breaking. *CrystEngComm*, *11*(3), 388–403. https://doi.org/10.1039/B810822F

Kissa, E. (2001). Fluorinated Surfactants and Repellents: Second Edition, Revised and Expanded Surfactant Science Series. Volume 97. By Erik Kissa (Consultant, Wilmington, DE). Marcel Dekker: New York. 2001. xiv + 616 pp. $195.00. ISBN 0-8247-0472-X. *Journal of the American Chemical Society*, *123*(36), 8882. https://doi.org/10.1021/ja015260a

Korolev, K., Golovanova, A. I., Maltseva, N. N., Lomovskiy, O. I., Salenko, V. L., & Boldyrev, V. V. (2003). Application of mechanical activation to decomposition of toxic chlorinated organic compounds. *Chem. Sustain. Dev.*, *11*, 489–496.

Lea, I. A., Pham, L. L., Antonijevic, T., Thompson, C., & Borghoff, S. J. (2022). Assessment of the applicability of the threshold of toxicological concern for per- and polyfluoroalkyl substances. *Regulatory Toxicology and Pharmacology*, *133*, 105190. https://doi.org/https://doi.org/10.1016/j.yrtph.2022.105190

Liu, J., & Lee, L. S. (2007). Effect of Fluorotelomer Alcohol Chain Length on Aqueous Solubility and Sorption by Soils. *Environmental Science & Technology*, *41*(15), 5357–5362. https://doi.org/10.1021/es070228n

Liu, Y., Pereira, A. D. S., & Martin, J. W. (2015). Discovery of C5–C17 Poly- and Perfluoroalkyl Substances in Water by In-Line SPE-HPLC-Orbitrap with In-Source Fragmentation Flagging. *Analytical Chemistry*, *87*(8), 4260–4268. https://doi.org/10.1021/acs.analchem.5b00039

Loiselle, S., Branca, M., Mulas, G., & Cocco, G. (1997). Selective Mechanochemical Dehalogenation of Chlorobenzenes over Calcium Hydride. *Environmental Science & Technology*, *31*(1), 261–265. https://doi.org/10.1021/es960398s

Lynch, A. J., & Rowland, C. A. (2005). *The History of Grinding*. https://api.semanticscholar.org/CorpusID:136546412

Marchini, M., Montanari, G., Casali, L., Martelli, M., Raggetti, L., Baláž, M., Baláž, P., & Maini, L. (2024). "What makes every work perfect is cooking and grinding": the ancient roots of mechanochemistry. *RSC Mechanochem.*, *1*(1), 123–129. https://doi.org/10.1039/D3MR00035D

Marinescu, I. D., Rowe, W. B., Dimitrov, B., & Ohmori, H. (2013). 16 - Tribochemistry of abrasive machining. In I. D. Marinescu, W. B. Rowe, B. Dimitrov, & H. Ohmori (Eds.), *Tribology of Abrasive Machining Processes (Second Edition)* (Second Edi, pp. 483–517). William Andrew Publishing. https://doi.org/https://doi.org/10.1016/B978-1-4377-3467-6.00016-1

Monagheddu, M., Mulas, G., Doppiu, S., Cocco, G., & Raccanelli, S. (1999). Reduction of Polychlorinated Dibenzodioxins and Dibenzofurans in Contaminated Muds by Mechanically Induced Combustion Reactions. *Environmental Science & Technology*, *33*(14), 2485–2488. https://doi.org/10.1021/es9809206

Nah, I. W., Hwang, K.-Y., & Shul, Y.-G. (2008). Effect of metal and glycol on mechanochemical dechlorination of polychlorinated biphenyls (PCBs). *Chemosphere*, *73*(1), 138–141. https://doi.org/10.1016/j.chemosphere.2008.04.051

O'Hagan, D. (2008). Understanding organofluorine chemistry. An introduction to the C–F bond. *Chem. Soc. Rev.*, *37*(2), 308–319. https://doi.org/10.1039/B711844A

Place, B. J., & Field, J. A. (2012). Identification of novel fluorochemicals in aqueous film-forming foams used by the US military. *Environmental Science and Technology*. https://doi.org/10.1021/es301465n

Rayne, S., & Forest, K. (2009). Perfluoroalkyl sulfonic and carboxylic acids: A critical review of physicochemical properties, levels and patterns in waters and wastewaters, and treatment methods. *Journal of Environmental Science and Health, Part A*, *44*(12), 1145–1199. https://doi.org/10.1080/10934520903139811

Rehman, A. U., Crimi, M., & Andreescu, S. (2023). Current and emerging analytical techniques for the determination of PFAS in environmental samples. *Trends in*

Environmental Analytical Chemistry, *37*, e00198. https://doi.org/https://doi.org/10.1016/j.teac.2023.e00198

Sadia, M., Nollen, I., Helmus, R., ter Laak, T. L., Béen, F., Praetorius, A., & van Wezel, A. P. (2023). Occurrence, Fate, and Related Health Risks of PFAS in Raw and Produced Drinking Water. *Environmental Science & Technology*, *57*(8), 3062–3074. https://doi.org/10.1021/acs.est.2c06015

Sepulvado, J. G., Blaine, A. C., Hundal, L. S., & Higgins, C. P. (2011). Occurrence and Fate of Perfluorochemicals in Soil Following the Land Application of Municipal Biosolids. *Environmental Science & Technology*, *45*(19), 8106–8112. https://doi.org/10.1021/es103903d

Shih, Y.-H., Blomberg, A. J., Jørgensen, L. H., Weihe, P., & Grandjean, P. (2022). Early-life exposure to perfluoroalkyl substances in relation to serum adipokines in a longitudinal birth cohort. *Environmental Research*, *204*, 111905. https://doi.org/https://doi.org/10.1016/j.envres.2021.111905

Stock, N. L., Lau, F. K., Ellis, D. A., Martin, J. W., Muir, D. C. G., & Mabury, S. A. (2004). Polyfluorinated Telomer Alcohols and Sulfonamides in the North American Troposphere. *Environmental Science & Technology*, *38*(4), 991–996. https://doi.org/10.1021/es034644t

Stock, N. L., Muir, D. C. G., & Mabury, S. (2010). Perfluoroalkyl compounds. *Persistent Organic Pollutants*, 25–70.

Stojakovic, J., & MacGillivray, L. R. (2017). 7.05 - Cocrystals and Templates to Control Solid-State [2+2] Photodimerizations. In J. L. Atwood (Ed.), *Comprehensive Supramolecular Chemistry II* (pp. 73–87). Elsevier. https://doi.org/https://doi.org/10.1016/B978-0-12-409547-2.12600-9

Strynar, M., Dagnino, S., McMahen, R., Liang, S., Lindstrom, A., Andersen, E., McMillan, L., Thurman, M., Ferrer, I., & Ball, C. (2015). Identification of Novel Perfluoroalkyl Ether Carboxylic Acids (PFECAs) and Sulfonic Acids (PFESAs) in Natural Waters Using Accurate Mass Time-of-Flight Mass Spectrometry (TOFMS). *Environmental Science & Technology*, *49*(19), 11622–11630. https://doi.org/10.1021/acs.est.5b01215

Sui, H., Rong, Y., Song, J., Zhang, D., Li, H., Wu, P., Shen, Y., & Huang, Y. (2018). Mechanochemical destruction of DDTs with Fe-Zn bimetal in a high-energy planetary ball mill. *Journal of Hazardous Materials*, *342*, 201–209. https://doi.org/https://doi.org/10.1016/j.jhazmat.2017.08.025

Takacs, Laszlo. (2013). The historical development of mechanochemistry. *Chem. Soc. Rev.*, *42*(18), 7649–7659. https://doi.org/10.1039/C2CS35442J

Takacs, Laszlo. (2018). Walthere Spring and his Rivalry with M. Carey Lea. *Bulletin*

for the History of Chemistry, *43*(1).

Takacs, Laszo. (2000). Quicksilver from Cinnabar: The first documented mechanochemical reaction? *JOM Journal of the Minerals, Metals and Materials Society*, *52*, 12–13. https://doi.org/10.1007/s11837-000-0106-0

Taylor, C. K. (1999). Fluorinated surfactants in practice. *Annu Surfactants Rev*, *2*, 271–316.

Thiessen, P. A.; Meyer, K.; Heinicke, G. . (1967). Grundlagen der Tribochemie. *Akademie Verlag*. https://doi.org/https://doi.org/10.1002/maco.19680190219

Thuens, S., Dreyer, A., Sturm, R., Temme, C., & Ebinghaus, R. (2008). Determination of the Octanol−Air Partition Coefficients (KOA) of Fluorotelomer Alcohols. *Journal of Chemical & Engineering Data*, *53*(1), 223–227. https://doi.org/10.1021/je700522f

Turner, L. P., Kueper, B. H., Jaansalu, K. M., Patch, D. J., Battye, N., El-Sharnouby, O., Mumford, K. G., & Weber, K. P. (2021). Mechanochemical remediation of perfluorooctanesulfonic acid (PFOS) and perfluorooctanoic acid (PFOA) amended sand and aqueous film-forming foam (AFFF) impacted soil by planetary ball milling. *Science of The Total Environment*, *765*, 142722. https://doi.org/https://doi.org/10.1016/j.scitotenv.2020.142722

United States Environmental Protection Agency. (2024). *PFAS National Primary Drinking Water Regulation 2024*. https://www.epa.gov/sdwa/and-polyfluoroalkyl-substances-pfas

USEPA. (2024). *EPA Efforts to Reduce Exposure to Carcinogens and Prevent Cancer*. https://www.epa.gov/environmental-topics/epa-efforts-reduce-exposure-carcinogens-and-prevent-cancer#:~:text=For two PFAS – perfluorooctanoic,developed the PFAS Strategic Roadmap.

Wang, Z., Cousins, I. T., Scheringer, M., & Hungerbühler, K. (2013). Fluorinated alternatives to long-chain perfluoroalkyl carboxylic acids (PFCAs), perfluoroalkane sulfonic acids (PFSAs) and their potential precursors. *Environment International*, *60*, 242–248. https://doi.org/10.1016/j.envint.2013.08.021

Wieczorek-Ciurowa, K., & Gamrat, K. (2007). Mechanochemicalsyntheses as an example of green processes. *Journal of Thermal Analysis and Calorimetry*, *88*(1), 213–217. https://doi.org/10.1007/s10973-006-8098-9

Williams, A. J., Gaines, L. G. T., Grulke, C. M., Lowe, C. N., Sinclair, G. F. B., Samano, V., Thillainadarajah, I., Meyer, B., Patlewicz, G., & Richard, A. M. (2022). Assembly and Curation of Lists of Per- and Polyfluoroalkyl Substances (PFAS) to Support Environmental Science Research. *Frontiers in*

Environmental Science, *10*. https://doi.org/10.3389/fenvs.2022.850019

Yan, J. H., Peng, Z., Lu, S. Y., Li, X. D., Ni, M. J., Cen, K. F., & Dai, H. F. (2007). Degradation of PCDD/Fs by mechanochemical treatment of fly ash from medical waste incineration. *Journal of Hazardous Materials*, *147*(1), 652–657. https://doi.org/https://doi.org/10.1016/j.jhazmat.2007.02.073

Yan, X., Liu, X., Qi, C., Wang, D., & Lin, C. (2015). Mechanochemical destruction of a chlorinated polyfluorinated ether sulfonate (F-53B{,} a PFOS alternative) assisted by sodium persulfate. *RSC Adv.*, *5*(104), 85785–85790. https://doi.org/10.1039/C5RA15337A

Zhang, K., Cao, Z., Huang, J., Deng, S., Wang, B., & Yu, G. (2016). Mechanochemical destruction of Chinese PFOS alternative F-53B. *Chemical Engineering Journal*, *286*, 387–393. https://doi.org/https://doi.org/10.1016/j.cej.2015.10.103

Zhang, K., Huang, J., Yu, G., Zhang, Q., Deng, S., & Wang, B. (2013). Destruction of Perfluorooctane Sulfonate (PFOS) and Perfluorooctanoic Acid (PFOA) by Ball Milling. *Environmental Science & Technology*, *47*(12), 6471–6477. https://doi.org/10.1021/es400346n

Zhang, K., Huang, J., Zhang, W., Yu, Y., Deng, S., & Yu, G. (2012). Mechanochemical degradation of tetrabromobisphenol A: performance, products and pathway. *Journal of Hazardous Materials*, *243*, 278—285. https://doi.org/10.1016/j.jhazmat.2012.10.034

Zhang, W., Wang, H., Jun, H., Yu, M., Wang, F., Zhou, L., & Yu, G. (2014). Acceleration and mechanistic studies of the mechanochemical dechlorination of HCB with iron powder and quartz sand. *Chemical Engineering Journal*, *239*, 185–191. https://doi.org/https://doi.org/10.1016/j.cej.2013.11.018

Zhang, X., Xue, L., Deji, Z., Wang, X., Liu, P., Lu, J., Zhou, R., & Huang, Z. (2022). Effects of exposure to per- and polyfluoroalkyl substances on vaccine antibodies: A systematic review and meta-analysis based on epidemiological studies. *Environmental Pollution*, *306*, 119442. https://doi.org/https://doi.org/10.1016/j.envpol.2022.119442

3 Use of a Horizontal Ball Mill to Remediate Per- and Polyfluoroalkyl Substances in Soil

3.1 Abstract

There is a need for destructive technologies for per- and polyfluoroalkyl substances (PFAS) in soil. While planetary ball mill have shown successful degradation of PFAS, there are issues surrounding scale up (maximum cylinder size is typically 0.5 L). While having lower energy outputs, horizontal ball mills, for which scale up is not a limiting factor, already exist at commercial/industrial sizes from the mining, metallurgic and agricultural industries, which could be re-purposed. This study evaluated the effectiveness of horizontal ball mills in degrading perfluorooctanesulfonate (PFOS), 6:2 fluorotelomer sulfonate (6:2 FTSA), and aqueous film forming foam (AFFF) spiked on nepheline syenite sand. Horizontal ball milling was also applied to two different soil types (sand dominant and clay dominant) collected from a firefighting training area (FFTA). Liquid chromatography tandem mass spectrometry was used to track 21 target PFAS throughout the milling process. High-resolution accurate mass spectrometry was also used to identify the presence and degradation of 19 non-target fluorotelomer substances, including 6:2 fluorotelomer sulfonamido betaine (FtSaB), 7:3 fluorotelomer betaine (FtB), and 6:2 fluorotelomer thioether amido sulfonate (FtTAoS). In the presence of potassium hydroxide (KOH), used as a co-milling reagent, PFOS, 6:2 FTSA, and the non-target fluorotelomer substances in the AFFF were found to undergo upwards of 81%, 97%, and 100% degradation, respectively. Despite the inherent added complexity associated with field soils, better PFAS degradation was observed on the FFTA soils over the spiked NSS, and more specifically, on the FFTA clay over the FFTA sand. These results held through scale-up, going from the 1 L to the 25 L cylinders. The results of this study support further scale-up in preparation for on-site pilot tests.

3.2 Introduction

Per- and polyfluoroalkyl substances are a class of chemicals that are used in a wide variety of consumer products and industrial processes. Their surfactant nature allows them to repel water, oil, and dirt, making them useful for consumer applications such as cosmetics, personal care products, clothing, textiles, cookware, and food packaging (Ameduri, 2018; Glüge et al., 2020; Herzke et al., 2012; Kwiatkowski et al., 2020; Liu et al., 2014; Robel et al., 2017; Schultes et al., 2018; Wang et al., 2020, 2014; Zafeiraki et al., 2014). Their high temperature resistance and ability to act as dispersants make them well-suited for use in firefighting foams, metal-plating

processes, and as lubricants in high performance machines (Mahinroosta and Senevirathna, 2020). Unfortunately, the same chemistry that makes PFAS so useful also makes some of them recalcitrant in nature due to a lack of, or limited, biodegradation pathways (Sima and Jaffé, 2021).

Some PFAS that have accumulated in the environment over time are now readily measureable in various environmental matrices (Hodgkins et al., 2019; Lin et al., 2020; Muir and Miaz, 2021; Newell et al., 2020; Podder et al., 2021; Zhu and Kannan, 2019), including soil (Bolan et al., 2021b; Garg et al., 2020; Mahinroosta and Senevirathna, 2020; O'Carroll et al., 2020; Pan et al., 2021). Many biowastes, including biosolids, composts, food wastes, and manures, are also major sources of PFAS contamination in the environment (Bolan et al., 2021a). PFOS was classified as a persistent organic pollutant (POP) in the Stockholm Convention in 2009 due to its toxicity, persistence, bioaccumulation potential, and global spread. As the full class of commercially available PFAS compounds continue to be studied, including shorter-chain perfluorinated compounds, longer-chain polyfluorinated compounds, and perfluorinated ethers (Wang et al., 2017), the potential toxic, persistent and bioaccumulative properties are also being investigated (Bao et al., 2017; Buck, 2015; Wang et al., 2017).

The occurrence of PFAS-impacted sites (Andrews et al., 2021; M. Liu et al., 2021; Milley et al., 2018) and the low concentrations deemed to be safe for several exposure pathways requires remedial technologies capable of eliminating them from environmental systems. While PFAS have been successfully removed from water using sorption-based technologies (Du et al., 2014; España et al., 2015; Phong Vo et al., 2020; Zhang et al., 2019), this results in the generation of secondary, concentrated waste streams. Lab-scale studies have also shown that PFAS can penetrate landfill liners (Di Battista et al., 2020). Traditional methods for destruction of persistent organic pollutants in soil, such as thermal treatment and chemical oxidation, have not yet been fully demonstrated for field implementation (Mahinroosta and Senevirathna, 2020). While hazardous waste combustion technologies (commercial incinerators, cement kilns, and lightweight aggregate kilns) were described by USEPA to have the greatest potential to destroy PFAS, additional research is needed to address uncertainties associated with the potential formation and control of products of incomplete combustion (PICs) (USEPA, 2020). Further, complex transformation chemistry complicates emissions capture, and the analytical measurement of residual and emitted/captured PFAS or PICs challenges current analytical abilities to achieve mass balance closure (Duchesne et al., 2020).

Over the last two decades, mechanochemistry has been used successfully to remediate environmental waste; notably, this has included other recalcitrant organic pollutants, such as dichlorodiphenyltrichloroethane (DDT) (Hall et al., 1996), hexachlorobenzene (HCB) (Cao et al., 1999; Korolev et al., 2003; Monagheddu et al., 1999; W. Zhang et al., 2014), polychlorinated biphenyls (PCBs) (Aresta et al.,

2004, 2003; Birke et al., 2006; Intini et al., 2007), polychlorinated dibenzo-p-dioxins (PCDDs) and polychlorinated dibenzofurans (PCDFs) (Yan et al., 2007), and tetrabromobisphenol A (Zhang et al., 2012). Mechanochemistry utilizes mechanical force to initiate chemical reactions that lead to the destruction of contaminants (Loiselle et al., 1997; Nah et al., 2008; Sui et al., 2018). This method stands out when considering both effectiveness and environmental benefits; it can be performed at ambient temperatures and pressures, and does not require the use of solvents, which allows it to be classified as a green technology (Wieczorek-Ciurowa and Gamrat, 2007).

Successful degradation of PFAS using ball milling has been shown for reagent powders (Cagnetta et al., 2017; Lu et al., 2017; Yan et al., 2015; Zhang et al., 2016, 2013), and for PFAS-impacted soils, both with and without the use of co-milling reagents (Turner et al., 2021). However, these studies are limited in terms of advancing a field-capable remedial technology because of their use of Planetary Ball Mills (PBMs). While PBMs create a very high-energy milling environment, capable of achieving accelerations of 50–100 g, the double axis of rotation (mimicking planetary motion) currently precludes easy scale-up beyond the benchtop (maximum size is typically 0.5 L cylinders). Alternatively, Horizontal Ball Mills (HBMs) function on a single axis of rotation. While this inherently produces a lower energy density as compared to PBMs – 100 to 1,000 times lower (Fokina et al., 2004) – large-scale HBMs are readily available, being prevalent in the mining, metallurgy and agricultural industries.

The objective of this research was to test the viability and effectiveness of a HBM for PFAS destruction. Proof of concept was first explored using nepheline syenite sand (NSS), spiked separately with PFOS, 6:2 FTSA, and a mixed formulation AFFF, in a 1 L cylinder. Complexity, and real-world applicability was then explored using two soil types, a predominantly sandy soil, and a predominantly clayey soil, that were collected from a FFTA, and a scale-up was performed, increasing the size of the cylinder to 25 L. The experimental design resulted in 18 trials with the spiked NSS, 12 trials with the FFTA sand and clay at the 1 L cylinder scale, and another 13 trials with the FFTA sand and clay at the 25 L cylinder scale, resulting in a total of 43 trials and 774 samples collected in duplicate across several time intervals. To ensure a more complete understanding of the PFAS degradation through ball milling, liquid chromatography tandem mass spectrometry (LC-MS/MS) was used to target 21 perfluorocarboxylic acids (PFCAs), perfluorosulfonic acids (PFSAs), and perfluorooctanesulfonamide (PFOSA) throughout the milling process, and high-resolution accurate mass spectrometry (LC-HRAM/MS) was used to identify the presence and degradation of 19 non-target fluorotelomer substances found in the AFFF formulation.

3.3 Materials and Methods

3.3.1 Ball Mill System

A 3-tier, long roll mill, model #803DVM, with each roller measuring 122 cm in length, was used for all testing. The overall dimensions of the mill are 144 cm length, 42 cm width, and 154 cm height. The machine has a speed range of between 50 and 300 rotations per minute (RPM). The 1 L cylinders used were ceramic (composition stated to be approximately 88.5% Al2O3, 6.5% SiO2, 2.8% ZrO2, and 1.3% MgO, with trace amounts of Fe2O3 and TiO2) and classified as size "00" (14 cm diameter, 14 cm height, and 7.0 cm opening). The corresponding internal cylinder volume is 1 L ± 5%, with a weight of 2.3 kg. The grinding media used with these cylinders consisted of cylindrical (2 cm diameter, 2 cm length), high-density, ultra-high fired burundum. Burundum is composed of approximately 96.34% Al2O3, 2.75% SiO2, 0.60% MgO, and 0.12% Na2, with trace amounts of Fe2O3 and CaO. The 25 L cylinders used were unlined stainless steel (Type 304) with internal lifter bars, and classified as size "6" (36 cm diameter, 27 cm height, and 20 cm opening). The corresponding internal volume is 25 L ± 5%, with a weight of 11 kg. The grinding media used in association with these cylinders was 2.9 cm diameter American Iron and Steel Institute (A.I.S.I.) 52100 chrome steel balls.

3.3.2 Reagents

Reagent grade PFOS (97%, CAS# 1763- 23-1) and 6:2 FTSA (97%, CAS# 1763-23-1) was purchased from Synquest Laboratories. The NSS was purchased from Unimin Canada (Unimin Canada Ltd. CAS# 37244-96-5, Al2KNaO8Si2, dry bulk density 1.5 g·cm3). Potassium hydroxide (KOH) was purchased from Sigma Aldrich (J.T. Baker 87.5%, CAS# 1310- 58-3). The AFFF used to spike the NSS was acquired directly from the tank of a firefighting vehicle. Characterization identified it as a mixed AFFF containing primarily National Foam PFAS components (FtSaB and FtSaAm), with small amounts of Ansul and/or Chemguard (FtTAoS), and Buckeye (FtB) (D'Agostino and Mabury, 2014; Field, Jennifer A, Sedlak, David, Alvarez-Cohen, 2017; Houtz et al., 2013). The FFTA sand and clay were obtained from a FFTA in Canada, which was used from 1955 to 1996. For each training exercise, approximately 3,000 L of fuel was sprayed into an unlined, 100 m by 100 m bermed area, ignited, and put out with firefighting foam. This occurred up to 50 times per year. Discussions with the site owners indicated that AFFF from 3M, Ansul, National Foam, Chemguard, as well as potentially Angus and Buckeye, were used at the site over time.

3.3.3 Experimental Design

Nepheline syenite sand (NSS) was amended using PFOS, 6:2 FTSA, and AFFF by first dissolving the PFAS in deionized water and mixing with the NSS in a slurry (1:5 wet to dry). PFAS-amended NSS batches, as well as the FFTA sand and clay, were dried at room temperature in a fume hood for 24 hours before being used in the mill. A 10:1 charge ratio (mass grinding media to mass soil) was selected based on the success of previous studies (Turner et al., 2021). Trials were also run with and without KOH as a co-milling reagent. When KOH was added, it was done at a 4:1 ratio (mass soil to mass KOH). For specific masses of media, soil and KOH added for each trial, see Table A-S1. Average starting concentrations in the spiked NSS trials were 6.1 mg/kg ± 1.7 mg/kg for PFOS, and 2.4 mg/kg ± 0.72 mg/kg for 6:2 FTSA. For PFOS, this resulted in an approximate KOH:PFAS mass ratio of 41,000:1, and for 6:2 FTSA, 104,000:1. Milling was carried out at 80 RPM for the 1 L cylinders and 45 RPM for the 25 L cylinders, which is approximately 60% of the critical speed in both instances. The critical speed is the rotational speed at which the centrifugal force keeps the grinding media stationary against the inner wall of the cylinder while it rotates, which precludes grinding (Rose and Sullivan, 1957). All ball milling trials were run in triplicate (with one extra FFTA clay at the 25 L scale), with duplicate samples being collected at each time interval. Samples were collected prior to the start of milling (T0), every 10 minutes across the first hour (i.e. T10, T20, T30, T40, T50 and T60), and then at the 2-hour (T120) and 3-hour (T180) marks.

3.3.4 Solid Sample Extraction

Samples were extracted in basic (0.1% ammonium hydroxide) high performance liquid chromatography (HPLC) grade methanol (CAS 67-56-1). Every 10th sample was spiked with 0.02 mL mass-labelled surrogate. Samples were then vortexed for 10 seconds, agitated on an end-over-end shaker at 65 RPM for 24 hours, then centrifuged at 4,000 RPM for 20 minutes, and diluted with basic methanol to reach ideal concentrations in the extracts before analysis.

3.3.5 Target PFAS Analysis

Sample pH was measured with litmus paper and adjusted to less than pH 10 with acetic acid. Sample extracts were analyzed using the multiple-reaction-monitoring (MRM) mode on an Agilent 6460 MS/MS coupled to an Agilent 1260 high-pressure liquid chromatography (HPLC) system using a 50 mm x 2.1 um ACME C18 analytical column and paired guard column with a 5-µL injection volume. Mobile phases consisted of 10 mM ammonium acetate in DI water (A) and 10 mM ammonium acetate in acetonitrile (B). The elution profile started at 90% A/10% B, transitioning to 100% B over 4 minutes, holding for 2 minutes, then equilibrating at starting conditions for 3 minutes. Blanks were all found to be below the detection

limit of 0.1 ng/g PFAS. All controls and replicates were within 30% of expected values. The complete list of targetable PFAS monitored can be found in Appendix A (Table A-S2). The Agilent 6460 MS/MS was run with the following source conditions: gas temperature of 250ºC, gas flow rate of 30 psi, sheath gas temperature of 300ºC, sheath gas flow of 12 L/min, negative capillary of 2500 V, and 0 nozzle voltage.

3.3.6 Non-target PFAS Analysis

Samples corresponding to T0 and T180 were analyzed on a ThermoFisher Exploris 120 Orbitrap coupled to a Vanquish UHPLC system using a 100 mm x 2.1 µm ACME C18 analytical column and paired guard column with a 15-µL injection volume. Mobile phases consisted of 0.1% acetic acid in DI water (A) and acetonitrile (B). The elution profile started at 90% A/10% B, transitioning to 100% B over 9 minutes, holding for 2 minutes, then equilibrating at starting conditions for 3 minutes. The complete list of non-target PFAS monitored can be found in Appendix A (Table A-S3). Global parameters for the ThermoFisher Exploris 120 Orbitrap HRAM/MS are outlined below. Internal mass calibration was performed using the RunStart EASY-IC (TM) system. A heated electrospray ionization source was used for the ionization of samples following HPLC separation. The HRAM/MS was run in dual polarity mode (voltage 3000+/ 3000-) with a static gas mode, sheath gas of 50 arbitrary units, auxiliary gas of 10 arbitrary units, sweep gas of 4 arbitrary units, ion transfer tube temperature of 325ºC, and vaporizer temperature of 350ºC. Scan parameters were set using a full scan mode (60,000 orbitrap resolution, RF lens 70%) with a 10 second expected LC peak width. Scan parameters also included an intensity triggered ddMS2 mode, with an isolation window of 1.2 m/z, a normalized collision energy type, HCD collision energy of 50%, and automatic scan range mode.

Initial samples were processed using Thermo Scientific FreeStyle® software. Within FreeStyle®, the Elemental Composition tool was used to determine initial suspect masses based on visual peak identification (elements in use: N, O, C, H, S, and F). Isotope simulation was used to identify additional non-target PFAS that were suspected based on the presence of other PFAS commonly found in the formulations. Where initial intensity allowed, MS2 profiles were used to confirm non-target compounds as fluorinated, and high-resolution masses measured were compared to those in literature (D'Agostino and Mabury, 2014; Field, Jennifer A, Sedlak, David, Alvarez-Cohen, 2017; Houtz et al., 2013). AFFF PFAS identities were also confirmed by analyzing National Foam, Ansul, 3M, and Buckeye formulations in inventory. Intensities for all identified PFAS precursors and non-fluorinated surfactants were normalized to the 6:2 FTSA calibration curve to allow for a semi-quantitative measure of the compounds (Charbonnet et al., 2021; Nickerson et al., 2021).

3.3.7 Free Fluoride Analysis

To quantitatively determine the amount of carbon-fluorine bond breakage, which can be used as a direct measure of ball milling efficiency, a free fluoride determination was performed on select samples. This method was modified from EPA Method 9214 for determining the fluoride content of soil and other solid material post-remediation, and has been used successfully for ball milling work previously (Turner et al., 2021). The main modification is the use of DI water as an extraction solution instead of total ionic strength adjustment buffer (TISAB), as this improved recoveries of spiked fluoride. In this method, 1.0 gram of ball-milled soil is mixed with 5 mL of DI water, adjusted to pH 5.5 with acetic acid, and mixed for 24 hours on an end-over-end shaker in 15 mL centrifuge tubes. After mixing, the sample is centrifuged at 4,000 RPM for 20 minutes and 2 mL of the supernatant is transferred via pipette to a clean 15 mL centrifuge tube. One (1) mL of TISAB is added to the 2 mL of supernatant and the pH is checked to ensure it is close to pH 5. The use of TISAB and pH control is important as TISAB prevents interferences from iron and aluminum ions, and pH control minimizes fluoride complex formation and hydroxide interferences. A fluoride ion selective electrode is then used to measure the amount of fluoride present in the solution, which is quantified using an external calibration curve. The sample is then spiked with a known amount of fluoride to measure matrix effects. In samples that had less than 70% recovery of the spike, a standard addition calibration curve was prepared.

Duplicate samples of the two PFOS-spiked soils were spiked with fluoride before analysis for QA/QC purposes. For samples that did not have significant matrix effects, the fluoride recovery was 92 ± 13%, indicating successful employment of the method.

3.4 Results and Discussion

3.4.1 Nepheline Syenite Sand Trials, 1 L Scale

Following the milling of dried NSS, and in the presence of KOH, PFOS was found to degrade up to 43±5% after three hours of total milling. Without KOH, PFOS underwent minimal degradation (19±12%). 6:2 FTSA was found to degrade rapidly in the presence of KOH, up to 88% in the first 10 minutes. After 3 hours, the total degradation reached 97±1%. Without KOH, no degradation of 6:2 FTSA occurred. Similar trends were observed in the AFFF spiked NSS, where 6:2 FTSA was the dominant PFAS present in the targeted suite. Total degradation of 91±2% and 23±13% was observed with and without KOH, respectively (Figure 3-1).

Perfluoropentanoic acid (PFPeA) was identified as being formed as a result of 6:2 FTSA degradation in both the native 6:2 FTSA and AFFF spiked NSS trials (Figure 3-1). Transformation of 6:2 FTSA into PFPeA has been shown in other studies (Lu

et al., 2017; Martin et al., 2019), with a hypothesized destruction sequence of 6:2 FTSA as a result of mechanochemical ball milling (using a PBM), with KOH, being provided in Lu et al. (2017). Their hypothesis starts with a dehydrofluorination at the 6:2 boundary, which, for 6:2 FTS, is surmised to be a weaker point in the molecule than at the functional head group (contrary to perfluorosulfonates). Fragmentation of the molecule occurs through hydroxyl radical attack; the attacking hydroxide remains bound to the perfluorinated moiety, but the negative charge is taken by the nearest fluorine, which detaches as a fluoride ion. The hydroxyl attack, followed by fluoride expulsion, is repeated for the second fluorine on the adjacent carbon, which generates an unstable radical intermediate with two hydroxyl groups attached to the same carbon. This leads to dehydration and transformation of the molecule into PFPeA. Another hydroxyl attack creates an excessive negative charge that leads to a formate removal, leaving a shorter perfluorinated radical behind. This cycle repeats until the molecule undergoes total mineralization. Concentrations of PFPeA peaked at approximately 1/10th the starting concentration of 6:2 FTSA within the first hour of milling, before being degraded in turn and finishing at comparable concentrations (0.018 to 0.049 mg/kg) as the 6:2 FTSA (0.040 to 0.091 mg/kg). PFPeA was not observed in any of the trials without KOH, presumably due to the lack of 6:2 FTSA degradation. No shorter-chained PFCAs were identified as a result of PFOS degradation.

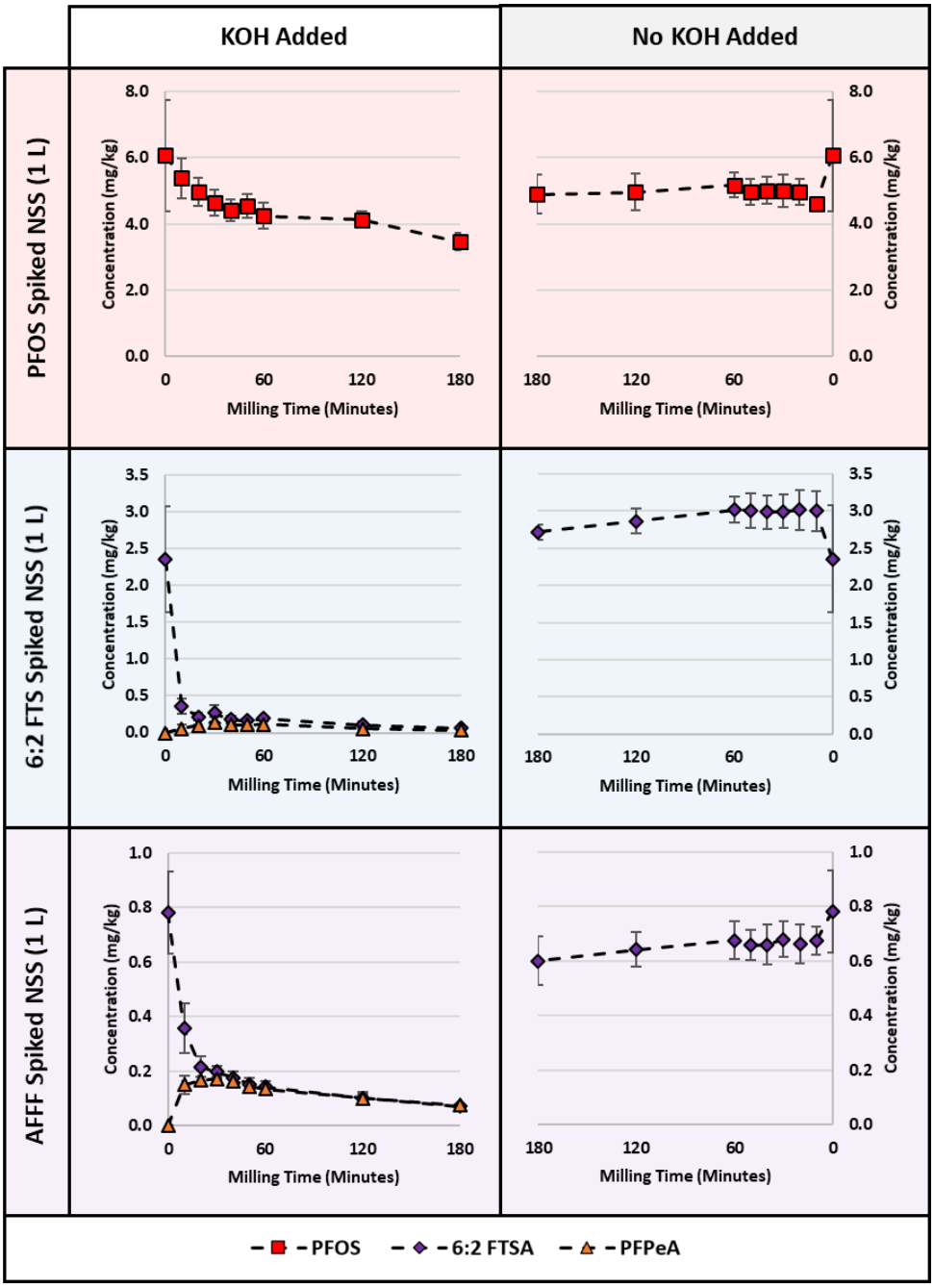

Figure 3-1: Degradation results for PFOS, 6:2 FTSA and AFFF spiked NSS trials, dried, with and without KOH, as a function of milling time (some error bars are too small to be visible).

Turner et al. (2021) used a PBM to destroy PFOS; when using a charge ratio of 33:1 (grinding media to soil), 81 and 98% PFOS degradation was measured after four hours, with and without the addition of KOH, respectively. When using a 12:1 charge ratio, they found 99 and 92% PFOS degradation after four hours. No significant additional degradation was noted beyond four hours with or without the addition of KOH, and although the addition of KOH resulted in an increase in the degradation kinetics in the first 15 minutes of milling in that study, statistical assessment indicated no significant influence of KOH on reducing PFOS concentrations overall (Turner et al., 2021). Given that degradation of PFOS was also shown to occur in our study without the requirement of any co-milling reagent, the greater PFOS degradation rates reported by Turner et al. (2021) is likely attributable to the PBM and the increased energy it is able to impart onto the soil as a result of the double axis of rotation. With the PBM, the PFOS degradation curve was noted to be drawn out without the use of KOH (Turner et al., 2021); using a HBM, the PFOS degradation pattern followed a more linear decay curve, regardless of the presence or absence of KOH. Lower PFOS degradation rates are expected in comparison to other PFAS as PFOS has generally been shown to be more recalcitrant. This is due in part to the protective nature of the sulfonate head group and the helical nature of the perfluorinated carbon chain. After removal of the functional group or a fluoride atom (C-F bond breakage), the fluorine atoms on the carbon chain relax out of their protective helical structure, making the rest of the molecule more vulnerable (Kowald et al., 2021; Patch et al., 2022). Several studies have investigated decomposition of PFAS from generated electrons that propose molecular cleavage along the perfluoroalkyl chain at C-F or C-C bonds (Bentel et al., 2019; Horst et al., 2020; Z. Zhang et al., 2014).

In the closest relevant study for 6:2 FTSA, where 6:2 FTSA as a potassium salt at 99% purity, was milled using a PBM with KOH, 100% degradation and resultant mineralization was achieved in less than one hour (Lu et al., 2017). While there has been no published work on 6:2 FTSA degradation without KOH, degradation was found to occur in PFOA-spiked NSS milling experiments using a PBM with KOH (Turner et al., 2021); in that study, up to 99% degradation was achieved, but notably, the same level of degradation was also achieved without the use of KOH.

The rapid degradation of 6:2 FTSA in the presence of KOH is likely due to the formation of hydroxy radicals, which have been shown capable of breaking C-H bonds (Lu et al., 2017; Zhang et al., 2013). The removal of hydrogen atoms from the chain may result in the formation of an alkene 6:2 FTSA, which can be readily cleaved with many of the radicals generated by the mechanochemical process. Without KOH, there are insufficient hydroxy radicals present to initiate the degradation. This is consistent with observations reported in literature, that the

ethylene linker (-CH2-CH2-) inhibits the degradation of fluorotelomers (Bentel et al., 2020; Dombrowski et al., 2018; Kucharzyk et al., 2017; Z. Liu et al., 2021; Ross et al., 2018). The presence of KOH also promotes PFAS degradation in other ways: (1) by acting as a hygroscopic substance, it absorbs water from its surroundings, which would otherwise inhibit reactive sites; and (2), KOH can also act as a tribomaterial, having the capacity to itself become activated by mechanochemical action and release radical electrons (Turner et al., 2021). However, as has been observed here, and previously (Turner et al., 2021), achieving PFAS degradation can be done without KOH. In these instances it has been surmised that fracture of the soil grains themselves will result in the generation of free electrons that go on to bombard the carbon-fluorine bonds (Turner et al., 2021). Overall results showed that while fluoride was detected in post-milled material, it was difficult to accurately quantify. This is due to a number of reasons, including low initial PFAS concentrations, complex matrix effects, and potential insoluble fluoride products.

Despite best efforts to homogenize the soil before ball milling, the variability of the PFAS concentrations before and throughout the milling process was due to the heterogeneous PFAS distribution within the soil. In general, greater variability between duplicates was observed in the T0 samples, as the milling process itself helps homogenize the material. However, caking of the material along the inside of the cylinder walls was occasionally observed, which would restrict this process. This was observed in PBMs when milling PFAS-impacted soil as well (Turner et al., 2021).

3.4.2 FFTA Sand and Clay Trials, 1 L Scale

Increasing complexity was achieved by using field soils collected from a FFTA; these trials also provide more ‘real-world’ study conditions. The dominant PFAS found in these soils through targeted analysis was determined to be PFOS and 6:2 FTSA.

Following 3 hours of milling, PFOS in the dry FFTA sand was found to undergo up to 69% degradation with KOH, and 15±2% degradation without KOH. As was observed in the native and AFFF 6:2 FTSA spiked trials, the associated 6:2 FTSA in the FFTA sand underwent near-complete degradation in the presence of KOH, and experienced no degradation without KOH. Following 3 hours of milling, PFOS in the dry FFTA clay was found to undergo up to 81% degradation with KOH, and 5±1% without KOH. Again, the associated 6:2 FTSA underwent near-complete degradation with KOH, and experienced no degradation without. Notably, better PFOS degradation was observed for both FFTA soils than for the spiked NSS, and most of the degradation occurred in the first 10 minutes (Figure 3-2). PFCAs (C4-

C8) were identified in the unmilled FFTA sand and clay, and were observed to fluctuate in concentration across the sampling intervals. This is due to the formation of PFCAs from fluorotelomer degradation and subsequent degradation of those same PFCAs.

PFAS degradation was shown in the same soils using a PBM and KOH (Turner et al., 2021); PFOS underwent 69±12% degradation after six hours in the FFTA sand, and 84±5% in the FFTA clay. 6:2 FTSA was not part of the analytical suite in that study. Here, results for the HBM are very similar to those produced by the PBM, including the results showing greater degradation in the FFTA clay than in the FFTA sand.

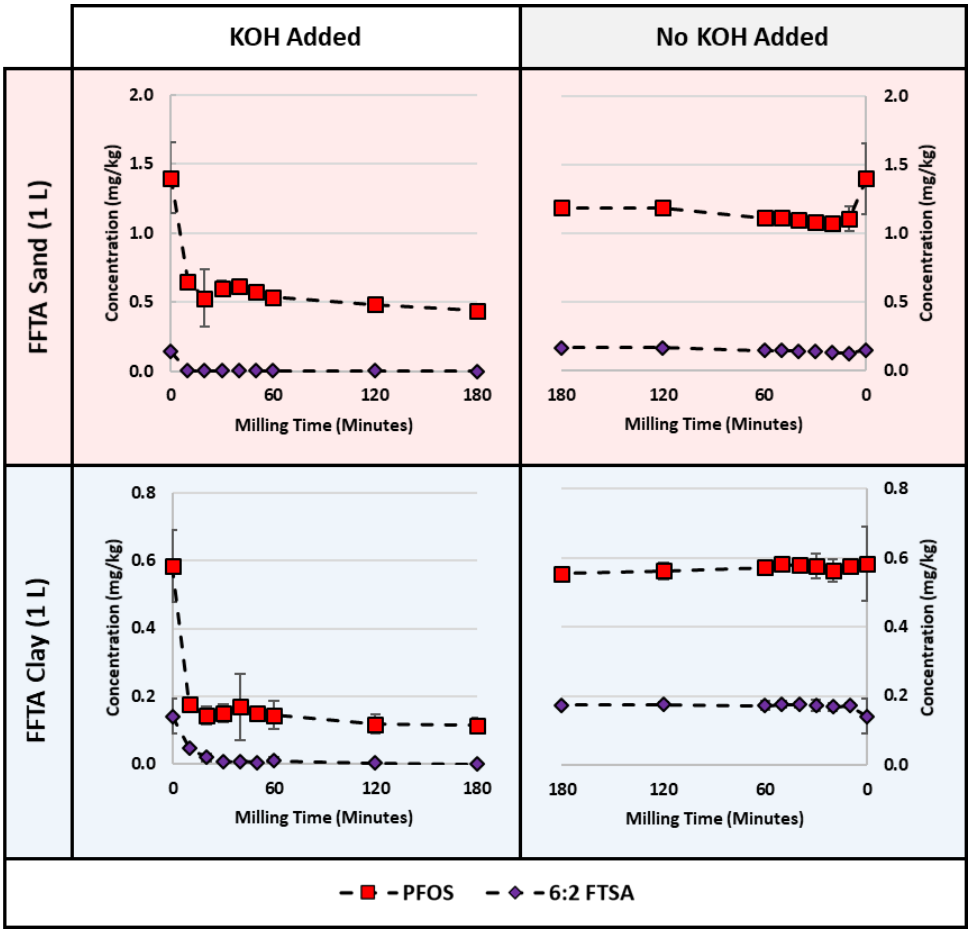

Figure 3-2: Degradation of PFOS and 6:2 FTSA on FFTA sand and clay, dried, with and without KOH, at the 1 L scale (some error bars are too small to be visible).

3.4.3 FFTA Sand and Clay Trials, 25 L Scale

A scale-up was explored for the FFTA sand and clay by increasing the cylinder volume size by a factor of 25. Similar results were obtained in comparison to the 1 L trials. For the FFTA sand, PFOS underwent up to 61% degradation with KOH after 3 hours of milling, and up to 67% without KOH, although much greater variability was noted in the latter trials. For the FFTA clay, PFOS underwent up to

85% degradation after 3 hours with KOH, and up to 12% degradation without KOH (Figure 3-3).

Other trends related to PFAS degradation remained similar at both the 1 L and 25 L scales as well, with milling of the FFTA clay outperforming that of the FFTA sand with respect to PFOS degradation, and with most of that degradation occurring in the first 10 minutes.

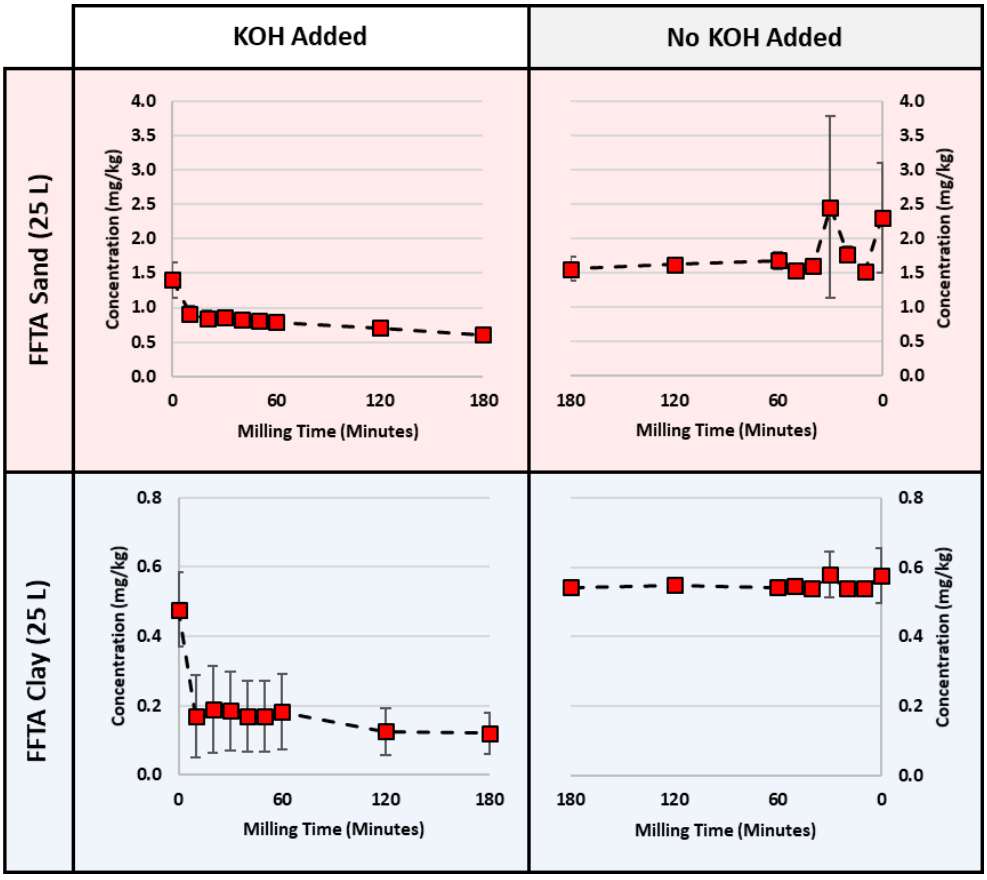

Figure 3-3: Degradation of PFOS on FFTA sand and clay, dried, with and without KOH at the 25 L scale (some error bars are too small to be visible).

3.4.4 Degradation of Non-target PFAS Precursors

While the PFAS composition has been documented for certain AFFF formulations in the scientific literature, chemical changes during natural weathering after release of the products occur and can pose a challenge when attempting to analyze PFAS present within AFFF formulations (Barzen-Hanson et al., 2017; D'Agostino and Mabury, 2014; Field, Jennifer A, Sedlak, David, Alvarez-Cohen, 2017). Analysis is further complicated by the fact that there are no analytical standards available for many of the PFAS present in AFFF, thereby requiring a semi-quantitative approach and high-resolution mass spectrometric techniques to even ascertain their presence. Typically, PFAS only represent 3 to 6% by weight in AFFF, with the other ingredients consisting of non-fluorinated surfactants, stabilizers, solubilizers, and other chemicals (Field, Jennifer A, Sedlak, David, Alvarez-Cohen, 2017; Houtz et al., 2013). When evaluating the remedial effectiveness of a technology on a relevant field soil, it is important to characterize all the PFAS present to allow for a more comprehensive evaluation of success. In this study, the AFFF-spiked NSS, as well as FFTA sand and clay, were analyzed before and after milling to identify the total degradation of non-target PFAS.

As was the case with the native 6:2 FTSA and 6:2 FTSA from AFFF trials (Figure 3-1), milling of the AFFF-spiked NSS in the presence of KOH led to near-complete degradation for all non-target PFAS present, as well as 6:2 FTSA (Figure 3-4). Without KOH, many of the non-target PFAS still underwent significant degradation, but fell short of complete degradation (generally in the 80-100% range).

HRAM/MS analysis of the FFTA sand and clay before and after milling also allowed for the identification of non-target PFAS that underwent degradation (Figure A-S1, S2). There was insufficient sample remaining for HRAM/MS analysis of the FFTA sand without KOH, but analysis of the unmilled and milled FFTA sand with KOH revealed a small amount of 6:2 FtSOAoS, which is a degradation product of 6:2 FtTAoS, the primary ingredient in Chemguard and Ansul AFFF formulations, as well as traces of 6:2 FtSaB, which derives from National Foam AFFF formulations, and 11:1:2 FtB, which is a class characteristic of Buckeye AFFF formulations (Field, Jennifer A, Sedlak, David, Alvarez-Cohen, 2017; Houtz et al., 2013). Once again, in the presence of KOH, complete degradation of the non-target PFAS was identified (Figure A-S1). Analysis of the FFTA clay revealed a small amount of 5:1:2 FtB, traces of other Buckeye compounds, as well as both 6:2 FtTAoS and 6:2 FtSOAoS. Complete degradation in the presence of KOH was observed, with degradation in the 80-100% range without KOH (Figure A-S2). All chromatograms and extracted ion chromatograms of the AFFF components found are provided in Appendix A (Figure AS3-S24).

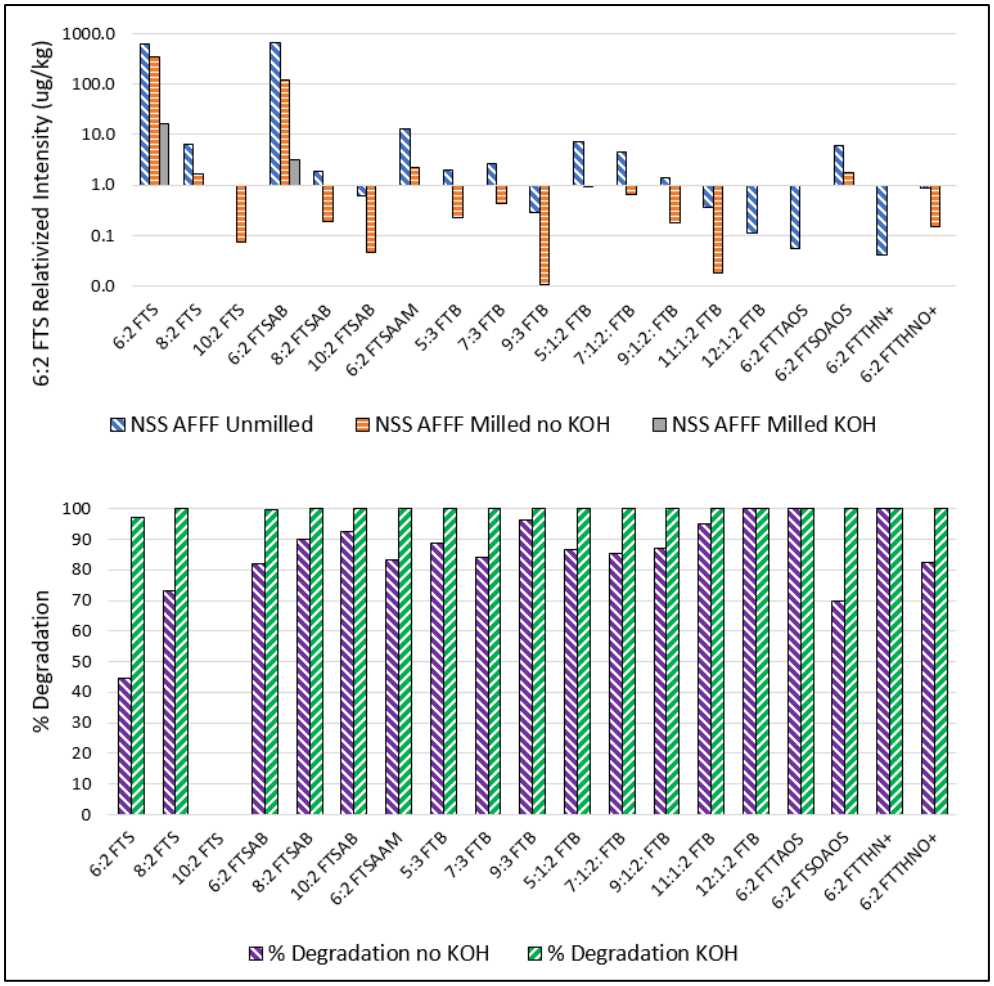

Figure 3-4: Relativized intensity (top) and relative degradation (bottom) of non-targeted PFAS found in the dried AFFF-spiked NSS, with and without KOH.

3.4.5 Comparison to Soil Quality Guidelines

The international soil guidelines for PFOS vary widely and change rapidly. At the time of writing, human health soil screening levels range from 0.0023 mg/kg (Norway) to 2 mg/kg (Australia); the USEPA uses a regional screening level of 1.26 mg/kg (ITRC, 2021). Starting PFOS concentrations in the NSS averaged 6.1 mg/kg, and between 0.4 and 2.9 mg/kg in the FFTA soils. Final concentrations ranged

between 3.0 and 5.6 mg/kg in the NSS and 0.1 to 1.7 mg/kg in the FFTA soils, making success dependent on which international soil quality guideline is applied.

Canada and Denmark are the only two countries that have a soil quality guideline for 6:2 FTSA; these values are 0.8 and 0.4 mg/kg, respectively (ITRC, 2021). These same guidelines also apply to PFPeA. With the average starting concentration of 6:2 FTSA in the NSS being 2.4 mg/kg, it exceeded guidelines in both countries. The final concentrations were, on average, 0.066 mg/kg, which put it in compliance in both countries. The production of PFPeA in the trials with KOH never exceeded either country's guideline (maximum value was 0.24 mg/kg), and finished at concentrations averaging 0.032 mg/kg. These comparisons show that in many cases the HBM can achieve international soil remediation standards for PFAS.

At present, the use of KOH seems to be required to get consistent and significant degradation of PFAS in soils when using a HBM. However, the use of KOH leads to pH increases beyond 12; thus, in a remedial setting, a buffering step would be needed post-milling to return the soil to environmentally acceptable pH levels (as determined by jurisdictional guidelines).

3.5 Conclusions

This study examined the effectiveness of a HBM for the mechanochemical degradation of PFAS in spiked NSS, as well as two different soil types, sand and clay, from a FFTA, with and without the use of KOH as a co-milling reagent, at two separate scales (1 L vs 25 L). A total of 21 targeted PFCAs, PFSAs, and PFOSA, as well as 19 non-target fluorotelomers were tracked through several time series sampling events. The summarized results (Table 3-1) for the dominant PFAS show that PFOS and 6:2 FTSA are readily degraded in the presence of KOH regardless of substrate type or scale. Whereas PFOS still experienced moderate degradation without KOH, 6:2 FTSA had minimal degradation. Given the similar chemical nature of PFOS and 6:2 FTSA, it was identified that the susceptibility of 6:2 FTSA to degradation in the presence of KOH is likely the result of hydroxy radicals generated from the KOH, which may result in a fluorotelomer-alkene structure that can be subsequently attacked by other radicals generated in the system.

This is the first study to identify that a HBM can degrade PFAS in soil, and that ball milling can near-completely degrade the non-target fluorotelomer PFAS found in modern AFFF formulations. Therefore, this technology can not only be potentially used for historical contaminated sites where the AFFF used was predominately PFSA-based, but it may also operate at enhanced effectiveness when dealing with sites that have used modern AFFF, or where modern AFFF has weathered significantly in-situ. Further, HRAM analysis has been able to show no major or easily identified fluorinated compounds formed as a byproduct of the milling procedure, which has been raised previously as a potential concern. This should be followed up with additional analysis in later studies, along with determining the

optimal amount of KOH needed to minimize alkalinity of the treated soil. Remediating PFAS in organic matter rich biowastes is hypothesized to be a challenge, with the organic material absorbing some of the energy imparted through the ball milling process, as well as the free radicals generated; future studies are being planned with these types of matrices. With its ability to rapidly degrade fluorotelomers, reduce grain size, and homogenize the feedstock, ball milling as a technology lends itself quite readily to incorporation into a treatment train approach (Ross et al., 2018), being complemented by a second, polishing step to reduce concentrations even further.

Table 3-1: Summary of results for targeted PFAS degradation.

Substrate Type	**Spiked PFAS**	**# trials**	**C_0 (mg/kg)**	**1 L Cylinder**	
				KOH	**no KOH**
NSS	PFOS	3	6.06	42.85 ± 4.81	
		3	6.06		19.36 ± 11.54
NSS	6:2 FTS	3	2.36	97.21 ± 0.90	
		3	2.36		-15.38 ± 5.10
NSS	AFFF	3	0.78	90.97 ± 1.76	
		3	0.78		23.30 ± 13.12
FFTA sand	PFOS	1	2.37	55.98	
		2	1.40	68.69 ± 1.91	
		3	1.40		14.99 ± 2.15
FFTA clay	PFOS	1	0.91	69.93	
		2	0.58	80.52 ± 0.31	
		3	0.58		5.01 ± 0.88
Substrate Type	**Spiked PFAS**	**# trials**	**C_0 (mg/kg)**	**25 L Cylinder**	
				KOH	**no KOH**
FFTA sand	PFOS	1	1.02	61.13	
		2	1.40	56.58 ± 2.40	
		1	0.65		66.54
		1	1.74		18.01
		1	2.87		41.73
FFTA clay	PFOS	1	0.36	84.95	
		1	0.57	75.47	
		2	0.50	66.63 ± 6.68	
		1	0.64		11.87
		2	0.51		-1.78 ± 5.60

3.6 Acknowledgements

Support for this research was provided by the Natural Sciences and Engineering Research Council (NSERC) of Canada (RGPIN-2018-04886; CRDPJ 530133-18) with industry sponsors Golder Associates Incorporated and Imperial Oil Limited.

3.7 References

Ameduri, B., 2018. Fluoropolymers: The Right Material for the Right Applications. Chem. – A Eur. J. 24, 18830–18841. https://doi.org/https://doi.org/10.1002/chem.201802708

Andrews, D.Q., Hayes, J., Stoiber, T., Brewer, B., Campbell, C., Naidenko, O. V, 2021. Identification of point source dischargers of per- and polyfluoroalkyl substances in the United States. AWWA Water Sci. 3, e1252. https://doi.org/https://doi.org/10.1002/aws2.1252

Aresta, M., Caramuscio, P., De Stefano, L., Pastore, T., 2003. Solid state dehalogenation of PCBs in contaminated soil using NaBH4. Waste Manag. 23, 315–319. https://doi.org/https://doi.org/10.1016/S0956-053X(03)00029-1

Aresta, M., Dibenedetto, A., Fragale, C., Pastore, T., 2004. High-energy milling to decontaminate soils polluted by polychlorobiphenyls and atrazine. Environ. Chem. Lett. 2, 1–4. https://doi.org/10.1007/s10311-003-0057-0

Bao, Y., Qu, Y., Huang, J., Cagnetta, G., Yu, G., Weber, R., 2017. First assessment on degradability of sodium p-perfluorous nonenoxybenzene sulfonate (OBS){,} a high volume alternative to perfluorooctane sulfonate in fire-fighting foams and oil production agents in China. RSC Adv. 7, 46948–46957. https://doi.org/10.1039/C7RA09728J

Barzen-Hanson, K.A., Roberts, S.C., Choyke, S., Oetjen, K., McAlees, A., Riddell, N., McCrindle, R., Ferguson, P.L., Higgins, C.P., Field, J.A., 2017. Discovery of 40 Classes of Per- and Polyfluoroalkyl Substances in Historical Aqueous Film-Forming Foams (AFFFs) and AFFF-Impacted Groundwater. Environ. Sci. Technol. https://doi.org/10.1021/acs.est.6b05843

Bentel, M.J., Liu, Z., Yu, Y., Gao, J., Men, Y., Liu, J., 2020. Enhanced Degradation of Perfluorocarboxylic Acids (PFCAs) by UV/Sulfite Treatment: Reaction Mechanisms and System Efficiencies at pH 12. Environ. Sci. Technol. Lett. 7, 351–357. https://doi.org/10.1021/acs.estlett.0c00236

Bentel, M.J., Yu, Y., Xu, L., Li, Z., Wong, B.M., Men, Y., Liu, J., 2019. Defluorination of Per- and Polyfluoroalkyl Substances (PFASs) with Hydrated

Electrons: Structural Dependence and Implications to PFAS Remediation and Management. Environ. Sci. Technol. 53, 3718–3728. https://doi.org/10.1021/acs.est.8b06648

Birke, V., Mattik, J., Runne, D., Benning, H., Zlatovic, D., 2006. Dechlorination of Recalcitrant Polychlorinated Contaminants Using Ball Milling, in: Kolodkin, V.M., Ruck, W. (Eds.), Ecological Risks Associated with the Destruction of Chemical Weapons. Springer Netherlands, Dordrecht, pp. 111–127.

Bolan, N., Sarkar, B., Vithanage, M., Singh, G., Tsang, D.C.W., Mukhopadhyay, R., Ramadass, K., Vinu, A., Sun, Y., Ramanayaka, S., Hoang, S.A., Yan, Y., Li, Y., Rinklebe, J., Li, H., Kirkham, M.B., 2021a. Distribution, behaviour, bioavailability and remediation of poly- and per-fluoroalkyl substances (PFAS) in solid biowastes and biowaste-treated soil. Environ. Int. 155, 106600. https://doi.org/https://doi.org/10.1016/j.envint.2021.106600

Bolan, N., Sarkar, B., Yan, Y., Li, Q., Wijesekara, H., Kannan, K., Tsang, D.C.W., Schauerte, M., Bosch, J., Noll, H., Ok, Y.S., Scheckel, K., Kumpiene, J., Gobindlal, K., Kah, M., Sperry, J., Kirkham, M.B., Wang, H., Tsang, Y.F., Hou, D., Rinklebe, J., 2021b. Remediation of poly- and perfluoroalkyl substances (PFAS) contaminated soils – To mobilize or to immobilize or to degrade? J. Hazard. Mater. https://doi.org/10.1016/j.jhazmat.2020.123892

Buck, R.C., 2015. Toxicology Data for Alternative ``Short-Chain'' Fluorinated Substances, in: DeWitt, J.C. (Ed.), Toxicological Effects of Perfluoroalkyl and Polyfluoroalkyl Substances. Springer International Publishing, Cham, pp. 451–477. https://doi.org/10.1007/978-3-319-15518-0_17

Cagnetta, G., Zhang, Q., Huang, J., Lu, M., Wang, B., Wang, Y., Deng, S., Yu, G., 2017. Mechanochemical destruction of perfluorinated pollutants and mechanosynthesis of lanthanum oxyfluoride: A Waste-to-Materials process. Chem. Eng. J. 316, 1078–1090. https://doi.org/https://doi.org/10.1016/j.cej.2017.02.050

Cao, G., Doppiu, S., Monagheddu, M., Orrù, R., Sannia, M., Cocco, G., 1999. Thermal and Mechanochemical Self-Propagating Degradation of Chloro-organic Compounds: The Case of Hexachlorobenzene over Calcium Hydride. Ind. Eng. Chem. Res. 38, 3218–3224. https://doi.org/10.1021/ie980790+

Charbonnet, J.A., Rodowa, A.E., Joseph, N.T., Guelfo, J.L., Field, J.A., Jones, G.D., Higgins, C.P., Helbling, D.E., Houtz, E.F., 2021. Environmental Source Tracking of Per- and Polyfluoroalkyl Substances within a Forensic Context: Current and Future Techniques. Environ. Sci. Technol. 55, 7237–7245. https://doi.org/10.1021/acs.est.0c08506

D’Agostino, L.A., Mabury, S.A., 2014. Identification of novel fluorinated surfactants in aqueous film forming foams and commercial surfactant concentrates. Environ. Sci. Technol. 48, 121–129. https://doi.org/10.1021/es403729e

Di Battista, V., Rowe, R.K., Patch, D., Weber, K., 2020. PFOA and PFOS diffusion through LLDPE and LLDPE coextruded with EVOH at 22 °C, 35 °C, and 50 °C. Waste Manag. 117, 93–103. https://doi.org/10.1016/j.wasman.2020.07.036

Dombrowski, P.M., Kakarla, P., Caldicott, W., Chin, Y., Sadeghi, V., Bogdan, D., Barajas-Rodriguez, F., Chiang, S.Y.D., 2018. Technology review and evaluation of different chemical oxidation conditions on treatability of PFAS. Remediation 28, 135–150. https://doi.org/10.1002/rem.21555

Du, Z., Deng, S., Bei, Y., Huang, Q., Wang, B., Huang, J., Yu, G., 2014. Adsorption behavior and mechanism of perfluorinated compounds on various adsorbents--a review. J. Hazard. Mater. 274, 443–454. https://doi.org/10.1016/j.jhazmat.2014.04.038

Duchesne, A.L., Brown, J.K., Patch, D.J., Major, D., Weber, K.P., Gerhard, J.I., 2020. Remediation of PFAS-Contaminated Soil and Granular Activated Carbon by Smoldering Combustion. Environ. Sci. Technol. 54, 12631–12640. https://doi.org/10.1021/acs.est.0c03058

España, V.A.A., Mallavarapu, M., Naidu, R., Naidu, R., 2015. Treatment technologies for aqueous perfluorooctanesulfonate (PFOS) and perfluorooctanoate (PFOA): A critical review with an emphasis on field testing. Environ. Technol. Innov. 4, 168–181.

Field, Jennifer A, Sedlak, David, Alvarez-Cohen, L., 2017. Characterization of the Fate and Biotransformation of Fluorochemicals in AFFF-Contaminated Groundwater at Fire/Crash Testing Military Sites.

Fokina, E., Budim, N., Kochnev, V., Chernik, G., 2004. Planetary mills of periodic and continuous action. J. Mater. Sci. 39, 5217–5221. https://doi.org/10.1023/B:JMSC.0000039213.44891.7d

Garg, S., Kumar, P., Mishra, V., Guijt, R., Singh, P., Dumée, L.F., Sharma, R.S., 2020. A review on the sources, occurrence and health risks of per-/poly-fluoroalkyl substances (PFAS) arising from the manufacture and disposal of electric and electronic products. J. Water Process Eng. 38, 101683. https://doi.org/https://doi.org/10.1016/j.jwpe.2020.101683

Glüge, J., Scheringer, M., Cousins, I.T., DeWitt, J.C., Goldenman, G., Herzke, D., Lohmann, R., Ng, C.A., Trier, X., Wang, Z., 2020. An overview of the uses of per- and polyfluoroalkyl substances (PFAS). Environ. Sci. Process. Impacts 22, 2345–2373. https://doi.org/10.1039/D0EM00291G

Hall, A.K., Harrowfield, J.M., Hart, R.J., McCormick, P.G., 1996. Mechanochemical Reaction of DDT with Calcium Oxide. Environ. Sci. Technol. 30, 3401–3407. https://doi.org/10.1021/es950680j

Herzke, D., Olsson, E., Posner, S., 2012. Perfluoroalkyl and polyfluoroalkyl substances (PFASs) in consumer products in Norway - a pilot study. Chemosphere 88, 980–987. https://doi.org/10.1016/j.chemosphere.2012.03.035

Hodgkins, L.M., Mulligan, R.P., McCallum, J.M., Weber, K.P., 2019. Modelling the transport of shipborne per- and polyfluoroalkyl substances (PFAS) in the coastal environment. Sci. Total Environ. 658, 602–613. https://doi.org/10.1016/j.scitotenv.2018.12.230

Horst, J., McDonough, J., Ross, I., Houtz, E., 2020. Understanding and Managing the Potential By-Products of PFAS Destruction. Groundw. Monit. \& Remediat. 40, 17–27. https://doi.org/https://doi.org/10.1111/gwmr.12372

Houtz, E.F., Higgins, C.P., Field, J.A., Sedlak, D.L., 2013. Persistence of Perfluoroalkyl Acid Precursors in AFFF-Impacted Groundwater and Soil. Environ. Sci. Technol. 47, 8187–8195. https://doi.org/10.1021/es4018877

Intini, G., Cangialosi, F., L.Liberti, D.Lupo, Notarnicola, M., Pastore, T., 2007. Mechanochemical treatment of contaminated marine sediments for PCB degradation. Chem. Sustain. Dev. 15, 147–156.

Korolev, K., Golovanova, A.I., Maltseva, N.N., Lomovskiy, O.I., Salenko, V.L., Boldyrev, V. V, 2003. Application of mechanical activation to decomposition of toxic chlorinated organic compounds. Chem. Sustain. Dev. 11, 489–496.

Kowald, C., Brorman, E., Shankar, S., Klemashevich, C., Staack, D., Pillai, S.D., 2021. PFOA and PFOS breakdown in experimental sand, laboratory-grade water, investigation-derived groundwater and wastewater effluent samples at 50 kGy electron beam dose. Radiat. Phys. Chem. 180, 109323. https://doi.org/https://doi.org/10.1016/j.radphyschem.2020.109323

Kucharzyk, K.H., Darlington, R., Benotti, M., Deeb, R., Hawley, E., 2017. Novel treatment technologies for PFAS compounds: A critical review. J. Environ. Manage. 204, 757–764. https://doi.org/10.1016/j.jenvman.2017.08.016

Kwiatkowski, C.F., Andrews, D.Q., Birnbaum, L.S., Bruton, T.A., DeWitt, J.C., Knappe, D.R.U., Maffini, M. V, Miller, M.F., Pelch, K.E., Reade, A., Soehl, A., Trier, X., Venier, M., Wagner, C.C., Wang, Z., Blum, A., 2020. Scientific Basis for Managing PFAS as a Chemical Class. Environ. Sci. Technol. Lett. 7, 532–543. https://doi.org/10.1021/acs.estlett.0c00255

Lin, Y., Jiang, J.-J., Rodenburg, L.A., Cai, M., Wu, Z., Ke, H., Chitsaz, M., 2020. Perfluoroalkyl substances in sediments from the Bering Sea to the western Arctic: Source and pathway analysis. Environ. Int. 139, 105699. https://doi.org/https://doi.org/10.1016/j.envint.2020.105699

Liu, M., Munoz, G., Vo Duy, S., Sauvé, S., Liu, J., 2021. Per- and Polyfluoroalkyl Substances in Contaminated Soil and Groundwater at Airports: A Canadian Case Study. Environ. Sci. Technol. https://doi.org/10.1021/acs.est.1c04798

Liu, X., Guo, Z., Krebs, K.A., Pope, R.H., Roache, N.F., 2014. Concentrations and trends of perfluorinated chemicals in potential indoor sources from 2007 through 2011 in the US. Chemosphere 98, 51–57. https://doi.org/10.1016/j.chemosphere.2013.10.001

Liu, Z., Bentel, M.J., Yu, Y., Ren, C., Gao, J., Pulikkal, V.F., Sun, M., Men, Y., Liu, J., 2021. Near-Quantitative Defluorination of Perfluorinated and Fluorotelomer Carboxylates and Sulfonates with Integrated Oxidation and Reduction. Environ. Sci. Technol. 55, 7052–7062. https://doi.org/10.1021/acs.est.1c00353

Loiselle, S., Branca, M., Mulas, G., Cocco, G., 1997. Selective Mechanochemical Dehalogenation of Chlorobenzenes over Calcium Hydride. Environ. Sci. Technol. 31, 261–265. https://doi.org/10.1021/es960398s

Lu, M., Cagnetta, G., Zhang, K., Huang, J., Yu, G., 2017. Mechanochemical mineralization of “very persistent” fluorocarbon surfactants – 6:2 fluorotelomer sulfonate (6:2FTS) as an example. Sci. Rep. 7, 17180. https://doi.org/10.1038/s41598-017-17515-7

Mahinroosta, R., Senevirathna, L., 2020. A review of the emerging treatment technologies for PFAS contaminated soils. J. Environ. Manage. 255, 109896. https://doi.org/10.1016/j.jenvman.2019.109896

Martin, D., Munoz, G., Mejia-Avendaño, S., Duy, S.V., Yao, Y., Volchek, K., Brown, C.E., Liu, J., Sauvé, S., 2019. Zwitterionic, cationic, and anionic perfluoroalkyl and polyfluoroalkyl substances integrated into total oxidizable precursor assay of contaminated groundwater. Talanta 195, 533–542. https://doi.org/https://doi.org/10.1016/j.talanta.2018.11.093

Milley, S.A., Koch, I., Fortin, P., Archer, J., Reynolds, D., Weber, K.P., 2018. Estimating the number of airports potentially contaminated with perfluoroalkyl and polyfluoroalkyl substances from aqueous film forming foam: A Canadian example. J. Environ. Manage. 222, 122–131. https://doi.org/10.1016/j.jenvman.2018.05.028

Monagheddu, M., Mulas, G., Doppiu, S., Cocco, G., Raccanelli, S., 1999. Reduction of Polychlorinated Dibenzodioxins and Dibenzofurans in Contaminated Muds by Mechanically Induced Combustion Reactions. Environ. Sci. Technol. 33, 2485–2488. https://doi.org/10.1021/es9809206

Muir, D., Miaz, L.T., 2021. Spatial and Temporal Trends of Perfluoroalkyl Substances in Global Ocean and Coastal Waters. Environ. Sci. Technol. 55, 9527–9537. https://doi.org/10.1021/acs.est.0c08035

Nah, I.W., Hwang, K.-Y., Shul, Y.-G., 2008. Effect of metal and glycol on mechanochemical dechlorination of polychlorinated biphenyls (PCBs). Chemosphere 73, 138–141. https://doi.org/10.1016/j.chemosphere.2008.04.051

Newell, C.J., Adamson, D.T., Kulkarni, P.R., Nzeribe, B.N., Stroo, H., 2020. Comparing PFAS to other groundwater contaminants: Implications for remediation. Remediat. J. 30, 7–26. https://doi.org/https://doi.org/10.1002/rem.21645

Nickerson, A., Rodowa, A.E., Adamson, D.T., Field, J.A., Kulkarni, P.R., Kornuc, J.J., Higgins, C.P., 2021. Spatial Trends of Anionic, Zwitterionic, and Cationic PFASs at an AFFF-Impacted Site. Environ. Sci. Technol. 55, 313–323. https://doi.org/10.1021/acs.est.0c04473

O'Carroll, D.M., Jeffries, T.C., Lee, M.J., Le, S.T., Yeung, A., Wallace, S., Battye, N., Patch, D.J., Manefield, M.J., Weber, K.P., 2020. Developing a roadmap to determine per- and polyfluoroalkyl substances-microbial population interactions. Sci. Total Environ. 712, 135994. https://doi.org/https://doi.org/10.1016/j.scitotenv.2019.135994

Pan, C.-G., Xiao, S.-K., Yu, K.-F., Wu, Q., Wang, Y.-H., 2021. Legacy and alternative per- and polyfluoroalkyl substances in a subtropical marine food web from the Beibu Gulf, South China: Fate, trophic transfer and health risk assessment. J. Hazard. Mater. 403, 123618. https://doi.org/https://doi.org/10.1016/j.jhazmat.2020.123618

Patch, D., O'Connor, N., Koch, I., Cresswell, T., Hughes, C., Davies, J.B., Scott, J., O'Carroll, D., Weber, K., 2022. Elucidating degradation mechanisms for a range of per- and polyfluoroalkyl substances (PFAS) via controlled irradiation studies. Sci.

Total Environ. 832, 154941. https://doi.org/https://doi.org/10.1016/j.scitotenv.2022.154941

Phong Vo, H.N., Ngo, H.H., Guo, W., Hong Nguyen, T.M., Li, J., Liang, H., Deng, L., Chen, Z., Hang Nguyen, T.A., 2020. Poly-and perfluoroalkyl substances in water and wastewater: A comprehensive review from sources to remediation. J. Water Process Eng. 36, 101393. https://doi.org/https://doi.org/10.1016/j.jwpe.2020.101393

Podder, A., Sadmani, A.H.M.A., Reinhart, D., Chang, N.-B., Goel, R., 2021. Per and poly-fluoroalkyl substances (PFAS) as a contaminant of emerging concern in surface water: A transboundary review of their occurrences and toxicity effects. J. Hazard. Mater. 419, 126361. https://doi.org/https://doi.org/10.1016/j.jhazmat.2021.126361

Robel, A.E., Marshall, K., Dickinson, M., Lunderberg, D., Butt, C., Peaslee, G., Stapleton, H.M., Field, J.A., 2017. Closing the Mass Balance on Fluorine on Papers and Textiles. Environ. Sci. Technol. 51, 9022–9032. https://doi.org/10.1021/acs.est.7b02080

Rose, H.E., Sullivan, R.M.E., 1957. A Treatise on the Internal Mechanics of Ball, Tube and Rod Mills. Constable, London.

Ross, I., McDonough, J., Miles, J., Storch, P., Thelakkat Kochunarayanan, P., Kalve, E., Hurst, J., S. Dasgupta, S., Burdick, J., 2018. A review of emerging technologies for remediation of PFASs. Remediation 28, 101–126. https://doi.org/10.1002/rem.21553

Schultes, L., Vestergren, R., Volkova, K., Westberg, E., Jacobson, T., Benskin, J.P., 2018. Per- and polyfluoroalkyl substances and fluorine mass balance in cosmetic products from the Swedish market: implications for environmental emissions and human exposure. Environ. Sci. Process. Impacts 20, 1680–1690. https://doi.org/10.1039/C8EM00368H

Sima, M.W., Jaffé, P.R., 2021. A critical review of modeling Poly- and Perfluoroalkyl Substances (PFAS) in the soil-water environment. Sci. Total Environ. 757, 143793. https://doi.org/https://doi.org/10.1016/j.scitotenv.2020.143793

Sui, H., Rong, Y., Song, J., Zhang, D., Li, H., Wu, P., Shen, Y., Huang, Y., 2018. Mechanochemical destruction of DDTs with Fe-Zn bimetal in a high-energy planetary ball mill. J. Hazard. Mater. 342, 201–209. https://doi.org/https://doi.org/10.1016/j.jhazmat.2017.08.025

Turner, L.P., Kueper, B.H., Jaansalu, K.M., Patch, D.J., Battye, N., El-Sharnouby, O., Mumford, K.G., Weber, K.P., 2021. Mechanochemical remediation of perfluorooctanesulfonic acid (PFOS) and perfluorooctanoic acid (PFOA) amended sand and aqueous film-forming foam (AFFF) impacted soil by planetary ball milling. Sci. Total Environ. 765, 142722. https://doi.org/https://doi.org/10.1016/j.scitotenv.2020.142722

USEPA, 2020. Interim Guidance on the Destruction and Disposal of Perfluoroalkyl and Polyfluoroalkyl Substances and Materials Containing Perfluoroalkyl and Polyfluoroalkyl Substances.

Wang, D.Z., Goldenman, G., Tugran, T., McNeil, A., Jones, M., 2020. Per- and polyfluoroalkylether substances: identity, production and use, Nordiske Arbejdspapirer. https://doi.org/10.6027/NA2020-901

Wang, Z., Cousins, I.T., Scheringer, M., Buck, R.C., Hungerbühler, K., 2014. Global emission inventories for C4-C14 perfluoroalkyl carboxylic acid (PFCA) homologues from 1951 to 2030, Part I: production and emissions from quantifiable sources. Environ. Int. 70, 62–75. https://doi.org/10.1016/j.envint.2014.04.013

Wang, Z., DeWitt, J.C., Higgins, C.P., Cousins, I.T., 2017. A Never-Ending Story of Per- and Polyfluoroalkyl Substances (PFASs)? Environ. Sci. Technol. 51, 2508–2518. https://doi.org/10.1021/acs.est.6b04806

Wieczorek-Ciurowa, K., Gamrat, K., 2007. Mechanochemicalsyntheses as an example of green processes. J. Therm. Anal. Calorim. 88, 213–217. https://doi.org/10.1007/s10973-006-8098-9

Yan, J.H., Peng, Z., Lu, S.Y., Li, X.D., Ni, M.J., Cen, K.F., Dai, H.F., 2007. Degradation of PCDD/Fs by mechanochemical treatment of fly ash from medical waste incineration. J. Hazard. Mater. 147, 652–657. https://doi.org/https://doi.org/10.1016/j.jhazmat.2007.02.073

Yan, X., Liu, X., Qi, C., Wang, D., Lin, C., 2015. Mechanochemical destruction of a chlorinated polyfluorinated ether sulfonate (F-53B{,} a PFOS alternative) assisted by sodium persulfate. RSC Adv. 5, 85785–85790. https://doi.org/10.1039/C5RA15337A

Zafeiraki, E., Costopoulou, D., Vassiliadou, I., Bakeas, E., Leondiadis, L., 2014. Determination of perfluorinated compounds (PFCs) in various foodstuff packaging materials used in the Greek market. Chemosphere 94, 169–176. https://doi.org/https://doi.org/10.1016/j.chemosphere.2013.09.092

Zhang, D.Q., Zhang, W.L., Liang, Y.N., 2019. Adsorption of perfluoroalkyl and polyfluoroalkyl substances (PFASs) from aqueous solution - A review. Sci. Total Environ. 694, 133606. https://doi.org/10.1016/j.scitotenv.2019.133606

Zhang, K., Cao, Z., Huang, J., Deng, S., Wang, B., Yu, G., 2016. Mechanochemical destruction of Chinese PFOS alternative F-53B. Chem. Eng. J. 286, 387–393. https://doi.org/https://doi.org/10.1016/j.cej.2015.10.103

Zhang, K., Huang, J., Yu, G., Zhang, Q., Deng, S., Wang, B., 2013. Destruction of Perfluorooctane Sulfonate (PFOS) and Perfluorooctanoic Acid (PFOA) by Ball Milling. Environ. Sci. Technol. 47, 6471–6477. https://doi.org/10.1021/es400346n

Zhang, K., Huang, J., Zhang, W., Yu, Y., Deng, S., Yu, G., 2012. Mechanochemical degradation of tetrabromobisphenol A: performance, products and pathway. J. Hazard. Mater. 243, 278—285. https://doi.org/10.1016/j.jhazmat.2012.10.034

Zhang, W., Wang, H., Jun, H., Yu, M., Wang, F., Zhou, L., Yu, G., 2014. Acceleration and mechanistic studies of the mechanochemical dechlorination of HCB with iron powder and quartz sand. Chem. Eng. J. 239, 185–191. https://doi.org/https://doi.org/10.1016/j.cej.2013.11.018

Zhang, Z., Chen, J.-J., Lyu, X.-J., Yin, H., Sheng, G.-P., 2014. Complete mineralization of perfluorooctanoic acid (PFOA) by γ-irradiation in aqueous solution. Sci. Rep. 4, 7418. https://doi.org/10.1038/srep07418

Zhu, H., Kannan, K., 2019. Distribution and partitioning of perfluoroalkyl carboxylic acids in surface soil, plants, and earthworms at a contaminated site. Sci. Total Environ. 647, 954–961. https://doi.org/https://doi.org/10.1016/j.scitotenv. 2018. 08.051

4 Mechanochemical Degradation of Per- and Polyfluoroalkyl Substances in Soil Using an Industrial-scale Horizontal Ball Mill With Comparisons of Key Operational Metrics

4.1 Abstract

Horizontal ball mills (HBMs) have been proven capable of remediating per- and polyfluoroalkyl substances (PFAS) in soil. Industrial-sized HBMs, which could easily be transported to impacted locations for on-site, ex-situ remediation, are readily available. This study examined PFAS degradation using an industrial-scale, 267 L cylinder HBM. This is the typical scale used in the industry before field application. Near-complete destruction of 6:2 fluorotelomer sulfonate (6:2 FTS), as well as the non-target PFAS in a modern fluorotelomer-based aqueous film forming foam (AFFF), was achieved when spiked onto nepheline syenite sand (NSS) and using potassium hydroxide (KOH) as a co-milling reagent. Perfluorooctanesulfonate (PFOS) showed much better and more consistent results with scale-up regardless of KOH. Perfluorooctanoate (PFOA) was examined for the first time using a HBM and behaved similarly to PFOS. Highly challenging field soils from a former firefighting training area (FFTA) were purposefully used to test the limits of the HBM. To quantify the effectiveness, free fluoride analysis was used; changes between unmilled and milled soil were measured up to 7.8 mg/kg, which is the equivalent of 12 mg/kg PFOS. Notably, this does not factor in insoluble fluoride complexes that may form in milled soils, so the actual amount of PFAS destroyed may be higher. Soil health, evaluated through the assessment of key microbial and associated plant health parameters, was not significantly affected as a result of milling, although it was characterized as poor to begin with. Leachability reached 100% in milled soil with KOH, but already ranged from 81 to 96% in unmilled soil. A limited assessment of the hazards associated with the inhalation of PFAS-impacted dust from ball-milling, as well as the cross-contamination potential to the environment, showed that the risk was low in both cases; however, precautions should always be taken.

4.2 Introduction

Per- and polyfluoroalkyl substances (PFAS) are a class of chemicals that have been manufactured and used in a variety of consumer products and industrial processes since the 1960s, which has led to a prevalence of PFAS impacted sites (Andrews et al., 2021; Lin et al., 2020; Milley et al., 2018; Phong Vo et al., 2020; Podder et al., 2021; Sunderland et al., 2019). Their recalcitrance in nature (Sima & Jaffé, 2021) and the extremely low concentrations deemed safe for drinking water consumption

(ITRC, 2021) have created a challenge (ATSDR, 2021; Schlezinger et al., 2020; Schrenk et al., 2020; Timmermann et al., 2020; U.S. National Toxicology Program, 2019a, 2019b). Available remedial options are often matrix-dependent. Remediation of PFAS in water is typically limited to sorption-based technologies (e.g., ion exchange resin, granular activated carbon, etc.) (Du et al., 2014; España et al., 2015; Phong Vo et al., 2020; D. Q. Zhang et al., 2019), which result in secondary waste streams. Destructive PFAS technologies for water are further developed than for soil, such as ultraviolet activated reduction (Bentel et al., 2019; Liu et al., 2022; O'Connor et al., 2023). While technologies are required to restore water to a useable state, addressing on-site sources is often best completed through soil remediation as soils can be an ongoing source of PFAS to the environment; however, again, 'dig and dump' practices simply move the problem and it is also suspect since PFAS have been shown to penetrate engineered liners (Di Battista et al., 2020; Rowe et al., 2023). Traditional impacted-soil destruction methods have not yet been fully demonstrated (Mahinroosta & Senevirathna, 2020). While advances have been made using thermal destruction, complex PFAS transformation chemistry complicates both emissions capture and mass balance closure (Crownover et al., 2019; Duchesne et al., 2020; Stoiber et al., 2020; Watanabe et al., 2016, 2018). Thus, there is a growing need for a simple, proven, PFAS soil destruction technology, especially one that can be conducted on-site.

Mechanochemical destruction of PFAS via ball milling is a candidate for such a technology. Ball mills are typically made up of a cylinder filled with grinding media (typically steel balls) and the product material to be milled. When the cylinder is rotated, the media and material are continually lifted inside the cylinder and cascade down, resulting in the milling of the material into finer sizes via impact and frictional forces. Each impact initiates chemical reactions that have been shown to cause the destruction of organic contaminants (Loiselle et al., 1997; Nah et al., 2008; Sui et al., 2018). Over the last two decades, ball milling has been used successfully to remediate other persistent organic pollutants (M Aresta et al., 2003; Michele Aresta et al., 2004; Birke et al., 2006; Cao et al., 1999; A. K. Hall et al., 1996; Intini et al., 2007; Korolev et al., 2003; Monagheddu et al., 1999; J. H. Yan et al., 2007; K. Zhang et al., 2012; W. Zhang et al., 2014), including PFAS (Cagnetta et al., 2017; Turner et al., 2021; X. Yan et al., 2015; K. Zhang et al., 2013, 2016). These PFAS studies all used planetary ball mills (PBMs), which are small benchtop devices, typically with cylinders less than 0.5 L, which have a double axis of rotation mimicking planetary motion. While this allows for a very high-energy milling environment, capable of achieving accelerations of 50–100 times the force of gravity, scale-up of PBMs beyond the benchtop is not currently possible, nor feasible. Conversely, horizontal ball mills (HBMs) are much simpler, having only a single axis of rotation. While this inherently produces a lower energy density compared to PBMs – 100 to 1,000 times lower (Fokina et al., 2004) – HBMs have now also been shown capable of remediating PFAS (Battye et al., 2022). Unlike PBMs, large-scale HBMs are

readily available, being prevalent in the mining, metallurgy and agricultural industries. Ball milling also stands out when considering not just feasibility, but sustainability. It can be performed at environmental temperatures and pressures, and does not require harsh solvents; these features led to Wieczorek-Ciurowa & Gamrat (2007) classifying it as a green technology.

In a general review of ball milling as a technology to remediate PFAS (Cagnetta et al., 2018), two significant issues were highlighted: 1) noise and fine powder release (related to worker safety); and 2) energy consumption (or operating cost). The first issue can be resolved through personal protective equipment (PPE) and emission capture. The second issue is contingent on the length of time that milling is required to be carried out. Recent studies using actual soils (Turner et al., 2021; 2023) have shown that PFAS degradation follows first order kinetics, with the majority of PFAS being degraded in the first 10–15 minutes. From these studies, the bigger issue was the diminishing degradation thereafter. Turner et al. (2023) provided evidence that PFAS degradation was linked to soil grain fracturing, a process that releases electrons and other surface reducing radicals, which assist in PFAS degradation through chemical reductive mechanisms. Various reductive-based mechanisms have been demonstrated in aqueous mediums (Patch et al., 2022; Trojanowicz et al., 2019, 2020). Parameters that influence particle size reduction include mill speed, which is determined as a percentage of the critical speed (the speed at which the centrifugal forces equal gravitational forces and balls stop falling from the shell), ball filling ratio, powder filling ratio (only valid in batch milling), ball size distribution (controlled in a batch milling setup), and grinding residence time. The optimal ball mill operating conditions will also vary with the material being treated.

The characteristics of the milled material that will have an impact on the milling performance are the material hardness, moisture content, feed particle size distribution, and target product size distribution. When ball mill grinding is being completed efficiently, i.e., where the factors of speed, powder, and grinding media filling ratios are optimized, the breakage rate of any given size fraction typically also follows a first order equation. Turner et al. (2023) showed the greatest proportion of grain fractures (i.e., particle size reduction) occurred in the first 15 minutes, supporting the link between grain fractures and PFAS degradation; however, the results were not consistent for all soil types examined, so soil mineralogy may also have an effect. Soil moisture content is also known to impact the rate of PFAS degradation (Turner et al., 2021) and Battye et al. (2022) found that 6:2 fluorotelomer sulfonate (FTS) required KOH as a co-milling agent in a HBM to achieve degradation at the 1 L and 25 L scales. Wet soils can be managed through a soil drying process, and the use of KOH leads to higher alkalinity in the soils, which would require secondary treatment after ball-milling. These would add additional operational costs. Further understanding is required so that PFAS remediation can be achieved to the local jurisdictional soil quality guidelines (or to complete mineralization) in the least amount of time to minimize energy consumption and

cost. Questions also remain regarding the status of post-milled soil; specifically, what the newly created physical, chemical, and biological properties are, and what that means for subsequent soil use (i.e., geotechnical properties, additional treatment, disposal requirements, etc.).

The aim of this study was to assess PFAS remediation using an industrial-scale, 267 L cylinder HBM, with simultaneous evaluation of key operational metrics to prepare the technology for future on-site remedial projects. The study consisted of four phases: 1) remedial trials using perfluorooctanesulfonate (PFOS), perfluorooctanoate (PFOA), 6:2 FTS, and aqueous film-forming foam (AFFF) spiked nepheline syenite sand (NSS); 2) remedial trials using two different soil types (a sandy silt and a silty sand) obtained from a firefighting training area (FFTA) at a North American airport; 3) evaluation of soil health and leachability in both unmilled and milled soil, and 4) a human health exposure assessment for PFAS-impacted dust intake via inhalation (and environmental cross-contamination evaluation).

4.3 Materials and Methods

4.3.1 Ball Mill Materials and Soil Preparation

Experimental trials were performed at the industrial-scale ball mill facilities of SGS Canada Inc. in Lakefield, Ontario. A custom process HBM from Titan Process Equipment Ltd was used for all ball mill trials. The internal cylinder volume was 267 L +/- 5% (0.61 m diameter, 0.91 m length) with internal lifter bars. Both the cylinder and lifter bars were composed of stainless steel. The grinding media filling ratios, powder ratios, and optimal speed were selected by SGS Canada Inc. based on prior testing. The grinding media was composed of mild steel and consisted of the following sizes (and weight percent used): 0.038 m (75%), 0.025 m (22.2%), and 0.013 m (2.8%). A 5:1 charge ratio was used (ratio of grinding media to soil by mass – 250 kg of media to 50 kg of soil). Milling was carried out in a dry batch mode at 42 RPM, which is 75% of the critical speed.

The NSS ($Al_2KNaO_8Si_2$) was purchased from Unimin Canada Ltd (CAS# 37244-96-5), and the potassium hydroxide (KOH) from Sigma Aldrich (87.5%, CAS# 1310-58-3). The PFOS (97%, CAS# 1763-23-1), PFOA (98%, CAS# 335-67-1), and 6:2 FTS (97%, CAS# 1763-23-1) were purchased from Synquest Laboratories. The AFFF used to spike the NSS was acquired directly from the tank of a firefighting vehicle and consisted of a modern fluorotelomer-dominant formulation containing 6:2 FtSaB and 6:2 FTS. The PFAS powders were dissolved in 4 L jugs of deionized water (0.125 +/- 0.005 g each), as was the AFFF (15 ml each). Each 50 kg soil charge was then spiked with 8 L of water (2 jugs) of the required PFAS/AFFF and placed in ovens at 30ºC to remove bulk water. They were then mixed by hand using a one-time use disposable scoop. For the PFOS and PFOA (spiked together), and 6:2 FTS,

this corresponds to 0.25 g of PFAS per 50 kg of soil, or 5 mg/kg. For the AFFF, assuming a density close to 1 leads to approximately 15 mg of AFFF per 50 kg of soil, or 0.3 mg/kg. Because of the non-target PFAS load in the AFFF, initial concentrations could not be exactly or entirely determined.

The FFTA soil was obtained from an airport in North America – Soil 1 (a sandy silt) and Soil 2 (a silty sand). The soil arrived in eight 45-gallon drums (full). To prepare the soil charges of 50 kg each, approximately one third of each drum was emptied into new drums to generate 1–2 additional drums for each soil type. All drums were then tumbled with a drum tumbler for 10 minutes to homogenize the material. Approximately 8–10 kg was removed from each drum of similar soil type, topping up from the final drum, as needed, to reach the desired 50 kg weight soil charge. These were then placed in ovens at 30ºC to remove bulk water.

It is important to note that drying the soil in an oven at 30ºC will not remove all moisture, but rather, will remove the bulk water resulting in a dry soil with latent moisture present. This was done to best represent the likely achievable state for any outdoor, field remediation project. Through preliminary trials, this level of drying was also shown to be sufficient to prevent soil from caking to the interior walls of the ball mill cylinder, which severely inhibits PFAS destruction.

4.3.2 Experimental Design

For each of the PFOS and PFOA (spiked together), 6:2 FTS, and AFFF spiked NSS charges, as well as the FFTA Soil 1 and Soil 2 charges, trials were run with and without KOH pellets as a co-milling reagent and replicated once; when used, the amount of KOH was set at 100:1 (mass soil to mass KOH) based on experimental necessity as lower ratios were found to cause severe caking inside the HBM (Battye et al. (2022) used a 4:1 ratio for their trials at the 1 L and 25 L scale). This resulted in an approximate KOH:PFAS mass ratio of 1,000:1 for the PFOS and PFOA trials (spiked together), and 2,000:1 for the 6:2 FTS trials. Equivalent mass ratios for the AFFF spiked NSS and FFTA soils cannot be accurately estimated due to the unquantifiable load of non-target PFAS. Three replicate trials of 6:2 FTS spiked NSS with KOH were performed and only a single trial without. In total, 12 trials were run using spiked NSS and 10 trials using FFTA soils. During each of these trials, duplicate soil samples were collected using a one-time use disposal plastic scoop prior to the start of milling (T0), every 10 minutes across the first hour (i.e., T10, T20, T30, T40, T50, and T60), after one and a half hours (T90), and after 2 hours (T120), with soil being collected from a variety of locations within the ball mill and composited to try and overcome heterogeneity issues. The milling parameters for each trial are provided in Table B-S1.

4.3.3 Sample Extraction and Analysis

Sample extraction followed the same procedures as those listed in Duchesne et al., (2020). Briefly, they were extracted by adding 5 mL of basic methanol (0.1% ammonium hydroxide v/v) to approximately 1.0 g of soil in a 15 mL c-tube, then vortexed for 30 seconds, then placed on an end-over-end shaker at 30 rotations per minute (RPM) for 48 hours. Samples were then centrifuged at 4000x RPM for 20 minutes, and a sub-sample was taken and diluted with water/methanol (50/50) into an high-performance liquid chromatography (HPLC) vial for analysis.

An Agilent 6460 MS/MS coupled to an Agilent 1260 HPLC system and a ThermoFisher Exploris 120 Orbitrap coupled to a Vanquish Ultra-High-Performance Liquid Chromatography (UHPLC) system (high-resolution accurate mass spectrometry – HRAM/MS) were used for target (Table B-S2) and non-target (Table B-S3) PFAS analysis, respectively. The associated analytical details can be found with those Tables.

A modified EPA Method 9214 was used for free fluoride analysis, which has been proven successful for other ball mill work (Turner et al., 2021), and the Synthetic Precipitation Leaching Procedure (SPLP) method was modified from USEPA 1312 SPLP and USGS FLT methods, with the main modifications being centrifugation instead of filtering, and an increase of the batch leachate pH from 5.5 to 7 (to better simulate natural conditions). Leachability estimates for unmilled and milled soil were calculated by dividing the concentration of target PFAS found in the soil after applying the SPLP leachate solution by the concentration of target PFAS found in the soil after extracting with basic methanol. For scenarios where the SPLP procedure resulted in more PFAS released than extracted by the methanolic extraction, leachability was reported as 100% (the reasons for this are discussed in Section 4.4.4.2). Full details regarding both these analyses are provided in Appendix B.

The VitTellus® Soil Health Suite was conducted by A&L Laboratories (A&L), located in London, Ontario, Canada. It is a soil health test used primarily by the agricultural industry to assess the chemical, physical, and biological balance of the soil, to assist in the development of agronomic strategies to improve crop yield and farm profitability. Additional details regarding this method have been included in Appendix B.

4.4 Results and Discussion

4.4.1 Nepheline Syenite Sand Trials

4.4.1.1 Target Analysis

At the 267 L scale, 6:2 FTS degradation reached 89 ± 26% in the first 10 minutes and 97% ± 29% after 120 minutes in the three trials with KOH (Figure 4-1a). Perfluoropentanoic acid (PFPeA) was identified as a degradation product, as it has been in other studies involving the degradation of 6:2 FTS (Battye et al., 2022; Lu et al., 2017; Martin et al., 2019). This is coincident with the hypothesized sequence of destruction (Lu et al., 2017). The PFPeA concentrations peaked at T10 (0.63 mg/kg), greater than those of 6:2 FTS for the same time interval (0.38 mg/kg), before being degraded in turn and finishing at slightly higher concentrations than those of 6:2 FTS (0.32 vs. 0.11 mg/kg). No other perfluorocarboxylic acids (PFCAs) were identified. In the single trial conducted without KOH, no significant degradation of 6:2 FTS was found to occur, and no quantifiable PFPeA was produced (Figure 4-1b). These results were similar to the previous study using a HBM at the 1 L and 25 L scales (Battye et al., 2022). The rapid degradation of 6:2 FTS in the presence of KOH is reported to be caused by the formation of hydroxy radicals, which can break C-H bonds (Lu et al., 2017; Zhang et al., 2013). With the removal of hydrogen atoms from the chain, the formation of an alkene 6:2 FTS may occur, which can be readily cleaved with many of the radicals generated by ball milling. Without KOH there are insufficient hydroxy radicals present and the ethylene linker of fluorotelomers (-CH2-CH2-) inhibits their ability to attack the carbon chain (Bentel et al., 2020; Dombrowski et al., 2018; Kucharzyk et al., 2017; Liu et al., 2021b; Ross et al., 2018).

In the AFFF spiked NSS, 6:2 FTS was determined to be the dominant PFAS in the target suite and similar degradation patterns were observed: 98% degradation after 120 minutes with KOH (Figure 4-1c). The average degradation after 10 minutes was noticeably less at 60%. It is hypothesized that the slower rate of degradation was caused by the presence and degradation of the additional non-target PFAS load. Evidence for this includes the fact that PFPeA concentrations immediately exceeded those of 6:2 FTS at T10 (0.088 mg/kg of PFPeA vs 0.0025 mg/kg of 6:2 FTS), and remained elevated after 120 minutes (0.039 mg/kg of PFPeA vs. 0.0012 mg/kg of 6:2 FTS). Despite the high value at T0 that creates the appearance of a degradation curve (Figure 4-1d), without KOH, we suspect no significant 6:2 FTS destruction actually occurred, which would be consistent with the results of the aforementioned 6:2 FTS spiked trials without KOH, as well as those from Battye et al. (2022). Further, there is no characteristic appearance of PFPeA.

Based on the target spike concentrations of 5 mg/kg, following 120 minutes of ball milling at the 267 L scale, PFOS and PFOA were found to undergo 70% and 74%

degradation in the two trials with KOH (Figure 4-1e), and 69% and 70% degradation in the two trials without (Figure 4-1f), with greater than 60% degradation achieved in the first 30 minutes in all cases. The degradation of PFOS in this study is significantly higher and more consistent than that observed in previous HBM work at the 1 L and 25 L scales (Battye et al., 2022). In Battye et al. (2022), PFOS degradation after 180 minutes was only 43 ± 5% and 19 ± 12% with and without KOH, respectively. The increased degradation at the larger 267 L scale is hypothesized to be due to the greater impact energy caused by the soil and media falling a longer distance (i.e., owing to the increased radius of the cylinder). Achieving significant degradation without KOH is notable because it avoids the negative effect of producing highly alkaline (pH 12–14) soil, which would need a pH adjustment step to bring it down to environmentally acceptable levels. PFOA was not used in the prior HBM work, but has been studied in NSS-spiked soils using a PBM (Turner et al., 2021, 2023); in those studies, PFOA degradation reached 90 to 97% with KOH, and 70 to 83% without, after 60 minutes. The greater degradation achieved in Turner et al., (2021, 2023) is attributable to the inherently higher energy output of the PBM. With respect to PFOS and PFOA, which have proven to be the most challenging PFAS to remediate using the HBM, the goal moving forward will be to find ways to re-start the high rate of degradation observed within the first 30 minutes of milling in the NSS trials. Turner et al. (2023) provided evidence that PFAS degradation was linked to soil grain fracturing because of the associated release of electrons; therefore, mixing the milled soil with residual PFAS with additional PFAS-impacted, or even non-impacted, unmilled soil may be all that is needed to do this.

A summary of the hypothesized destruction mechanisms that account for the findings observed herein (as well as those appearing in Chapter 3) is provided in Appendix B.

Heterogeneity in soils, especially at T0, have been noted to be a challenge (Battye et al., 2022; Turner et al., 2021). The average measured T0 values here were 2.1 ± 1.0 mg/kg for PFOS and 2.2 ± 0.42 mg/kg for PFOA, which are below the target spike concentrations of 5 mg/kg. The discrepancy seems to be largely a mixing issue as high variability existed in the T0 measurements, with precision increasing substantially past T0, aided by the natural mixing process that occurs through milling (standard deviations beyond T0 averaged 0.14 and 0.21 mg/kg for PFOS and PFOA, respectively, showing up to an order of magnitude improvement). These latter time points provide clear evidence of degradation. Since the challenge of characterizing bulk soil concentrations increases proportionately with volume, future work will benefit from identifying ways to more thoroughly homogenize and characterize the soils prior to milling them.

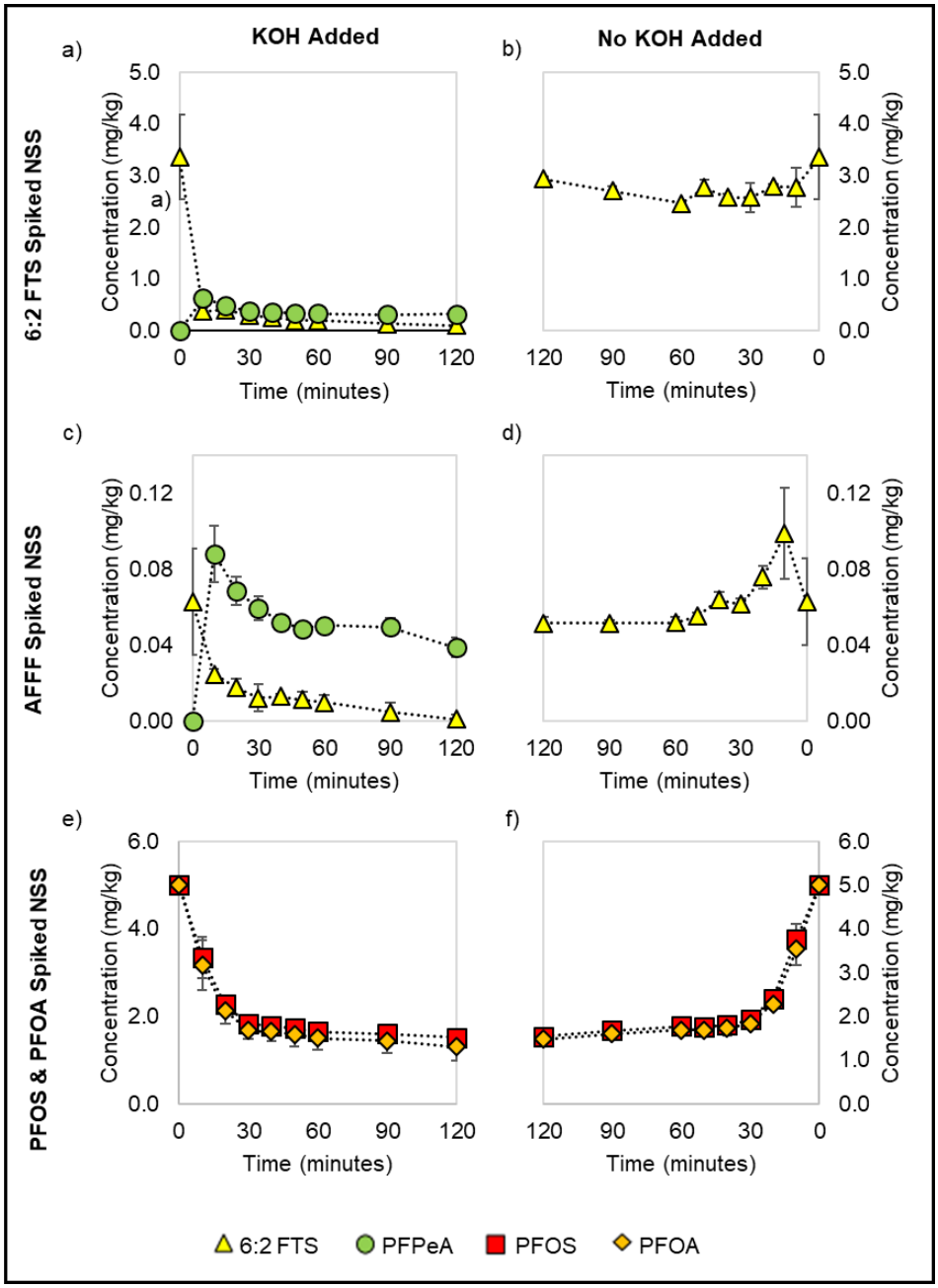

Figure 4-1: MS/MS results for 6:2 FTS, AFFF, and PFOS and PFOA spiked NSS trials, dried, with and without KOH, as a function of milling time (some error bars are too small to be visible). Nominal values were used for PFOS and PFOA for T0 (therefore, no error bars).

4.4.1.2 Non-target Analysis

The AFFF-spiked NSS was also analyzed by HRAM/MS to identify the initial non-target PFAS present as well as the fluorinated degradation products. The data obtained was semi-quantitative because quantification was based on a standard that was not the same as the identified compounds. 6:2 fluorotelomer sulfonamido betaine (FtSaB) was determined to be the dominant initial PFAS compound, averaging 2.0 mg/kg when normalized against the quantifiable 6:2 FTS, which had an average initial concentration of 1.1 mg/kg. Several other non-target PFAS were detected at trace concentrations. With KOH, near-complete degradation was achieved for both 6:2 FtSaB and 6:2 FTS (96% each) (Figure 4-2a). Significant by-products of the degradation included 6:2 fluorotelomer unsaturated sulfonamide (FtUSam), PFPeA, and perfluorobutanoic acid (PFBA) (Figure 4-2b). PFPeA increased the most, achieving an upper concentration of 0.85 mg/kg at T10. After 120 minutes it remained the most prevalent with a concentration of 0.25 mg/kg. Without KOH, 6:2 FtSaB degradation only reached 35% and 6:2 FTS did not undergo any significant degradation (Figure 4-2c). Additional by-products were measured in these trials, including 6:2 fluorotelomer sulfonamido amines (FtSaAm) and 6:2 fluorotelomer sulfonamide (FtSam) (Figure 4-2d). In these trials, 6:2 FtUSam increased beyond PFPeA to a maximum concentration of 0.054 mg/kg, which was still much lower than the remaining 6:2 FtSaB and 6:2 FTS concentrations (1.2 and 0.98 mg/kg, respectively).

Based on the observed transformation products, the hypothesized sequence of degradation is illustrated in Figure 4-3. 6:2 FtSaB is proposed to degrade into either 6:2 FtSaAm or 6:2 FtSam. 6:2 FtSaAm then transforms into 6:2 FtSam, followed by conversion into either 6:2 FtUSam or 6:2 FTS. This sequential pathway is the same as that described in O'Conner et al. (2023) for the destruction of PFAS by aqueous electrons in a UV/sulfite/iodide system. In contrast to that study, PFPeA and PFBA were also observed here, which are concluded to be the degradation products of both 6:2 FtUSam and 6:2 FTS. The degradation of 6:2 FTS into PFPeA and PFBA has been put forth by others (Lu et al., 2017). Conceivably, perfluoropropanoic acid (PFPA) and trifluoroacetic acid (TFA) might also be produced from the step-wise degradation of PFPeA and PFBA, which is why they were included in Figure 4-3, but these PFAS were not detected analytically here. This may also imply that their existence in ball mill remediation is short-lived.

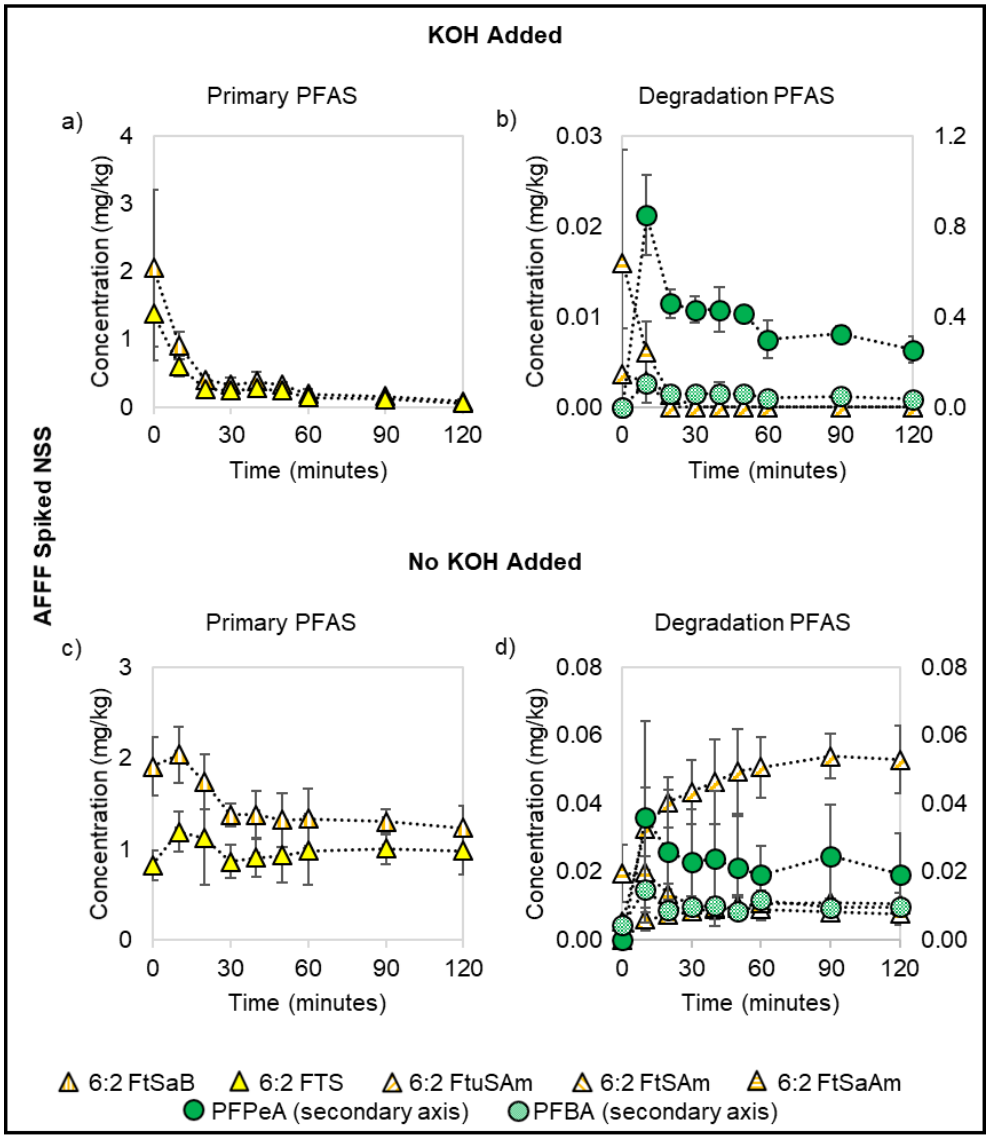

Figure 4-2: HRAM/MS results for AFFF spiked NSS trials, dried, with and without KOH, as a function of milling time (some error bars are too small to be visible). Non-target PFAS concentrations were semi-quantified using 6:2 FTS.

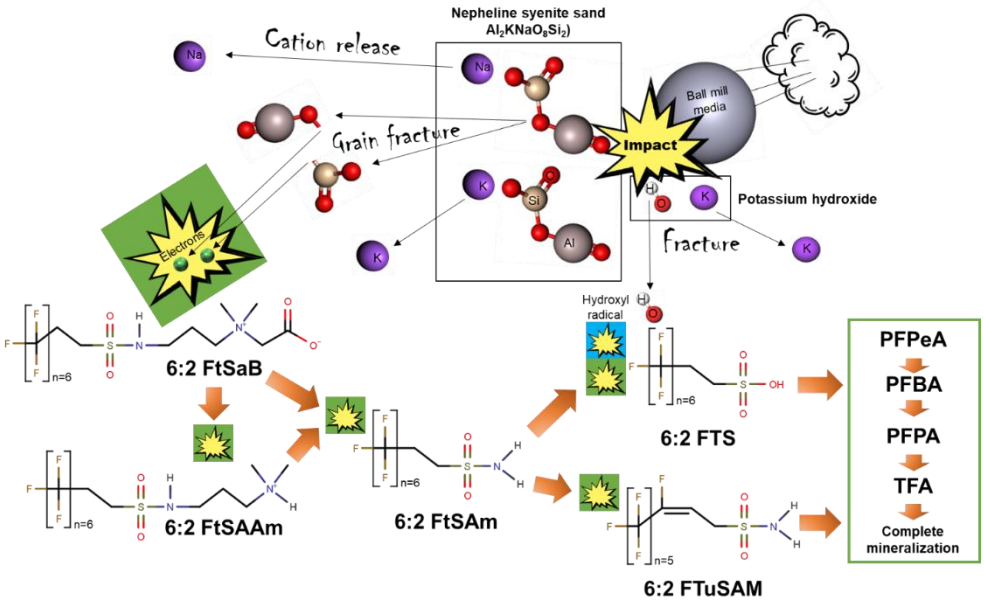

Figure 4-3: Hypothesized sequence of 6:2 FtSaB degradation based on observed by-product formation identified through HRAM/MS. While KOH may be involved in the degradation of all PFAS, it appears to be required only for 6:2 FTS (using a HBM).

4.4.2 FFTA Soil Trials

Soil from a PFAS-impacted field site was used to test the limits of the HBM. The site had two FFTAs, both operational for over 60 years, with various AFFF mixtures used (the most recent ones reported to be Ansul Ansulite, Angus Fire Tridol, and Solberg Re-Healing Training Foam). Both target and non-target analysis was employed. In Soil 1, PFOS was determined to be the dominant compound (up to 5.6 mg/kg), followed by 6:2 FTS (up to 4.5 mg/kg). 8:2 FTS was also detected in Soil 1 at concentrations up to 2.6 mg/kg. Initial screening analyses also showed various PFCAs, perfluoroalkyl sulfonamides (PFSAms), and fluorotelomer betaines (FtBs), but these ended up being below detection in the final analysis because of the dilution levels required to quantify the dominant PFAS. In Soil 2, PFOS was also the dominant compound, though at significantly lower concentrations (up to 0.36 mg/kg). This was followed by 6:2 FTS (up to 0.063 mg/kg). 8:2 FTS was not detected in Soil 2. Similar to Soil 1, various PFCAs, PFSAms, and FtBs were observed in preliminary analyses, but were rendered non-detect in the final analyses

as a result of required dilution, as were FtSam and PFOSA, which were present only in untreated Soil 2.

For Soil 1, with KOH, PFOS, 6:2 FTS, and 8:2 FTS underwent 31 ± 5.4, 17 ± 5.9, and 33 ± 17% degradation, respectively (Figure 4-4a); without KOH, degradation of these compounds was 50 ± 31%, 46 ± 13%, and 55 ± 14%, respectively (Figure 4-4b). The apparent observation of more PFAS destruction without KOH than with KOH (based on the PFOS, 6:2 FTS, and 8:2 FTS concentrations alone) was originally unexpected, as previous studies and experiments earlier in this work have identified the importance of KOH as a co-milling reagent. In the case where KOH was used, it is hypothesized that a significant quantity of uncharacterized non-target PFAS compounds were undergoing degradation and converting into PFOS, 6:2 FTS, and 8:2 FTS, off-setting the actual degradation of these compounds. Evidence for this is more apparent in Soil 2, where concentrations of PFOS, 6:2 FTS, and 8:2 FTS were found to increase following milling (Figure 4-4c,d). This was likely dominant in Soil 2 due to the lower concentrations of target PFAS than compared to Soil 1.

Because of the difficulties in characterizing the PFAS and the complexities created through PFAS transformation, free-fluoride analysis was used to provide better insights into ball milling effectiveness and PFAS destruction. In Soil 1, the change in extractable fluorine from unmilled to milled soil was 6.0 ± 0.21 mg/kg and 3.4 ± 0.37 mg/kg with and without KOH, respectively (Figure 4-4a,b), proving that more PFAS was indeed degraded in the presence of KOH. In Soil 2, despite the significantly increased concentrations of PFOS, 6:2 FTS, and 8:2 FTS, the change in extractable fluoride was 7.8 ± 0.17 mg/kg and 2.6 ± 0.22 mg/kg with and without KOH, respectively (Figure 4-4c,d), suggesting that the total organofluorine load in these soils may be similar, but the amount of known (i.e., target) PFAS is lower in Soil 2. For context on PFAS destruction, the upper free fluoride amounts measured in Soil 1 and Soil 2 represent the equivalent of 9.2 and 12 mg/kg of PFOS, respectively.

Turner et al. (2023) showed that fluoride can be both generated and lost during ball milling with soil. While the generation of fluoride is largely attributable to the destruction of PFAS, fluoride loss is thought to be due to the formation of insoluble fluoride complexes, such as Si-F (Turner et al., 2023). Fluoride loss was measured by Turner et al. (2023) to be up to 95% depending on soil type (range was 64 to 95%). This finding explains the lack of fluoride recovery in previous ball mill work using soils (Battye et al., 2022; Turner et al., 2023). Free fluoride loss would result in an underrepresentation of the amount of PFAS destroyed.

As energy consumption (or operating cost) was listed as a significant consideration in the evaluation of ball milling as a remedial technology (Cagnetta et al., 2018), the power requirements were tracked as part of the FFTA soil trials. These were observed to be fairly steady throughout the duration of each 50 kg soil trial at 0.22 kWh per trial, which works out to 0.0044 kWh / kg soil, or 4.4 kWh / tonne. Based on actual free fluoride increases measured before and after milling, converted into equivalent PFOS concentrations, the power requirements per mg/kg PFOS destroyed were 0.024 and 0.018 kWh / mg/kgPFOS for Soil 1 and Soil 2, respectively. Notably, these values do not account for insoluble fluoride complexes that may have formed in these soils; therefore, the power requirements per mg/kg PFAS destroyed are likely lower.

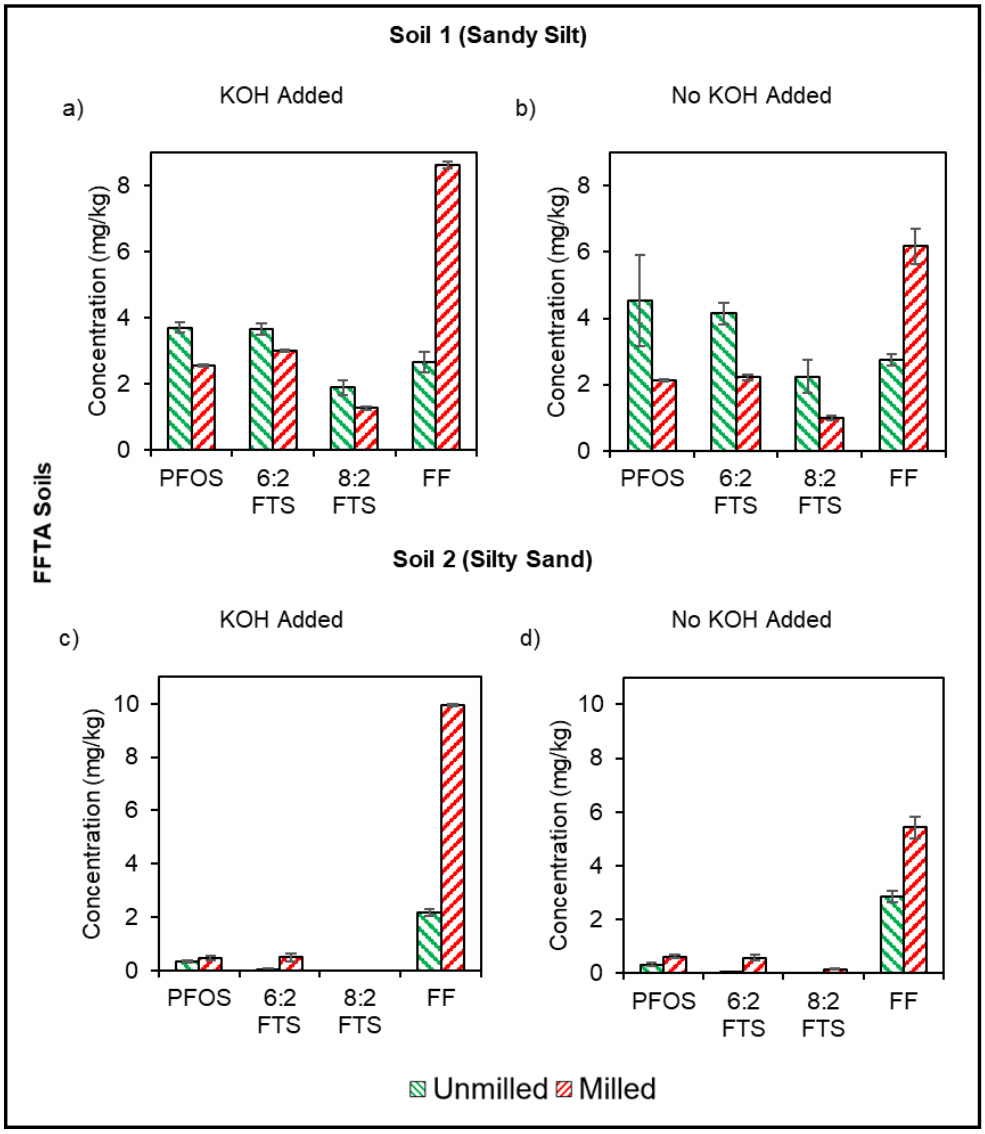

Figure 4-4: Initial (unmilled) and final (milled) concentrations of detectable PFAS, as well as the associated free fluoride results, for FFTA Soil 1 and 2, dried, with and without KOH.

4.4.3 Challenges and Future Design Considerations

The experiments conducted herein represent the first attempted scale-up of ball milling to destroy PFAS. Several logistical and analytical opportunities were identified to guide future optimization. These are discussed below along with our proposed future design considerations.

Heterogeneity of PFAS concentrations, primarily in unmilled soil (i.e., T0), created a degree of uncertainty, which will likely be proportional with increasing soil volumes. The standard mixing technique used to homogenize soil is tumbling, which is essentially the same process as ball milling, but without the media (in fact, ball milling is a recognized mixing technique). However, even without steel grinding media, tumbling soil may initiate PFAS degradation as the soil particles themselves act as media, grinding and colliding against each other (Lange, 2023). Thus, this technique cannot be used. Incomplete mixing was concluded to be the main cause of the high standard deviations related to the PFOS and PFOA T0 values in the NSS trials, which is why nominal concentration values (mass of PFAS added to mass of soil) were used. To overcome this limitation, modifications to the experimental design, such as sieving all soil to <2 mm particle size, collecting a greater number of T0 replicates, and using larger subsample sizes during extraction should be investigated in subsequent work.

With several other studies having identified the difficulty of quantifying total PFAS present in AFFF impacted matrices due to the presence of PFSA and PFCA precursors (Anderson et al., 2016; Guelfo & Higgins, 2013; McDonough et al., 2019; Patch et al., 2024), there are opportunities to optimize analytical procedures. Advances in analytical methodology, specifically for ball milling investigations, have since been published in parallel works. In recent ball milling work Turner (2024), several complementary analytical techniques were used with great success to help quantify total PFAS concentrations in soils, including liquid chromatography – triple quadrupole tandem mass spectrometry (LC-MS/MS), liquid chromatography – high resolution mass spectrometry (LC-HRMS), a thermally activated direct total oxidizable precursor (dTOP) assay (Göckener et al., 2020, 2021, 2023), and a modified reducible organic fluorine (ROF) assay, using an ultra-violet (UV) activated sulfite/ iodide reduction (UV/S/I) (O'Connor et al., 2023), to quantify the extractable organic fluorine (EOF) by destroying all PFAS and generating fluoride that could then be detected via a fluoride ion selective electrode (ISE). The incorporation of these analytical methodologies and the evaluation of their effectiveness for scaled up ball milling should be the focus of future work. Further work should also investigate complimentary analytical techniques, including X-ray

diffraction analysis (XRD) and proton induced gamma-ray emission (PIGE) to assist with interpretation and understanding of insoluble fluoride complex development.

4.4.4 Milled vs Unmilled Soil Evaluations

4.4.4.1 Evaluation of Soil Quality

Ideally, soil remediated for PFAS on-site using a mobile ball mill set-up would be put directly back into the excavation from which it came after it met jurisdictional soil quality guidelines; however, soil quality is based on other parameters besides PFAS. An evaluation of soil quality was conducted using an analytical package common in the agricultural industry, and is referred to as "soil health". In this context, soil health conveys the potential for soils to support agriculture; namely, the growth of plants on the basis of nutrient content and other general chemistry metrics. Microbiological activity can also be measured, which gives an indication of the extent to which soil before and after treatment houses biological microorganisms. While these measured endpoints are not typically used in contaminated site ecological risk assessment, we use them here to determine the potential for the milled soil to support macro-scale organisms and plants, and as a basic evaluation to inform beneficial re-use. Unmilled and milled soil samples were sent to A&L Canada Laboratories (A&L) for their VitTellus® Soil Health analysis and evaluation package. Briefly, it includes the measurement of chemical and physical soil parameters, and uses an algorithm developed by A&L to yield a numerical soil health index value that has been shown to be correlated to crop yield (Verhallen, 2023). The package also reports the presence and abundance of key microbes ('biological quality'), carbon dioxide (CO2) respiration, and mineralizable nitrogen (see Appendix B for more details).

The results showed significant increases in the phytoavailable concentrations of certain inorganic elements in both soil types after milling – most notably magnesium, calcium, and sodium – that were unaffiliated with any of the ball mill materials used (Figure 4-5a,b). It is hypothesized that these elements are released from the crystalline structures of the soil grains as they break apart during milling (Figure 4-3) and become more soluble.

It is notable that poor soil health of starting soils can detract from consequential comparisons to the post-milled soils. All parameters for Soil 1 (sandy silt), initially classified 'low' or 'very low', remained similar after milling, but decreased in the milled samples where KOH was used (Table 4-1). For Soil 2 (silty sand), notable decreases were observed in biological quality, CO2 respiration, and mineralizable nitrification release, even in the milled material without KOH, whereas the soil

health index remained the same. Measurements for all parameters decreased in Soil 2 with KOH (Table 4-1).

Not surprisingly, KOH impacts soil pH. Previous studies used a 4:1 ratio of soil to KOH, which resulted in pH levels in excess of 14 (Battye et al., 2022; Turner et al., 2021). Using a lower soil to KOH ratio of 100:1 in the present study resulted in pH levels of 10, relative to unmilled soil pH of 9.2 (soil 1) and 7.1 (soil 2) (Table 4-1). While these levels would still likely exceed soil quality guidelines, which typically range from about 6-8, it represents a significant improvement. It would be beneficial to determine the least amount of KOH required to achieve the desired PFAS destruction results.

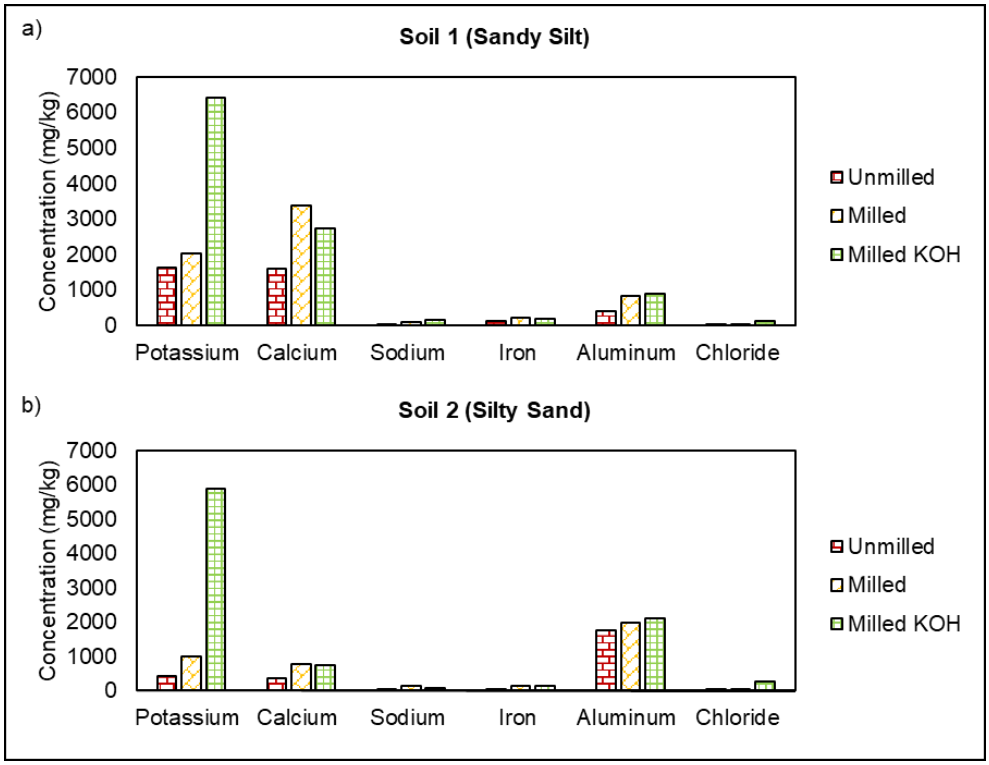

Figure 4-5: Summary of selected phytoavailable inorganic element parameters for unmilled, milled, and milled with KOH, for FFTA Soil 1 and Soil 2.

Table 4-1: Summary of key soil health parameters for unmilled, milled, and milled with KOH, soil samples. Evaluations of "low", "very low", etc., were provided by A&L in the laboratory report.

	Unmilled	Milled	Milled KOH
	Soil 1 (Sandy Silt)		
pH	9.2	9	10.4
Soil Health Index[1]	23 (low)	24 (low)	17 (very low)
Biological Quality[2]	1 (very low)	1 (very low)	0 (none)
CO_2 Respiration (ppm)[3]	5 (low)	5 (low)	2 (low)
Mineralizable Nitrogen	12	12	6
Cation Exchange Capacity (m_{eq}/ 100g)	14	26	34
PFAS Leachability (%)	81	92	100
	Soil 2 (Silty Sand)		
pH	7.1	8	10.2
Soil Health Index[1]	16 (very low)	16 (very low)	10 (very low)
Biological Quality[2]	3 (medium)	1 (very low)	0 (none)
CO_2 Respiration (ppm)[3]	20 (moderate)	7 (low)	2 (low)
Mineralizable Nitrogen	36	16	6
Cation Exchange Capacity (m_{eq}/ 100g)	4	9	20
PFAS Leachability (%)	96	94	100

[1]The Soil Health Index classification is based on a 0 – 60 relative scale that gives an indication of Soil Health ranging from low (0) to high (60). In soils with a low VitTellus® Soil Health Index, plant and nutrient levels do not support optimum microbiological levels resulting in lower nutrient utilization efficiency and lower yields. In soils with a high VitTellus® Soil Health Index, plant and nutrient levels support greater microbiological activity resulting in greater nutrient uptake efficiency and higher yields.

[2]Biological Quality is classified as follows: 0-1: Very Low Soil Microbial Activity - Associated with dry sandy soils and little to no organic matter; 1-2.5: Low Soil Microbial Activity - Soil is marginal in terms of biological activity and organic matter; 2.5-3.5: Medium Soil Microbial Activity - Soil is in moderately balanced condition; 3.5-4: Ideal Soil Microbial Activity - Soil is well supplied with organic matter and has an active population of microorganisms; >4: Unusually High Soil Microbial Activity - Soil has very high level of microbial activity and may have excessive organic matter.

[3]CO2 Respiration is classified as follows: 0-5: Little biological activity - Soil is depleted of organic matter, Biomass < 100 ppm; 6-30: Moderate to Low - Low in organic matter and microbial activity; 31-60: Moderate Level - Soil is approaching ideal levels, applications of active organic matter still recommended; 61-100: Moderate to high - ideal balance of biological activity and adequate organic matter level; >100: High N potential soil - Soil is well supplied with organic matter.

4.4.4.2 Leachability

Synthetic Precipitation Leaching Procedure (SPLP) analysis (at pH 7) was completed on unmilled and milled FFTA Soil 1 and 2 samples (Table 4-1). Based on the target PFAS results, an average of 81% and 96% of the PFAS leached out of the unmilled Soil 1 and 2 samples, respectively. In milled samples, the averages were 92% and 94%, and in milled samples with KOH it reached 100% for both soil types.

The increase in PFAS leachability as a result of milling is likely due to a number of factors. Ball milling transforms PFSAs into PFCAs and degrades long-chain PFAS into shorter-chain PFAS. Short-chain PFCAs tend to be more mobile and readily leach from soils. Significant increases in short-chain PFCAs were observed in both soil types but are likely to be particularly responsible for the big increase in leachability observed between unmilled to milled soil for Soil 1 (sandy silt), 81 to 92 %, respectively. Conversely, in Soil 2 (silty sand), no significant difference in leachability was observed between unmilled (96 %) and milled soil (94 %); however, leachability was notably high to begin with, which may be a result of original soil type (i.e. sandy soils generally have lower organic matter and higher permeability, leading to greater PFAS leaching compared to soils with finer grain sizes or organic carbon content). Soil organic matter can bind to PFAS, reducing leachability, but would be destroyed to some extent during milling, nullifying the effect. The final factor in our experiments leading to increased leachability is pH, which gets raised significantly due to the addition of KOH. Higher pH is known to increase the leachability of some PFAS, which it clearly does here, for both soil types.

Since leachability of PFAS is generally high to begin with, especially anionic PFAS in low-organic material media, from a practical perspective, the difference between unmilled and milled soil is considered relatively unimportant; however, with the use of KOH resulting in 100% PFAS leachability, this could be viewed positively should secondary soil treatment options be employed, such as soil washing, as a polishing step. Alternatively, it would be expected that leachability would revert back to normal once the treated soil pH is buffered.

4.4.5 Assessment of Dust Inhalation

In dry field conditions, the fine-grained portion of PFAS-impacted soil at surface would be expected to be picked up, carried and deposited at some distance in moderate to high winds. While studies have shown many anthropogenic contaminants being mobilized in this way, those related to PFAS are limited (Borthakur et al., 2022; Ismail et al., 2023). Instead, most studies looking at PFAS in dust have been focused inside residential homes and/or fire stations, where the source of PFAS is expected to originate from commercial products (de la Torre et al., 2019; S. M. Hall et al., 2020; Savvaides et al., 2021; Young et al., 2021). In some

cases, the data was used to perform human health exposure assessment for dust intake via oral ingestion (de la Torre et al., 2019).

Ball milling creates dust. This was shown on the FFTA soils by conducting basic textural analyses before and after milling. The Sandy Silt (Soil 1) started with only 16 % (by weight) passing through a #200 sieve (0.075 mm); after milling, that increased to 77 %. And the Silty Sand (Soil 2) initially had 30 % pass the #200 sieve; this increased to an average of 67% post-milling. Grain size analyses were completed at all sampling time intervals. The greatest change consistently occurred in the first interval (from T0 to T20). Only minor grain size changes were observed following that. Any untreated fugitive dust emissions could pose a potential exposure risk for operators. Personal powered air purification respirators (PAPRs) were used by all personnel in the present study and negligible dust mass was obtained. Additionally, two air sampling cyclone units were used to capture respirable-sized particles on a filter cassette. One of these units was positioned next to the ball mill hatch, and another was approximately 5 m away. They were turned on at the beginning of each day and left to run the entire work day. At the end of the experiment (approximately 30 hours of collection time), the filters were removed and brought back to the laboratory for standard, target PFAS soil analysis.

The present study was a controlled pilot scale evaluation of dust and PFAS on dust. The ball mill area was serviced by a 3,000 cubic feet per minute (CFM) Donaldson Torit DW-6 dust collection unit, equipped with high efficiency particulate air (HEPA) filters with a moveable, 20 cm diameter intake hose. This is a standard procedure during ball milling to protect workers from dust and the intake hose was set up next to the ball mill hatch. The associated dust bin for this unit was checked at the end of each week for possible dust sample collection and analysis; however, there was consistently insufficient quantity for analysis. A measurable quantity of PFAS (sum of PFOS, PFOA, and 6:2 FTS) was found on the glass polyurethane foam (PUF) air filter that was caged above the Donaldson Torit DW-6 exhaust vent, but the corresponding air concentrations were negligible compared to the amounts measured in the two air sampling cyclone units.

While the visually detectable dust was zero during operation of the ball mill, and minimal when the hatch was opened to collect soil samples, dust in the air was noticeably present during batch cleanouts following each trial. The PFAS total mass (sum of PFOS, PFOA, and 6:2 FTS) in the air sampling cyclone unit closest to the ball mill was 0.21 µg, and 0.11 µg in the unit 5 m away (Table 4-2); however, a measurable mass of dust could not be obtained with available instrumentation. This is evidence of the small amount of dust that escaped. Cleanouts took place in front of the ball mill (next to the cyclone dust collector beside the ball mill hatch), and

separation of the processed soil and grinding media took place on a large vibrating sieve located between the two cyclone dust collectors. This may account for the similar amounts of PFAS measured at both collectors.

Air concentrations were calculated from the total mass of PFAS (referred to above and in Table 4-2) and the known volume that passed through the cyclone dust collectors (3.6 m^3; 2 L/min air flow rate as per manufacturer's specifications x 30 h). These air concentrations were applied to generic exposure factors to evaluate the potential for inhalation of PFAS impacted dust in areas near ball-milling operations (Table 4-2). Canadian guidance was followed (Health Canada, 2021a), including the selection of toxicological reference values (TRVs) (Health Canada, 2021b) in the toxicity assessment step of the risk assessment, because the ball-milling study was conducted in Canada. Canadian risk assessment guidance is very similar to guidance from other jurisdictions (e.g., USEPA, 1989). Other jurisdictions were additionally considered for the toxicity assessment.

The toxicity assessment identified TRVs for PFOS, PFOA, and 6:2 FTS separately (Health Canada, 2019, 2021a), and for the sum of four PFAS compounds (only PFOS and PFOA values were available in the present study) (Schrenk et al., 2020). The USEPA has suggested lower TRVs for PFOS and PFOA (USEPA, 2022); although these values are interim at present, they were also used to assess dust intake by workers. Health Canada and the European Union have proposed maximum limits of PFAS in water based on sums of a large suite of compounds (European Union, 2020; Health Canada, 2023) but the health-based derivations of the proposed limits have not been published. For the purposes of the present study, we derived a TRV from the lower of these values, which was the Health Canada (2023) value of 30 ng/L, assuming exposure factors described in Health Canada (2018).

The risk characterization summarized in Table 4-2 suggests that there is negligible risk from exposure to the PFAS in the collected dust as the hazard quotients (dose/TRV) were all less than 0.2 (Health Canada, 2021a), except for the sum of four PFAS compounds (in this case only PFOS and PFOA), which gave a hazard quotient of 3.6, or the very protective interim USEPA values (USEPA, 2022) are used. The orders of magnitude differences seen in the TRVs and resulting hazard quotients associated with updates and reconsideration of PFAS toxicity – USEPA (2016) vs USEPA (2022) – highlights the dynamic nature of PFAS risk assessment, with a trend towards more protective values. Therefore, proper precautions should always be taken when working with PFAS-impacted materials. This is particularly relevant for ball-milling methods like the one used in the present paper. Even if the ball mill remediation technology were to use a continuous feed system as expected for on-site remediation, with forced-air fine particulate soil removal to eliminate the need for

repetitive cleanouts, workers conducting general maintenance and/or repair work may still be exposed to dust. As such, it is advisable that appropriate health and safety procedures, including the use of personal protective equipment (PPE), be followed.

From an environmental or hypothetical field set-up perspective, these results are also positive in that they show that even in a basic batch ball mill setup, little PFAS-impacted dust escaped that might lead to cross-contamination of the area in which the ball mill is placed. The assessment of dust inhalation performed herein was based on limited and preliminary results and should be validated in other scenarios and scales.

Table 4-2: Summary of dust concentrations in air and risk calculations for exposure to PFAS via dust inhalation for 10 hours per day.

Parameter	PFOS	PFOA	6:2 FTS	PFOS+PFOA	Sum PFAS
Mass on filter nearest ball mill (µg)	0.119	0.071	0.024	0.19	0.21
Mass on filter 5 m distant (µg)	0.063	0.032	0.016	0.1	0.11
Maximum C_{air} (mg/m^3)*	3.31E-05	1.97E-05	6.67E-06	5.28E-05	5.83E-05
Inhalation rate of air (m^3/d)	10 hours/day x 1.4 m^3/hour** = 14				
Dose (mg/kg BW-day)†	6.55E-06	3.91E-06	1.32E-06	1.05E-05	1.16E-05
TRV-1 (mg/kg BW-day)	6.0E-05[1]	2.1E-05[1]	2.1E-05[12]‡	6.3E-04[3]	3.2E-06[45]‡
TRV-2 (mg/kg BW-day)	7.9E-09[6]	1.5E-09[6]	-	-	-
Hazard quotient-1 (Dose/TRV)	0.11	0.19	0.063	0.017	3.6
Hazard quotient-2	829	2604			

*C_{air} (mg/m^3) = (mass on filter (µg)/1000 µg/mg)/86.4 m^3)

**From Health Canada 2021a, construction/utility worker exposure factors, Appendix E.

†Example calculation: 2.7E-07 mg/kg BW-day = 33.1 mg/m^3 x 14 m^3/day x 1 (relative absorption factor)/70.7 kg (body weight, BW, from Health Canada 2021a)

[1]Health Canada (2021b)

[2]Health Canada (2019)

[3]EFSA (2020)

[4]Health Canada (2023)

[5]Health Canada (2018)

[6]USEPA (2022)

‡The drinking water screening value for 6:2 FTS is identical to that for PFOA and therefore the same TRV is used. For the sum of all PFAS, the proposed drinking water value of 30 ng/L in Health Canada 2023 was converted to a TRV using exposure factors used in Health Canada 2018 as follows: {[(30 ng/L)/1,000,000 mg/ng] x 1.5 L/day (water ingestion rate)}/(70.7 kg body weight x 0.2 allocation factor for drinking water) = 3.2E-06 mg/kg BW-day.

4.5 Conclusions

This was an industrial-scale study evaluating a 267 L cylinder HBM for remediation of PFAS in soil. Comparisons of soil health and PFAS leachability on both unmilled and milled soil were also conducted, as was an evaluation of the potential risk associated with dust intake via oral ingestion to operators while milling, and to the environmental through for cross-contamination. Scale-up continued to show the HBM's effectiveness at destroying 6:2 FTS and other non-target PFAS with KOH under controlled conditions. For these types of PFAS, there is growing confidence that the HBM could be used for field trials. While better and more consistent degradation of PFOS and PFOA was observed with scale-up under controlled conditions, attributed to the greater collision energy imparted onto the soil as a result of the increased falling distance of the media, and the use of KOH is not required, limited degradation after 30 minutes remains an issue that needs to be overcome. Mixing of the PFAS-impacted milled material with unmilled impacted or non-impacted soil may be enough to re-start higher rates of degradation by providing fresh grains that can be cracked to release additional electrons by reductive breakdown mechanisms.

Field soils are inherently more complex naturally, but to test the limits of the HBM, two soils from a FFTA that had been in operation for over 60 years, with a wide variety of elevated PFAS concentrations, were selected. To quantify effectiveness, free fluoride analysis was needed. The maximum increase in extractable fluoride from unmilled to milled samples was 7.8 ± 0.17 mg/kg, which represents the equivalent of 12 mg/kg PFOS. This value does not account for insoluble fluoride complexes, which may form in milled soils; therefore, the actual amount of PFAS destroyed may be greater, but more work is required to confirm this.

Notable observations between the unmilled and milled soil included: increases in various inorganic elements, which are released when the mineral's crystal lattice is fractured during milling; soil health, evaluated through the assessment of key microbial and associated plant health parameters, was not significantly affected as a result of milling, although it was characterized as poor to begin with; and leachability reached 100% in milled soil with KOH, but already ranged from 81 to 96% in unmilled soil. Although the use of KOH leads to environmentally unacceptable alkalinity of the treated soil, the resulting 100% PFAS leachability could be beneficial to secondary soil treatment options, such as soil washing.

The risk associated with inhalation of PFAS impacted dust was negligible using current TRVs; however, the evaluation of PFAS toxicity is a dynamic field, with a trend towards higher levels of protection, so precautions should always be taken when working with PFAS-impacted materials. The results also suggest that the risk of environmental cross-contamination is small. A continuous feed ball mill system (as opposed to the batch system employed for scientific study), as expected to be

used for on-site remediation, would eliminate the need for repetitive cleanouts and further limit operator exposure (and the surrounding environment) to dust, in addition to being a more efficient setup. Complete elimination of dust exposure is unlikely, however, making an evaluation of appropriate PPE and risk management measures a necessity.

4.6 Acknowledgements

Support for this research was provided by the Natural Sciences and Engineering Research Council (NSERC) of Canada (RGPIN-2018-04886; CRDPJ 530133-18) with industry sponsors WSP Canada Inc. and Imperial Oil Limited.

4.7 References

Anderson, R. H., Long, G. C., Porter, R. C., & Anderson, J. K. (2016). Occurrence of select perfluoroalkyl substances at U.S. Air Force aqueous film-forming foam release sites other than fire-training areas: Field-validation of critical fate and transport properties. Chemosphere, 150, 678–685. https://doi.org/https://doi.org/10.1016/j.chemosphere.2016.01.014

Andrews, D. Q., Hayes, J., Stoiber, T., Brewer, B., Campbell, C., & Naidenko, O. V. (2021). Identification of point source dischargers of per- and polyfluoroalkyl substances in the United States. AWWA Water Science, 3(5), e1252. https://doi.org/https://doi.org/10.1002/aws2.1252

Aresta, M, Caramuscio, P., De Stefano, L., & Pastore, T. (2003). Solid state dehalogenation of PCBs in contaminated soil using NaBH4. Waste Management, 23(4), 315–319. https://doi.org/https://doi.org/10.1016/S0956-053X(03)00029-1

Aresta, Michele, Dibenedetto, A., Fragale, C., & Pastore, T. (2004). High-energy milling to decontaminate soils polluted by polychlorobiphenyls and atrazine. Environmental Chemistry Letters , 2(1), 1–4. https://doi.org/10.1007/s10311-003-0057-0

ATSDR. (2021). Toxicological Profile for Perfluoroalkyls - Release May 2021. https://www.atsdr.cdc.gov/toxprofiles/tp200.pdf

Battye, N. J., Patch, D. J., Roberts, D. M. D., O'Connor, N. M., Turner, L. P., Kueper, B. H., Hulley, M. E., & Weber, K. P. (2022). Use of a horizontal ball mill to remediate per- and polyfluoroalkyl substances in soil. Science of The Total Environment, 835, 155506. https://doi.org/https://doi.org/10.1016/j.scitotenv.2022.155506

Bentel, M. J., Yu, Y., Xu, L., Li, Z., Wong, B. M., Men, Y., & Liu, J. (2019). Defluorination of Per- and Polyfluoroalkyl Substances (PFASs) with Hydrated Electrons: Structural Dependence and Implications to PFAS Remediation and Management. Environmental Science & Technology, 53(7), 3718–3728. https://doi.org/10.1021/acs.est.8b06648

Birke, V., Mattik, J., Runne, D., Benning, H., & Zlatovic, D. (2006). Dechlorination of Recalcitrant Polychlorinated Contaminants Using Ball Milling. In V. M. Kolodkin & W. Ruck (Eds.), Ecological Risks Associated with the Destruction of Chemical Weapons (pp. 111–127). Springer Netherlands.

Borthakur, A., Leonard, J., Koutnik, V. S., Ravi, S., & Mohanty, S. K. (2022). Inhalation risks of wind-blown dust from biosolid-applied agricultural lands: Are they enriched with microplastics and PFAS? Current Opinion in Environmental Science & Health, 25, 100309. https://doi.org/https://doi.org/10.1016/j.coesh.2021.100309

Cagnetta, G., Huang, J., & Yu, G. (2018). A mini-review on mechanochemical treatment of contaminated soil: From laboratory to large-scale. Critical Reviews in Environmental Science and Technology, 48(7–9), 723–771. https://doi.org/10.1080/10643389.2018.1493336

Cagnetta, G., Zhang, Q., Huang, J., Lu, M., Wang, B., Wang, Y., Deng, S., & Yu, G. (2017). Mechanochemical destruction of perfluorinated pollutants and mechanosynthesis of lanthanum oxyfluoride: A Waste-to-Materials process. Chemical Engineering Journal, 316, 1078–1090. https://doi.org/https://doi.org/10.1016/j.cej.2017.02.050

Cao, G., Doppiu, S., Monagheddu, M., Orrù, R., Sannia, M., & Cocco, G. (1999). Thermal and Mechanochemical Self-Propagating Degradation of Chloro-organic Compounds: The Case of Hexachlorobenzene over Calcium Hydride. Industrial & Engineering Chemistry Research, 38(9), 3218–3224. https://doi.org/10.1021/ie980790+

Crownover, E., Oberle, D., Kluger, M., & Heron, G. (2019). Perfluoroalkyl and polyfluoroalkyl substances thermal desorption evaluation. Remediation Journal, 29(4), 77–81. https://doi.org/https://doi.org/10.1002/rem.21623

de la Torre, A., Navarro, I., Sanz, P., & de los Ángeles Mártinez, M. (2019). Occurrence and human exposure assessment of perfluorinated substances in house dust from three European countries. Science of The Total Environment, 685, 308–314. https://doi.org/https://doi.org/10.1016/j.scitotenv.2019.05.463

Di Battista, V., Rowe, R. K., Patch, D., & Weber, K. (2020). PFOA and PFOS diffusion through LLDPE and LLDPE coextruded with EVOH at 22 °C, 35 °C, and 50 °C. Waste Management (New York, N.Y.), 117, 93–103. https://doi.org/10.1016/j.wasman.2020.07.036

Du, Z., Deng, S., Bei, Y., Huang, Q., Wang, B., Huang, J., & Yu, G. (2014). Adsorption behavior and mechanism of perfluorinated compounds on various adsorbents--a review. Journal of Hazardous Materials, 274, 443–454. https://doi.org/10.1016/j.jhazmat.2014.04.038

Duchesne, A. L., Brown, J. K., Patch, D. J., Major, D., Weber, K. P., & Gerhard, J. I. (2020). Remediation of PFAS-Contaminated Soil and Granular Activated Carbon by Smoldering Combustion. Environmental Science & Technology, 54(19), 12631–12640. https://doi.org/10.1021/acs.est.0c03058

España, V. A. A., Mallavarapu, M., Naidu, R., & Naidu, R. (2015). Treatment technologies for aqueous perfluorooctanesulfonate (PFOS) and perfluorooctanoate (PFOA): A critical review with an emphasis on field testing. Environmental Technology and Innovation, 4, 168–181.

European Union. (2020). Directive (EU) 2020/2184 of the European Parliament and of the Council of 16 December 2020 on the quality of water intended for human consumption (recast). Official Journal of the European Union, 23.12.2020. https://eur-lex.europa.eu/legal-content/EN/TXT/PDF/?uri=CELEX:32020L2184

Fokina, E., Budim, N., Kochnev, V., & Chernik, G. (2004). Planetary mills of periodic and continuous action. Journal of Materials Science, 39, 5217–5221. https://doi.org/10.1023/B:JMSC.0000039213.44891.7d

Göckener, B., Eichhorn, M., Lämmer, R., Kotthoff, M., Kowalczyk, J., Numata, J., Schafft, H., Lahrssen-Wiederholt, M., & Bücking, M. (2020). Transfer of Per- and Polyfluoroalkyl Substances (PFAS) from Feed into the Eggs of Laying Hens. Part 1: Analytical Results Including a Modified Total Oxidizable Precursor Assay. Journal of Agricultural and Food Chemistry, 68(45), 12527–12538. https://doi.org/10.1021/acs.jafc.0c04456

Göckener, B., Fliedner, A., Rüdel, H., Fettig, I., & Koschorreck, J. (2021). Exploring unknown per- and polyfluoroalkyl substances in the German environment – The total oxidizable precursor assay as helpful tool in research and regulation. Science of The Total Environment, 782, 146825. https://doi.org/https://doi.org/10.1016/j.scitotenv.2021.146825

Göckener, B., Fliedner, A., Weinfurtner, K., Rüdel, H., Badry, A., & Koschorreck, J. (2023). Tracking down unknown PFAS pollution – The direct TOP assay in spatial monitoring of surface waters in Germany. Science of The Total Environment, 898, 165425. https://doi.org/https://doi.org/10.1016/j.scitotenv.2023.165425

Guelfo, J. L., & Higgins, C. P. (2013). Subsurface Transport Potential of Perfluoroalkyl Acids at Aqueous Film-Forming Foam (AFFF)-Impacted Sites. Environmental Science & Technology, 47(9), 4164–4171. https://doi.org/10.1021/es3048043

Hall, A. K., Harrowfield, J. M., Hart, R. J., & McCormick, P. G. (1996). Mechanochemical Reaction of DDT with Calcium Oxide. Environmental Science & Technology, 30(12), 3401–3407. https://doi.org/10.1021/es950680j

Hall, S. M., Patton, S., Petreas, M., Zhang, S., Phillips, A. L., Hoffman, K., & Stapleton, H. M. (2020). Per- and Polyfluoroalkyl Substances in Dust Collected from Residential Homes and Fire Stations in North America. Environmental Science & Technology, 54(22), 14558–14567. https://doi.org/10.1021/acs.est.0c04869

Health Canada. (2019). Water talk: Summary of drinking water values for PFOS, PFOA and other PFAS. https://www.canada.ca/en/services/health/publications/healthy-living/water-talk-drinking-water-screening-values-perfluoroalkylated-substances.html

Health Canada. (2021a). Federal Contaminated Site Risk Assessment in Canada: Guidance on Human Health Preliminary Quantitative Risk Assessment (PQRA). Version 3.0. https://publications.gc.ca/collections/collection_2021/sc-hc/H129-114-2021-eng.pdf

Health Canada. (2021b). Federal Contaminated Site Risk Assessment in Canada: Toxicological Reference Values (TRVs), Version 3.0. https://publications.gc.ca/collections/collection_2021/sc-hc/H129-108-2021-eng.pdf

Health Canada. (2023). Draft objective for per- and polyfluoroalkyl substances in Canadian drinking water: Overview. https://www.canada.ca/en/health-canada/programs/consultation-draft-objective-per-polyfluoroalkyl-substances-canadian-drinking-water/overview.html

Intini, G., Cangialosi, F., L.Liberti, D.Lupo, Notarnicola, M., & Pastore, T. (2007). Mechanochemical treatment of contaminated marine sediments for PCB degradation. Chemistry for Sustainable Development, 15, 147–156.

Ismail, U. M., Elnakar, H., & Khan, M. F. (2023). Sources, Fate, and Detection of Dust-Associated Perfluoroalkyl and Polyfluoroalkyl Substances (PFAS): A Review. Toxics, 11(4). https://doi.org/10.3390/toxics11040335

ITRC. (2021). PFAS Fact Sheets. PFAS Water and Soil Values Table Excel File. https://pfas-1.itrcweb.org/fact-sheets/ (accessed 2021-06-08)

Korolev, K., Golovanova, A. I., Maltseva, N. N., Lomovskiy, O. I., Salenko, V. L., & Boldyrev, V. V. (2003). Application of mechanical activation to decomposition of toxic chlorinated organic compounds. Chem. Sustain. Dev., 11, 489–496.

Kudo, N. (2015). Metabolism and Pharmacokinetics. In Toxicological Effects of Perfluoroalkyl and Polyfluoroalkyl Substances (J. C. DeWitt (ed.)). Humana Press.

Lange, F. (2023). Analysis of leachable, extractable, and non-extractable PFAS in contaminated soils – how to measure "total PFAS"? Fluoros 2023.

Lin, Y., Jiang, J.-J., Rodenburg, L. A., Cai, M., Wu, Z., Ke, H., & Chitsaz, M. (2020). Perfluoroalkyl substances in sediments from the Bering Sea to the western Arctic: Source and pathway analysis. Environment International, 139, 105699. https://doi.org/https://doi.org/10.1016/j.envint.2020.105699

Liu, Z., Chen, Z., Gao, J., Yu, Y., Men, Y., Gu, C., & Liu, J. (2022). Accelerated Degradation of Perfluorosulfonates and Perfluorocarboxylates by UV/Sulfite + Iodide: Reaction Mechanisms and System Efficiencies. Environmental Science & Technology, 56(6), 3699–3709. https://doi.org/10.1021/acs.est.1c07608

Loiselle, S., Branca, M., Mulas, G., & Cocco, G. (1997). Selective Mechanochemical Dehalogenation of Chlorobenzenes over Calcium Hydride. Environmental Science & Technology, 31(1), 261–265. https://doi.org/10.1021/es960398s

Lu, M., Cagnetta, G., Zhang, K., Huang, J., & Yu, G. (2017). Mechanochemical mineralization of "very persistent" fluorocarbon surfactants – 6:2 fluorotelomer sulfonate (6:2FTS) as an example. Scientific Reports, 7(1), 17180. https://doi.org/10.1038/s41598-017-17515-7

Mahinroosta, R., & Senevirathna, L. (2020). A review of the emerging treatment technologies for PFAS contaminated soils. Journal of Environmental Management, 255, 109896. https://doi.org/10.1016/j.jenvman.2019.109896

Martin, D., Munoz, G., Mejia-Avendaño, S., Duy, S. V., Yao, Y., Volchek, K., Brown, C. E., Liu, J., & Sauvé, S. (2019). Zwitterionic, cationic, and anionic perfluoroalkyl and polyfluoroalkyl substances integrated into total oxidizable

precursor assay of contaminated groundwater. Talanta, 195, 533–542. https://doi.org/https://doi.org/10.1016/j.talanta.2018.11.093

McDonough, C. A., Guelfo, J. L., & Higgins, C. P. (2019). Measuring Total PFASs in Water: The Tradeoff between Selectivity and Inclusivity. Current Opinion in Environmental Science & Health, 7, 13–18. https://doi.org/10.1016/j.coesh.2018.08.005

Milley, S. A., Koch, I., Fortin, P., Archer, J., Reynolds, D., & Weber, K. P. (2018). Estimating the number of airports potentially contaminated with perfluoroalkyl and polyfluoroalkyl substances from aqueous film forming foam: A Canadian example. Journal of Environmental Management, 222, 122–131. https://doi.org/10.1016/j.jenvman.2018.05.028

Monagheddu, M., Mulas, G., Doppiu, S., Cocco, G., & Raccanelli, S. (1999). Reduction of Polychlorinated Dibenzodioxins and Dibenzofurans in Contaminated Muds by Mechanically Induced Combustion Reactions. Environmental Science & Technology, 33(14), 2485–2488. https://doi.org/10.1021/es9809206

Nah, I. W., Hwang, K.-Y., & Shul, Y.-G. (2008). Effect of metal and glycol on mechanochemical dechlorination of polychlorinated biphenyls (PCBs). Chemosphere, 73(1), 138–141. https://doi.org/10.1016/j.chemosphere.2008.04.051

O'Connor, N., Patch, D., Noble, D., Scott, J., Koch, I., Mumford, K. G., & Weber, K. (2023). Forever no more: Complete mineralization of per- and polyfluoroalkyl substances (PFAS) using an optimized UV/sulfite/iodide system. The Science of the Total Environment, 888, 164137. https://doi.org/10.1016/j.scitotenv.2023.164137

Olsen, G. W., Mair, D. C., Lange, C. C., Harrington, L. M., Church, T. R., Goldberg, C. L., Herron, R. M., Hanna, H., Nobiletti, J. B., Rios, J. A., Reagen, W. K., & Ley, C. A. (2017). Per- and polyfluoroalkyl substances (PFAS) in American Red Cross adult blood donors, 2000-2015. Environmental Research, 157, 87–95. https://doi.org/10.1016/j.envres.2017.05.013

Patch, D., O'Connor, N., Koch, I., Cresswell, T., Hughes, C., Davies, J. B., Scott, J., O'Carroll, D., & Weber, K. (2022). Elucidating degradation mechanisms for a range of per- and polyfluoroalkyl substances (PFAS) via controlled irradiation studies. Science of The Total Environment, 832, 154941. https://doi.org/https://doi.org/10.1016/j.scitotenv.2022.154941

Patch, D., O'Connor, N., Vereecken, T., Murphy, D., Munoz, G., Ross, I., Glover, C., Scott, J., Koch, I., Sauvé, S., Liu, J., & Weber, K. (2024). Advancing PFAS characterization: Enhancing the total oxidizable precursor assay with improved

sample processing and UV activation. Science of The Total Environment, 909, 168145. https://doi.org/https://doi.org/10.1016/j.scitotenv.2023.168145

Petersen, M. S., Halling, J., Jørgensen, N., Nielsen, F., Grandjean, P., Jensen, T. K., & Weihe, P. (2018). Reproductive Function in a Population of Young Faroese Men with Elevated Exposure to Polychlorinated Biphenyls (PCBs) and Perfluorinated Alkylate Substances (PFAS). International Journal of Environmental Research and Public Health, 15(9). https://doi.org/10.3390/ijerph15091880

Phong Vo, H. N., Ngo, H. H., Guo, W., Hong Nguyen, T. M., Li, J., Liang, H., Deng, L., Chen, Z., & Hang Nguyen, T. A. (2020). Poly-and perfluoroalkyl substances in water and wastewater: A comprehensive review from sources to remediation. Journal of Water Process Engineering, 36, 101393. https://doi.org/https://doi.org/10.1016/j.jwpe.2020.101393

Podder, A., Sadmani, A. H. M. A., Reinhart, D., Chang, N.-B., & Goel, R. (2021). Per and poly-fluoroalkyl substances (PFAS) as a contaminant of emerging concern in surface water: A transboundary review of their occurrences and toxicity effects. Journal of Hazardous Materials, 419, 126361. https://doi.org/https://doi.org/10.1016/j.jhazmat.2021.126361

Rappazzo, K. M., Coffman, E., & Hines, E. P. (2017). Exposure to Perfluorinated Alkyl Substances and Health Outcomes in Children: A Systematic Review of the Epidemiologic Literature. International Journal of Environmental Research and Public Health, 14(7). https://doi.org/10.3390/ijerph14070691

Rowe, R. K., Barakat, F. B., Patch, D., & Weber, K. (2023). Diffusion and partitioning of different PFAS compounds through thermoplastic polyurethane and three different PVC-EIA liners. Science of The Total Environment, 892, 164229. https://doi.org/https://doi.org/10.1016/j.scitotenv.2023.164229

Savvaides, T., Koelmel, J. P., Zhou, Y., Lin, E. Z., Stelben, P., Aristizabal-Henao, J. J., Bowden, J. A., & Godri Pollitt, K. J. (2021). Prevalence and Implications of Per- and Polyfluoroalkyl Substances (PFAS) in Settled Dust. Current Environmental Health Reports, 8(4), 323–335. https://doi.org/10.1007/s40572-021-00326-4

Schlezinger, J. J., Puckett, H., Oliver, J., Nielsen, G., Heiger-Bernays, W., & Webster, T. F. (2020). Perfluorooctanoic acid activates multiple nuclear receptor pathways and skews expression of genes regulating cholesterol homeostasis in liver of humanized PPARα mice fed an American diet. Toxicology and Applied Pharmacology, 405, 115204. https://doi.org/https://doi.org/10.1016/j.taap.2020.115204

Schrenk, D., Bignami, M., Bodin, L., Chipman, J. K., del Mazo, J., Grasl-Kraupp, B., Hogstrand, C., Hoogenboom, L., Leblanc, J. C., Nebbia, C. S., Nielsen, E., Ntzani, E., Petersen, A., Sand, S., Vleminckx, C., Wallace, H., Barregård, L., Ceccatelli, S., Cravedi, J. P., … Schwerdtle, T. (2020). Risk to human health related to the presence of perfluoroalkyl substances in food. EFSA Journal, 18(9), e06223. https://doi.org/10.2903/j.efsa.2020.6223

Sima, M. W., & Jaffé, P. R. (2021). A critical review of modeling Poly- and Perfluoroalkyl Substances (PFAS) in the soil-water environment. Science of The Total Environment, 757, 143793. https://doi.org/https://doi.org/10.1016/j.scitotenv.2020.143793

Stoiber, T., Evans, S., & Naidenko, O. V. (2020). Disposal of products and materials containing per- and polyfluoroalkyl substances (PFAS): A cyclical problem. Chemosphere, 260, 127659. https://doi.org/10.1016/j.chemosphere.2020.127659

Sui, H., Rong, Y., Song, J., Zhang, D., Li, H., Wu, P., Shen, Y., & Huang, Y. (2018). Mechanochemical destruction of DDTs with Fe-Zn bimetal in a high-energy planetary ball mill. Journal of Hazardous Materials, 342, 201–209. https://doi.org/https://doi.org/10.1016/j.jhazmat.2017.08.025

Sunderland, E. M., Hu, X. C., Dassuncao, C., Tokranov, A. K., Wagner, C. C., & Allen, J. G. (2019). A review of the pathways of human exposure to poly- and perfluoroalkyl substances (PFASs) and present understanding of health effects. Journal of Exposure Science & Environmental Epidemiology, 29(2), 131–147. https://doi.org/10.1038/s41370-018-0094-1

Timmermann, C. A. G., Jensen, K. J., Nielsen, F., Budtz-Jørgensen, E., van der Klis, F., Benn, C. S., Grandjean, P., & Fisker, A. B. (2020). Serum Perfluoroalkyl Substances, Vaccine Responses, and Morbidity in a Cohort of Guinea-Bissau Children. Environmental Health Perspectives, 128(8), 87002. https://doi.org/10.1289/EHP6517

Trojanowicz, M., Bartosiewicz, I., Bojanowska-Czajka, A., Kulisa, K., Szreder, T., Bobrowski, K., Nichipor, H., Garcia-Reyes, J. F., Nałęcz-Jawecki, G., Męczyńska-Wielgosz, S., & Kisała, J. (2019). Application of ionizing radiation in decomposition of perfluorooctanoate (PFOA) in waters. Chemical Engineering Journal, 357, 698–714. https://doi.org/https://doi.org/10.1016/j.cej.2018.09.065

Trojanowicz, M., Bartosiewicz, I., Bojanowska-Czajka, A., Szreder, T., Bobrowski, K., Nałęcz-Jawecki, G., Męczyńska-Wielgosz, S., & Nichipor, H. (2020). Application of ionizing radiation in decomposition of perfluorooctane sulfonate

(PFOS) in aqueous solutions. Chemical Engineering Journal, 379, 122303. https://doi.org/https://doi.org/10.1016/j.cej.2019.122303

Tsai, M.-S., Lin, C.-Y., Lin, C.-C., Chen, M.-H., Hsu, S. H. J., Chien, K.-L., Sung, F.-C., Chen, P.-C., & Su, T.-C. (2015). Association between perfluoroalkyl substances and reproductive hormones in adolescents and young adults. International Journal of Hygiene and Environmental Health, 218(5), 437–443. https://doi.org/10.1016/j.ijheh.2015.03.008

Turner, L. P., Kueper, B. H., Jaansalu, K. M., Patch, D. J., Battye, N., El-Sharnouby, O., Mumford, K. G., & Weber, K. P. (2021). Mechanochemical remediation of perfluorooctanesulfonic acid (PFOS) and perfluorooctanoic acid (PFOA) amended sand and aqueous film-forming foam (AFFF) impacted soil by planetary ball milling. Science of The Total Environment, 765, 142722. https://doi.org/https://doi.org/10.1016/j.scitotenv.2020.142722

Turner, L. P., Kueper, B. H., Patch, D. J., & Weber, K. P. (2023). Elucidating the relationship between PFOA and PFOS destruction, particle size and electron generation in amended media commonly found in soils. Science of The Total Environment, 888, 164188. https://doi.org/https://doi.org/10.1016/j.scitotenv.2023.164188

U.S. National Toxicology Program. (2019a). Toxicity Report 96: NTP Technical Report on The Toxicity Studies of Perfluoroalkyl Sulfonates (Perfluorobutane Sulfonic Acid, Perfluorohexane Sulfonate Potassium Salt, and Perfluorooctane Sulfonic Acid). https://ntp.niehs.nih.gov/ntp/htdocs/st_rpts/tox096_508.pdf?utm_source=direct&utm_medium=prod&utm_campaign=ntpgolinks&utm_term=tox096

U.S. National Toxicology Program. (2019b). Toxiciy Report 97: NTP Technical Report on The Toxicity Studies of Perfluoroalkyl Carboxylates (Perfluorohexanoic Acid, Perfluorooctanoic Acid, Perfluorononanoic Acid, and Perfluorodecanoic Acid). https://ntp.niehs.nih.gov/ntp/htdocs/st_rpts/tox097_508.pdf?utm_source=direct&utm_medium=prod&utm_campaign=ntpgolinks&utm_term=tox097

USEPA, U. S. E. P. A. (2022). Technical Fact Sheet: Drinking Water Health Advisories for Four PFAS (PFOA, PFOS, GenX chemicals, and PFBS). https://www.epa.gov/system/files/documents/2022-06/technical-factsheet-four-PFAS.pdf

Verhallen, A. (2023). Soil Health as it Relates to Yield. Ontario Soil and Crop Improvement Association. https://www.osciaresearch.org/current-projects/soil-health-as-relates-yield-2020/

Watanabe, N., Takata, M., Takemine, S., & Yamamoto, K. (2018). Thermal mineralization behavior of PFOA, PFHxA, and PFOS during reactivation of granular activated carbon (GAC) in nitrogen atmosphere. Environmental Science and Pollution Research, 25(8), 7200–7205. https://doi.org/10.1007/s11356-015-5353-2

Watanabe, N., Takemine, S., Yamamoto, K., Haga, Y., & Takata, M. (2016). Residual organic fluorinated compounds from thermal treatment of PFOA, PFHxA and PFOS adsorbed onto granular activated carbon (GAC). Journal of Material Cycles and Waste Management, 18. https://doi.org/10.1007/s10163-016-0532-x

Yan, J. H., Peng, Z., Lu, S. Y., Li, X. D., Ni, M. J., Cen, K. F., & Dai, H. F. (2007). Degradation of PCDD/Fs by mechanochemical treatment of fly ash from medical waste incineration. Journal of Hazardous Materials, 147(1), 652–657. https://doi.org/https://doi.org/10.1016/j.jhazmat.2007.02.073

Yan, X., Liu, X., Qi, C., Wang, D., & Lin, C. (2015). Mechanochemical destruction of a chlorinated polyfluorinated ether sulfonate (F-53B{,} a PFOS alternative) assisted by sodium persulfate. RSC Adv., 5(104), 85785–85790. https://doi.org/10.1039/C5RA15337A

Young, A. S., Sparer-Fine, E. H., Pickard, H. M., Sunderland, E. M., Peaslee, G. F., & Allen, J. G. (2021). Per- and polyfluoroalkyl substances (PFAS) and total fluorine in fire station dust. Journal of Exposure Science & Environmental Epidemiology, 31(5), 930–942. https://doi.org/10.1038/s41370-021-00288-7

Zhang, D. Q., Zhang, W. L., & Liang, Y. N. (2019). Adsorption of perfluoroalkyl and polyfluoroalkyl substances (PFASs) from aqueous solution - A review. The Science of the Total Environment, 694, 133606. https://doi.org/10.1016/j.scitotenv.2019.133606

Zhang, K., Cao, Z., Huang, J., Deng, S., Wang, B., & Yu, G. (2016). Mechanochemical destruction of Chinese PFOS alternative F-53B. Chemical Engineering Journal, 286, 387–393. https://doi.org/https://doi.org/10.1016/j.cej.2015.10.103

Zhang, K., Huang, J., Yu, G., Zhang, Q., Deng, S., & Wang, B. (2013). Destruction of Perfluorooctane Sulfonate (PFOS) and Perfluorooctanoic Acid (PFOA) by Ball Milling. Environmental Science & Technology, 47(12), 6471–6477. https://doi.org/10.1021/es400346n

Zhang, K., Huang, J., Zhang, W., Yu, Y., Deng, S., & Yu, G. (2012). Mechanochemical degradation of tetrabromobisphenol A: performance, products and pathway. Journal of Hazardous Materials, 243, 278—285. https://doi.org/10.1016/j.jhazmat.2012.10.034

Zhang, W., Wang, H., Jun, H., Yu, M., Wang, F., Zhou, L., & Yu, G. (2014). Acceleration and mechanistic studies of the mechanochemical dechlorination of HCB with iron powder and quartz sand. Chemical Engineering Journal, 239, 185–191. https://doi.org/https://doi.org/10.1016/j.cej.2013.11.018

5 Mechanochemical Degradation of Per- and Polyfluoroalkyl Substances in Soil From a Firefighter Training Area at Three Scales

5.1 Abstract

Mechanochemistry, and more specifically, ball milling, has been proven capable of remediating per-and polyfluoroalkyl substances (PFAS) in soil. While benchtop planetary ball mills (PBMs) are uncontestably more efficient due to the much greater energy the media (e.g., steel balls) can impart onto the material to be milled, scale-up of these devices beyond the benchtop is not practical. Conversely, horizontal ball mills (HBMs) are available in a wide variety of sizes. Suitably-sized machines could easily be transported to an impacted site for on-site remediation. As a final step before the first field-trial, this study tested the effectiveness of ball milling PFAS-impacted soil from a former firefighting training area (FFTA) at three different scales: a benchtop-scale PBM (0.25 L cylinder), a commercial-scale HBM (1.0 L cylinder), and an industrial-scale HBM (267 L cylinder). Results showed that with the right milling parameters the majority of the non-target PFAS load, up to 93 % on a HBM system, can be degraded (using the PBM it was up to 97 %). The amount of potassium hydroxide (KOH) used as a co-milling reagent was the critical factor and the results suggest a preferential order to PFAS degradation. Other influential factors include media:soil ratios and soil moisture content. Attempts to restart higher rates of degradation showed some indications of success. Overall, the technology works, and further study of these critical factors will make on-site field remediation efforts more efficient and cost-effective.

5.2 Introduction

Per- and polyfluoroalkyl substances (PFAS) are a class of chemicals identified by one or more carbon-fluorine moieties (-CF2 or -CF3) (Wang et al., 2021). They were manufactured and used for a variety of consumer and industrial products and processes since the 1960s (Andrews et al., 2021). Many PFAS are extremely recalcitrant in nature due to a complete lack of, or having limited, biodegradation pathways (Sima & Jaffé, 2021). Because of their toxicity, persistence, bioaccumulation potential, and global spread, perfluorooctane sulfonic acid (PFOS) was listed as a persistent organic pollutant (POP) in Annex B (restriction) of the Stockholm Convention in 2009. Perfluorooctanoic acid (PFOA), part of a group of PFAS called perfluorocarboxylic acids (PFCAs), was listed in Annex A (elimination) in 2019. This was followed by perfluorohexane sulfonic acid (PFHxS) in 2022, and more recently, the entire PFCA group was made a candidate for listing.

Despite this, PFOS, and other PFAS sharing similar characteristics, are still produced in several countries for use in aqueous film forming foam (AFFF), metal plating, electric and electronic parts, photo imaging, hydraulic fluids, and textiles.

The historical use and ongoing production of PFAS has impacted environmental matrices worldwide (Armitage et al., 2006; Ferrey et al., 2012; Garnett et al., 2022; Giesy et al., 2006; Guelfo & Higgins, 2013; Houtz et al., 2013; Kim & Kannan, 2007; Martin et al., 2003; Pan & You, 2010; Rankin et al., 2016). The most significant point sources generally include firefighting training areas (FFTAs) (Barzen-Hanson, Davis, et al., 2017; Barzen-Hanson, Roberts, et al., 2017; Milley et al., 2018; Munoz et al., 2017), where, historically, AFFF was hosed repeatedly on the ground over many years, often with little or no containment. At many of these locations, even though PFAS is no longer being applied, the soil itself now acts as a point source that continues to impact the underlying groundwater, which can then go on to affect private water supply wells and surface water ecosystems. Coupled with more diffuse sources, like landfills, PFAS released to the environment often ends up in waste water treatment plants (WWTPs). Because of this, many biowastes, including biosolids, composts, food wastes, and manures, also become significant sources of PFAS contamination (Bolan et al., 2021) that are then widely reapplied in the environment, causing further impacts.

The most common pathway of exposure for humans is through drinking water, and regulatory values are extremely low. Canada has established a drinking water quality objective of 30 ng/L for the sum total of 25 specific PFAS (Health Canada, 2024). In Europe, total PFAS in drinking water is limited at 500 ng/L, with individual PFAS limited at 100 ng/L (Sadia et al., 2023). And in the United States, the USEPA set Maximum Contaminant Levels for PFOS / PFOA at 4 ng/L, PFHxS, perfluorononanoic acid (PFNA), and hexafluoropropylene oxide dimer acid (HFPO-DA) at 10 ng/L, and a hazard index of 1 (unitless) for mixtures of PFHxS, PFNA, HFPO-DA, and perfluorobutane sulfonate (PFBS) under the Clean Water Act (United States Environmental Protection Agency, 2024). At these extremely low levels, PFAS-free soil becomes critical; otherwise, it will leach the PFAS to surface water and groundwater, which can become drinking water sources for humans. Comparing the levels of PFOS, PFOA, PFHxS, and PFNA in various global environmental media (i.e., rainwater, soils, and surface waters), Cousins et al. (2024) concluded that the levels of PFOA and PFOS in rainwater is often greater than the USEPA's Lifetime Drinking Water Health Advisory levels (0.004 ng/L PFOA and 0.02 ng/L PFOS); the sum of those four PFAS in rainwater is often above the Danish drinking water limit value (2 ng/L); PFOS in rainwater is often above the Environmental Quality Standard for Inland European Union Surface Water (0.65 ng/L); and atmospheric deposition also leads to global soils being ubiquitously

impacted and to be often above proposed Dutch guideline values (>0.1 μg/kg dry weight (dw) of either PFOS or PFOA).

On the remediation front, sorption-based technologies (e.g., ion exchange resin, granular activated carbon, etc.) (Du et al., 2014; España et al., 2015; Phong Vo et al., 2020; D. Q. Zhang et al., 2019) continue to dominate yet result in secondary waste streams. Destructive PFAS technologies are few and mostly geared towards water, such as ultraviolet activated reduction (Bentel et al., 2019; Z. Liu et al., 2022; O'Connor et al., 2023). To address many of the significant PFAS point sources currently present in the environment, such as those present at FFTAs, a PFAS-destruction technology for soil is needed. Traditional methods of destruction for POPs in soil, such as thermal treatment and chemical oxidation, have not yet been fully demonstrated for PFAS (Mahinroosta & Senevirathna, 2020). Hazardous waste combustion technologies making use of commercial incinerators and kilns were considered to have the greatest potential to destroy PFAS, but additional research is needed to address uncertainties associated with the potential formation and control of products of incomplete combustion (PICs) (USEPA, 2020). Complex transformation chemistry complicates emissions capture, and the analytical measurement of residual and emitted / captured PFAS or PICs challenges current analytical abilities to achieve mass balance closure (Duchesne et al., 2020).

The mechanochemical processes that occur inside ball mills enable solid state reactions from mechanical action (Friščić, 2018; Kajdas, 2005) that are not otherwise attainable in ambient conditions. With excitation periods around 10^{-7} s (Kajdas, 2005; Kaupp, 2009; Marinescu et al., 2013), the number of reactions taking place even over a small unit of time is significant and can result in surface plasma generation, piezoelectric effects, and high energy emission of electrons, ions, radicals, neutral particles, or photons that can destroy POPs (M Aresta et al., 2003; Michele Aresta et al., 2004; Birke et al., 2006; Cao et al., 1999; Hall et al., 1996; Intini et al., 2007; Korolev et al., 2003; Monagheddu et al., 1999; J. H. Yan et al., 2007; K. Zhang et al., 2012; W. Zhang et al., 2014). Successful destruction of PFAS using ball mills was first shown with planetary ball mills (PBMs) and PFAS powders (Cagnetta et al., 2017; Lu et al., 2017; Lv et al., 2018; Wang et al., 2021; X. Yan et al., 2015; N. Yang et al., 2023; K. Zhang et al., 2013, 2016; W. Zhang et al., 2014), but has since been shown in porous media and actual field soils (Battye et al., 2022, 2024; Gobindlal et al., 2023a,b; Turner et al., 2021, 2023; N. Yang et al., 2023). Among the variety of co-milling reagents explored, KOH has emerged as the most successful for PFAS destruction (Ateia et al., 2021; Lu et al., 2017; Turner et al., 2021; K. Zhang et al., 2013), as it provides a potassium ion for free fluoride to form soluble potassium fluoride (KF) (Ateia et al., 2021; Turner et al., 2021; K. Zhang et

al., 2013), which can be measured for mass balance calculations, thereby proving PFAS defluorination / destruction.

PFAS degradation in soil in ball mills has been shown to follow first order kinetics (Turner et al. 2023), with the vast majority of PFAS often being degraded by the time the first confirmatory sample is collected (typically within the first 15 minutes of milling). Thereafter, diminishing returns take hold. Finding a way to restart those initially high degradation rates is key to making ball milling a more cost-effective field technology. Turner et al. (2023) showed the greatest proportion of grain fractures (i.e., particle size reduction) also occurred in the first milling interval, suggesting a link between this and PFAS destruction. Grain fracturing releases electrons and other surface reducing radicals that assist in PFAS degradation through chemical reductive mechanisms (Gobindlal, Shields, et al., 2023; Gobindlal, Zujovic, et al., 2023; Turner et al., 2023). Various reductive-based mechanisms have also been demonstrated in aqueous mediums (Patch et al., 2022; Trojanowicz et al., 2019, 2020). Conversely, Battye et al. (2022) found that 6:2 fluorotelomer sulfonate (FTS) required KOH as a co-milling agent in a horizontal ball mill (HBM) to achieve degradation at the 1 L and 25 L scales. This suggests some PFAS may only break down through chemical oxidative mechanisms. KOH can lead to unacceptably high alkalinity in milled soils, so a secondary treatment step would be required, if used, to return it to environmentally / regulatory acceptable levels. Soil moisture has also been shown to inhibit the rate of PFAS degradation (Turner et al., 2021). While wet soils can be managed in the field using a soil drying process, having to carry out any additional steps adds to operational costs, so having a full understanding of these factors is beneficial.

Challenges remain with respect to analytical characterization. There are currently 14,735 individual PFAS listed on the USEPA's CompTox Chemicals Dashboard (v2.4.1, accessed October 8, 2024). This is in part a result of manufacturers altering their PFAS formulations as each new regulatory restriction was introduced. These 'modern' PFAS formulations include such varieties as fluorotelomers (e.g., 6:2 fluorotelomer sulfonate (FtS), 6:2 fluorotelomer alcohol (FtOH), and 6:2 fluorotelomer sulfonamido betaine (FtSaB)), perfluoroethers (e.g., GenX), and perfluorosulfonamides (FSAs) (Barzen-Hanson & Field, 2015; Gomis et al., 2015; Heydebreck et al., 2015; Rayne & Forest, 2009; Strynar et al., 2015; Wang et al., 2013). AFFF formulations are highly variable in terms of the PFAS they contain, as they vary by both manufacturer and year (Houtz et al., 2013; Place & Field, 2012). FFTAs that operated for many years would have been exposed to many different formulations. Further, these 'modern' formulations are not persistent in the environment, but will transform into a series of other PFAS, ultimately ending in more recalcitrant, regulated PFAS (Caverly Rae et al., 2015; Gannon et al., 2016;

Gomis et al., 2015; Hoke et al., 2016; Wang et al., 2015). For example, 6:2 FtOH (unregulated) degrades into 6:2 fluorotelomer unsaturated aldehyde (6:2 FtUAl) (unregulated), which will in turn degrade into regulated PFCAs (Folkerson et al., 2023; Rand et al., 2014). Less than 50 PFAS can easily be quantified, referred to as target PFAS (e.g., PFOS); others, referred to as non-target PFAS (e.g., 6:2 FtOH), can only be semi-quantified because there are no readily available reference standards. Further, some PFAS are charged and can be anionic (e.g., perfluoroalkyl acids (PFAAs)) and fluorotelomer sulfonates (FtSs)), cationic (e.g., perfluoroalkyl sulfonamido amines (PSAAms)), or zwitterionic (e.g., fluorotelomer betaines (FtBs) and fluorotelomer sulfonamido betaines (FtSaBs)). Several classes of PFAS are neutral and / or volatile, which makes them unable to be detected using standard liquid chromatography-mass spectrometry (LC-MS) techniques (Rehman et al., 2023). Mass balance studies on abiotic and biotic samples using fluorine have shown that a large proportion of the extractable organic fluorine (EOF) (15 to 99 %) remains unidentified (Y. Liu et al., 2015). While extensive progress has been made in analyzing PFAS over the years, achieving complete characterization remains elusive. Attempting to do so requires multiple techniques, not all of which are readily available or affordable, and all requiring extensive operator expertise and experience.

This study sought to evaluate the effectiveness of ball milling PFAS-impacted soil derived from a former FFTA at three scales: a benchtop PBM (0.25 L cylinder), a commercial-scale HBM (1.0 L cylinder), and an industrial-scale HBM (267 L cylinder). Ball milling parameters were varied to examine the effects of various amounts of KOH, media:soil ratios, moisture content, as well as means to restart the higher rates of degradation typically observed in the first few minutes of milling.

5.3 Materials and Methods

5.3.1 Ball Mills and Associated Materials

At the benchtop scale, a Retsch PM 100 benchtop PBM was used with a vertically oriented, 0.25 L stainless steel cylinder, and 90 x 0.010 m and 10 x 0.015 m spherical stainless steel media. At the commercial scale, a U.S. Stoneware 3-tier long roll HBM (model #803DVM) was used (1.44 m length, 0.42 m width, and 1.54 m height) with 1 L ceramic (88.5 % Al_2O_3, 6.5 % SiO_2, 2.8 % ZrO_2, and 1.3 % MgO, with trace amounts of Fe_2O_3 and TiO_2) cylinders (size “00”: 0.14 m diameter, 0.14 m height, and 0.07 m opening) and cylindrical (0.02 m diameter, 0.02 m length), high-density, ultra-high fired burundum media (96.34 % Al_2O_3, 2.75 % SiO_2, 0.60 % MgO, and 0.12 % Na_2, with trace amounts of Fe_2O_3 and CaO). And at the industrial scale, a

Titan Process Equipment Ltd HBM was used, with a 267 L stainless steel cylinder (0.61 m diameter, 0.91 m length) with stainless steel internal lifter bars, and American Iron and Steel Institute (A.I.S.I.) 52100 chrome steel media, consisting of the following sizes (and weight percent used): 0.038 m (75 %), 0.025 m (22.2 %), and 0.013 m (2.8 %).

The soil was obtained from a former firefighting training area (FFTA) located in western Canada.

The KOH (87.5 %, CAS# 1310-58-3) was obtained from Sigma Aldrich.

Details of milling parameters (i.e., masses of grinding media, soil, and KOH) used in the various trials is summarized in Appendix C, Table S1.

5.3.2 Sample Extraction and Analysis by LC-MS/MS and LC-HRMS

Approximately 1.0 g of soil was extracted in 5 mL basic (0.1 % ammonium hydroxide v/v) high performance liquid chromatography (HPLC) grade methanol (CAS 67-56-1) in a 15 mL c-tube. Every 10 samples were spiked with 0.02 mL mass-labelled surrogate (5 mg/L, M2PFOS, Wellington Laboratories). Samples were vortexed for 30 s, then placed on an end-over-end shaker at 30 rotations per minute (RPM) for 48 h. Samples were then centrifuged at 4,000 RPM for 20 minutes and diluted with basic methanol to reach ideal concentrations in the extract. Sample pH was measured and adjusted to less than pH 10 with acetic acid (for samples where KOH was included).

Sample extracts were analyzed using the multiple-reaction-monitoring (MRM) mode on an Agilent 6460 MS/MS coupled to an Agilent 1260 high-pressure liquid chromatography (HPLC) system (LC-MS/MS) using a 50 mm × 2.1 µm ACME C18 analytical column and paired guard column with a 5-µL injection volume. Mobile phases consisted of 10 mM ammonium acetate in DI water (A) and 10 mM ammonium acetate in acetonitrile (B). The elution profile started at 90 % A / 10 % B, transitioning to 100 % B over 4 minutes, holding for 2 minutes, then equilibrating at starting conditions for 3 minutes. Blanks were all found to be below the detection limit of 0.1 ng/g PFAS. All controls and replicates were within 30 % of expected values. The Agilent 6460 MS/MS was run with the following source conditions: gas temperature of 250 °C, gas flow rate of 30 psi, sheath gas temperature of 300 °C, sheath gas flow of 12 L/min, negative capillary of 2500 V, and 0 nozzle voltage. A list of target analytes is provided in Appendix C, Table S2.

Samples were also analyzed on a ThermoFisher Exploris 120 Orbitrap coupled to a Vanquish UHPLC system (LC-HRMS) using a 100 mm × 2.1 µm ACME C18

analytical column and paired guard column with a 15-µL injection volume. Mobile phases consisted of 0.1 % acetic acid in DI water (A) and acetonitrile (B). The elution profile started at 90 % A / 10 % B, transitioning to 100 % B over 9 minutes, holding for 2 minutes, then equilibrating at starting conditions for 3 minutes. Internal mass calibration was performed using the RunStart EASY-IC™ system. A heated electrospray ionization source was used for the ionization of samples following HPLC separation and was run in dual polarity mode (voltage 3000+/ 3000-) with a static gas mode, sheath gas of 50 arbitrary units, auxiliary gas of 10 arbitrary units, sweep gas of 4 arbitrary units, ion transfer tube temperature of 325 °C, and vaporizer temperature of 350 °C. Scan parameters were set using a full scan mode (60,000 orbitrap resolution, RF lens 70 %) with a 10 s expected LC peak width. Scan parameters also included an intensity triggered ddMS2 mode, with an isolation window of 1.2 m/z, a normalized collision energy type, HCD collision energy of 50 %, and automatic scan range mode.

Initial samples were processed using Thermo Scientific FreeStyle® software. Within FreeStyle®, the Elemental Composition tool was used to determine initial suspect masses based on visual peak identification (elements in use: nitrogen, oxygen, carbon, hydrogen, sulphur, and fluorine). Isotope simulation was used to identify additional non-target PFAS that were suspected based on the presence of other PFAS commonly found in the formulations. Where initial intensity allowed, MS2 profiles were used to confirm non-target compounds as fluorinated, and high-resolution masses measured were compared to those in literature (D'Agostino & Mabury, 2014; Field, Jennifer A, Sedlak, David, Alvarez-Cohen, 2017; Houtz et al., 2013). AFFF PFAS identities were also confirmed by analyzing National Foam, Ansul, 3M, and Buckeye formulations in inventory. Intensities for all identified PFAS precursors and non-fluorinated surfactants were normalized to the 6:2 FtS calibration curve to allow for a semi-quantitative measure of the compounds (Charbonnet et al., 2021; Nickerson et al., 2021). A list of the non-target analytes covered is provided in Appendix C, Table S3.

5.4 Results and Discussion

5.4.1 Initial Soil Characterization

The non-target PFAS analysis associated with the soil used for the smaller scale experiments (i.e., PBM and 1 L HBM) identified 7:1:2 and 9:1:2 FtB as the dominant compounds. The semi-quantified values were averaged from 24 initial soil (or time 0 – T0) samples and the concentrations were 6.1 ± 2.3 and 5.5 ± 2.5 mg/kg, respectively. Secondary non-target PFAS included 11:1:2, 7:3, and 9:3 FtB, which

had average concentrations of 1.2 ± 0.73, 1.2 ± 0.43, and 1.1 ± 0.50 mg/kg, respectively. Other FtBs, as well as 6:2 FtSaB, were identified, but the average concentrations for these were all below 0.18 mg/kg. The primary target PFAS identified in these samples were PFOS and 8:2 FTS. Concentrations averaged 1.1 ± 0.35 and 0.77 ± 0.24 mg/kg, respectively. Various PFCAs, PFOSA, and 6:2 FTS were identified but the average concentrations for these were all below 0.09 mg/kg. The experiments conducted with the industrial-scale HBM (267 L) used soil from the same storage/shipping barrels as for the smaller scale trials but were carried out 22 months later. The non-target PFAS analysis identified the same dominant compounds, 7:1:2 and 9:1:2 FtB, but at significantly lower concentrations. Averaged from 28 T0 samples, the concentrations were 0.95 ± 0.17 and 0.53 ± 0.08 mg/kg, respectively. The secondary non-target PFAS also included some notable differences. In decreasing order of concentration: 6:2 FtUSam (0.25 ± 0.02 mg/kg), 7:3 FtB (0.13 ± 0.03 mg/kg), 5:1:2 FtB (0.09 ± 0.01 mg/kg), 9:3 FtB (0.08 ± 0.01 mg/kg), 6:2 FtSaB (0.06 ± 0.01 mg/kg), 11:1:2 FTB (0.06 ± 0.01 mg/kg), 6:2 FtSam (0.05 ± 0.004 mg/kg). Other non-target PFAS detected had average concentrations below 0.01 mg/kg. The primary target PFAS in these samples remained PFOS and 8:2 FTS, with averaged concentrations of 0.44 ± 0.03 and 0.35 ± 0.04 mg/kg, respectively. Other target PFAS were identified but average concentrations were all below 0.03 mg/kg.

Heterogeneity is likely the main factor in the different PFAS concentrations observed in the soil associated with the industrial-scale HBM due to the much larger volumes of soil used. Although the soil was excavated from the same site, the volume of soil excavated would have meant extending the excavation both laterally and vertically, both of which would result in varying PFAS concentrations. In particular, PFAS concentrations typical decrease significantly with depth. Interestingly, however, the presence of several known PFAS transformation products (e.g., 6:2 FtUSam, 6:2 FtSaB, 6:2 FtSam) in the list of notable, but secondary, non-target PFAS suggests some transformation had occurred while the soil sat in the storage/shipping barrels in the time between the smaller scale and larger scale experiments were run.

5.4.2 Critical Factor: KOH

In terms of PFAS degradation, the greatest successes in this study were in the trials where the most KOH was used, which was using a soil:KOH ratio of 10:1 (Figure 5-1). Using the benchtop-scale PBM with a 5:1 media:soil ratio (Figure 5-1 a), the primary non-target PFAS, 7:1:2 and 9:1:2 FtB, both underwent permanent, near-complete degradation in the first 10 minutes. A similar trend occurred for 11:1:2

FtB. 7:3 and 9:3 FtB degraded significantly in the first 10 minutes, 92 and 90 %, respectively; however, concentrations of both increased significantly from T10 to T20 (326 and 279 %, respectively), and again from T30 or T40 (74 and 73 %, respectively). Moderate degradation occurred thereafter and the final concentrations were down 65 and 53 %, respectively, from T0. Similar success was observed under the same milling parameters using the commercial-scale HBM (Figure 5-1 b) for 7:1:2, 9:1:2, and 11:1:2 FtB (permanent, near-complete degradation in the first 10 minutes). 7:3 and 9:3 FtB were reduced 77 and 79 %, respectively, after 20 minutes of milling, but then trended higher, ultimately finishing 1.8 % higher and 20 % lower, respectively, from T0.

Notably, this level of success was also achieved where a 3:1 media:soil ratio was used (along with the 10:1 soil:KOH ratio). In both the benchtop-scale PBM (Figure 5-1 c) and commercial-scale HBM (Figure 5-1 d), 7:1:2, 9:1:2, and 11:1:2 FtB all underwent permanent, near-complete degradation in the first 10 minutes. With the benchtop-scale PBM, the concentrations of 7:3 and 9:3 FtB generally trended continuously downward at a slower rate, ultimately finishing 85 and 82 % lower than T0, respectively. With the commercial-scale HBM, 7:3 FtB increased 26 % from T0 to T10 but then dropped 81 % from T10 to T20. After that, concentrations oscillated but remained relatively stable overall. 9:3 FtB decreased 2.5 % from T0 to T10 and then a further 74 % from T10 to T20 before steadying.

KOH ratios of 10:1 were not used in the industrial-scale HBM because these higher KOH ratios led to severe caking inside the mill during previous studies (Battye et al., 2024).

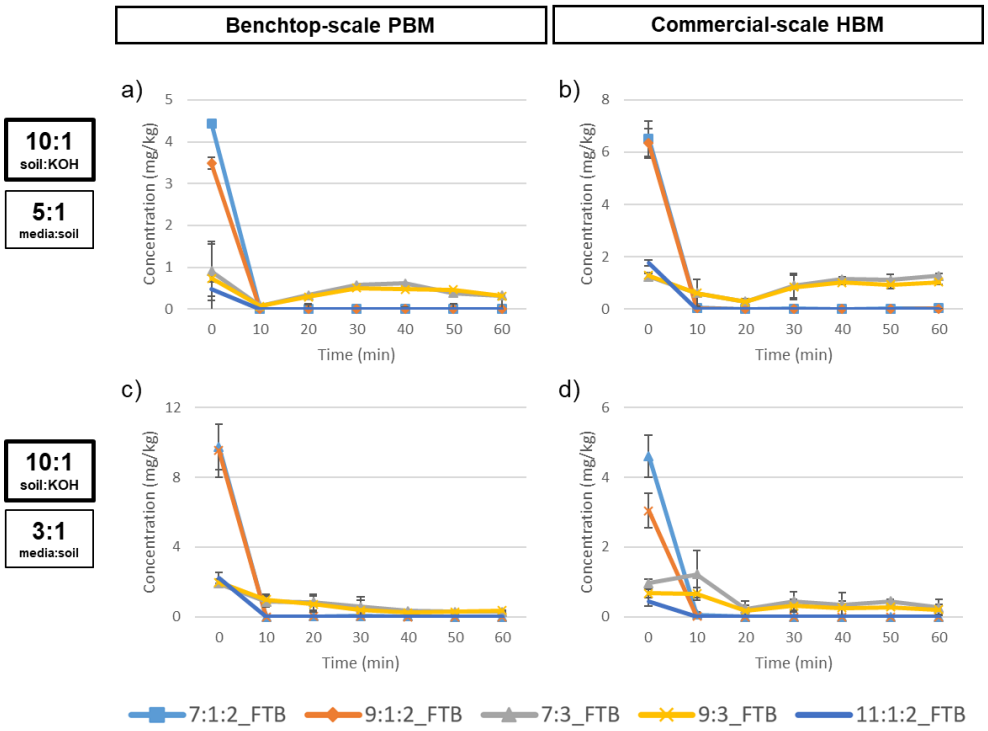

Figure 5-1. Results for benchtop-scale PBM and commercial-scale HBM for 7:1:2, 9:1:2, 11:1:2, 7:3, and 9:3 FtB, using 10:1 soil:KOH ratios along with 5:1 and 3:1 media:soil ratios. Soil was dried for all trials. Data points are presented as means of triplicate samples ± standard deviation.

Insignificant PFAS degradation was observed when lesser amounts of KOH was used (Figure 5-2). With the benchtop-scale PBM and a KOH ratio of 100:1 (and a 5:1 media:soil ratio) (Figure 5-2 a), 7:1:2 and 9:1:2 FtB actually increased in concentration up until T50. Concentrations decreased from T50 to T60, but still finished 40 and 43 % greater than their respective T0 concentrations. 11:1:2 FtB followed a similar pattern and finished 34 % higher. 7:3 and 9:3 FtB also peaked at T50 but saw steeper trends across the first 20 minutes. They finished 141 and 129 % higher, respectively. When no KOH was added (Figure 5-2 d), 7:1:2 FtB increased 37 % from T0 to T10, held relatively steady from T10 to T40, then decreased substantially from T40 to T50 (31 %) and from T50 to T60 (28 %). A similar pattern was observed for 7:3 FtB, where concentrations were up 38 % from T0 to T10, were relatively steady from T10 to T40, and then decreased 20 % from T40 to T50, and

from 32 % from T50 to T60. 9:1:2, 9:3, and 11:1:2 FtB all remained largely unchanged over the course of milling.

With the commercial-scale HBM and a KOH ratio of 100:1, degradation occurred at much slower rates (Figure 5-2 b). After 60 minutes, 7:1:2 and 9:1:2 FtB had degraded 32 and 35 %, respectively, with most of the degradation happening in the first 10 minutes, 35 and 31 %, respectively. 7:3, 9:3, and 11:1:2 FtB were degraded 26, 31, and 39 %, respectively, with most of the degradation happening in the first 10 minutes. Concentrations then remained relatively uniform for the rest of the milling period. When no KOH was used (Figure 5-2 e), 7:1:2, 9:1:2 11:1:2, 7:3, and 9:3 FtB (Figure 5-2) all behaved similarly throughout milling, increasing from T0 to T20, decreasing from T20 to T50, and increasing again from T50 to T60. Ultimately, there were no significant differences in concentrations in any of these PFAS from start to finish.

With the industrial-scale HBM and a KOH ratio of 100:1 (Figure 5-2 c), 7:1:2, 9:1:2, and 11:1:2 FtB degraded 10, 23, and 46 %, respectively, over the course of milling. 7:3 and 9:3 FtB showed significant increases of 196 and 133 %, respectively. The limited degradation here was surprising as the 100:1 soil:KOH ratio was shown to be successful (i.e., near-complete destruction was achieved) in Battye el al. (2024) for 6:2 FTS originating from a modern AFFF spiked onto nepheline syenite sand (NSS). Also in that study, PFOS and PFOA, spiked onto NSS, underwent 70 and 74 % degradation, respectively, with KOH, and 69 and 70 % degradation, respectively, without. Although neither the target nor non-target analysis results in that study showed conclusive success with the FFTA field soils, free fluoride analysis showed increases between unmilled and milled soil of up to 7.8 mg/kg, which is the equivalent of 12 mg/kg PFOS. On that basis, there was evidence to suggest the 100:1 KOH ratio could be successful at this scale. In the trials without KOH (Figure 5-2 f), 7:1:2, 9:1:2, and 11:1:2 FtB increased insignificantly, 2.9, 2.8, and 0.67 %, respectively, over the course of milling, as did 7:3 and 9:3 FtB, 3.9 and 1.1 %, respectively.

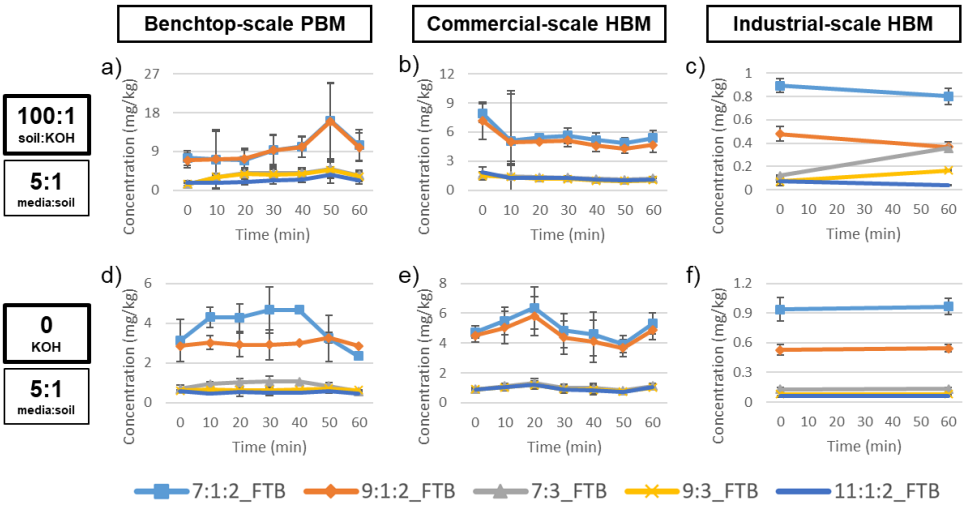

Figure 5-2. LC-HRMS results for all three scales for 7:1:2, 9:1:2, 11:1:2, 7:3, and 9:3 FtB for 100:1 soil:KOH ratios and no KOH. Soil was dried and 5:1 media:soil ratios were used in all trials. Data points are presented as means of triplicate samples ± standard deviation for the benchtop-scale PBM and commercial-scale HBM, and means of duplicate samples across duplicate trials ± standard deviation for the industrial-scale HBM.

Using the benchtop-scale PBM with 10:1 soil:KOH ratios, the primary target PFAS, PFOS and 8:2 FTS, were degraded by 54 and 63 % in the 5:1 media:soil trials, respectively (Appendix C, Figure S1), and 25 and 87 % in the 3:1 media:soil trials, respectively (Appendix C, Figure S2). While the degradation of these two PFAS was relatively consistent across the milling period in the 3:1 trial, in the 5:1 trial, after initial decreases in the first 10 minutes, both PFAS then increased before decreasing again in the final 20 minutes. Although present at much lower concentrations to begin with, relatively speaking, significant increases of various target PFCAs, as well as PFOSA and 6:2 FTS, were observed in the first 10 minutes of milling. While most of these PFAS underwent some reduction after that, in the 5:1 media:soil trials, this was followed by a period of increase between T20 and T40, after which downward trends were re-established, generally after T40. In the 3:1 media:soil trials, many of these PFAS were still trending higher after the same time period. Using 100:1 soil:KOH and 5:1 media:soil ratios, PFOS and 8:2 FTS increased, 53 and 110 %, respectively (Appendix C, Figure S1). All other measurable target PFAS were relatively stable throughout milling. Without KOH, PFOS and 8:2 FTS were both relatively stable throughout milling, until T40 when PFOS decreased 23 %

(from T40 to T50), and then a further 16 % (from T50 to T60). Total reductions for both PFOS and 8:2 FTS ended up being 31 and 6.0 %, respectively (Appendix C, Figure S1). Of the other target PFAS, 6:2 FTS and PFBA had upward trends across most of the milling period; the others were relatively stable.

Using the commercial-scale HBM with 10:1 soil:KOH ratios, PFOS and 8:2 FTS were reduced by 31 and 24 % in the 5:1 media:soil trials, respectively (Appendix C, Figure S1), and 24 and 72 % in the 3:1 media:soil trials, respectively (Appendix C, Figure S2). Notably, in the 5:1 media:soil trials, 8:2 FTS was initially degraded 67 % after 20 minutes before an upward trend was initiated that erased most of the early gains. Conversely, PFOS maintained relatively similar amounts of degradation throughout milling. In the 3:1 media:soil trials, after early degradation of both PFOS (from T0 to T10) and 8:2 FTS (from T20 to T30), oscillating, but relative stable trends were generally maintained. Although present at much lower concentrations, relatively speaking, significant increases of various target PFCAs were observed in the first 20 minutes of milling in the 5:1 media:soil trials. These generally degraded to residual concentrations by the end of milling, except for PFBA, which spiked 63 % from T50 to T60. In the 3:1 media:soil trials, the upward trends generally continued for all secondary target PFAS. With 100:1 soil:KOH ratios (Appendix C, Figure S1), PFOS was degraded 50 % overall, with much of that occurring in the first 10 minutes (32 %). 8:2 FTS degraded 54 % in the first 10 minutes, but then increased 123 % from T10 to T20. Slight degradation was observed after that and it finished 14 % lower than T0 concentrations. Various other PFCAs spiked at T10, but were similar to starting concentrations again by T20, except for PFBA, which spiked again (at roughly a quarter of the magnitude) at T30. Without KOH (Appendix C, Figure S1), concentrations remained similar start to finish, with PFOS down 2.2 % overall and 8:2 FTS up 0.66 % overall, with little fluctuation throughout. Trends for all secondary target PFAS were also generally flat throughout milling.

Using the industrial-scale HBM with 100:1 soil:KOH and 5:1 media:soil ratios, PFOS and 8:2 FTS were degraded 27 and 11 %, respectively, the majority of which happened between T15 and T30 (Appendix C, Figure S3). PFHpA was the only target PFAS measured in these trials, and appeared only at T15 in both trials. Without KOH, degradation was 7.5 and 5.2 % for PFOS and 8:2 FTS, respectively, with concentrations of both PFAS remaining relatively flat throughout milling (Appendix C, Figure S3). No other target PFAS were detected in these trials.

The changes observed in the trials with the greatest amounts of KOH suggest there may be a preferential sequence of PFAS degradation. First, there was large-scale degradation of the long-chain FtBs. Whether this preference is on par with short-chain FtBs is difficult to discern as short-chain FtBs undergo degradation and

creation (from their longer-chain precursor compounds) simultaneously. This also appears true for short-chain FTSs and PFCAs. The degradation of 8:2 FTS was greater than that of PFOS, and was also potentially being created in some of the trials. PFOS, known for being extremely recalcitrant, would be expected to be one of the last PFAS to undergo destruction, which it does here. PFOS also experienced some increases in concentrations, but these may have been within the range of analytical uncertainty or heterogeneity. Alternatively, this observed "creation" could have come from the release from previously non-extractable regions of soil. Similar degradation patterns were observed and similar conclusions made for PFOS in the field soils used in Battye et al (2024), which originated from a different site.

Reduction processes have been shown to degrade PFAS in the following order: PFCAs > PFSAs > fluorotelomers (Bentel et al., 2019; Z. Liu et al., 2021; O'Connor et al., 2023). Conversely, oxidation processes have been shown to degrade fluorotelomers first, followed by PFCAs, with PFSAs being the most resistant (Bruton & Sedlak, 2017; Ross et al., 2018; Vecitis et al., 2009; L. Yang et al., 2020). Our results herein, which more closely follow the latter degradation pathway, along with the clear dependence on the amount of KOH present, suggests oxidation was the limiting chemical reaction pathway during milling. Battye et al (2022; 2024) showed that 6:2 FTS destruction in a horizontal ball mill required KOH (i.e. nucleophilic substitution reactions based on the presence of OH-). With the dominant AFFF species present in our impacted soils being fluorotelomers, KOH is expected to take on extra importance. This is not to suggest that reduction processes did not take place or that they are not required to initiate mechanistic degradation; this has been shown to be the case in previous work where success was achieved using a horizontal ball mill to destroy PFOS and PFOA without the use of KOH (Battye et al., 2024; Battye et al., 2022). Rather, we are suggesting that both reductive and oxidative degradation of PFAS occurs in a ball mill and harnessing both processes may be both necessary and optimal in achieving complete degradation of all PFAS present, especially where complex PFAS mixtures are present, such as they are when dealing with AFFF sources.

It is clear from the results of both the benchtop-scale PBM and commercial-scale HBM that the majority of the non-target PFAS load can be degraded in actual field soils provided sufficient KOH is used. For the trials with 10:1 soil:KOH ratio (including both the 5:1 and 3:1 media:soil ratios), total degradation ranged between 92 and 97 % for the benchtop-scale PBM, and 82 and 93 % for the commercial-scale HBM (calculated using all identified, semi-quantified, non-target PFAS via LC-HRMS). Also clear was that a soil:KOH ratio of 100:1 was not sufficient, nor were the trials without KOH. This is despite success having previously been achieved using the 100:1 soil:KOH ratio on the same industrial horizontal ball mill (Battye et

al., 2024). It is acknowledged that those successes were most apparent for the trials where spiked NSS was used at target concentrations of 5 mg/kg. Although neither the target nor non-target analysis results in that study showed conclusive success with the FFTA field soils, free fluoride analysis showed increases between unmilled and milled soil of up to 7.8 mg/kg, which is the equivalent of 12 mg/kg PFOS. Initially, it was thought that field soils may present more of a challenge because they are inherently more complex both chemically and physically than pristine NSS spiked under controlled conditions, or that PFAS may sorb differently to field soils either initially or over the course of weathering, which may make them more recalcitrant. In combination with the successes using field soils at the smaller scales in this study, it now seems that the issue may simply be that FFTA soils typically have much higher overall PFAS concentrations, and therefore, require correspondingly higher amounts of KOH. If this is true, challenges remain. Liberal amounts of KOH cannot simply be thrown into a ball mill because, being hygroscopic, it introduces moisture and leads to caking inside the mill, which inhibits PFAS degradation both chemically and physically. And even if it could, such a blunt approach is not ideal because increasing amounts of KOH lead to increasingly high alkalinity in the soil. At the 100:1 soil:KOH ratio, pH tends to be in excess of 10, and at the 10:1 ratio, it tends to be in excess of 12. Such pH levels are environmentally unacceptable and treated soil under these conditions would require a pH adjustment step to lower it back to acceptable levels. Commensurate with that, would be the added costs associated with that extra step, not just in relation to the purchase of the KOH, but also for the other reagents required in the pH adjustment step. Accurately characterizing all PFAS present in AFFF is known to be challenging (Anderson et al., 2016; Guelfo & Higgins, 2013; McDonough et al., 2019; Patch et al., 2024). Mass balance studies using fluorine have shown that a large proportion of the available EOF (15 to 99 %) can go unidentified (Y. Liu et al., 2015). This may be due to neutrally-charged and / or volatile PFAS species being present (Rehman et al., 2023), which would require different analytical methods to be employed for full PFAS identification, such as fluorine inductively coupled plasma mass spectrometry (F-ICP-MS), fluorine nuclear magnetic resonance imaging (19F-NMR), combustion ion chromatography (CIC), gas chromatography mass spectrometry (GC-MS), surface enhanced raman scattering spectroscopy (SERS), and photon induced gamma emission (PIGE) (Heuckeroth et al., 2021; Lewis et al., 2023; Rehman et al., 2023; Tabassum et al., 2024), none of which are readily available commercially for PFAS analysis. Modern AFFF formulations are also composed entirely of non-target PFAS, which at best can only be semi-quantified using LC-HRMS.

A well-documented laboratory issue that may also apply to field soils relates to the organic matter content; many authors have shown that the Total Oxidation Precursor

(TOP) assay results in incomplete oxidation of the PFAA precursors due to oxidant exhaustion caused by dissolved organic matter competition (Patch et al., 2024). Hydroxyl radicals break down organic molecules through hydrogen atom abstraction mechanisms and if this action is preferential to PFAS destruction, a similar outcome would ensue where the hydroxyl radicals would be consumed breaking down organic matter instead of PFAS. Notably, in one inter-laboratory study examining the TOP assay, PFCA variation in post-oxidation samples, based on relative percent difference, was found to be as high as 67 %, with one sample high in total organic carbon differing more than 85 % (Nolan et al., 2019). Other factors might include mineralogy, grain size, other contaminants, etc.

5.4.3 Media:Soil Ratios

Two different variations of the 3:1 media to soil ratio were performed using the industrial-scale HBM. The standard method, comparative to those performed at the smaller scales in this study, kept the mass of media the same (250 kg), but the soil mass was increased to 83 kg (from 50 kg). In the other 3:1 variation, the typical mass of soil was kept the same (50 kg), but the mass of the media was reduced to 150 kg. From a field remediation standpoint, using the 250:83 kg media:soil ratio would be preferable as it would allow more soil to be processed per unit time; however, doing so results in an exceedance of the typically accepted mill volume most efficient for comminution (40 % fill volume). All trials discussed in this section were run with a 100:1 soil:KOH ratio.

In the 250:83 kg trials (Figure 5-3 a), 7:1:2 FtB underwent a significant increase in concentration (140 %). Although of lesser concentrations, 9:1:2 FtB and 11:1:2 FtB saw similar percent increases, 101 and 110 %, respectively. These substantial increases were not observed in the 150:50 kg trials (Figure 5-3 b), where 7:1:2 FtB increased by only 0.97 %, and 9:1:2 FtB and 11:1:2 FtB decreased by 14 and 38 %, respectively. Notably, such changes were also not observed in any of the previously discussed KOH trials at the same scale (Figure 5-2 c,f). The only similarities between the two sets of 3:1 trials at this scale were the outcomes for 7:3 and 9:3 FtB, which saw increases of 251 and 188 % in the 250/83 kg trials, respectively, and 276 and 199 % in the 150/50 kg trials, respectively. PFOS in the 250/83 kg trials was generally stable with concentrations fluctuating mildly, but never by more than 10 %. Final degradation was only 3.5 and 5.2 % in the two trials. Conversely, 8:2 FTS almost consistently increased in concentration, ending up 36 and 38 % overall in each trial, with the greatest increases, 36 % in both trials, occurring at T15. In the 150/50 kg trials, PFOS appeared to undergo slightly more variation, but also remained below 10 % variation at each sampling interval, except for a 12 %

reduction at T30 in one of the trials. Final degradation values were 2.5 and 14 % in the two trials. 8:2 FTS behaved similarly in the 250/83 kg trials, but with slightly lower values; overall, concentrations increased 24 and 35 % in each trial, with the greatest increases, 20 and 45 %, occurring at T15 in each of the trials.

There are two possibilities for the substantial increase in concentrations of 7:1:2 and 9:1:2 FtB (and others) in the 250/83 kg trials. As they occurred without any corresponding degradation of any other identified PFAS: 1) the LC-HRMS analysis did not identify all the non-target precursors in the T0 soil, which then transformed into the target and non-target PFAS that were identified, or 2) the identifiable PFAS were not fully extracted in the T0 analysis due to matrix and/or weathering effects. As discussed earlier, characterization of all PFAS in AFFF is challenging; therefore, failure to identify all potential non-target precursors in the T0 soil is a distinct possibility. In this case, the unidentified precursors would have had to be such that transformation into X:1:2 and X:3 FtBs would be necessary. If poor extraction is to blame, we would only expect it to occur in the T0 samples because the soil within a ball mill is quickly reduced to fine flour. Any PFAS harboured within the crystalline structure of individual soil grains would be rapidly released in the first few minutes of milling, which would then appear in subsequent analyses. Given that the source of soil was for the same for all trials herein (i.e., from the same storage/shipping barrels), one would expect a certain level of consistency across all trials. This was not the case, as substantial increases of 7:1:2 and 9:1:2 FtB were not observed in any of the other trials discussed thus far (150/50 kg trials, and all KOH variant trials). Lower PFAS degradation might be expected in the 250/83 kg trials due to sub-optimal ball mill loading (based on the industry's general understanding of maximum comminution efficiency); if that was the case, the previously non-extracted PFAS would have been liberated through milling, but subsequent degradation would have been poor and the increased concentrations would have remained present until the end of milling. Conversely, in the 150/50 kg trials, and the trials with 10:1 soil:KOH ratios, the previously non-extracted PFAS would have been liberated through milling, but the more optimal milling conditions would have led to that PFAS being degraded such that no evidence of it remained. This latter theory is flawed in that the trials with 100:1 soil:KOH ratios and those without KOH were concluded to have been unsuccessful; therefore, similar spikes in concentrations should have appeared. Better analytical characterization techniques would be required to gain further insight into this, such as free fluoride analysis.

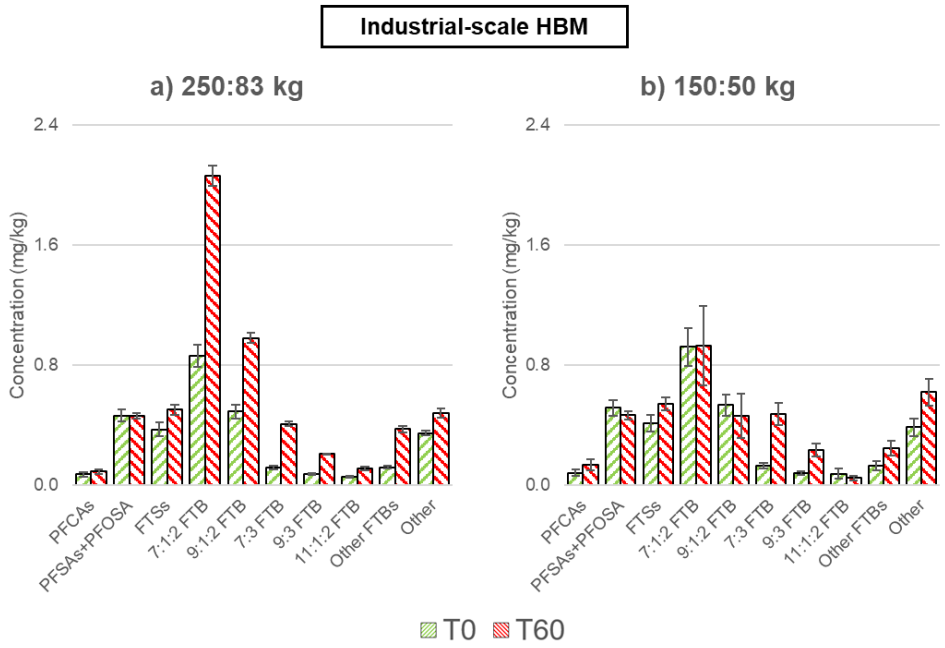

Figure 5-3: Results for industrial-scale HBM for two variations of the 3:1 media:soil ratio – 250 kg media to 83 kg soil (250:83 kg), and 150 kg media to 50 kg soil (150:50 kg). Soil was dried and 100:1 soil:KOH was used in all trials. Data points are presented as means of duplicate samples across duplicate trials ± standard deviation.

5.4.4 Soil Moisture Content

Two trials were run using soil that had not been dried (coupled with a 5:1 media:soil ratio and a 100:1 soil:KOH ratio) (Figure 5-4 a). Similarities to the 250/83 kg trials (Figure 5-3 a) were observed; in particular, 7:1:2 FtB underwent a significant increase in concentration (93 %). 9:1:2 FtB and 11:1:2 FtB increased by 80 and 158 %, respectively, and 7:3 and 9:3 FtB increased by 314 and 279 %, respectively. PFOS fluctuated over the course of milling and remained within 10 % of the starting concentrations. 8:2 FTS increased 28 % overall in both trials, with the greatest increases, 27 % in T15 in one trial, and in the other, 15 % at T15, followed by 20 % at T30. Concentrations were little changed after that. The appropriate comparison to make here is to the dried soil version with 100:1 soil:KOH ratio (Figure 5-2 c). Taken together, this data is consistent with the previously discussed topic of unidentified non-target precursors in the T0 soil and/or poor extraction in the T0 analysis due to

matrix and/or weathering effects. If the later, the sub-optimal milling conditions would be related to soil moisture, which would also be expected to inhibit degradation, preventing the further degradation of 7:1:2 and 9:1:2 FtB, leaving behind the evidence of the concentration spikes.

5.4.5 Attempt to Restart Higher Rates of Degradation

Based on speculations by Turner et al. (2023) that PFAS degradation is owed to soil grain fracturing, which releases electrons and other surface reducing radicals, three trials were run where 16.7 kg of soil (1/3 of the original soil charge) was removed from the mill after 45 minutes and an equivalent amount of PFAS-free sand added back in. In the first iteration of this (Figure 5-4 b), the soil was determined to have been incompletely dried, as minor caking was observed around the interior of the mill. The results for this iteration showed similarities to the trials where the soil was not dried (Figure 5-4 a), as well as to the 250/83 kg trials (Figure 5-3 a) in that 7:1:2 FtB underwent a significant increase in concentration (100 %). 9:1:2 and 11:1:2 FtB also increased by 78 and 80 %, respectively, and 7:3 and 9:3 FtB increased by 260 and 201 %, respectively. In the other two iterations where the soil was completely dried, in general there was greater similarity to the 100:1 soil:KOH trials (Figure 5-2 c) and the 150/50 kg trials (Figure 5-3 b). 7:1:2 increased by 12 %, 9:1:2 and 11:1:2 FtB decreased by 3.7 and 10 %, respectively, and 7:3 and 9:3 FtB increased by 135 and 98 %, respectively. Overall, PFOS concentrations decreased between 28 and 37 %, and 8:2 FTS increased between 20 and 38 %.

In relation to the stated purpose of these trials, there is evidence of success in restarting PFAS degradation following the typical diminishing returns often observed following the first 10-15 minutes of milling. Replacing impacted soil with PFAS-free soil would have resulted in a significant dilution (1/3 existing concentrations). For PFOS, based on the T45 concentrations in the three trials performed, 0.499, 0.476, and 0.455 mg/kg, we would expect dilution alone to lower these concentrations to 0.332, 0.318, and 0.303 mg/kg. The actual T60 concentrations measured were 0.389, 0.315, and 0.311, which are not significantly different than those estimated; however, for 8:2 FTS, the T45 concentrations were 0.442, 0.422, and 0.438 mg/kg. The expected diluted concentrations would be 0.295, 0.281, and 0.292 mg/kg. The actual T60 concentrations measured were 0.438, 0.421, and 0.434, which are largely the same as at T45. This suggests that the addition of PFAS-free sand was indeed successful in spurring additional degradation of precursors to 8:2 FTS in the final 15 minutes of milling that had otherwise remained relatively stable following the first big increase from T0 to T15. It also adds weight to the potential that preferential degradation of PFAS is occurring, as 8:2 FTS, a

potential product of transformation from long-chain precursors in the fluorotelomer group, was seen to be created, whereas PFOS, a PFSA, was not. This data is also consistent with the previously discussed topic of unidentified non-target precursors in the T0 soil and/or poor extraction in the T0 analysis due to matrix and/or weathering effects. Here, again, the spikes in 7:1:2 and 9:1:2 FtB are only present in the trial that had higher soil moisture (Figure 5-4 b), which would be expected to inhibit further degradation and leave behind the evidence of the concentration spikes.

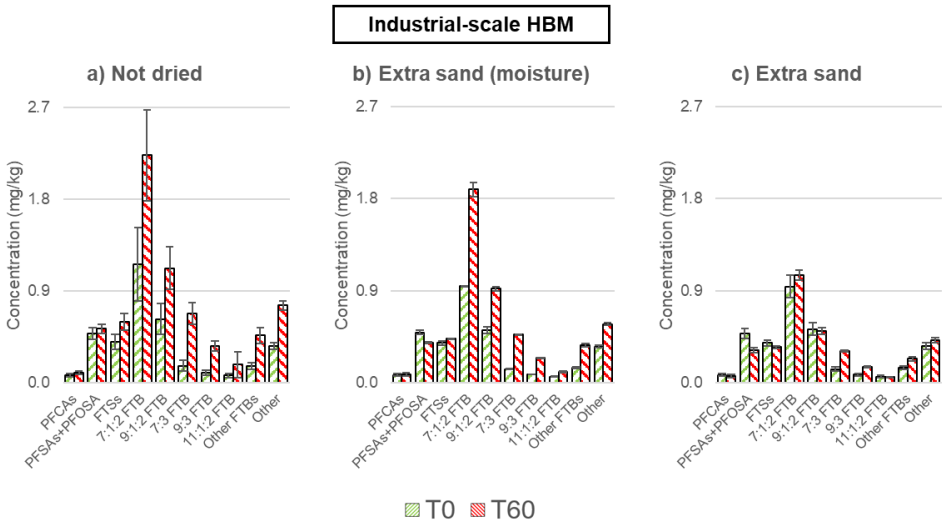

Figure 5-4: Results for industrial-scale HBM for undried soil, and where extra, PFAS-free sand added after T45. All trials used a 5:1 media:soil ratio and a 100:1 soil:KOH ratio. Data points for a) and c) are presented as means of duplicate samples across duplicate trials ± standard deviation. Data points for b) are presented as duplicate samples but for a single trial ± standard deviation.

5.5 Conclusions

In preparation for the first on-site field remediation, this study tested the effectiveness of ball milling PFAS-impacted soil derived from a FFTA at three scales: a benchtop-scale planetary ball mill (0.25 L cylinder), a commercial-scale horizontal ball mill (1.0 L cylinder), and an industrial-scale horizontal ball mill (267 L cylinder).

Results showed that with the right milling parameters the majority of the non-target PFAS load, up to 93 % on a horizontal ball mill system, can be degraded in actual field soils. KOH was shown to be the critical factor, yet the optimal amount remains unknown. It is considered probable that the amount of KOH required will be a function of the total initial PFAS concentration; however, this is a challenge because AFFF is difficult to fully characterize and modern formulations are composed entirely of non-target PFAS, which can only be semi-quantified. Additional analytical techniques may be needed, not all of which are readily available. There is also a practical limit to the amount of KOH that can used because at larger scale it leads to severe caking.

Overall, the results suggest preferential PFAS destruction with proportionately greater degradation of the long-chain FtBs happening over the identified short-chain FtBs, 8:2 FTS and PFOS. Notably, however, short-chain FtBs undergo degradation and creation (from their longer-chain precursors) simultaneously, as do short-chain FTSs and PFCAs. There were also indications of 8:2 FTS and PFOS being created, albeit to a much more minor degree. PFOS in particular is known for being extremely recalcitrant, and would be expected to be one of the last PFAS to undergo destruction.

Media:soil ratios and moisture content are other influential factors that need to be considered carefully. Experiments where 1/3 of the original soil charge was removed after T45 and an equivalent amount of PFAS-free sand was added provided some indication that the faster reaction rates often observed in the first minutes of milling before diminishing returns ensue can be reinitiated. Further work to create more degradation from this is required.

Overall, the technology remains promising, and further study of the highlighted influential factors will make on-site field remediation efforts more efficient and cost-effective.

5.6 Acknowledgements

Support for this research was provided by the Natural Sciences and Engineering Research Council (NSERC) of Canada (RGPIN-2018-04886; CRDPJ 530133-18) with industry sponsors WSP Canada Inc. and Imperial Oil Limited.

5.7 References

Anderson, R. H., Long, G. C., Porter, R. C., & Anderson, J. K. (2016). Occurrence of select perfluoroalkyl substances at U.S. Air Force aqueous film-forming foam release sites other than fire-training areas: Field-validation of critical fate and

transport properties. Chemosphere, 150, 678–685. https://doi.org/https://doi.org/10.1016/j.chemosphere.2016.01.014

Andrews, D. Q., Hayes, J., Stoiber, T., Brewer, B., Campbell, C., & Naidenko, O. V. (2021). Identification of point source dischargers of per- and polyfluoroalkyl substances in the United States. AWWA Water Science, 3(5), e1252. https://doi.org/https://doi.org/10.1002/aws2.1252

Aresta, M, Caramuscio, P., De Stefano, L., & Pastore, T. (2003). Solid state dehalogenation of PCBs in contaminated soil using NaBH4. Waste Management, 23(4), 315–319. https://doi.org/https://doi.org/10.1016/S0956-053X(03)00029-1

Aresta, Michele, Dibenedetto, A., Fragale, C., & Pastore, T. (2004). High-energy milling to decontaminate soils polluted by polychlorobiphenyls and atrazine. Environmental Chemistry Letters , 2(1), 1–4. https://doi.org/10.1007/s10311-003-0057-0

Armitage, J., Cousins, I. T., Buck, R. C., Prevedouros, K., Russell, M. H., MacLeod, M., & Korzeniowski, S. H. (2006). Modeling Global-Scale Fate and Transport of Perfluorooctanoate Emitted from Direct Sources. Environmental Science & Technology, 40(22), 6969–6975. https://doi.org/10.1021/es0614870

Ateia, M., Skala, L. P., Yang, A., & Dichtel, W. R. (2021). Product analysis and insight into the mechanochemical destruction of anionic PFAS with potassium hydroxide. Journal of Hazardous Materials Advances, 3, 100014. https://doi.org/https://doi.org/10.1016/j.hazadv.2021.100014

Barzen-Hanson, K. A., Davis, S. E., Kleber, M., & Field, J. A. (2017). Sorption of Fluorotelomer Sulfonates, Fluorotelomer Sulfonamido Betaines, and a Fluorotelomer Sulfonamido Amine in National Foam Aqueous Film-Forming Foam to Soil. Environmental Science & Technology, 51(21), 12394–12404. https://doi.org/10.1021/acs.est.7b03452

Barzen-Hanson, K. A., & Field, J. A. (2015). Discovery and Implications of C2 and C3 Perfluoroalkyl Sulfonates in Aqueous Film-Forming Foams and Groundwater. Environmental Science & Technology Letters, 2(4), 95–99. https://doi.org/10.1021/acs.estlett.5b00049

Barzen-Hanson, K. A., Roberts, S. C., Choyke, S., Oetjen, K., McAlees, A., Riddell, N., McCrindle, R., Ferguson, P. L., Higgins, C. P., & Field, J. A. (2017). Discovery of 40 Classes of Per- and Polyfluoroalkyl Substances in Historical Aqueous Film-Forming Foams (AFFFs) and AFFF-Impacted Groundwater. Environmental Science and Technology. https://doi.org/10.1021/acs.est.6b05843

Battye, N. J., Patch, D. J., Roberts, D. M. D., O'Connor, N. M., Turner, L. P., Kueper, B. H., Hulley, M. E., & Weber, K. P. (2022). Use of a horizontal ball mill to remediate per- and polyfluoroalkyl substances in soil. Science of The Total Environment, 835, 155506. https://doi.org/https://doi.org/10.1016/j.scitotenv.2022.155506

Battye, N., Patch, D., Koch, I., Monteith, R., Roberts, D., O'Connor, N., Kueper, B., Hulley, M., & Weber, K. (2024). Mechanochemical degradation of per- and polyfluoroalkyl substances in soil using an industrial-scale horizontal ball mill with comparisons of key operational metrics. Science of the Total Environment, 928, 172274. https://doi.org/10.1016/j.scitotenv.2024.172274

Bentel, M. J., Yu, Y., Xu, L., Li, Z., Wong, B. M., Men, Y., & Liu, J. (2019). Defluorination of Per- and Polyfluoroalkyl Substances (PFASs) with Hydrated Electrons: Structural Dependence and Implications to PFAS Remediation and Management. Environmental Science & Technology, 53(7), 3718–3728. https://doi.org/10.1021/acs.est.8b06648

Birke, V., Mattik, J., Runne, D., Benning, H., & Zlatovic, D. (2006). Dechlorination of Recalcitrant Polychlorinated Contaminants Using Ball Milling. In V. M. Kolodkin & W. Ruck (Eds.), Ecological Risks Associated with the Destruction of Chemical Weapons (pp. 111–127). Springer Netherlands.

Bolan, N., Sarkar, B., Vithanage, M., Singh, G., Tsang, D. C. W., Mukhopadhyay, R., Ramadass, K., Vinu, A., Sun, Y., Ramanayaka, S., Hoang, S. A., Yan, Y., Li, Y., Rinklebe, J., Li, H., & Kirkham, M. B. (2021). Distribution, behaviour, bioavailability and remediation of poly- and per-fluoroalkyl substances (PFAS) in solid biowastes and biowaste-treated soil. Environment International, 155, 106600. https://doi.org/https://doi.org/10.1016/j.envint.2021.106600

Bruton, T. A., & Sedlak, D. L. (2017). Treatment of Aqueous Film-Forming Foam by Heat-Activated Persulfate Under Conditions Representative of In Situ Chemical Oxidation. Environmental Science & Technology, 51(23), 13878–13885. https://doi.org/10.1021/acs.est.7b03969

Cagnetta, G., Zhang, Q., Huang, J., Lu, M., Wang, B., Wang, Y., Deng, S., & Yu, G. (2017). Mechanochemical destruction of perfluorinated pollutants and mechanosynthesis of lanthanum oxyfluoride: A Waste-to-Materials process. Chemical Engineering Journal, 316, 1078–1090. https://doi.org/https://doi.org/10.1016/j.cej.2017.02.050

Cao, G., Doppiu, S., Monagheddu, M., Orrù, R., Sannia, M., & Cocco, G. (1999). Thermal and Mechanochemical Self-Propagating Degradation of Chloro-organic

Compounds: The Case of Hexachlorobenzene over Calcium Hydride. Industrial & Engineering Chemistry Research, 38(9), 3218–3224. https://doi.org/10.1021/ie980790+

Caverly Rae, J. M., Craig, L., Slone, T. W., Frame, S. R., Buxton, L. W., & Kennedy, G. L. (2015). Evaluation of chronic toxicity and carcinogenicity of ammonium 2,3,3,3-tetrafluoro-2-(heptafluoropropoxy)-propanoate in Sprague–Dawley rats. Toxicology Reports, 2, 939–949. https://doi.org/https://doi.org/10.1016/j.toxrep.2015.06.001

Charbonnet, J. A., Rodowa, A. E., Joseph, N. T., Guelfo, J. L., Field, J. A., Jones, G. D., Higgins, C. P., Helbling, D. E., & Houtz, E. F. (2021). Environmental Source Tracking of Per- and Polyfluoroalkyl Substances within a Forensic Context: Current and Future Techniques. Environmental Science & Technology, 55(11), 7237–7245. https://doi.org/10.1021/acs.est.0c08506

Cousins, I. T., Johansson, J. H., Salter, M. E., Sha, B., & Scheringer, M. (2022). Outside the Safe Operating Space of a New Planetary Boundary for Per- and Polyfluoroalkyl Substances (PFAS). Environmental Science & Technology, 56(16), 11172–11179. https://doi.org/10.1021/acs.est.2c02765

D'Agostino, L. A., & Mabury, S. A. (2014). Identification of novel fluorinated surfactants in aqueous film forming foams and commercial surfactant concentrates. Environmental Science & Technology, 48(1), 121–129. https://doi.org/10.1021/es403729e

Du, Z., Deng, S., Bei, Y., Huang, Q., Wang, B., Huang, J., & Yu, G. (2014). Adsorption behavior and mechanism of perfluorinated compounds on various adsorbents--a review. Journal of Hazardous Materials, 274, 443–454. https://doi.org/10.1016/j.jhazmat.2014.04.038

Duchesne, A. L., Brown, J. K., Patch, D. J., Major, D., Weber, K. P., & Gerhard, J. I. (2020). Remediation of PFAS-Contaminated Soil and Granular Activated Carbon by Smoldering Combustion. Environmental Science & Technology, 54(19), 12631–12640. https://doi.org/10.1021/acs.est.0c03058

España, V. A. A., Mallavarapu, M., Naidu, R., & Naidu, R. (2015). Treatment technologies for aqueous perfluorooctanesulfonate (PFOS) and perfluorooctanoate (PFOA): A critical review with an emphasis on field testing. Environmental Technology and Innovation, 4, 168–181.

Ferrey, M. L., Wilson, J. T., Adair, C., Su, C., Fine, D. D., Liu, X., & Washington, J. W. (2012). Behavior and Fate of PFOA and PFOS in Sandy Aquifer Sediment.

Groundwater Monitoring \& Remediation, 32(4), 63–71. https://doi.org/https://doi.org/10.1111/j.1745-6592.2012.01395.x

Field, Jennifer A, Sedlak, David, Alvarez-Cohen, L. (2017). Characterization of the Fate and Biotransformation of Fluorochemicals in AFFF-Contaminated Groundwater at Fire/Crash Testing Military Sites. https://apps.dtic.mil/sti/pdfs/AD1037940.pdf

Folkerson, A. P., Schneider, S. R., Abbatt, J. P. D., & Mabury, S. A. (2023). Avoiding Regrettable Replacements: Can the Introduction of Novel Functional Groups Move PFAS from Recalcitrant to Reactive? Environmental Science & Technology, 57(44), 17032–17041. https://doi.org/10.1021/acs.est.3c06232

Friščić, T. (2018). Mechanochemistry in Co-crystal Synthesis. In C. B. Aakeröy & A. S. Sinha (Eds.), Co-crystals: Preparation, Characterization and Applications (p. 0). The Royal Society of Chemistry. https://doi.org/10.1039/9781788012874-00147

Gannon, S. A., Fasano, W. J., Mawn, M. P., Nabb, D. L., Buck, R. C., Buxton, L. W., Jepson, G. W., & Frame, S. R. (2016). Absorption, distribution, metabolism, excretion, and kinetics of 2,3,3,3-tetrafluoro-2-(heptafluoropropoxy)propanoic acid ammonium salt following a single dose in rat, mouse, and cynomolgus monkey. Toxicology, 340, 1–9. https://doi.org/10.1016/j.tox.2015.12.006

Garnett, J., Halsall, C., Winton, H., Joerss, H., Mulvaney, R., Ebinghaus, R., Frey, M., Jones, A., Leeson, A., & Wynn, P. (2022). Increasing Accumulation of Perfluorocarboxylate Contaminants Revealed in an Antarctic Firn Core (1958–2017). Environmental Science & Technology, 56(16), 11246–11255. https://doi.org/10.1021/acs.est.2c02592

Giesy, J. P., Mabury, S. A., Martin, J. W., Kannan, K., Jones, P. D., Newsted, J. L., & Coady, K. (2006). Perfluorinated Compounds in the Great Lakes. In R. A. Hites (Ed.), Persistent Organic Pollutants in the Great Lakes (pp. 391–438). Springer Berlin Heidelberg. https://doi.org/10.1007/698_5_046

Gobindlal, K., Shields, E., Whitehill, A., Weber, C. C., & Sperry, J. (2023). Mechanochemical destruction of per- and polyfluoroalkyl substances in aqueous film-forming foams and contaminated soil. Environ. Sci.: Adv., 2(7), 982–989. https://doi.org/10.1039/D3VA00099K

Gobindlal, K., Zujovic, Z., Jaine, J., Weber, C. C., & Sperry, J. (2023). Solvent-Free, Ambient Temperature and Pressure Destruction of Perfluorosulfonic Acids under Mechanochemical Conditions: Degradation Intermediates and Fluorine Fate.

Environmental Science & Technology, 57(1), 277–285. https://doi.org/10.1021/acs.est.2c06673

Gomis, M. I., Wang, Z., Scheringer, M., & Cousins, I. T. (2015). A modeling assessment of the physicochemical properties and environmental fate of emerging and novel per- and polyfluoroalkyl substances. The Science of the Total Environment, 505, 981–991. https://doi.org/10.1016/j.scitotenv.2014.10.062

Guelfo, J. L., & Higgins, C. P. (2013). Subsurface Transport Potential of Perfluoroalkyl Acids at Aqueous Film-Forming Foam (AFFF)-Impacted Sites. Environmental Science & Technology, 47(9), 4164–4171. https://doi.org/10.1021/es3048043

Hall, A. K., Harrowfield, J. M., Hart, R. J., & McCormick, P. G. (1996). Mechanochemical Reaction of DDT with Calcium Oxide. Environmental Science & Technology, 30(12), 3401–3407. https://doi.org/10.1021/es950680j

Health Canada. (2024). Objective for Canadian Drinking Water Quality Per- and Polyfluoroalkyl Substances.

Heuckeroth, S., Nxumalo, T. N., Raab, A., & Feldmann, J. (2021). Fluorine-Specific Detection Using ICP-MS Helps to Identify PFAS Degradation Products in Nontargeted Analysis. Analytical Chemistry, 93(16), 6335–6341. https://doi.org/10.1021/acs.analchem.1c00031

Heydebreck, F., Tang, J., Xie, Z., & Ebinghaus, R. (2015). Alternative and Legacy Perfluoroalkyl Substances: Differences between European and Chinese River/Estuary Systems. Environmental Science & Technology, 49(14), 8386–8395. https://doi.org/10.1021/acs.est.5b01648

Hoke, R. A., Ferrell, B. D., Sloman, T. L., Buck, R. C., & Buxton, L. W. (2016). Aquatic hazard, bioaccumulation and screening risk assessment for ammonium 2,3,3,3-tetrafluoro-2-(heptafluoropropoxy)-propanoate. Chemosphere, 149, 336–342. https://doi.org/10.1016/j.chemosphere.2016.01.009

Houtz, E. F., Higgins, C. P., Field, J. A., & Sedlak, D. L. (2013). Persistence of Perfluoroalkyl Acid Precursors in AFFF-Impacted Groundwater and Soil. Environmental Science & Technology, 47(15), 8187–8195. https://doi.org/10.1021/es4018877

Intini, G., Cangialosi, F., L.Liberti, D.Lupo, Notarnicola, M., & Pastore, T. (2007). Mechanochemical treatment of contaminated marine sediments for PCB degradation. Chemistry for Sustainable Development, 15, 147–156.

Kajdas, C. K. (2005). Importance of the triboemission process for tribochemical reaction. Tribology International, 38(3), 337–353. https://doi.org/https://doi.org/10.1016/j.triboint.2004.08.017

Kaupp, G. (2009). Mechanochemistry: the varied applications of mechanical bond-breaking. CrystEngComm, 11(3), 388–403. https://doi.org/10.1039/B810822F

Kim, S.-K., & Kannan, K. (2007). Perfluorinated Acids in Air, Rain, Snow, Surface Runoff, and Lakes: Relative Importance of Pathways to Contamination of Urban Lakes. Environmental Science & Technology, 41(24), 8328–8334. https://doi.org/10.1021/es072107t

Korolev, K., Golovanova, A. I., Maltseva, N. N., Lomovskiy, O. I., Salenko, V. L., & Boldyrev, V. V. (2003). Application of mechanical activation to decomposition of toxic chlorinated organic compounds. Chem. Sustain. Dev., 11, 489–496.

Lewis, R. E., Huang, C.-H., White, J. C., & Haynes, C. L. (2023). Using 19F NMR to Investigate Cationic Carbon Dot Association with Per- and Polyfluoroalkyl Substances (PFAS). ACS Nanoscience Au, 3(5), 408–417. https://doi.org/10.1021/acsnanoscienceau.3c00022

Liu, Y., Pereira, A. D. S., & Martin, J. W. (2015). Discovery of C5–C17 Poly- and Perfluoroalkyl Substances in Water by In-Line SPE-HPLC-Orbitrap with In-Source Fragmentation Flagging. Analytical Chemistry, 87(8), 4260–4268. https://doi.org/10.1021/acs.analchem.5b00039

Liu, Z., Bentel, M. J., Yu, Y., Ren, C., Gao, J., Pulikkal, V. F., Sun, M., Men, Y., & Liu, J. (2021). Near-Quantitative Defluorination of Perfluorinated and Fluorotelomer Carboxylates and Sulfonates with Integrated Oxidation and Reduction. Environmental Science and Technology, 55(10), 7052–7062. https://doi.org/10.1021/acs.est.1c00353

Liu, Z., Chen, Z., Gao, J., Yu, Y., Men, Y., Gu, C., & Liu, J. (2022). Accelerated Degradation of Perfluorosulfonates and Perfluorocarboxylates by UV/Sulfite + Iodide: Reaction Mechanisms and System Efficiencies. Environmental Science & Technology, 56(6), 3699–3709. https://doi.org/10.1021/acs.est.1c07608

Lu, M., Cagnetta, G., Zhang, K., Huang, J., & Yu, G. (2017). Mechanochemical mineralization of “very persistent” fluorocarbon surfactants – 6:2 fluorotelomer sulfonate (6:2FTS) as an example. Scientific Reports, 7(1), 17180. https://doi.org/10.1038/s41598-017-17515-7

Lv, H., Wang, N., Zhu, L., Zhou, Y., Li, W., & Tang, H. (2018). Alumina-mediated mechanochemical method for simultaneously degrading perfluorooctanoic acid and synthesizing a polyfluoroalkene. Green Chem., 20(11), 2526–2533. https://doi.org/10.1039/C8GC00854J

Mahinroosta, R., & Senevirathna, L. (2020). A review of the emerging treatment technologies for PFAS contaminated soils. Journal of Environmental Management, 255, 109896. https://doi.org/10.1016/j.jenvman.2019.109896

Marinescu, I. D., Rowe, W. B., Dimitrov, B., & Ohmori, H. (2013). 16 - Tribochemistry of abrasive machining. In I. D. Marinescu, W. B. Rowe, B. Dimitrov, & H. Ohmori (Eds.), Tribology of Abrasive Machining Processes (Second Edition) (Second Edi, pp. 483–517). William Andrew Publishing. https://doi.org/https://doi.org/10.1016/B978-1-4377-3467-6.00016-1

Martin, J. W., Mabury, S. A., Solomon, K. R., & Muir, D. C. G. (2003). Bioconcentration and tissue distribution of perfluorinated acids in rainbow trout (Oncorhynchus mykiss). Environmental Toxicology and Chemistry, 22(1), 196–204. https://doi.org/https://doi.org/10.1002/etc.5620220126

McDonough, C. A., Guelfo, J. L., & Higgins, C. P. (2019). Measuring Total PFASs in Water: The Tradeoff between Selectivity and Inclusivity. Current Opinion in Environmental Science & Health, 7, 13–18. https://doi.org/10.1016/j.coesh.2018.08.005

Milley, S. A., Koch, I., Fortin, P., Archer, J., Reynolds, D., & Weber, K. P. (2018). Estimating the number of airports potentially contaminated with perfluoroalkyl and polyfluoroalkyl substances from aqueous film forming foam: A Canadian example. Journal of Environmental Management, 222, 122–131. https://doi.org/10.1016/j.jenvman.2018.05.028

Monagheddu, M., Mulas, G., Doppiu, S., Cocco, G., & Raccanelli, S. (1999). Reduction of Polychlorinated Dibenzodioxins and Dibenzofurans in Contaminated Muds by Mechanically Induced Combustion Reactions. Environmental Science & Technology, 33(14), 2485–2488. https://doi.org/10.1021/es9809206

Munoz, G., Desrosiers, M., Duy, S. V., Labadie, P., Budzinski, H., Liu, J., & Sauvé, S. (2017). Environmental Occurrence of Perfluoroalkyl Acids and Novel Fluorotelomer Surfactants in the Freshwater Fish Catostomus commersonii and Sediments Following Firefighting Foam Deployment at the Lac-Mégantic Railway Accident. Environmental Science & Technology, 51(3), 1231–1240. https://doi.org/10.1021/acs.est.6b05432

Nickerson, A., Rodowa, A. E., Adamson, D. T., Field, J. A., Kulkarni, P. R., Kornuc, J. J., & Higgins, C. P. (2021). Spatial Trends of Anionic, Zwitterionic, and Cationic PFASs at an AFFF-Impacted Site. Environmental Science & Technology, 55(1), 313–323. https://doi.org/10.1021/acs.est.0c04473

Nolan, A., Grimison, C., Lavetz, R., Slee, D., Lim, C., Centner, M., McGrath, S., Symons, B., & Bowles, K. (2019). Improving measurement reliability of the PFAS top assay. Proceedings of the 8th International Contaminated Site Remediation Conference, 633. https://www.crccare.com/files/dmfile/CleanUp2019Proceedings_FINAL.pdf

O'Connor, N., Patch, D., Noble, D., Scott, J., Koch, I., Mumford, K. G., & Weber, K. (2023). Forever no more: Complete mineralization of per- and polyfluoroalkyl substances (PFAS) using an optimized UV/sulfite/iodide system. The Science of the Total Environment, 888, 164137. https://doi.org/10.1016/j.scitotenv.2023.164137

Pan, G., & You, C. (2010). Sediment–water distribution of perfluorooctane sulfonate (PFOS) in Yangtze River Estuary. Environmental Pollution, 158(5), 1363–1367. https://doi.org/https://doi.org/10.1016/j.envpol.2010.01.011

Patch, D., O'Connor, N., Koch, I., Cresswell, T., Hughes, C., Davies, J. B., Scott, J., O'Carroll, D., & Weber, K. (2022). Elucidating degradation mechanisms for a range of per- and polyfluoroalkyl substances (PFAS) via controlled irradiation studies. Science of The Total Environment, 832, 154941. https://doi.org/https://doi.org/10.1016/j.scitotenv.2022.154941

Patch, D., O'Connor, N., Vereecken, T., Murphy, D., Munoz, G., Ross, I., Glover, C., Scott, J., Koch, I., Sauvé, S., Liu, J., & Weber, K. (2024). Advancing PFAS characterization: Enhancing the total oxidizable precursor assay with improved sample processing and UV activation. Science of The Total Environment, 909, 168145. https://doi.org/https://doi.org/10.1016/j.scitotenv.2023.168145

Phong Vo, H. N., Ngo, H. H., Guo, W., Hong Nguyen, T. M., Li, J., Liang, H., Deng, L., Chen, Z., & Hang Nguyen, T. A. (2020). Poly-and perfluoroalkyl substances in water and wastewater: A comprehensive review from sources to remediation. Journal of Water Process Engineering, 36, 101393. https://doi.org/https://doi.org/10.1016/j.jwpe.2020.101393

Place, B. J., & Field, J. A. (2012). Identification of novel fluorochemicals in aqueous film-forming foams used by the US military. Environmental Science and Technology, 46(13), 7120–7127. https://doi.org/10.1021/es301465n

Rand, A. A., Rooney, J. P., Butt, C. M., Meyer, J. N., & Mabury, S. A. (2014). Cellular toxicity associated with exposure to perfluorinated carboxylates (PFCAs) and their metabolic precursors. Chemical Research in Toxicology, 27(1), 42–50. https://doi.org/10.1021/tx400317p

Rankin, K., Mabury, S. A., Jenkins, T. M., & Washington, J. W. (2016). A North American and global survey of perfluoroalkyl substances in surface soils: Distribution patterns and mode of occurrence. Chemosphere, 161, 333–341. https://doi.org/https://doi.org/10.1016/j.chemosphere.2016.06.109

Rayne, S., & Forest, K. (2009). Perfluoroalkyl sulfonic and carboxylic acids: A critical review of physicochemical properties, levels and patterns in waters and wastewaters, and treatment methods. Journal of Environmental Science and Health, Part A, 44(12), 1145–1199. https://doi.org/10.1080/10934520903139811

Rehman, A. U., Crimi, M., & Andreescu, S. (2023). Current and emerging analytical techniques for the determination of PFAS in environmental samples. Trends in Environmental Analytical Chemistry, 37, e00198. https://doi.org/https://doi.org/10.1016/j.teac.2023.e00198

Ross, I., McDonough, J., Miles, J., Storch, P., Thelakkat Kochunarayanan, P., Kalve, E., Hurst, J., S. Dasgupta, S., & Burdick, J. (2018). A review of emerging technologies for remediation of PFASs. Remediation, 28(2), 101–126. https://doi.org/10.1002/rem.21553

Sadia, M., Nollen, I., Helmus, R., ter Laak, T. L., Béen, F., Praetorius, A., & van Wezel, A. P. (2023). Occurrence, Fate, and Related Health Risks of PFAS in Raw and Produced Drinking Water. Environmental Science & Technology, 57(8), 3062–3074. https://doi.org/10.1021/acs.est.2c06015

Sima, M. W., & Jaffé, P. R. (2021). A critical review of modeling Poly- and Perfluoroalkyl Substances (PFAS) in the soil-water environment. Science of The Total Environment, 757, 143793. https://doi.org/https://doi.org/10.1016/j.scitotenv.2020.143793

Strynar, M., Dagnino, S., McMahen, R., Liang, S., Lindstrom, A., Andersen, E., McMillan, L., Thurman, M., Ferrer, I., & Ball, C. (2015). Identification of Novel Perfluoroalkyl Ether Carboxylic Acids (PFECAs) and Sulfonic Acids (PFESAs) in Natural Waters Using Accurate Mass Time-of-Flight Mass Spectrometry (TOFMS). Environmental Science & Technology, 49(19), 11622–11630. https://doi.org/10.1021/acs.est.5b01215

Tabassum, S., Ahmed, A., Rahman, S., Tithi, M., Mehjabin, M., & Dristy, J. (2024). Recent Advancements in Per- and Polyfluoroalkyl Substances (PFAS) Detection by Sensors and Surface-Enhanced Raman Scattering (SERS) Method: A Review. https://doi.org/10.20944/preprints202401.1557.v1

Trojanowicz, M., Bartosiewicz, I., Bojanowska-Czajka, A., Kulisa, K., Szreder, T., Bobrowski, K., Nichipor, H., Garcia-Reyes, J. F., Nałęcz-Jawecki, G., Męczyńska-Wielgosz, S., & Kisała, J. (2019). Application of ionizing radiation in decomposition of perfluorooctanoate (PFOA) in waters. Chemical Engineering Journal, 357, 698–714. https://doi.org/https://doi.org/10.1016/j.cej.2018.09.065

Trojanowicz, M., Bartosiewicz, I., Bojanowska-Czajka, A., Szreder, T., Bobrowski, K., Nałęcz-Jawecki, G., Męczyńska-Wielgosz, S., & Nichipor, H. (2020). Application of ionizing radiation in decomposition of perfluorooctane sulfonate (PFOS) in aqueous solutions. Chemical Engineering Journal, 379, 122303. https://doi.org/https://doi.org/10.1016/j.cej.2019.122303

Turner, L. P. (2024). Mechanochemical destruction of per- and polyfluoroalkyl substances in environmental media by planetary ball milling. Queen's University.

Turner, L. P., Kueper, B. H., Jaansalu, K. M., Patch, D. J., Battye, N., El-Sharnouby, O., Mumford, K. G., & Weber, K. P. (2021). Mechanochemical remediation of perfluorooctanesulfonic acid (PFOS) and perfluorooctanoic acid (PFOA) amended sand and aqueous film-forming foam (AFFF) impacted soil by planetary ball milling. Science of The Total Environment, 765, 142722. https://doi.org/https://doi.org/10.1016/j.scitotenv.2020.142722

Turner, L. P., Kueper, B. H., Patch, D. J., & Weber, K. P. (2023). Elucidating the relationship between PFOA and PFOS destruction, particle size and electron generation in amended media commonly found in soils. Science of The Total Environment, 888, 164188. https://doi.org/https://doi.org/10.1016/j.scitotenv.2023.164188

United States Environmental Protection Agency. (2024). PFAS National Primary Drinking Water Regulation 2024. https://www.epa.gov/sdwa/and-polyfluoroalkyl-substances-pfas

USEPA. (2020). Interim Guidance on the Destruction and Disposal of Perfluoroalkyl and Polyfluoroalkyl Substances and Materials Containing Perfluoroalkyl and Polyfluoroalkyl Substances. https://www.epa.gov/pfas/interim-guidance-destroying-and-disposing-certain-pfas-and-pfas-containing-materials-are-not?msclkid=787b040ca5f111ecaf45067b86b7ed53

Vecitis, C. D., Park, H., Cheng, J., Mader, B. T., & Hoffmann, M. R. (2009). Treatment technologies for aqueous perfluorooctanesulfonate (PFOS) and perfluorooctanoate (PFOA). Frontiers of Environmental Science & Engineering in China, 3(2), 129–151. https://doi.org/10.1007/s11783-009-0022-7

Wang, Z., Buser, A. M., Cousins, I. T., Demattio, S., Drost, W., Johansson, O., Ohno, K., Patlewicz, G., Richard, A. M., Walker, G. W., White, G. S., & Leinala, E. (2021). A New OECD Definition for Per- and Polyfluoroalkyl Substances. Environmental Science & Technology, 55(23), 15575–15578. https://doi.org/10.1021/acs.est.1c06896

Wang, Z., Cousins, I. T., Scheringer, M., & Hungerbuehler, K. (2015). Hazard assessment of fluorinated alternatives to long-chain perfluoroalkyl acids (PFAAs) and their precursors: Status quo, ongoing challenges and possible solutions. Environment International, 75, 172–179. https://doi.org/https://doi.org/10.1016/j.envint.2014.11.013

Wang, Z., Cousins, I. T., Scheringer, M., & Hungerbühler, K. (2013). Fluorinated alternatives to long-chain perfluoroalkyl carboxylic acids (PFCAs), perfluoroalkane sulfonic acids (PFSAs) and their potential precursors. Environment International, 60, 242–248. https://doi.org/10.1016/j.envint.2013.08.021

Yan, J. H., Peng, Z., Lu, S. Y., Li, X. D., Ni, M. J., Cen, K. F., & Dai, H. F. (2007). Degradation of PCDD/Fs by mechanochemical treatment of fly ash from medical waste incineration. Journal of Hazardous Materials, 147(1), 652–657. https://doi.org/https://doi.org/10.1016/j.jhazmat.2007.02.073

Yan, X., Liu, X., Qi, C., Wang, D., & Lin, C. (2015). Mechanochemical destruction of a chlorinated polyfluorinated ether sulfonate (F-53B{,} a PFOS alternative) assisted by sodium persulfate. RSC Adv., 5(104), 85785–85790. https://doi.org/10.1039/C5RA15337A

Yang, L., He, L., Xue, J., Ma, Y., Xie, Z., Wu, L., Huang, M., & Zhang, Z. (2020). Persulfate-based degradation of perfluorooctanoic acid (PFOA) and perfluorooctane sulfonate (PFOS) in aqueous solution: Review on influences, mechanisms and prospective. Journal of Hazardous Materials, 393, 122405. https://doi.org/https://doi.org/10.1016/j.jhazmat.2020.122405

Yang, N., Yang, S., Ma, Q., Beltran, C., Guan, Y., Morsey, M., Brown, E., Fernando, S., Holsen, T. M., Zhang, W., & Yang, Y. (2023). Solvent-Free Nonthermal Destruction of PFAS Chemicals and PFAS in Sediment by Piezoelectric Ball Milling. Environmental Science & Technology Letters, 10(2), 198–203. https://doi.org/10.1021/acs.estlett.2c00902

Zhang, D. Q., Zhang, W. L., & Liang, Y. N. (2019). Adsorption of perfluoroalkyl and polyfluoroalkyl substances (PFASs) from aqueous solution – A review. The Science of the Total Environment, 694, 133606. https://doi.org/10.1016/j.scitotenv.2019.133606

Zhang, K., Cao, Z., Huang, J., Deng, S., Wang, B., & Yu, G. (2016). Mechanochemical destruction of Chinese PFOS alternative F-53B. Chemical Engineering Journal, 286, 387–393. https://doi.org/https://doi.org/10.1016/j.cej.2015.10.103

Zhang, K., Huang, J., Yu, G., Zhang, Q., Deng, S., & Wang, B. (2013). Destruction of Perfluorooctane Sulfonate (PFOS) and Perfluorooctanoic Acid (PFOA) by Ball Milling. Environmental Science & Technology, 47(12), 6471–6477. https://doi.org/10.1021/es400346n

Zhang, K., Huang, J., Zhang, W., Yu, Y., Deng, S., & Yu, G. (2012). Mechanochemical degradation of tetrabromobisphenol A: performance, products and pathway. Journal of Hazardous Materials, 243, 278—285. https://doi.org/10.1016/j.jhazmat.2012.10.034

Zhang, W., Wang, H., Jun, H., Yu, M., Wang, F., Zhou, L., & Yu, G. (2014). Acceleration and mechanistic studies of the mechanochemical dechlorination of HCB with iron powder and quartz sand. Chemical Engineering Journal, 239, 185–191. https://doi.org/https://doi.org/10.1016/j.cej.2013.11.018

6 Chapter 6: Overall Conclusions and Recommendations

The overall goal of this work was to develop a simple and efficient PFAS-destruction technique for impacted soils using a horizontal ball mill (HBM). PFAS are present in a wide variety of commercial and industrial products, have been classified as POPs as they are toxic, extremely resistant to degradation, bioaccumulate in food chains, and have long-half lives in humans. While success had previously been shown using PBMs, these types of mills are not conducive to scale-up beyond the benchtop. Conversely, HBMs have a simpler rotational mechanism and already exist at large scales. If shown to be successful, appropriately sized HBMs could easily be re-purposed and mobilized for on-site remedial purposes. To achieve the stated goal, the following objectives were identified:

1. Assess, for the first time, whether a HBM is capable of remediating PFAS impacted soil.

2. Scale up the HBM to an industrial size typically used by the industry before field applications.

3. Compare geophysical and geochemical properties in both unmilled and milled soil, as well as health and safety factors to provide insight into critical logistical and operational concerns pertinent to a field remediation project deployment.

4. In preparation for the first in-field ball milling pilot test, perform a final evaluation of PFAS destruction via ball milling using an AFFF impacted field soil at three scales, evaluating influential factors such as KOH and soil:media ratios, soil moisture content, as well as a method to restart higher rates of degradation.

A summary of the outcomes from each objective are provided below, followed by some overarching conclusions, and recommendations for future study.

6.1 Use of a Horizontal Ball Mill to Remediate Per- and Polyfluoroalkyl Substances in Soil

This study sought to determine whether a HBM could be used to destroy PFAS in a soil matrix. Spiked NSS, as well as two different field soils, a sand and a clay, were tested with and without the use of KOH as a co-milling reagent, at two separate scales (cylinder sizes of 1 L and 25 L). A total of 21 targeted PFCAs, PFSAs, and PFOSA, as well as 19 non-target fluorotelomers were tracked across several time series sampling events. The following conclusions are presented:

1. In the presence of KOH, PFOS and 6:2 FTS were successfully degraded, up to 81% and 97%, respectively. Substrate type and scale were not found to be significant factors in terms of degradation.

2. KOH was critical for the degradation of 6:2 FTS; without it, no degradation occurred. Conversely, PFOS experienced moderate degradation without KOH.

3. Given the similar chemical nature of PFOS and 6:2 FTS, it was identified that the susceptibility of 6:2 FTS to degrade in the presence of KOH is likely the result of hydroxy radicals generated from the KOH, which may result in a fluorotelomer-alkene structure that can be subsequently attacked by other radicals generated in the system.

4. Near-complete degradation of all non-target fluorotelomer PFAS was achieved, which are the primary PFAS components in modern AFFF formulations.

5. HRAM analysis showed no major or easily identified fluorinated compounds formed as a by-product of the milling procedure.

6. Given these results, HBMs should be effective at remediating both modern day and historically contaminated sites, where different AFFF formulations with varying PFAS compositions were used.

6.2 Scale-up to an Industrial-sized Horizontal Ball Mill

Based on the previous success using a commercial-scale HBM, this study examined scale up to an industrial-sized HBM. With a cylinder size of 267 L, this is the typical scale used in the industry before field application. The following conclusions were made:

1. Scale-up continued to show effectiveness at destroying 6:2 FTS (up to 97 %) and other non-target PFAS (up to 96 %) with KOH in spiked NSS.

2. Better and more consistent degradation of PFOS and PFOA was observed with scale-up in spiked NSS trials, and the use of KOH was again shown not to be required for those two PFAS (70 % and 74 %, respectively, with KOH, and 69 % and 70 %, respectively, without).

3. The improved degradation of PFOS and PFOA in the above trials was attributed to the greater collision energy imparted onto the soil as a result of the increased falling distance of the media. If shown to be correct, this would bode well for further scale-up.

4. Limited degradation of PFOS and PFOA after 30 minutes remains a significant issue that needs to be overcome.

5. The results associated with the complex field soils were more ambiguous due to the assumed creation and destruction of target PFAS taking place simultaneously throughout the milling process. To quantify milling effectiveness, free fluoride analysis was used; the increase in extractable fluoride from unmilled to milled samples represented the equivalent of 12 mg/kg PFOS, which was considered a success.

6. The above value does not account for insoluble fluoride complexes that are known to form in milled soils; therefore, the actual amount of PFAS destroyed could be even greater.

6.3 Comparisons of Key Operational Metrics in Milled and Unmilled Soil Relevant to a Field Deployment

In addition to the examination of PFAS destruction, comparisons of soil health and PFAS leachability on both unmilled and milled soil at the industrial scale were conducted, as well as an evaluation of the potential risk associated with dust intake via oral ingestion to operators while milling, and to the environment through PFAS impacted dust dispersal. Results and conclusions for these tests were as follows:

1. Increases in various inorganic elements, which are released when the individual soil grain crystal lattices are fractured during milling;

2. Soil health, evaluated through the assessment of key microbial and associated plant health parameters, was not significantly affected as a result of milling, although it was characterized as poor to begin with;

3. Leachability reached 100% in milled soil with KOH, but already ranged from 81 to 96% in unmilled soil.

4. Although the use of KOH leads to environmentally unacceptable alkalinity of the treated soil, the resulting 100% PFAS leachability could be beneficial to secondary soil treatment options, such as soil washing. Otherwise, a secondary buffering step would be required before putting the soil back into the excavation.

5. The risk associated with inhalation of PFAS impacted dust was negligible using current TRVs; however, the evaluation of PFAS toxicity is a dynamic field, with a trend towards higher levels of protection, so precautions should always be taken when working with PFAS-impacted materials.

6. The above results also suggest that the risk of environmental cross-contamination is small from fugitive dust and/or emissions.

6.4 Complete Workup of a Field Soil at Three Scales to Finalize Our Understanding of the Critical Elements of PFAS Destruction

In preparation for the first on-site field remediation pilot test, this study evaluated the effectiveness of ball milling PFAS-impacted soil originating from a modern AFFF collected from an FFTA field site at three scales: a benchtop-scale PBM (0.25 L cylinder), a commercial-scale HBM (1.0 L cylinder), and an industrial-scale HBM (267 L cylinder). A summary of the findings are presented below.

1. Results showed that with the right milling parameters the majority of the non-target PFAS load, up to 93 % on a HBM system, can be degraded in actual field soils (on the PBM it was up to 97 %).

2. KOH was shown to be the critical factor, yet the optimal amount remains unknown.

3. The amount of KOH required is likely a function of the total initial PFAS concentration; however, this is challenging because AFFF is difficult to fully characterize and modern formulations are composed entirely of non-target PFAS, which can only be semi-quantified. Additional analytical techniques are needed, not all of which are readily available commercially. There is also a practical limit to the amount of KOH that can used because at larger scale it leads to severe caking.

4. Results suggest preferential PFAS destruction with proportionately greater degradation of the long-chain FtBs happening over the identified short-chain FtBs, 8:2 FTS and PFOS. Notably, short-chain FtBs, FTSs, and PFCAs undergo degradation and creation (from their longer-chain precursors) simultaneously. There was also evidence herein that 8:2 FTS and PFOS were being created.

5. Media:soil ratios and moisture content are other influential factors that need to be considered carefully.

6. Experiments where 1/3 of the original soil charge was removed after T45 and an equivalent amount of PFAS-free sand was added provided some indication that the faster reaction rates often observed in the first minutes of milling before diminishing returns ensue can be reinitiated.

6.5 Overarching Conclusions

The ball milling trials conducted for this thesis used and compared results at a variety of different scales. In large part, what was used was what was available. Notably, the different mills and grinding media consisted of different materials. The cylinder for the PBM was stainless steel, and spherical stainless steel media was used. The 1 L HBM cylinder was ceramic and the media was cylindrical burundum. For the 25 L HBM, the cylinder was stainless steel and the media was spherical chrome steel. And for the 267 L HBM, the cylinder was stainless steel and the media was mild steel. As different materials are known to create different reactions and outcomes when milling, it was thought that these differences may have an effect; however, it they did, they were not noticeable or significant.

It is also worth noting that at the time of writing, there is still no other viable PFAS destruction technology for soil that can be mobilized to PFAS-impacted sites. Thus, ball milling remains at the forefront in terms of potential.

6.6 Recommendations

The following recommendations are suggested for further study and to further enhance the efficiency of the technology and reduce operating costs:

1. Because of the complex mixtures of both target and non-target PFAS typically found in PFAS-impacted soils, standard analytical methods alone provide insufficient characterization and understanding. Although not always employed, this is true for all remedial methods, not just ball milling. To overcome this, a multitude of standard methods, used in complementary fashion, alongside several novel methods recently published, are needed to gain a full understanding of the reactions and ultimate success of the technology. Notably, this creates a hurdle for most researchers, as not all methods are readily available.

2. Determining the optimal amount of KOH is needed to maximize PFAS destruction, while minimizing alkalinity in the treated soil; however, higher alkalinity also increases PFAS leachability, which could be taken advantage of, such as in a treatment train approach that seeks to strip any residual PFAS from the soil after milling before it is put back into the excavation.

3. If the required amount of KOH cannot be used in large-scale HBMs because of caking, an alternate co-milling reagent will have to found that can achieve the same goal, while also allowing complete fluoride recovery for mass balance calculations. Alternatively, instead of fighting moisture, it is recommended that experiments be run that embrace it, saturating the system

so that caking is no longer an issue and putting in the required amount of KOH. While moisture is known to inhibit PFAS destruction, Turner et al. (2020) was able to overcome saturated conditions with KOH to degrade PFOS and PFOA.

4. A continuous feed ball mill system (as opposed to the batch system employed for scientific study), should be tested for on-site remediation. Such a system would be more efficient in terms of time, and therefore cost. It would also eliminate the need for repetitive cleanouts, which would further limit operator exposure to PFAS dust, as well as the surrounding environment. Complete elimination of dust exposure is unlikely, however, making an evaluation of appropriate PPE and risk management measures a necessity.

5. If the above points can be achieved, trials attempting to treat organic matter rich biowastes would be beneficial as they often contain PFAS. Doing so is hypothesized to be extra challenging, as the organic material is expected to absorb a portion of the energy imparted through the milling process, as well as the free radicals generated. The same would be true for spent activated carbon, which is often used for treating PFAS impacted water, and which creates a secondary waste stream product.

Appendix A – Supplementary Information for Chapter 3

Successful use of a horizontal ball mill to remediate per- and polyfluoroalkyl substances in soil

Nicholas J. Battye†, David J. Patch†, Dylan M. D. Roberts†, Natalia O'Connor†, Lauren P. Turner‡, Bernard H. Kueper‡, Kela P. Weber†.*

† Environmental Sciences Group, Department of Chemistry and Chemical Engineering, Royal Military College of Canada, Kingston, ON, Canada.

‡ Department of Civil Engineering, Queen's University, Kingston, ON, Canada.

* Corresponding Author: Kela P. Weber, email: Kela.Weber@rmc.ca, phone: 613-541-6000 ext. 3633.

KEYWORDS: per- and polyfluoroalkyl substances, PFAS, mechanochemical destruction, horizontal ball mill, aqueous film forming foam, AFFF, firefighting training area, FFTA.

TABLE OF CONTENTS

Table S1: Horizontal ball mill trial details.

Jar size	Soil Type	Mass grinding media (kg)	Mass soil (kg)	Mass KOH (kg)
1 L jar	NSS - PFOS	0.988	0.0786	0.0196
	NSS - PFOS	0.988	0.0982	-
	NSS - 6:2 FTSA	0.988	0.0786	0.0196
	NSS - 6:2 FTSA	0.988	0.0982	-
	NSS - AFFF	0.988	0.0786	0.0196
	NSS - AFFF	0.988	0.0982	-
	FFTA sand	0.988	0.0786	0.0196
	FFTA sand	0.988	0.0982	-
	FFTA clay	0.988	0.0786	0.0196
	FFTA clay	0.988	0.0982	-
25 L jar	FFTA sand	28	2.2	0.55
	FFTA sand	28	2.75	-
	FFTA clay	28	2.2	0.55
	FFTA clay	28	2.75	-

Table S2: Targeted PFAS analyzed using LC-MS/MS.

PFAS Class	PFAS Name	Abbreviation
Perfluorocarboxylic Acids (PFCA) (C_xF_{2x}-1COOH)	Trifluoroacetic acid	TFA
	Perfluoropropanoic acid	PFPA
	Perfluorobutanoic acid	PFBA
	Perfluoropentanoic acid	PFPeA
	Perfluorohexanoic acid	PFHxA
	Perfluoroheptanoic acid	PFHpA
	Perfluorooctanoic acid	PFOA
	Perfluorononanoic acid	PFNA
	Perfluorodecanoic acid	PFDA
	Perfluoroundecanoic acid	PFUnDA
	Perfluorododecanoic acid	PFDoDA
Perfluorosulfonic Acids (PFSA) ($C_xF_{2x+1}SO_3H$)	Perfluorobutane sulfonic acid	PFBS
	Perfluorohexane sulfonic acid	PFHxS
	Perfluorooctane sulfonic acid	PFOS
Fluorotelomer Sulfonic Acids (FTSA) ($C_xF_{2x+}1C_nH_{2n}SO_3H$)	6:2 fluorotelomer sulfonate	6:2 FTSA
Perfluorosulfonamide (PFOSA) ($C_xF_{2x+}1SO_2NH_2$)	Perfluorooctane sulfonamide	PFOSA

Table S3: Non-targeted PFAS identified and analyzed using LC-HRAM/MS.

Compound name	Abbreviated Name	Chemical Formula	Accurate Mass	Theoretical Mass	Mass Error
Octyl sulfate	OS	C8H17SO4	209.0854	209.08530	0.48
Decyl sulfate	DS	C10H21SO4	237.1165	237.11660	-0.42
6:2 Fluorotelomer sulfonates	6:2 FtSA	C8H4F13SO3	426.9676	426.96790	-0.70
8:2 Fluorotelomer sulfonates	8:2 FtSA	C10H4F17SO3	526.9613	526.96152	-0.42
10:2 Fluorotelomer sulfonates	10:2 FtSA	C12H4F21SO3	626.9550	626.95513	-0.21
6:2 Fluorotelomer sulfonamido betaines	6:2 FtSaB	C15H18N2F13SO4	569.0782	569.07852	-0.56
6:2 Fluorotelomer sulfonamido betaines	6:2 FtSaB	C15H20N2F13SO4	571.0924	571.09307	-1.17
8:2 Fluorotelomer sulfonamido betaines	8:2 FtSaB	C17H18N2F17SO4	669.0720	669.07213	-0.19
10:2 Fluorotelomer sulfonamido betaines	10:2 FtSaB	C19H18N2F21SO4	769.0657	769.06574	-0.05
6:2 Fluorotelomer sulfonamido amines	6:2 FtSaAm	C13H18N2F13SO2	513.0875	513.08759	-0.18
6:2 Fluorotelomer thioether amido sulfonates	6:2 FtTAoS	C15H17NF13S2O4	586.0394	586.03969	-0.49
6:2 Fluorotelomer sulfonyl amido sulfonates	6:2 FtSoAoS	C15H17NF13S2O5	602.0344	602.03460	-0.33
6:2 Fluorotelomer thiohydroxy ammonium	6:2 FtTHN	C14H19NF13SO	496.0975	496.09743	0.14
Oxidized 6:2 Fluorotelomer thiohydroxy ammonium	6:2 FtTHNO	C14H19NF13SO2	512.0920	512.09234	-0.66
5:3 Fluorotelomer betaines	5:3 FtB	C12H15NF11O2	414.0923	414.09217	0.31
5:1:2 Fluorotelomer betaines	5:1:2 FtB	C12H14NF12O2	432.0826	432.08274	-0.32
7:3 Fluorotelomer betaines	7:3 FtB	C14H15NF15O2	514.0856	514.08578	-0.35
7:1:2 Fluorotelomer betaines	7:1:2 FtB	C14H14NF16O2	532.0762	532.07636	-0.30
9:3 Fluorotelomer betaines	9:3 FtB	C16H15NF19O2	614.0795	614.07939	0.18
9:1:2 Fluorotelomer betaines	9:1:2 FtB	C16H14NF20O2	632.0698	632.06997	-0.27
11:1:2 Fluorotelomer betaines	11:1:2 FtB	C18H14NF24O2	732.0634	732.06358	-0.25
13:1:2 Fluorotelomer betaines	13:1:2 FtB	C20H14NF28O2	832.0573	832.05719	0.13

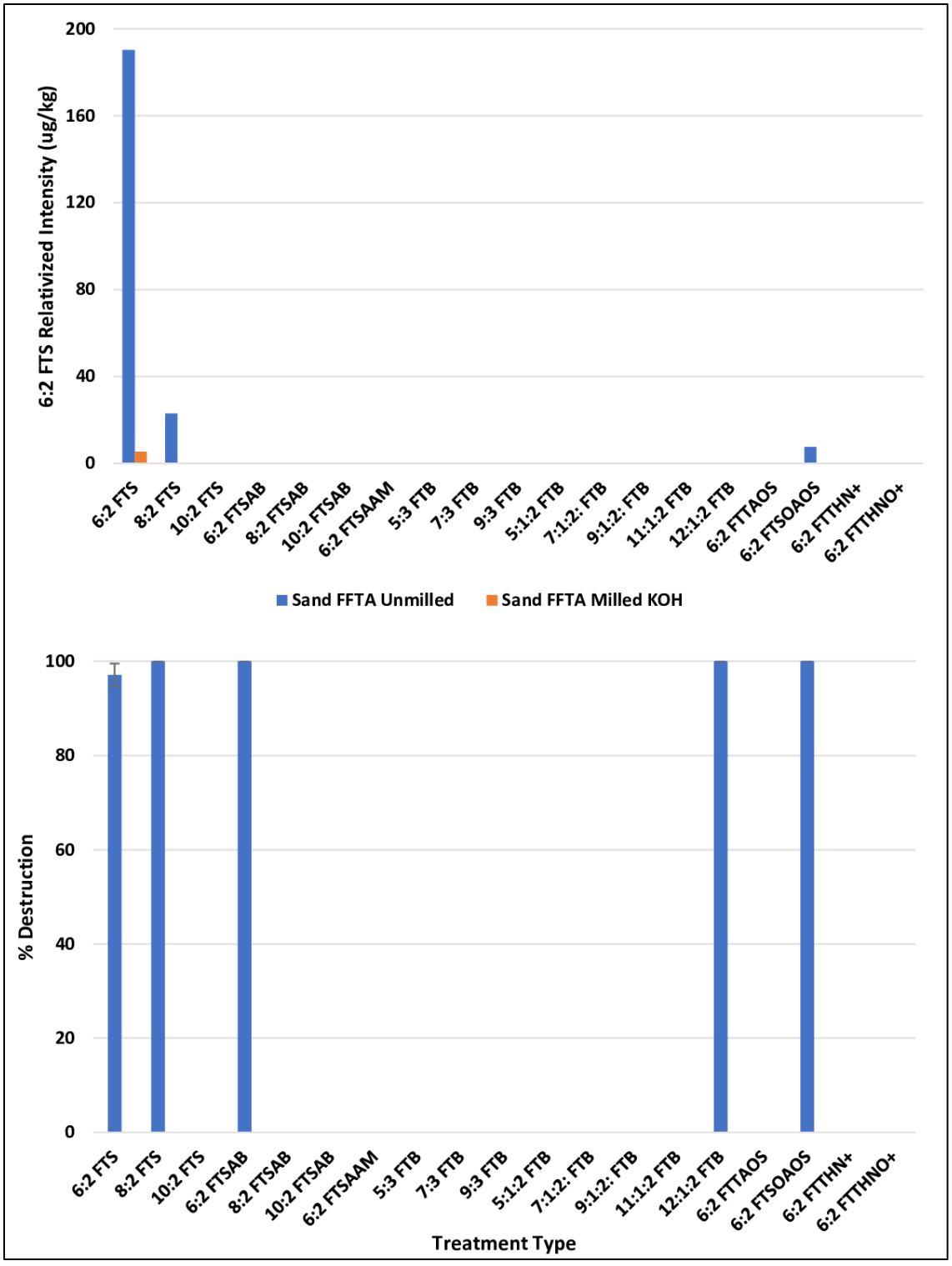

Figure S1: Relativized intensity (top) and relative degradation (bottom) of non-targeted PFAS found in the FFTA sand with KOH.

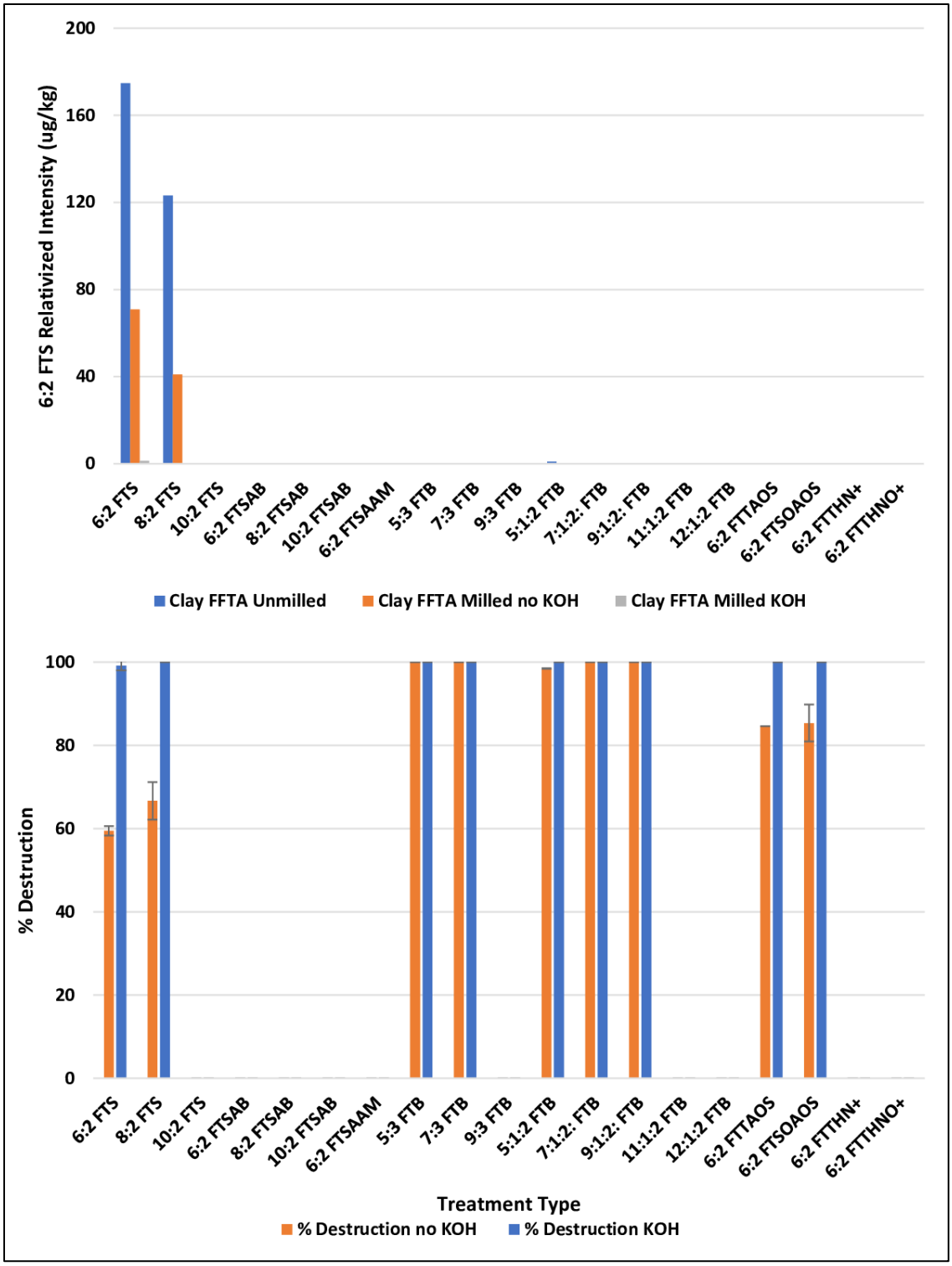

Figure S2: Relativized intensity (top) and relative degradation (bottom) of non-targeted PFAS found in the FFTA clay with and without KOH.

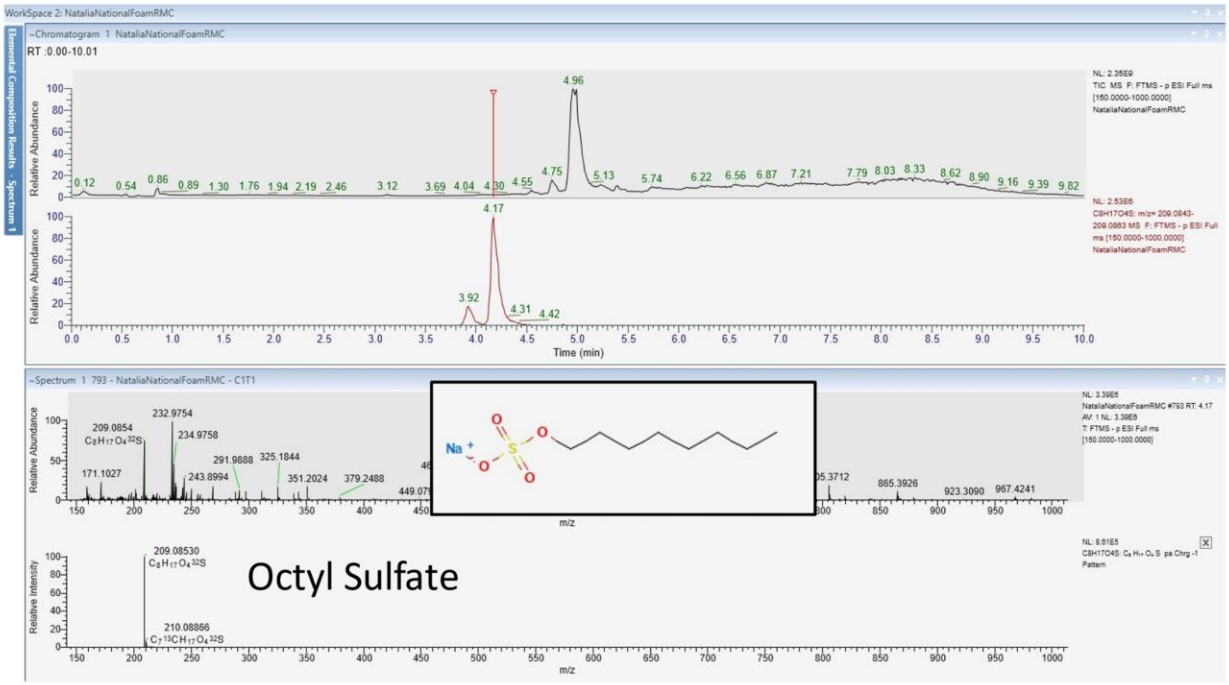

Figure S3: Chromatogram and extracted ion chromatogram of AFFF component in the mixed National Foam sample.

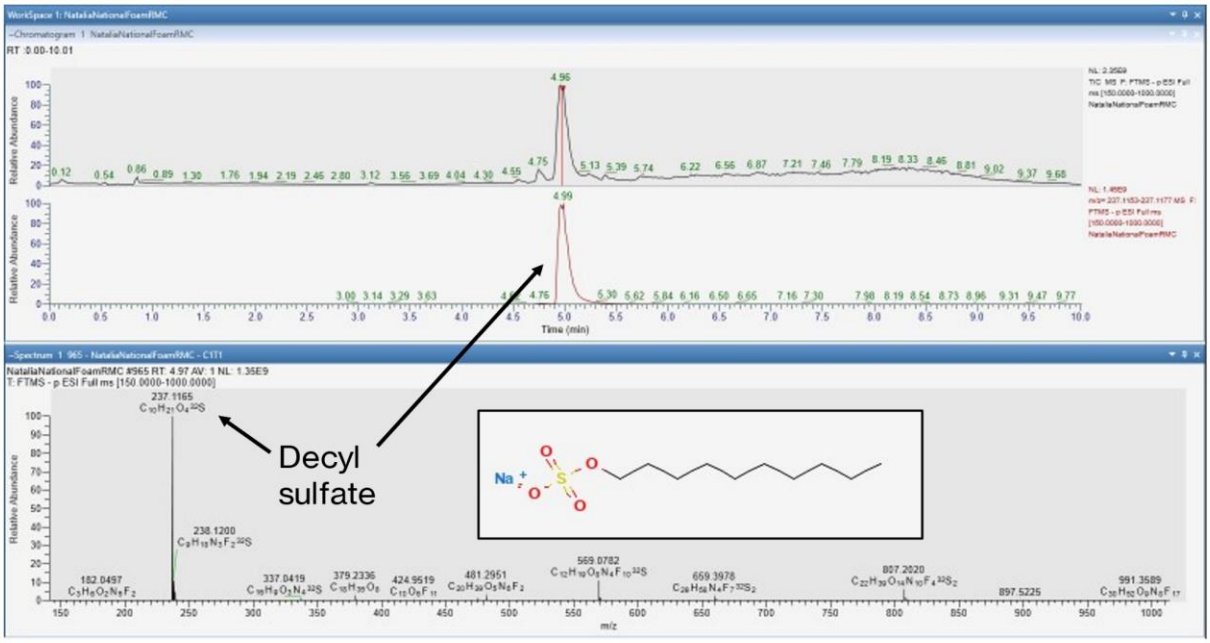

Figure S4: Chromatogram and extracted ion chromatogram of AFFF component in the mixed National Foam sample.

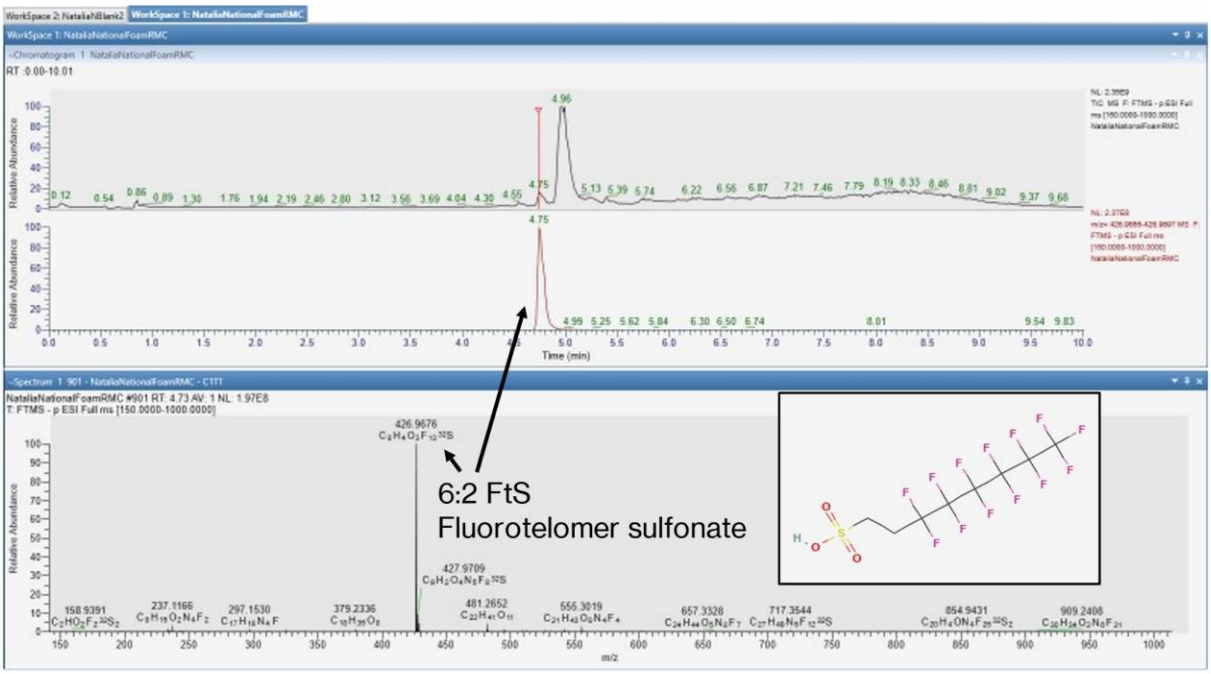

Figure S5: Chromatogram and extracted ion chromatogram of AFFF component in the mixed National Foam sample.

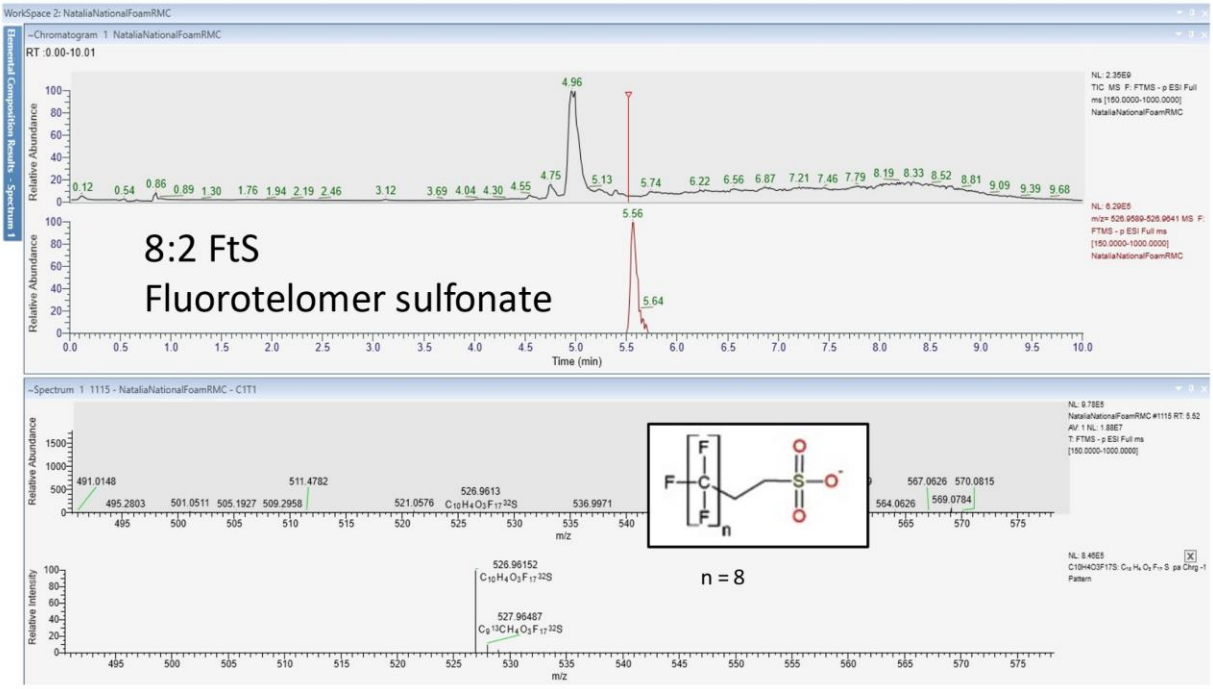

Figure S6: Chromatogram and extracted ion chromatogram of AFFF component in the mixed National Foam sample.

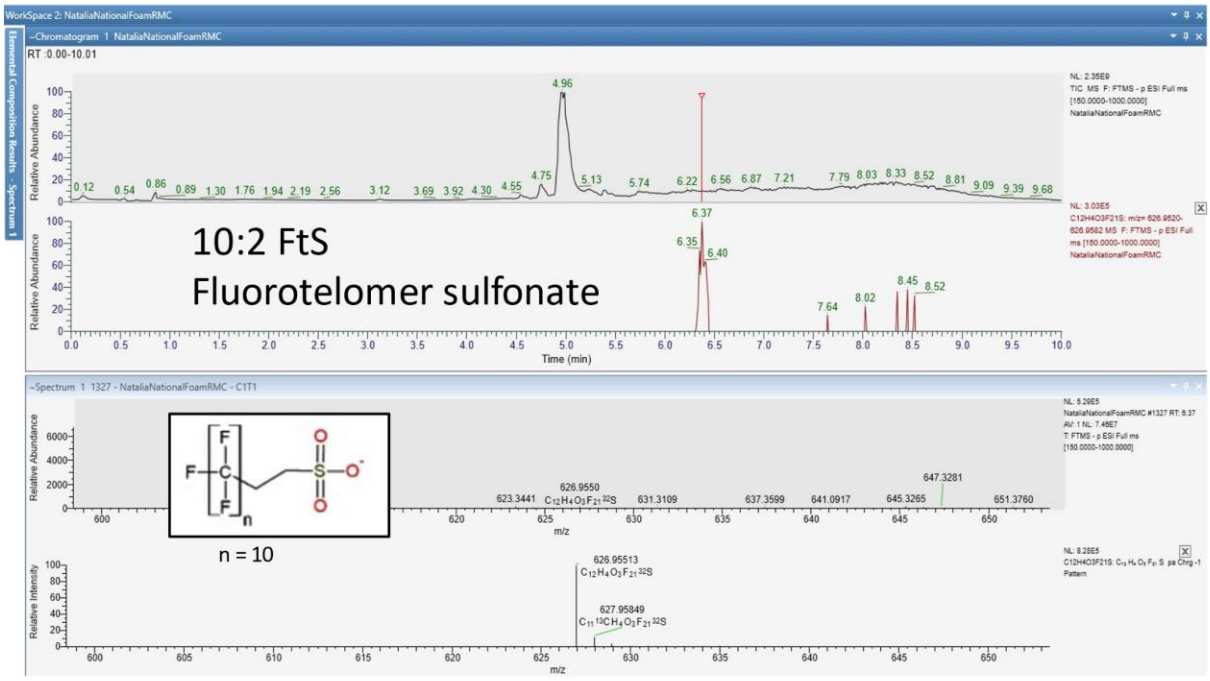

Figure S7: Chromatogram and extracted ion chromatogram of AFFF component in the mixed National Foam sample.

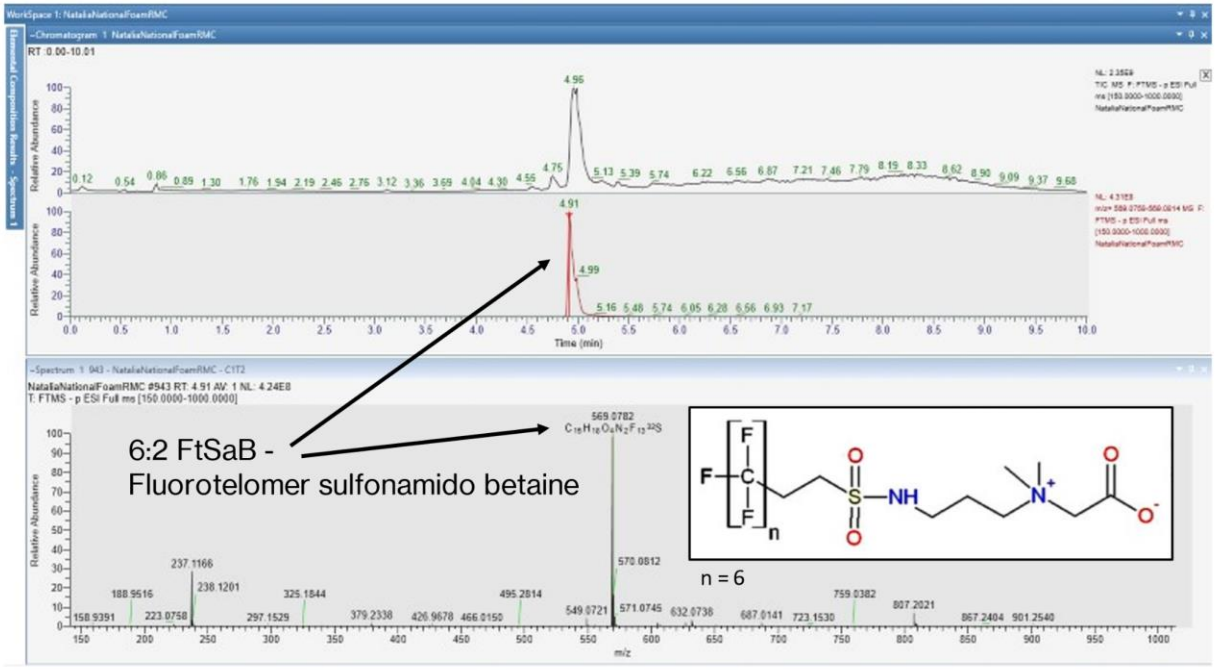

Figure S8: Chromatogram and extracted ion chromatogram of AFFF component in the mixed National Foam sample.

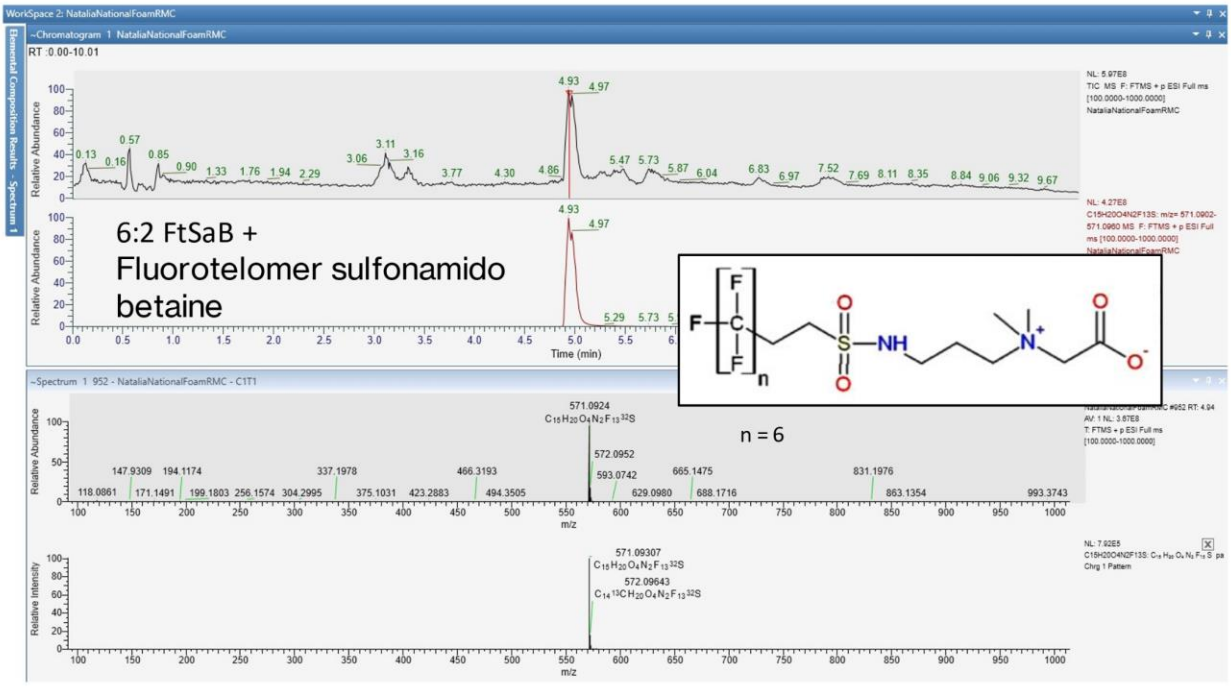

Figure S9: Chromatogram and extracted ion chromatogram of AFFF component in the mixed National Foam sample.

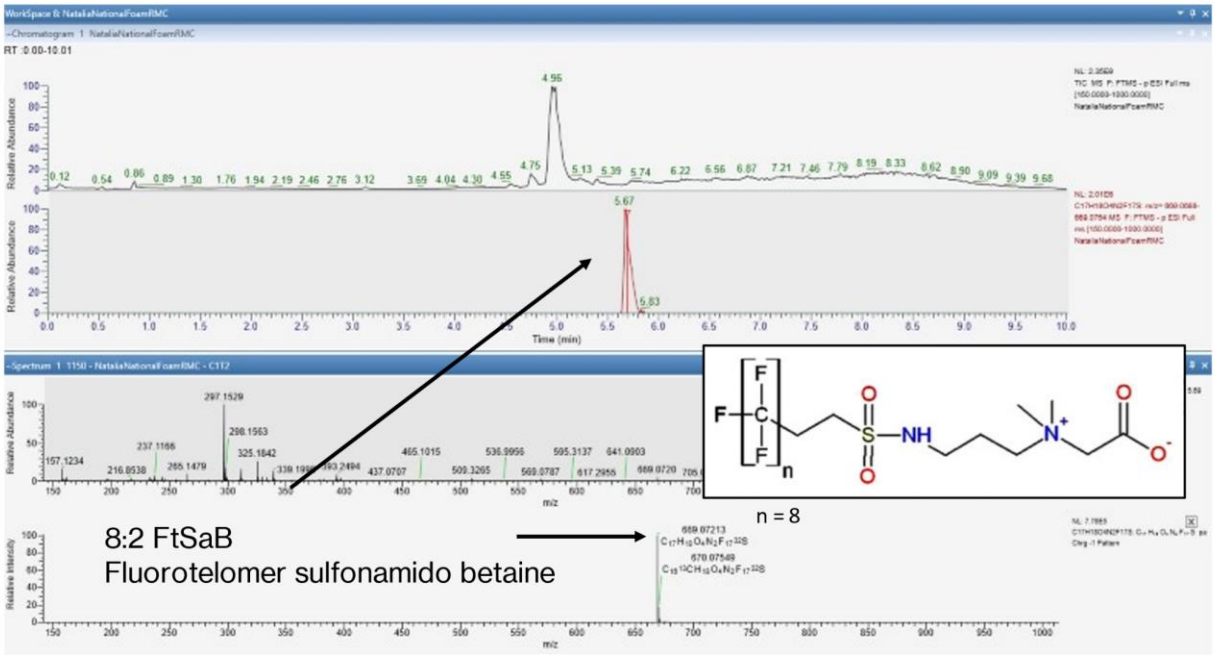

Figure S10: Chromatogram and extracted ion chromatogram of AFFF component in the mixed National Foam sample.

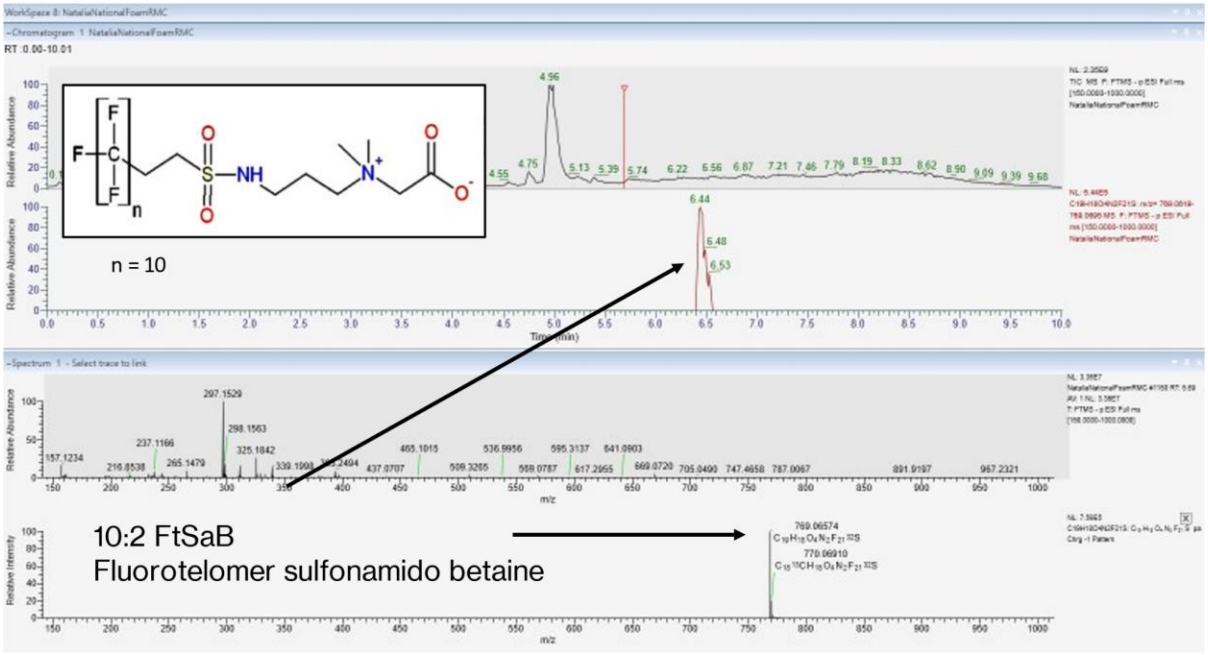

Figure S11: Chromatogram and extracted ion chromatogram of AFFF component in the mixed National Foam sample.

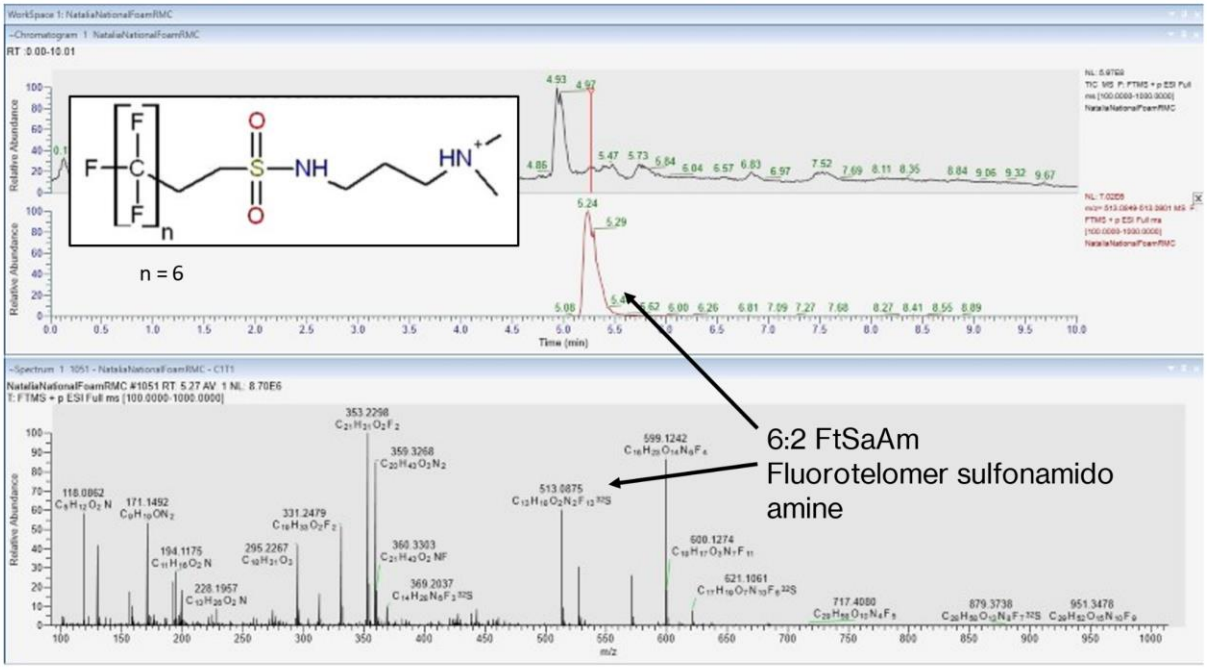

Figure S12: Chromatogram and extracted ion chromatogram of AFFF component in the mixed National Foam sample.

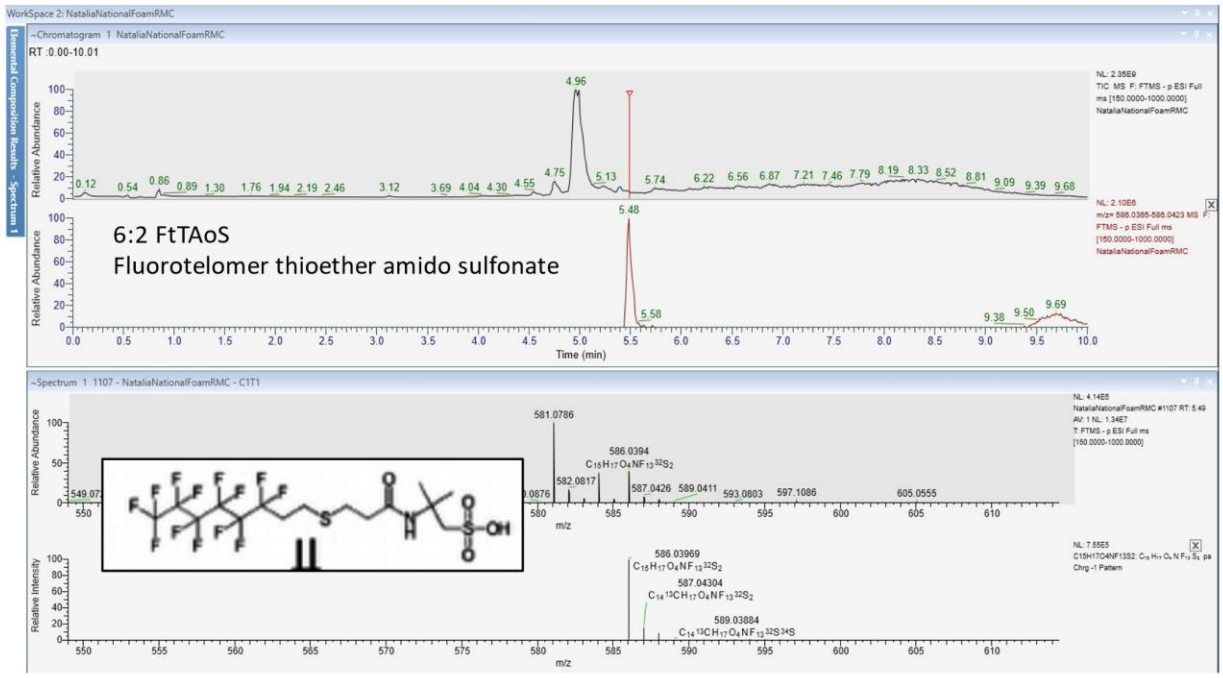

Figure S13: Chromatogram and extracted ion chromatogram of AFFF component in the mixed National Foam sample.

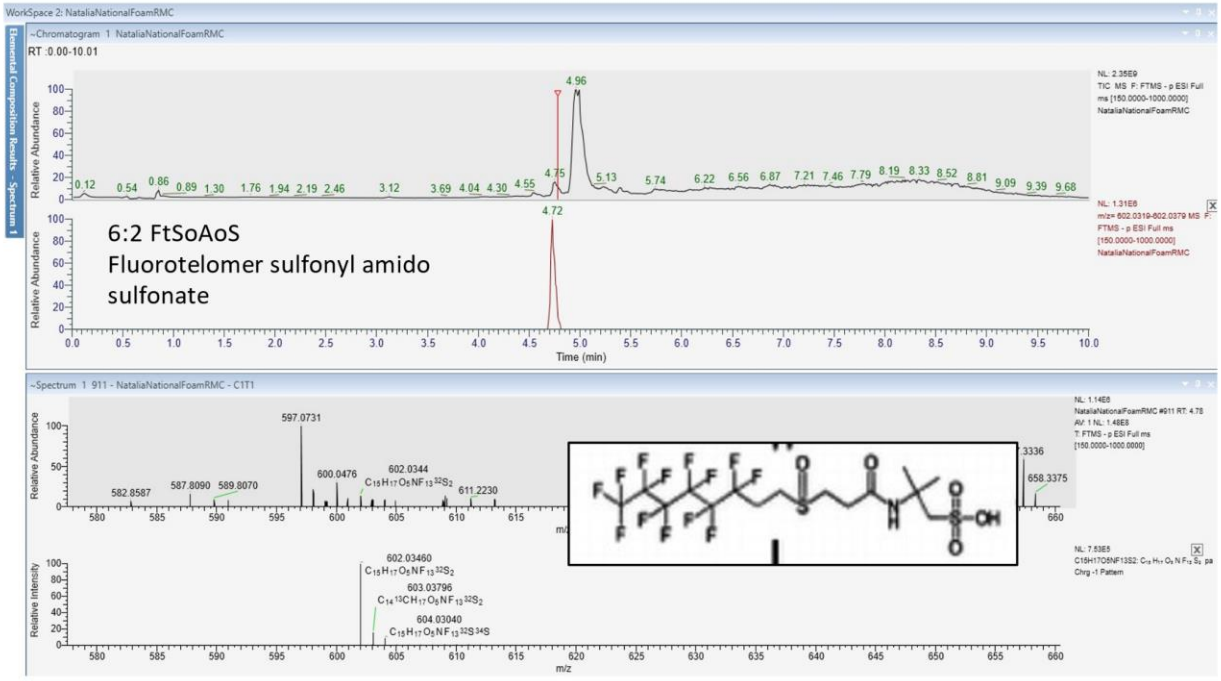

Figure S14: Chromatogram and extracted ion chromatogram of AFFF component in the mixed National Foam sample.

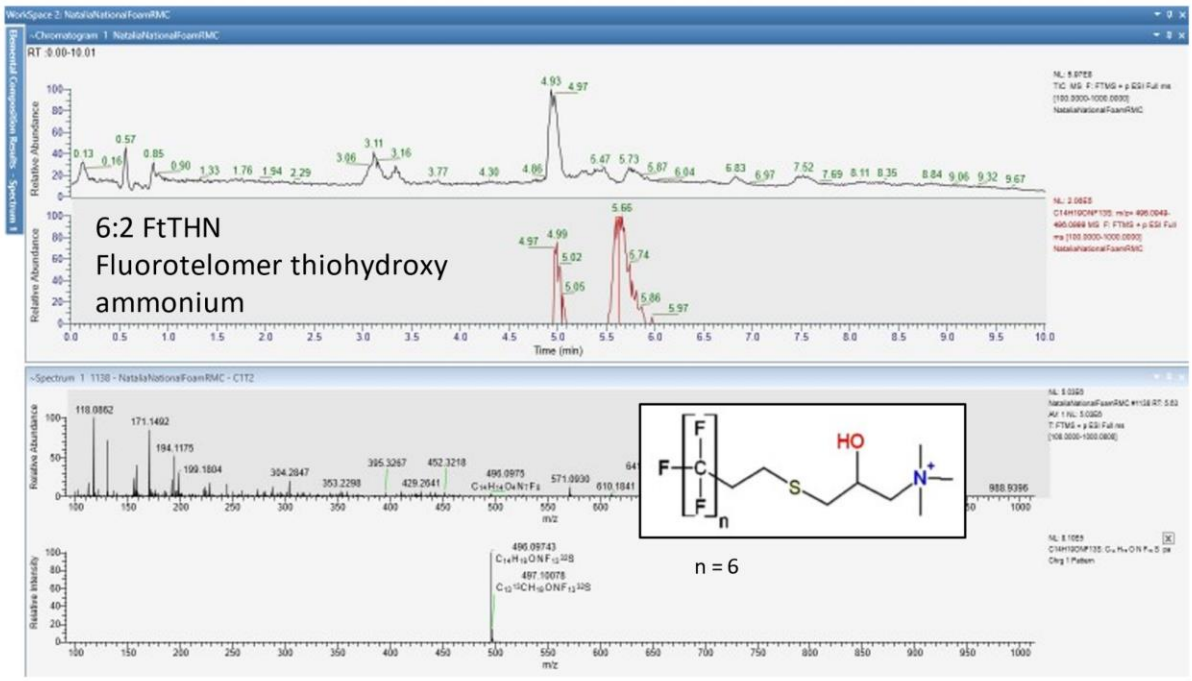

Figure S15: Chromatogram and extracted ion chromatogram of AFFF component in the mixed National Foam sample.

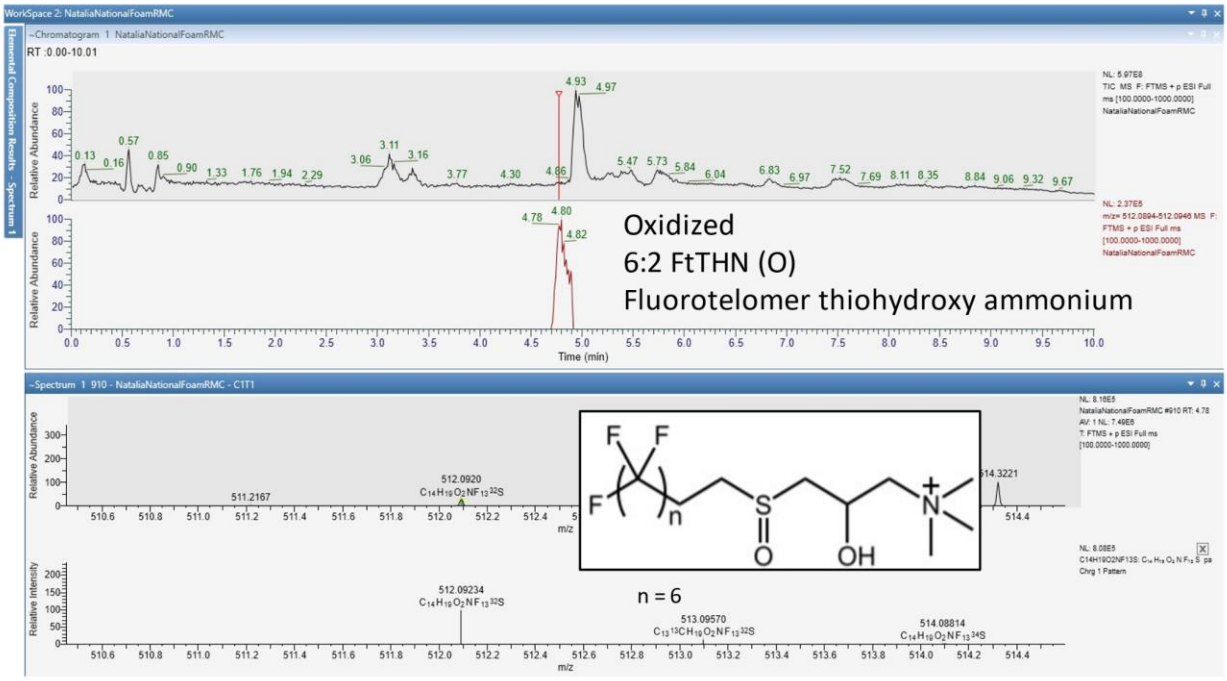

Figure S16: Chromatogram and extracted ion chromatogram of AFFF component in the mixed National Foam sample.

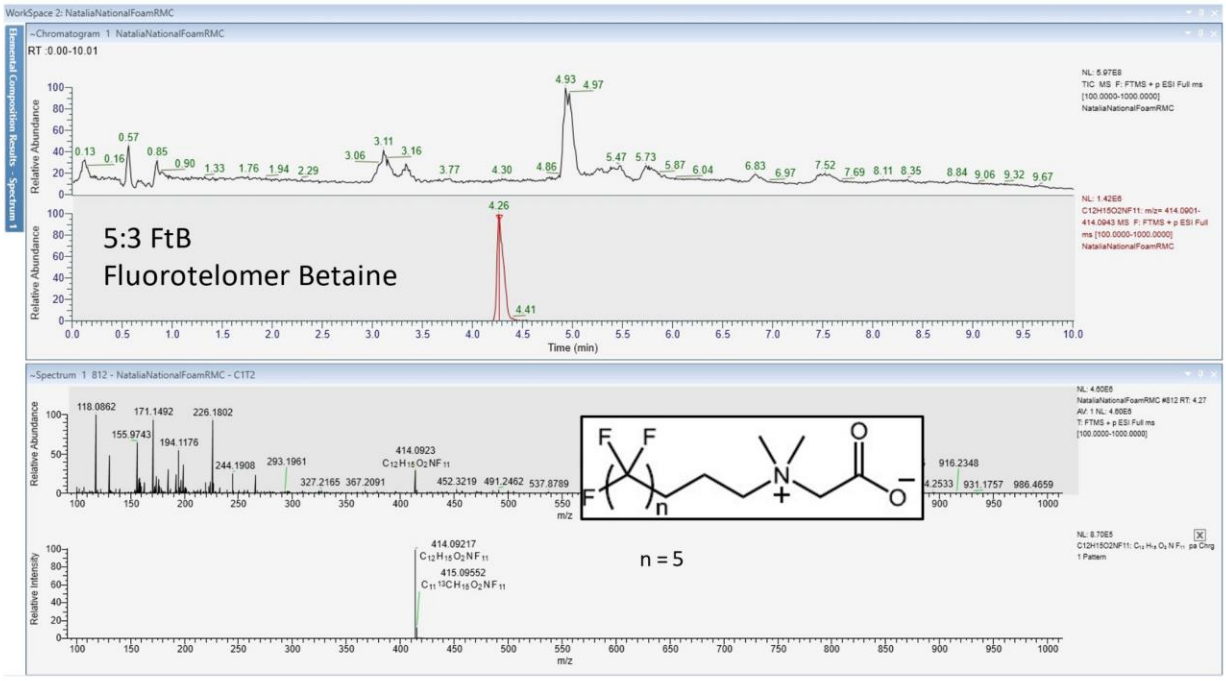

Figure S17: Chromatogram and extracted ion chromatogram of AFFF component in the mixed National Foam sample.

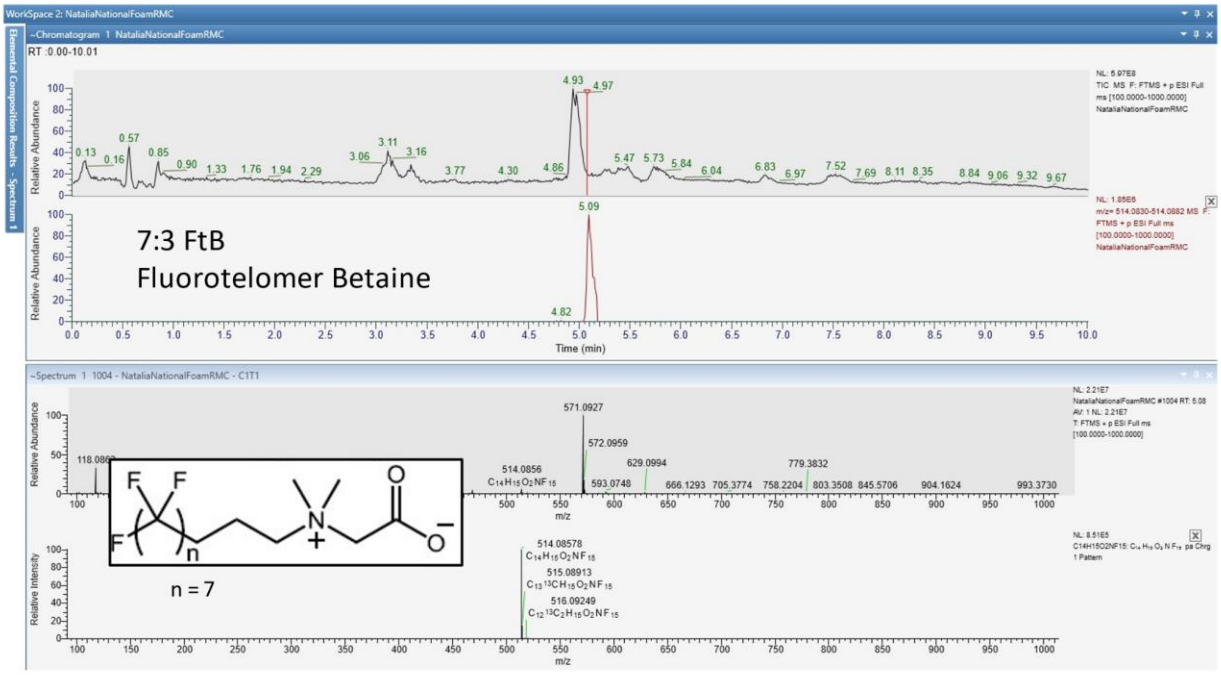

Figure S18: Chromatogram and extracted ion chromatogram of AFFF component in the mixed National Foam sample.

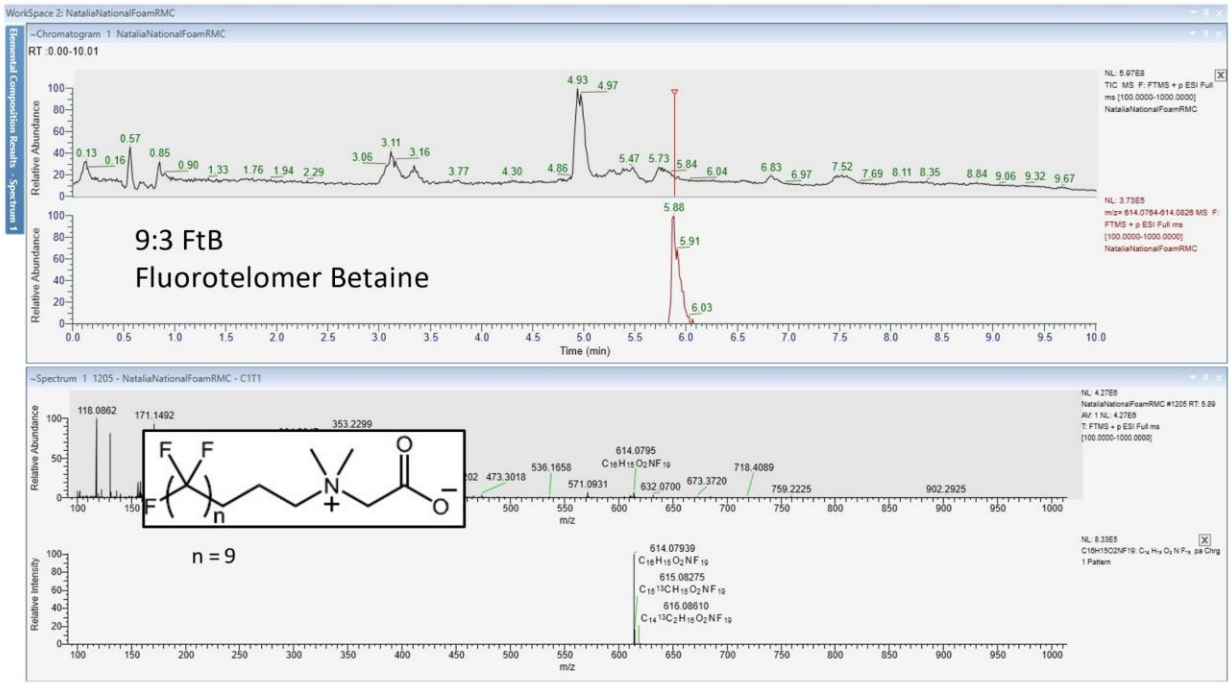

Figure S19: Chromatogram and extracted ion chromatogram of AFFF component in the mixed National Foam sample.

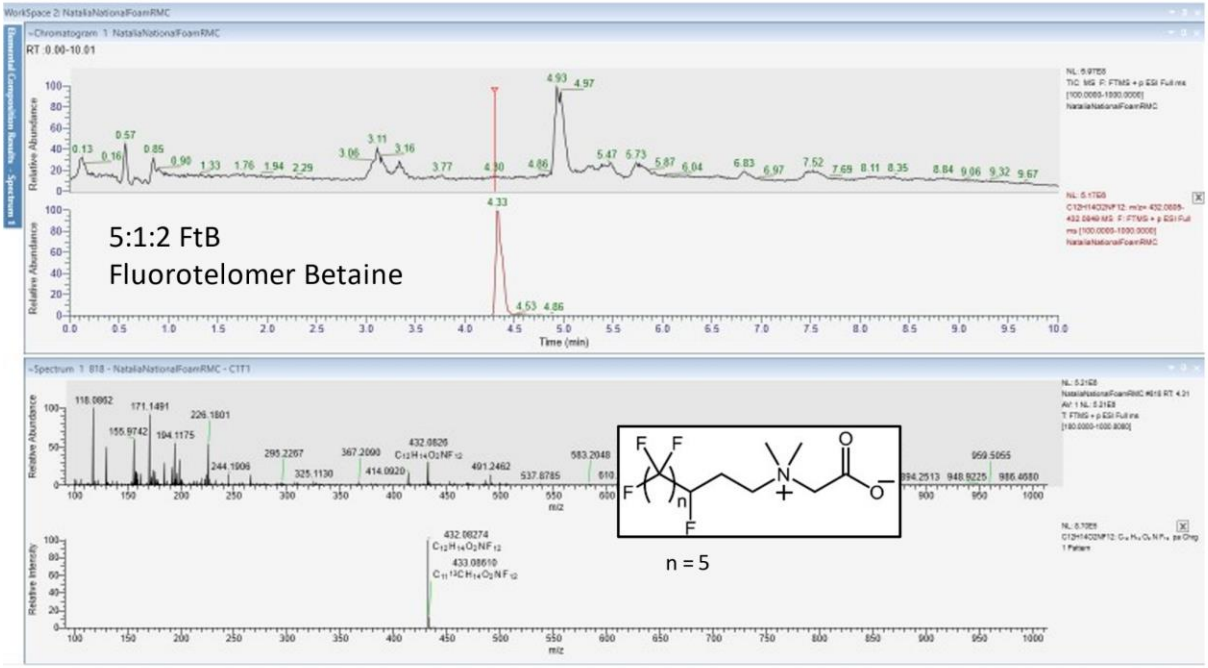

Figure S20: Chromatogram and extracted ion chromatogram of AFFF component in the mixed National Foam sample.

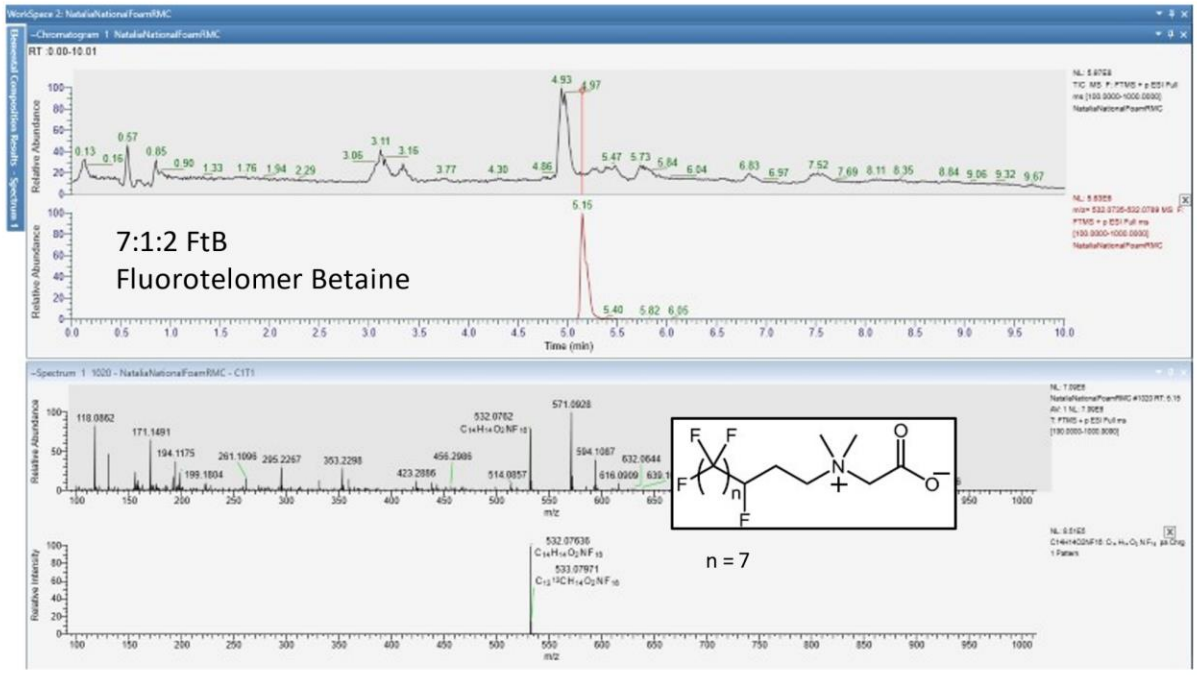

Figure S21: Chromatogram and extracted ion chromatogram of AFFF component in the mixed National Foam sample.

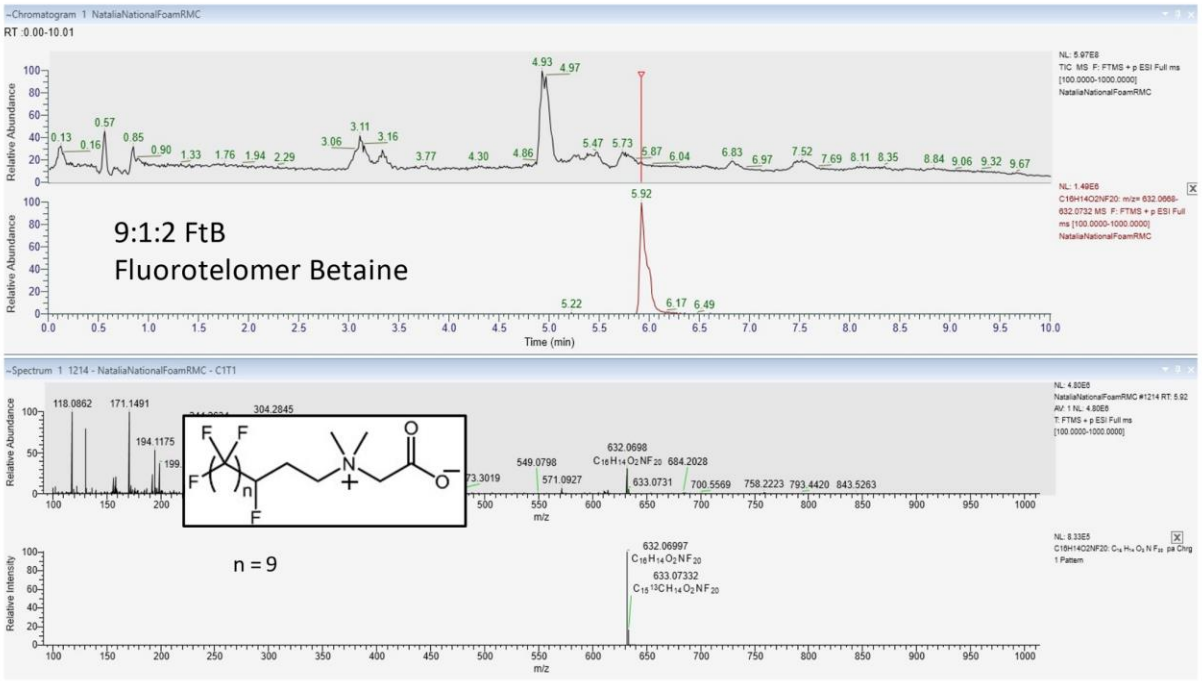

Figure S22: Chromatogram and extracted ion chromatogram of AFFF component in the mixed National Foam sample.

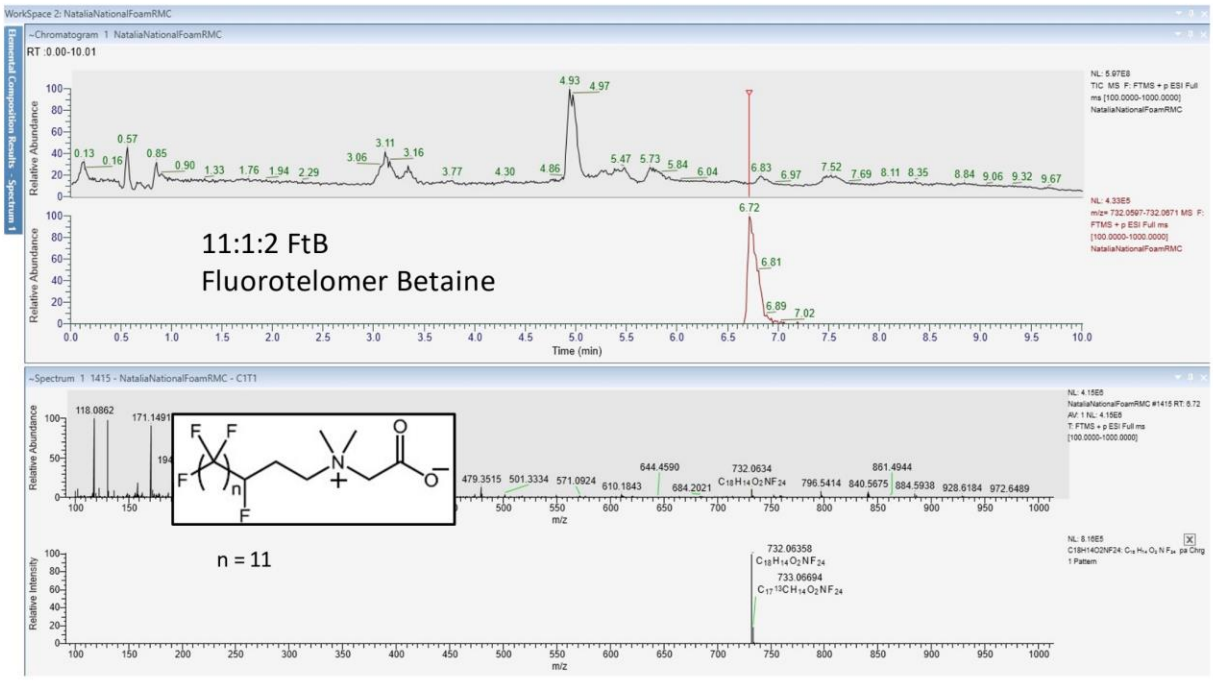

Figure S23: Chromatogram and extracted ion chromatogram of AFFF component in the mixed National Foam sample.

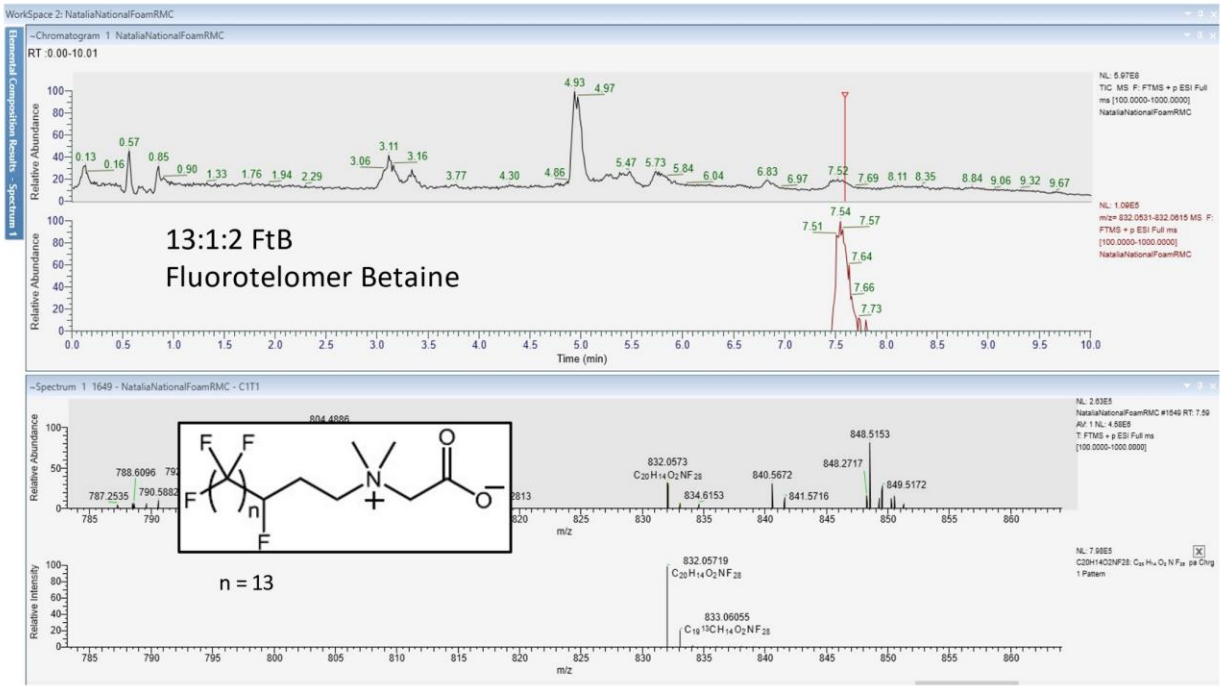

Figure S24: Chromatogram and extracted ion chromatogram of AFFF component in the mixed National Foam sample.

Appendix B – Supplementary Information for Chapter 4

Mechanochemical degradation of per- and polyfluoroalkyl substances in soil using an industrial-scale horizontal ball mill with comparisons of key operational metrics

Nicholas J. Battye†, David J. Patch†, Ryan Monteith‡, Dylan M. D. Roberts†, Natalia M. O'Connor†, Bernard H. Kueper†, Michael E. Hulley†, Kela P. Weber†.*

† Environmental Sciences Group, Department of Chemistry and Chemical Engineering, Royal Military College of Canada, Kingston, ON, Canada.

‡SGS Canada Inc., Lakefield, ON, Canada.

† Department of Civil Engineering, Queen's University, Kingston, ON, Canada.

† Environmental Sciences Group, Department of Civil Engineering, Royal Military College of Canada, Kingston, ON, Canada.

*Corresponding Author: Kela P. Weber (Kela.Weber@rmc.ca). Royal Military College of Canada, PO Box 17000, Station Forces, Kingston, Ontario, Canada, K7K 7B4.

KEYWORDS: PFAS, AFFF, mechanochemistry, ball mill, soil, remediation

TABLE OF CONTENTS

Table S1: Horizontal ball mill trial details.

Soil Type	Mass grinding media (kg)	Mass soil (kg)	Mass KOH (kg)
NSS - PFOS&PFOA	250	50	0.5
NSS - PFOS&PFOA	250	50	0.5
NSS - PFOS&PFOA	250	50	-
NSS - PFOS&PFOA	250	50	-
NSS - 6:2 FTSA	250	50	0.5
NSS - 6:2 FTSA	250	50	0.5
NSS - 6:2 FTSA	250	50	0.5
NSS - 6:2 FTSA	250	50	-
NSS - AFFF	250	50	0.5
NSS - AFFF	250	50	0.5
NSS - AFFF	250	50	-
NSS - AFFF	250	50	-
FFTA Soil 1 (sandy silt)	250	50	0.5
FFTA Soil 1 (sandy silt)	250	50	0.5
FFTA Soil 1 (sandy silt)	250	50	-
FFTA Soil 1 (sandy silt)	250	50	-
FFTA Soil 1 (sandy silt) - spiked	250	50	0.5
FFTA Soil 1 (sandy silt) - spiked	250	50	0.5
FFTA Soil 2 (silty sand)	250	50	0.5
FFTA Soil 2 (silty sand)	250	50	0.5
FFTA Soil 2 (silty sand)	250	50	-
FFTA Soil 2 (silty sand)	250	50	-

Table S2: Targeted PFAS analyzed using LC-MS/MS.

PFAS Class	PFAS Name	Abbreviation
Perfluorocarboxylic Acids (PFCA) (C_xF_{2x}-1COOH)	Trifluoroacetic acid	TFA
	Perfluoropropanoic acid	PFPA
	Perfluorobutanoic acid	PFBA
	Perfluoropentanoic acid	PFPeA
	Perfluorohexanoic acid	PFHxA
	Perfluoroheptanoic acid	PFHpA
	Perfluorooctanoic acid	PFOA
	Perfluorononanoic acid	PFNA
	Perfluorodecanoic acid	PFDA
	Perfluoroundecanoic acid	PFUnDA
	Perfluorododecanoic acid	PFDoDA
Perfluorosulfonic Acids (PFSA) ($C_xF_{2x+1}SO_3H$)	Perfluorobutane sulfonic acid	PFBS
	Perfluorohexane sulfonic acid	PFHxS
	Perfluorooctane sulfonic acid	PFOS
Fluorotelomer Sulfonic Acids (FTSA) ($C_xF_{2x+}1C_nH_{2n}SO_3H$)	6:2 fluorotelomer sulfonate	6:2 FTSA
Perfluorosulfonamide (PFOSA) ($C_xF_{2x+}1SO_2NH_2$)	Perfluorooctane sulfonamide	PFOSA

Table S3: Non-targeted PFAS identified and analyzed using LC-HRAM/MS.

Compound name	Abbreviated Name	Chemical Formula	Accurate Mass	Theoretical Mass	Mass Error
Octyl sulfate	OS	C8H17SO4	209.0854	209.08530	0.48
Decyl sulfate	DS	C10H21SO4	237.1165	237.11660	-0.42
6:2 Fluorotelomer sulfonates	6:2 FtSA	C8H4F13SO3	426.9676	426.96790	-0.70
8:2 Fluorotelomer sulfonates	8:2 FtSA	C10H4F17SO3	526.9613	526.96152	-0.42
10:2 Fluorotelomer sulfonates	10:2 FtSA	C12H4F21SO3	626.9550	626.95513	-0.21
6:2 Fluorotelomer sulfonamido betaines	6:2 FtSaB	C15H18N2F13SO4	569.0782	569.07852	-0.56
6:2 Fluorotelomer sulfonamido betaines	6:2 FtSaB	C15H20N2F13SO4	571.0924	571.09307	-1.17
8:2 Fluorotelomer sulfonamido betaines	8:2 FtSaB	C17H18N2F17SO4	669.0720	669.07213	-0.19
10:2 Fluorotelomer sulfonamido betaines	10:2 FtSaB	C19H18N2F21SO4	769.0657	769.06574	-0.05
6:2 Fluorotelomer sulfonamido amines	6:2 FtSaAm	C13H18N2F13SO2	513.0875	513.08759	-0.18
6:2 Fluorotelomer thioether amido sulfonates	6:2 FtTAoS	C15H17NF13S2O4	586.0394	586.03969	-0.49
6:2 Fluorotelomer sulfonyl amido sulfonates	6:2 FtSoAoS	C15H17NF13S2O5	602.0344	602.03460	-0.33
6:2 Fluorotelomer thiohydroxy ammonium	6:2 FtTHN	C14H19NF13SO	496.0975	496.09743	0.14
Oxidized 6:2 Fluorotelomer thiohydroxy ammonium	6:2 FtTHNO	C14H19NF13SO2	512.0920	512.09234	-0.66
5:3 Fluorotelomer betaines	5:3 FtB	C12H15NF11O2	414.0923	414.09217	0.31
5:1:2 Fluorotelomer betaines	5:1:2 FtB	C12H14NF12O2	432.0826	432.08274	-0.32
7:3 Fluorotelomer betaines	7:3 FtB	C14H15NF15O2	514.0856	514.08578	-0.35
7:1:2 Fluorotelomer betaines	7:1:2 FtB	C14H14NF16O2	532.0762	532.07636	-0.30
9:3 Fluorotelomer betaines	9:3 FtB	C16H15NF19O2	614.0795	614.07939	0.18
9:1:2 Fluorotelomer betaines	9:1:2 FtB	C16H14NF20O2	632.0698	632.06997	-0.27
11:1:2 Fluorotelomer betaines	11:1:2 FtB	C18H14NF24O2	732.0634	732.06358	-0.25
13:1:2 Fluorotelomer betaines	13:1:2 FtB	C20H14NF28O2	832.0573	832.05719	0.13

Target PFAS Analysis using LC-MS/MS

Sample pH was measured with litmus paper and adjusted to less than pH 10 with acetic acid. Sample extracts were analyzed using the multiple-reaction-monitoring (MRM) mode on an Agilent 6460 MS/MS coupled to an Agilent 1260 high-pressure liquid chromatography (HPLC) system using a 50 mm × 2.1 um ACME C18 analytical column and paired guard column with a 5-µL injection volume. Mobile phases consisted of 10 mM ammonium acetate in DI water (A) and 10 mM ammonium acetate in acetonitrile (B). The elution profile started at 90% A/10% B, transitioning to 100% B over 4 minutes, holding for 2 minutes, then equilibrating at starting conditions for 3 minutes. Blanks were all found to be below the detection limit of 0.1 ng/g PFAS. All controls and replicates were within 30% of expected values. The Agilent 6460 MS/MS was run with the following source conditions: gas temperature of 250 °C, gas flow rate of 30 psi, sheath gas temperature of 300 °C, sheath gas flow of 12 L/min, negative capillary of 2500 V, and 0 nozzle voltage.

Non-target PFAS Analysis using HRAM/MS

Samples were analyzed on a ThermoFisher Exploris 120 Orbitrap coupled to a Vanquish UHPLC system using a 100 mm × 2.1 µm ACME C18 analytical column and paired guard column with a 15-µL injection volume. Mobile phases consisted of 0.1% acetic acid in DI water (A) and acetonitrile (B). The elution profile started at 90% A/10% B, transitioning to 100% B over 9 minutes, holding for 2 minutes, then equilibrating at starting conditions for 3 minutes. Internal mass calibration was performed using the RunStart EASY-IC (TM) system. A heated electrospray ionization source was used for the ionization of samples following HPLC separation. The HRAM/MS was run in dual polarity mode (voltage 3000+/ 3000-) with a static gas mode, sheath gas of 50 arbitrary units, auxiliary gas of 10 arbitrary units, sweep gas of 4 arbitrary units, ion

transfer tube temperature of 325 °C, and vaporizer temperature of 350 °C. Scan parameters were set using a full scan mode (60,000 orbitrap resolution, RF lens 70%) with a 10 seconds expected LC peak width. Scan parameters also included an intensity triggered ddMS2 mode, with an isolation window of 1.2 m/z, a normalized collision energy type, HCD collision energy of 50%, and automatic scan range mode.

Initial samples were processed using Thermo Scientific FreeStyle® software. Within FreeStyle®, the Elemental Composition tool was used to determine initial suspect masses based on visual peak identification (elements in use: N, O, C, H, S, and F). Isotope simulation was used to identify additional non-target PFAS that were suspected based on the presence of other PFAS commonly found in the formulations. Where initial intensity allowed, MS2 profiles were used to confirm non-target compounds as fluorinated, and high-resolution masses measured were compared to those in literature (D'Agostino & Mabury, 2014; Field, Jennifer A, Sedlak, David, Alvarez-Cohen, 2017; Houtz et al., 2013). AFFF PFAS identities were also confirmed by analyzing National Foam, Ansul, 3 M, and Buckeye formulations in inventory. Intensities for all identified PFAS precursors and non-fluorinated surfactants were normalized to the 6:2 FTS calibration curve to allow for a semi-quantitative measure of the compounds (Charbonnet et al., 2021; Nickerson et al., 2021).

Free-Fluoride Analysis

A modified EPA Method 9214 was used to determine the fluoride content of milled samples. This method has been used successfully for ball milling work previously (Turner et al., 2021). The main modification is the use of DI water as an extraction solution instead of total ionic strength adjustment buffer (TISAB), as this improved recoveries of spiked fluoride. In this method, 1.0 g of ball-milled soil is mixed with 5 mL of DI water, adjusted to pH 5.5 with acetic acid, and mixed

for 24 hours on an end-over-end shaker in 15 mL centrifuge tubes. After mixing, the sample is centrifuged at 4000 RPM for 20 minutes and 2 mL of the supernatant is transferred via pipette to a clean 15 mL centrifuge tube. One (1) mL of TISAB is added to the 2 mL of supernatant and the pH is checked to ensure it is close to pH 5. The use of TISAB and pH control is important as TISAB prevents interferences from iron and aluminum ions, and pH control minimizes fluoride complex formation and hydroxide interferences. A fluoride ion selective electrode is then used to measure the amount of fluoride present in the solution, which is quantified using an external calibration curve. The sample is then spiked with a known amount of fluoride to measure matrix effects.

Synthetic Precipitation Leachate Procedure

The Synthetic Precipitation Leachate Procedure (SPLP) method used was modified from USEPA 1312 SPLP and USGS FLT methods, with the main modifications being centrifugation instead of filtering and an increase of the batch leachate pH from 5.5 to 7 (to better simulate natural conditions). A batch leachate method was employed utilizing a 20:1 ratio of leachate (pH 7 deionized water) to solid (pre/post milled material). The soil was not sieved before use but grain size was less than 2 millimeters. Samples were agitated for 18+/-2 hours on an end-over-end rotary system, centrifuged at 4000 RPM, decanted and sub-sampled. Leachate was centrifuged to avoid uncertainty surrounding PFAS loss that has been noted in literature because of filtration. Samples were then diluted 10X in basic methanol to reduce matrix effects and analyzed using targeted PFAS method.

VitTellus Soil Health Test

VitTellus is a soil health test that assesses the chemical, physical and biological balance of the soil. It provides a unique analysis and soil health index that is highly correlated to yield and the

presence of a combination of disease suppressive and bio-stimulating organisms in the plant microbiome (root zone). Based on eight years of intensive research, assessing over 400 factors related to soil health and yield, it has been proven to confirm predicted yields to actual yields with a correlation of 93%. The assessment typically leads to agronomic strategies to improve soil health, which drives greater nutrient utilization, higher crop yields and greater farm profitability.

The VitTellus Soil Health Test includes a Soil Health index, Solvita CO_2, PMN (potential mineralizable nitrogen), Reactive C (carbon), standard fertility test results, and A&L crop production recommendations. The Soil Health index is a 0 – 60 relative scale which gives an indication of Soil Health ranging from low (0) to high (60). In soils with a low VitTellus Soil Health Index, plant and nutrient levels do not support optimum microbiological levels resulting in lower nutrient utilization efficiency and lower yields. In soils with a high VitTellus Soil Health Index, plant and nutrient levels support greater microbiological activity resulting in greater nutrient uptake efficiency and higher yields. Reactive C (in ppm) is a measure of the available carbon sources for soil microbes and is based on the Cornell Assessment of Soil Health of Active Carbon. For a medium textured soil the classifications are Very Low (0-400), Low (400-500), Medium (500-600), High (600-700), and Very High (>700). A result of 600 ppm or greater indicates sufficient carbon sources are available for soil microbes to flourish. The Solvita CO_2-C Test (in ppm) is a metric that provides a measure of the microbial activity on the soil. Between 60 and 100 ppm suggests good microbial activity. The Soil Health Test also outlines soil chemistry ranges for good soil health as compared to actual test results for several parameters, including pH, e K/Mg Ratio, %K, %Mg, and %Ca. Results that fall into the desired ranges provide good nutrient balance for plants to support soil microbe communities.

Destruction Mechanism Hypothesis Summary

Using a horizontal ball mill, it has been shown that KOH is required to degrade 6:2 FTS, whereas PFOS and PFOA do not (Battye et al., 2022; 2024). Lu et al. (2017) hypothesized a destruction sequence of 6:2 FTS based on their mechanochemical ball milling work using a planetary ball mill, with KOH (Figure S1, below). The hypothesis surmises that the presence of KOH alone, leading to an increase in pH, immediately causes 6:2 FTS transformation through a base catalyzed reaction consisting of dehydrofluorination. This is shown to occur at the 6:2 boundary, which is thought to be a weaker point in the molecule than at the functional head group (contrary to perfluorosulfonates). An alkene structure is formed whereby subsequent fragmentation of the molecule occurs through hydroxyl radical attack at C_3-C_4. The attacking hydroxide remains bound to the perfluorinated moiety, but the negative charge is taken by the nearest fluorine, which detaches as a fluoride ion. The hydroxyl attack, followed by fluoride expulsion, is repeated for the second fluorine on the adjacent carbon, which generates an unstable radical intermediate with two hydroxyl groups attached to the same carbon. This leads to dehydration and transformation of the molecule into PFPeA. Notably, PFPeA was identified as a degradation product of 6:2 FTS in both Lu et al. (2017) and Martin et al. (2019), as well as in all native 6:2 FTS and AFFF spiked NSS trials performed in both Battye et al. (2002) and Battye et al. (2024). Another hydroxyl attack creates an excessive negative charge that leads to a formate removal, leaving a shorter perfluorinated radical behind. This cycle repeats until the molecule undergoes total mineralization.

An entirely reductive mechanism of destruction (i.e., no KOH) was provided in Turner et al. (2023). Figure S2 below shows the hypothesized sequence of destruction for PFOS. The proposed mechanism shows an alpha carbon attack but it was acknowledged that attack can occur anywhere along the carbon chain. C–F bond breakage occurs from electrons, either directly, or through attack

of the head group and rearrangement of the electrons to the alpha carbon (2). This creates a perfluoroalkyl radical that interacts with other reactive species to generate OH substituted structures (3, 8, 16), all of which were consistently detected in Turner et al. (2023) trials using both silica sand and nepheline syenite sand, but only periodically in trace amounts in ground calcite and marble. Unlike experiments using KOH, it was surmised that, here, electrons generated from the mechanochemical activation of the media must be interacting with water (atmospheric water vapour and/or soil moisture). The perfluoroalkyl radicals react with this water, generating the by-product structures observed (structures 3, 5, 8, 14 and 16). SiO_2 in contact with water has been observed to produce hydroxyl radicals and their generation has been modelled (Governa et al., 2002; Narayanasamy and Kubicki, 2005; Wang et al., 2000). After two OH substitutions on a carbon, a more stable ketonic structure is formed, and water is emitted (5 to 6 and 10 to 11). Emission of $HCOO^-$ or CO_2 then results in generation of a PFCA of one less a CF2 moiety (18). This process then repeats.

The reason that reductive destruction alone works for PFOS and PFOA (shown in both Turner et al. (2023) and Battye et al. (2024)) and not for 6:2 FTS may be because of the associated bond dissociation energies (BDEs) associated with the individual C–F bonds on each of the their respective carbon-chain structures. These were modelled by Bentel et al. (2019) and are shown for various PFAS in Figure S3. Although 6:2 FTS, PFOS, and PFOA are not explicitly shown, the structures shown for (c) – 6:2 FTCA, and (d) – PFNA, in particular, are good representations of 6:2 FTS and PFOS, respectively, as the only difference would be a sulfonate head group instead of the indicated carboxylate head group. And (d) – PFNA, is also a good representation of PFOA as the only difference would be one less CF_2 moiety. What the BDEs show is that, the longer the perfluorinated chain, the greater the number C–F bonds with lower BDEs, and thus, the more

susceptible it is to reductive attack, specifically, somewhere in the middle of the carbon chain, which may be why there were no measurable PFAS by-products observed in Battye et al. (2022) and Battye etl al. (2024) for the simple PFOS and PFOA spiked NSS trials. The two unsaturated carbons on 6:2 FTS actually lead to higher C–F BDEs on the overall carbon chain, making it more resistant to reductive destruction than PFOS. Granted, the average C–H BDE is much lower, around 99 kcal/mol^{-1}, which would make the C–H bond more susceptible to dissociation, but the likely follow-up addition would be another H for no net change overall. With respect to PFOA (and other PFCAs), the carboxylate head group also leads to lower C–F BDEs on the adjacent CF2, which makes head group disassociation more probable in PFCAs. This is not the case for sulfonates.

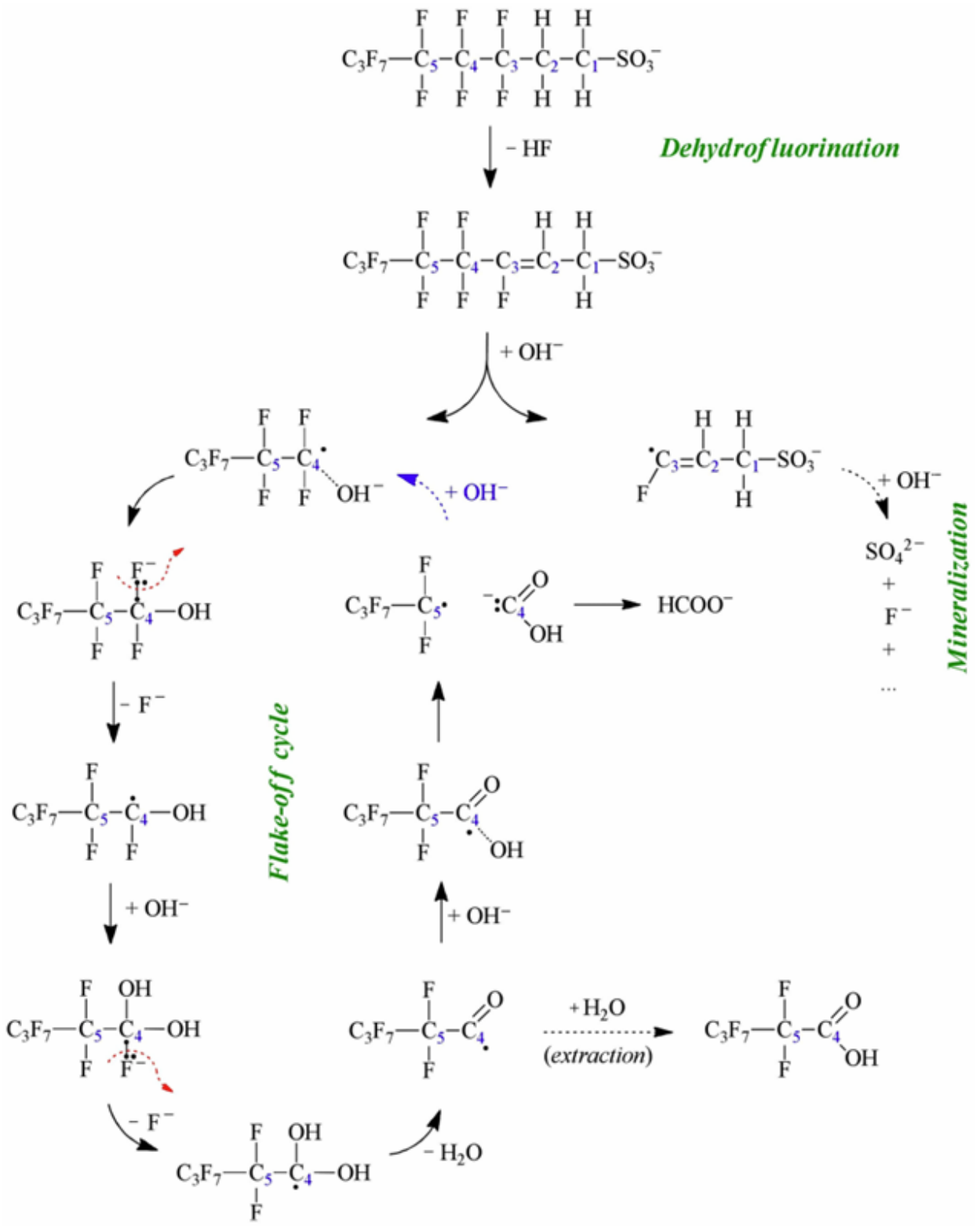

Figure S1: Proposed reaction mechanism for the mechanochemical destruction of 6:2 FTS (from Lu et al (2017)).

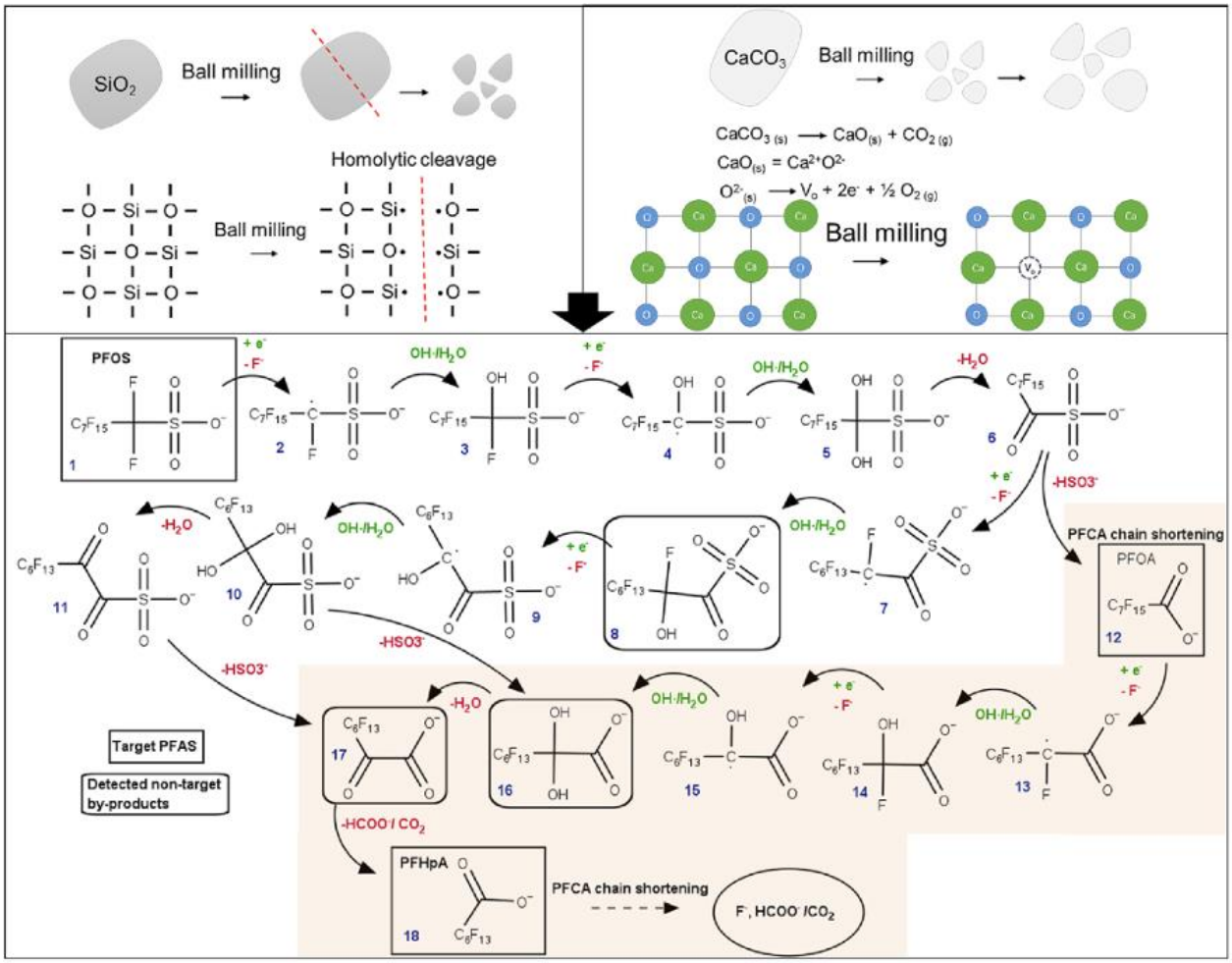

Figure S2: Proposed mechanism of destruction for PFOS and PFOA by planetary ball milling (from Turner et al 2023)).

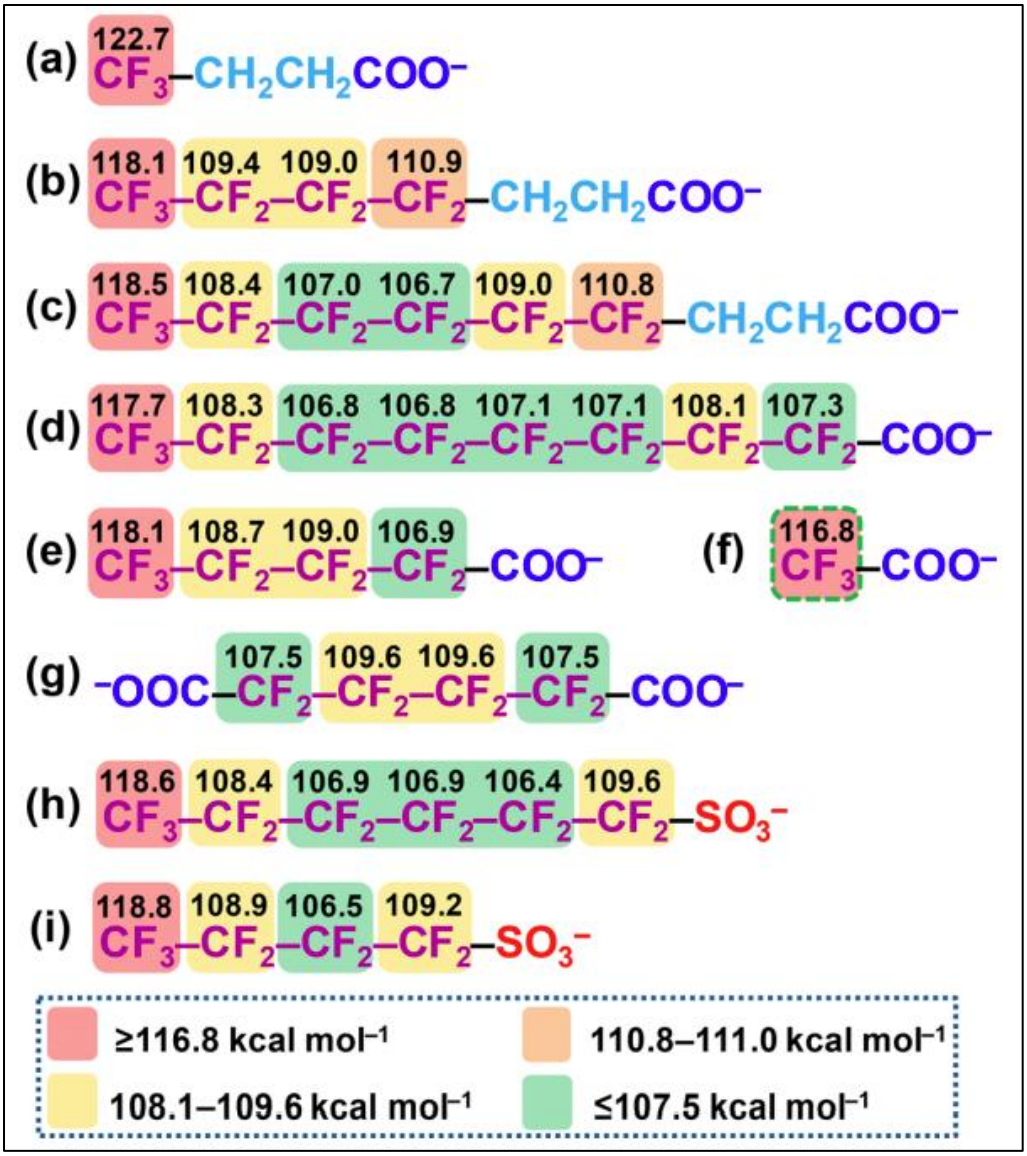

Figure S3: Calculated C−F bond dissociation energies (BDEs) (kcal mol^{-1}) of selected PFAS (from Bentel et al (2019)).

Appendix C – Supplementary Information for Chapter 5

Mechanochemical degradation of per- and polyfluoroalkyl substances in soil from a firefighter training area at three scales

Nicholas J. Battye†, David J. Patch†, Dean Morrow†, Michael E. Hulley†, Kela P. Weber†.*

† Environmental Sciences Group, Department of Chemistry and Chemical Engineering, Royal Military College of Canada, Kingston, ON, Canada.

† Environmental Sciences Group, Department of Civil Engineering, Royal Military College of Canada, Kingston, ON, Canada.

*Corresponding Author: Kela P. Weber (Kela.Weber@rmc.ca). Royal Military College of Canada, PO Box 17000, Station Forces, Kingston, Ontario, Canada, K7K 7B4.

KEYWORDS: PFAS, AFFF, mechanochemistry, ball mill, soil, remediation

TABLE OF CONTENTS

Table S1: Milling parameter details.

Cylinder size	Milling Parameters	Mass grinding media (kg)	Mass soil (kg)	Mass KOH (kg)
0.25 L cylinder (PBM)	5:1 media:soil; 10:1 soil:KOH	0.4950	0.0990	0.0099
	5:1 media:soil; 100:1 soil:KOH	0.4950	0.0990	0.0010
	5:1 media:soil; no KOH	0.4950	0.0990	-
	3:1 media:soil; 10:1 soil:KOH	0.4950	0.1500	0.0150
1 L cylinder (HBM)	5:1 media:soil; 10:1 soil:KOH	1.00	0.200	0.020
	5:1 media:soil; 100:1 soil:KOH	1.00	0.200	0.002
	5:1 media:soil; no KOH	1.00	0.200	-
	3:1 media:soil; 10:1 soil:KOH	1.00	0.300	0.030
267 L cylinder (HBM)	5:1 media:soil; 10:1 soil:KOH	-	-	-
	5:1 media:soil; 100:1 soil:KOH	250	50	0.5
	5:1 media:soil; no KOH	250	50	-
	3:1 media:soil; 10:1 soil:KOH	250	83	0.5
	3:1 media:soil; 10:1 soil:KOH	150	50	0.5

Table S2: Targeted PFAS analyzed using LC-MS/MS.

PFAS Class	PFAS Name	Abbreviation
Perfluorocarboxylic Acids (PFCA) (C_xF_{2x}-1COOH)	Trifluoroacetic acid	TFA
	Perfluoropropanoic acid	PFPA
	Perfluorobutanoic acid	PFBA
	Perfluoropentanoic acid	PFPeA
	Perfluorohexanoic acid	PFHxA
	Perfluoroheptanoic acid	PFHpA
	Perfluorooctanoic acid	PFOA
	Perfluorononanoic acid	PFNA
	Perfluorodecanoic acid	PFDA
	Perfluoroundecanoic acid	PFUnDA
	Perfluorododecanoic acid	PFDoDA
	Perfluorotridecanoic acid	PFTrDA
	Perfluorotetradecanoic acid	PFTeDA
Perfluorosulfonic Acids (PFSA) ($C_xF_{2x+1}SO_3H$)	Perfluorobutane sulfonic acid	PFBS
	Perfluorohexane sulfonic acid	PFHxS
	Perfluoroheptane sulfonic acid	PFHpS
	Perfluorooctane sulfonic acid	PFOS
	Perfluorodecane sulfonic acid	PFDS
	Perfluorododecane sulfonic acid	PFDoS
Fluorotelomer Sulfonic Acids (FTSA) ($C_xF_{2x+}1C_nH_{2n}SO_3H$)	6:2 fluorotelomer sulfonate	6:2 FTSA
	8:2 fluorotelomer sulfonate	8:2 FTSA
Perfluorosulfonamide (PFOSA) ($C_xF_{2x+}1SO_2NH_2$)	Perfluorooctane sulfonamide	PFOSA

Table S3: Non-targeted PFAS identified and analyzed using LC-HRAM/MS.

Compound name	Abbreviated Name	Chemical Formula	Accurate Mass	Theoretical Mass	Mass Error
Octyl sulfate	OS	C8H17SO4	209.0854	209.08530	0.48
Decyl sulfate	DS	C10H21SO4	237.1165	237.11660	-0.42
6:2 Fluorotelomer sulfonates	6:2 FtSA	C8H4F13SO3	426.9676	426.96790	-0.70
8:2 Fluorotelomer sulfonates	8:2 FtSA	C10H4F17SO3	526.9613	526.96152	-0.42
10:2 Fluorotelomer sulfonates	10:2 FtSA	C12H4F21SO3	626.9550	626.95513	-0.21
6:2 Fluorotelomer sulfonamido betaines	6:2 FtSaB	C15H18N2F13SO4	569.0782	569.07852	-0.56
6:2 Fluorotelomer sulfonamido betaines	6:2 FtSaB	C15H20N2F13SO4	571.0924	571.09307	-1.17
8:2 Fluorotelomer sulfonamido betaines	8:2 FtSaB	C17H18N2F17SO4	669.0720	669.07213	-0.19
10:2 Fluorotelomer sulfonamido betaines	10:2 FtSaB	C19H18N2F21SO4	769.0657	769.06574	-0.05
6:2 Fluorotelomer sulfonamido amines	6:2 FtSaAm	C13H18N2F13SO2	513.0875	513.08759	-0.18
6:2 Fluorotelomer thioether amido sulfonates	6:2 FtTAoS	C15H17NF13S2O4	586.0394	586.03969	-0.49
6:2 Fluorotelomer sulfonyl amido sulfonates	6:2 FtSoAoS	C15H17NF13S2O5	602.0344	602.03460	-0.33
6:2 Fluorotelomer thiohydroxy ammonium	6:2 FtTHN	C14H19NF13SO	496.0975	496.09743	0.14
Oxidized 6:2 Fluorotelomer thiohydroxy ammonium	6:2 FtTHNO	C14H19NF13SO2	512.0920	512.09234	-0.66
5:3 Fluorotelomer betaines	5:3 FtB	C12H15NF11O2	414.0923	414.09217	0.31
5:1:2 Fluorotelomer betaines	5:1:2 FtB	C12H14NF12O2	432.0826	432.08274	-0.32
7:3 Fluorotelomer betaines	7:3 FtB	C14H15NF15O2	514.0856	514.08578	-0.35
7:1:2 Fluorotelomer betaines	7:1:2 FtB	C14H14NF16O2	532.0762	532.07636	-0.30
9:3 Fluorotelomer betaines	9:3 FtB	C16H15NF19O2	614.0795	614.07939	0.18
9:1:2 Fluorotelomer betaines	9:1:2 FtB	C16H14NF20O2	632.0698	632.06997	-0.27
11:1:2 Fluorotelomer betaines	11:1:2 FtB	C18H14NF24O2	732.0634	732.06358	-0.25
13:1:2 Fluorotelomer betaines	13:1:2 FtB	C20H14NF28O2	832.0573	832.05719	0.13

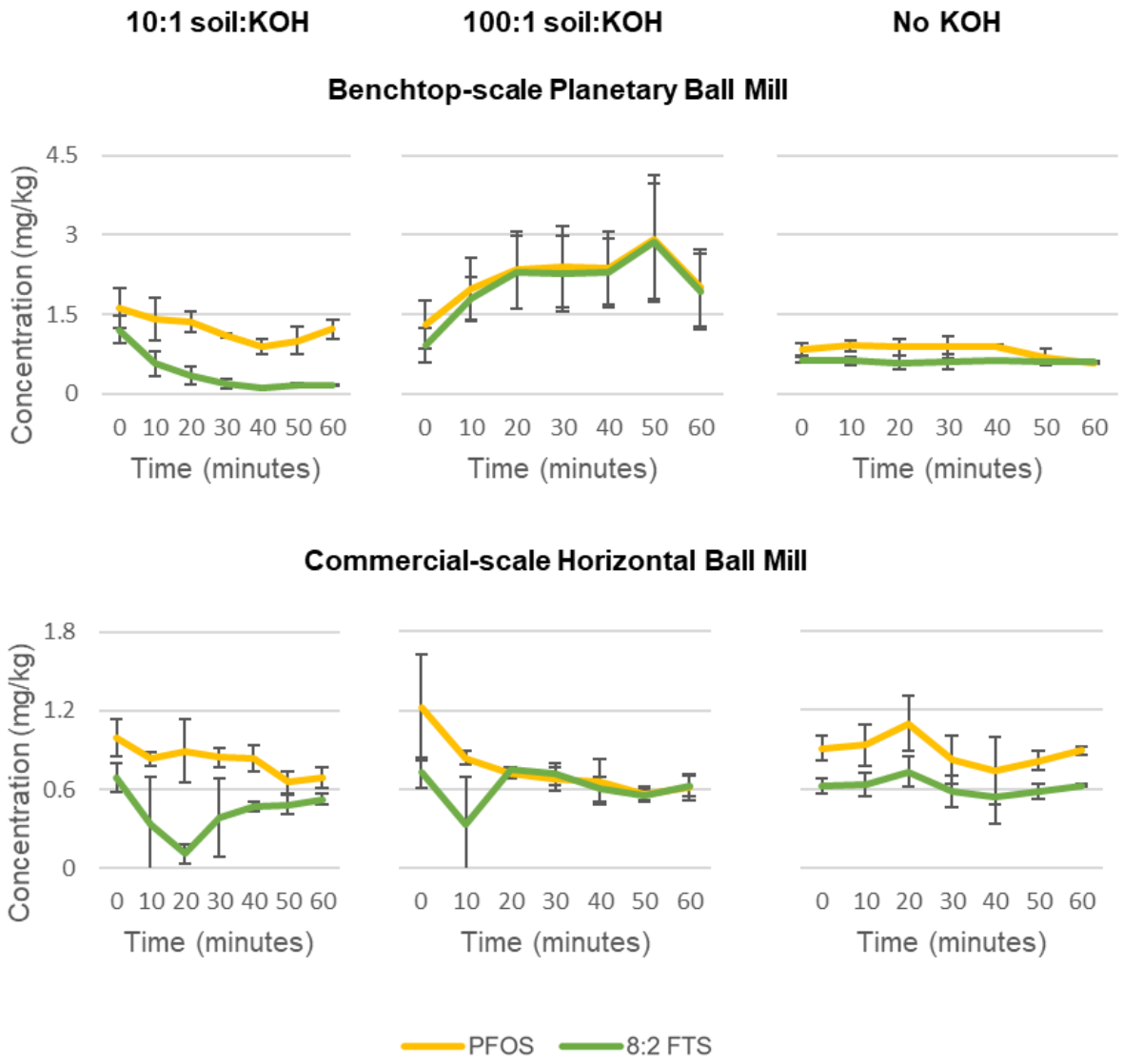

Figure S1: Results for benchtop-scale PBM and commercial-scale HBM for PFOS and 8:2 FTS, using 10:1 and 100:1 soil:KOH ratios, and no KOH. Soil was dried and 5:1 media:soil ratios were used for all trials. Data points are presented as means of triplicate samples ± standard deviation.

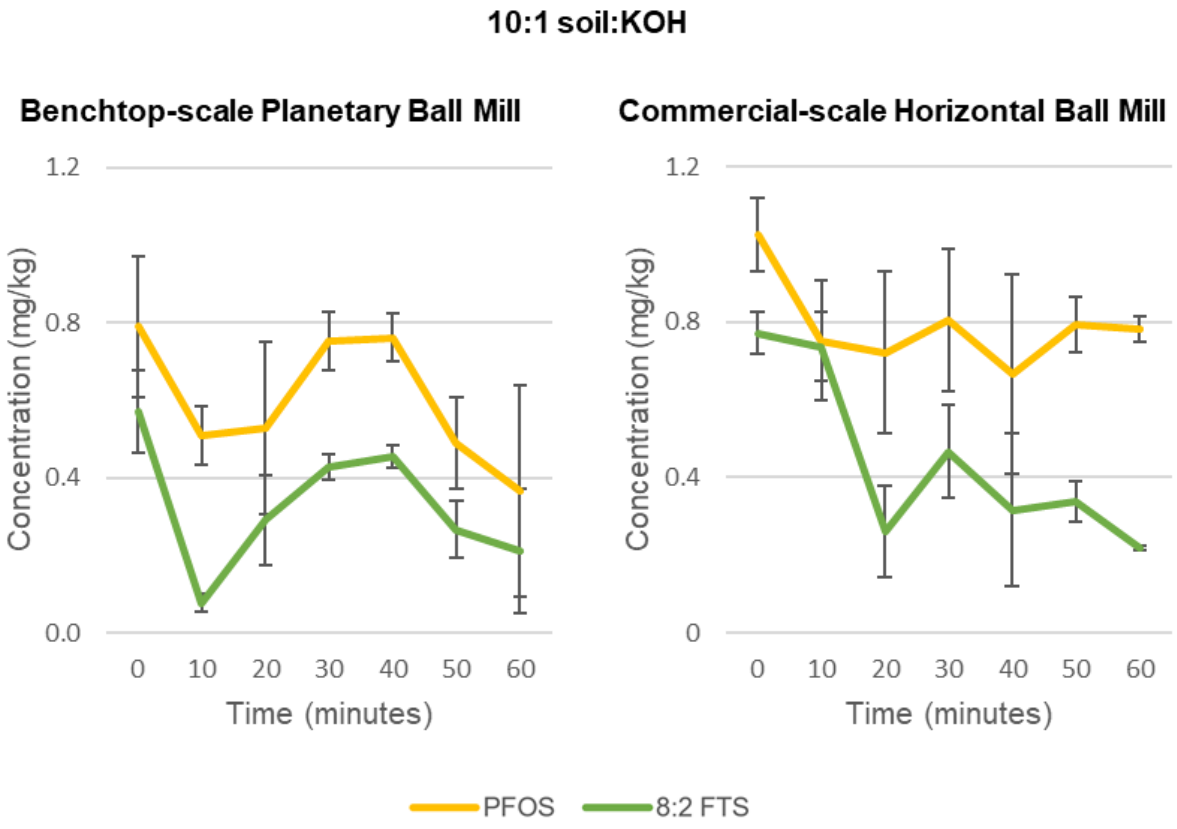

Figure S2: Results for benchtop-scale PBM and commercial-scale HBM for PFOS and 8:2 FTS, using 10:1 soil:KOH and 3:1 media:soil ratios. Soil was dried for all trials. Data points are presented as means of triplicate samples ± standard deviation.

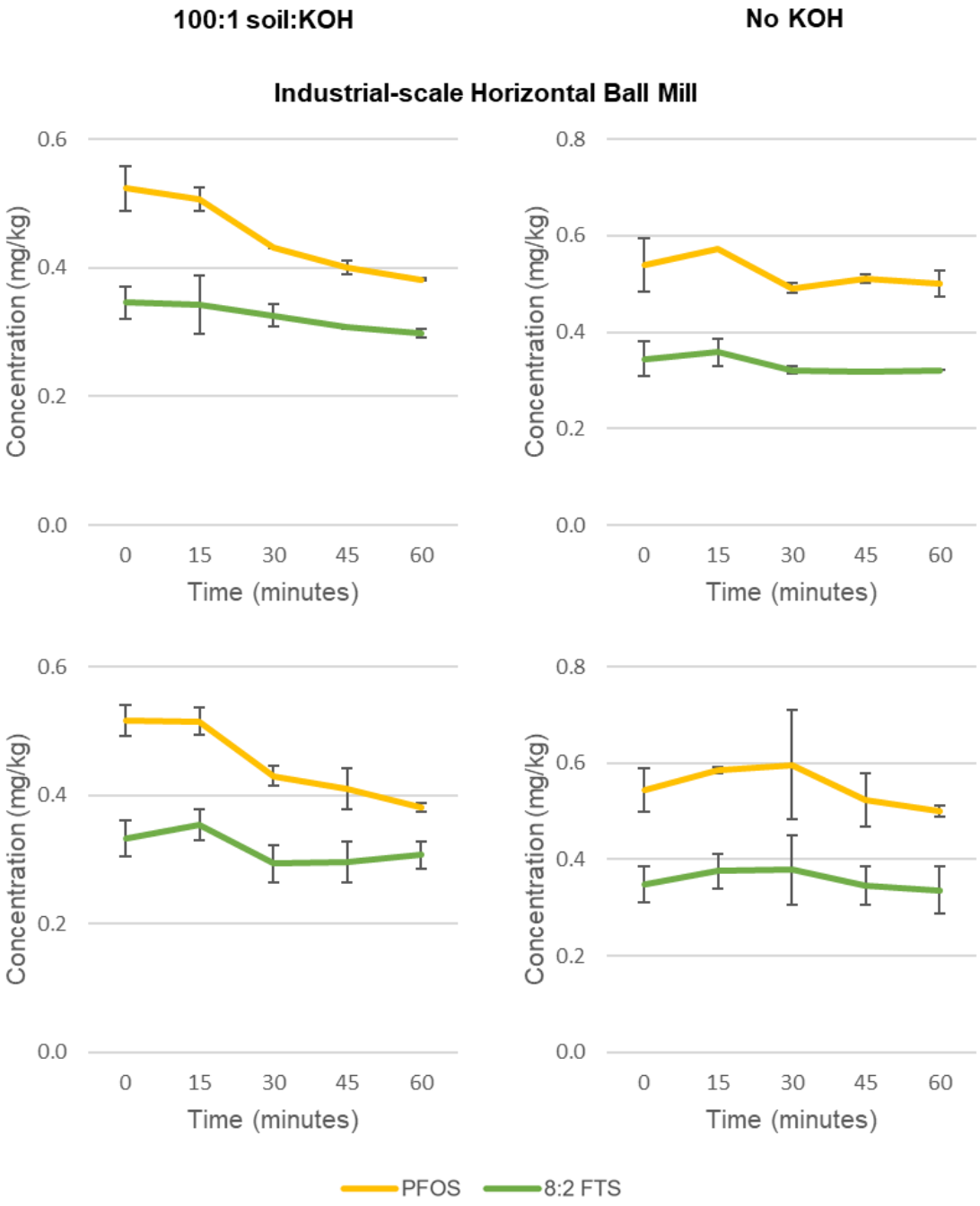

Figure S3: Results for industrial-scale HBM for PFOS and 8:2 FTS, using 100:1 soil:KOH ratios, and no KOH. Soil was dried and 5:1 media:soil ratios were used for all trials. Data points are presented as means of duplicate samples ± standard deviation.